Report No. CDOT-DTD-R-2004-8
Final Report

DRILLED SHAFT DESIGN FOR SOUND BARRIER

WALLS, SIGNS, AND SIGNALS

Jamal Nusairat

Robert Y. Liang

Rick Engel

Dennis Hanneman

Naser Abu-Hejleh

Ke Yang

October 2004

COLORADO DEPARTMENT OF TRANSPORTATION
RESEARCH BRANCH

1. Report No. CDOT-DTD-R-2004-8	2. Government Accession No.	3. Recipient's Catalog No.	
4. Title and Subtitle DRILLED SHAFT DESIGN FOR SOUND BARRIER WALLS, SIGNS, AND SIGNALS		5. Report Date June 2004	
		6. Performing Organization Code	
7. Author(s) Jamal Nusairat, Robert Y. Liang, Rick Engel, Dennis Hanneman, Naser Abu-Hejleh, and Ke Yang		8. Performing Organization Report No. CDOT-DTD-R-2004-8	
9. Performing Organization Name and Address E. L. Robinson Engineering of Ohio Co. 6209 Riverside Drive, Suite 100, Dublin, OH 43017, and Geocal, Inc. 13900 E. Florida Ave., Unit D, Aurora, CO 80012-5821		10. Work Unit No. (TRAIS)	
		11. Contract or Grant No. Study # 80.19	
12. Sponsoring Agency Name and Address Colorado Department of Transportation - Research 4201 E. Arkansas Ave. Denver, CO 80222		13. Type of Report and Period Covered Final Report, June 2002-June 2004	
		14. Sponsoring Agency Code	

15. Supplementary Notes
Prepared in cooperation with the US Department of Transportation, Federal Highway Administration

16. Abstract: The Colorado Department of Transportation (CDOT) uses drilled shafts to support the noise barrier walls and the large overhead signs and signals placed alongside the highways. These structures are subjected to predominantly lateral loads from wind. Current CDOT design for the drilled shafts is very conservative and lacks uniformity, which could lead to high construction costs for these shafts. CDOT commissioned a research study with the objective of identifying/developing uniform and improved design methods for these structures. Toward these goals, existing analysis methods for both capacity estimate and load-deflection predictions of drilled shafts supporting sound barrier walls, signs, and signals and typical soil and rock formations in Colorado are presented in a comprehensive manner. This includes the practice of CDOT engineers and consultants for design methods and geotechnical investigation, AASHTO design methods and specifications, and the design practice of the Ohio DOT. The accuracy of selected design methods for lateral and torsional responses of drilled shafts was evaluated by comparing predictions from these methods with measured "true" capacity and deflections from lateral and torsional load tests reported in the literature, performed in Ohio, and two new lateral load tests performed in this study as a part of the CDOT construction project along I-225 where noise barriers walls were constructed. A comprehensive geotechnical investigation program was also carried out at the two new lateral load test sites that included a pressuremeter test, Standard Penetration Test (SPT), laboratory triaxial CU tests, and direct shear tests. This allowed for evaluation of the accuracy of various testing methods employed for determining the soil parameters required in the lateral design methods. Finite element modeling have been developed and validated against the new load test data. Additional consideration of possible loading rate effect, cyclic loading effect, and ground water table fluctuations on the soil resistance are discussed. The appropriateness of the recommended factor of safety (FS) for the Broms method was further verified with LRFD calibration.

Implementation: Consider both strength limit state and serviceability limit state for design of sound walls. For the strength limit, use the Broms method and a FS of two. For the serviceability limit, use COM624p (LPILE) to estimate the lateral deflection of the drilled shaft. The permissible lateral deflection should be established by the structural engineers based on engineering judgment, structural, and aesthetic concerns. The study provides some recommendations for the permissible lateral deflections. A standard special note for performing instrumented lateral load tests has been developed, which can be adopted by CDOT engineers or consultants in developing their design plans. Appropriate geotechnical test methods are recommended for obtaining relevant cohesive and cohesionless soil parameters for various analysis methods: capacity method, deflection method, and finite element method. These included the use of triaxial and direct shear tests, pressuremeter tests, and SPT based on Liang's correlation charts. These recommendations will result in more uniform, consistent, and cost-effective design in future CDOT sound wall projects. The proposed design/analysis approach for the I-225 project has been shown to reduce the required drilled shaft length by 25% compared to the original CDOT design approach.

17. Keywords Lateral, torsional, sound wall, sign, signals, drilled shaft, load test, p-y analysis, capacity	18. Distribution Statement No restrictions. This document is available to the public through the National Technical Information Service 5825 Port Royal Road, Springfield, VA 22161.

19. Security Classif. (of this report) Unclassified	20. Security Classif. (of this page) Unclassified	21. No. of Pages 414	22. Price

Form DOT F 1700.7 (8-72)   Reproduction of completed page authorized

CONVERSION TABLE

U. S. Customary System to SI to U. S. Customary System
(multipliers are approximate)

Multiply (symbol)	by	To Get (symbol)	Multiply	by	To Get
LENGTH					
Inches (in)	25.4	millimeters (mm)	mm	0.039	in
Feet (ft)	0.305	meters (m)	m	3.28	ft
yards (yd)	10.914	meters (m)	m	1.09	yd
miles (mi)	1.61	kilometers (km)	m	0.621	mi
AREA					
square inches (in^2)	645.2	square millimeters (mm^2)	mm^2	0.0016	in^2
square feet (ft^2)	0.093	square meters (m^2)	m^2	10.764	ft^2
square yards (yd^2)	0.836	square meters (m^2)	m^2	1.195	yd^2
acres (ac)	0.405	hectares (ha)	ha	2.47	ac
square miles (mi^2)	2.59	square kilometers (km^2)	km^2	0.386	mi^2
VOLUME					
fluid ounces (fl oz)	29.57	milliliters (ml)	ml	0.034	fl oz
gallons (gal)	3.785	liters (l)	l	0.264	gal
cubic feet (ft^3)	0.028	cubic meters (m^3)	m^3	35.71	ft^3
cubic yards (yd^3)	0.765	cubic meters (m^3)	m^3	1.307	yd^3
MASS					
ounces (oz)	28.35	grams (g)	g	0.035	oz
pounds (lb)	0.454	kilograms (kg)	kg	2.202	lb
short tons (T)	0.907	megagrams (Mg)	Mg	1.103	T
TEMPERATURE (EXACT)					
Farenheit (°F)	5(F-32)/9 (F-32)/1.8	Celcius (° C)	° C	1.8C+32	° F
ILLUMINATION					
foot candles (fc)	10.76	lux (lx)	lx	0.0929	fc
foot-Lamberts (fl)	3.426	candela/m (cd/m)	cd/m	0.2919	fl
FORCE AND PRESSURE OR STRESS					
poundforce (lbf)	4.45	newtons (N)	N	.225	lbf
poundforce (psi)	6.89	kilopascals (kPa)	kPa	.0145	psi

Drilled Shaft Design for Sound Barrier Walls, Signs, and Signals

By

Jamal Nusairat, E. L. Robinson Engineering of Ohio Co.
Robert Y. Liang, The University of Akron
Rick Engel, E. L. Robinson Engineering of Ohio Co.
Dennis Hanneman, Geocal, Inc.
Naser Abu-Hejleh, Colorado Dept. of Transportation
Ke Yang, The University of Akron

ACKNOWLEDGEMENTS

EXECUTIVE SUMMARY

The Colorado Department of Transportation (CDOT) adopts the use of drilled shafts to support sound barrier walls, overhead signs, and signals. The primary loading to these foundation elements are lateral loads, moments, and torsion. Due to complexities of the nature of soil-shaft interaction under these applied loads, the geotechnical design of these drilled shafts has been very conservative. There has been a lack of uniformity in design and analysis methods and design criteria, in terms of factor of safety against ultimate capacity failure as well as the allowable deflection (serviceability under working load). Methods for determining pertinent soil parameters needed in both types of analysis (ultimate capacity and deflection prediction) have not been consistently evaluated for their applicability and accuracy. Realizing the importance of these issues, CDOT commissioned a research study with the objective of identifying/developing uniform and improved design method for sound walls, signs, and signals.

Toward these goals, existing analysis methods for both capacity estimate and load-deflection predictions of drilled shafts supporting sound barrier walls, signs, and signals are presented in a comprehensive manner. Typical soil and rock formations in Colorado are also summarized in a comprehensive manner. Then, the practice of CDOT and consultants for the design methods and geotechnical investigation for sound walls, signs, and signals are thoroughly discussed and evaluated. The AASHTO guidelines and specifications as well as the practice of the Ohio DOT are reviewed and discussed.

The accuracy of the selected simple analysis methods for lateral and torsional responses of drilled shafts was evaluated by comparing predictions from these simple methods with measured "true" capacity and deflections from lateral load tests. The simple methods for lateral response include the Broms method, COM624P method, sheet piling method, caissons program developed at CDOT, Brinch Hansen method, and NAVFAC DM-7 method. The simple methods for torsional response include two methods used by the Florida DOT and a method developed by Richard Osmun for the Colorado DOT. Data for evaluation of these methods were obtained from hypothetical cases, several load test databases carefully selected from literature, and from Ohio's load tests results. Tentative recommendations on lateral and torsional design methods were made.

LRFD calibration of the compiled load tests suggested that FS of 2 for the Broms method is appropriate. Additional consideration of possible loading rate effect, cyclic loading effect, ground water table fluctuations, and effect of lateral force induced moment on the soil resistance are discussed and accounted for in the study recommendations.

For further evaluation of design methods for Colorado's sound walls, the research team has conducted two fully instrumented lateral load tests on drilled shafts constructed at a sand soil deposit and a clay soil deposit, respectively, near Denver, Colorado. The two lateral load tests were performed as a part of the CDOT construction project along I-225 where noise barriers walls were constructed. Instruments were placed to measure the applied lateral loads and the induced lateral movements and strains of the drilled shafts at different depths. The measured load test data included lateral loads, lateral shaft head movements, and strains and deflections along the entire depth of the test shafts at each lateral load increment. A comprehensive geotechnical investigation program was also carried out at the two lateral load test sites that included the pressuremeter test, SPT, as well as laboratory triaxial UC tests and direct shear tests on the soil samples taken from the lateral load test sites. This also allowed for evaluations of the accuracy of various testing methods for determining the soil parameters for the design methods for sound walls. Using a validated FEM modeling technique, the two Colorado load tests were simulated and a very accurate estimate of p-y curve parameters was generated.

Implementation Statement

Appropriate analysis methods and the accompanying geotechnical test methods for determining the soil parameters were recommended in this report (see Chapter 5 for justification).

For CDOT Structural Engineers and Consultants
Current CDOT practice for overhead signs and signals could continue.

The following two simple uniform strength limit state and serviceability limit state design methods are recommended to determine the required drilled shaft length of sound walls (use larger predicted length from the two methods). For the strength limit, use the Broms method and

a F.S. of two to determine the required drilled shaft length. Lateral soil resistance in the upper 1.5 D (D is the shaft diameter) of the shaft is neglected in Broms method for cohesive soils, so no additional depth should be neglected as may be recommended in the geotechnical report. For the serviceability limit, use COM624P (LPILE) to estimate the lateral deflection of the drilled shaft. From the drilled shaft performance viewpoint and to be consistent with the strength limit, the authors of this report recommended a permissible lateral deflection of 1 inch. Mr. Dick Osmun from Staff Bridge recommends limiting the deformation for signs and signals to the soil's elastic limit under repetitive loading estimated with LPILE to avoid accumulation of irrecoverable deformation with cyclic wind loads. Other suggestions for the permissible lateral deflection are presented in Chapter 8.

The most accurate design method for drilled shafts is to conduct a load test on test shafts constructed as planned in the construction project. Chapter 7 provides a standard special note for performing instrumented lateral load tests, which can be adopted by CDOT engineers or consultants in developing their design plans. The load tests are expensive and therefore are only considered for large projects where testing could lead to large cost savings to the project. Finite element modeling should be considered in large or very critical projects with uncommon field and loading conditions.

For CDOT Geotechnical Engineers and Consultants

Estimate the highest possible elevation for ground water level (GWL). The most appropriate soil testing method to determine the cohesive soil parameters required for the Broms and COM624P methods are:

- The triaxial CU test or direct shear test as described in Chapter 5 of this report.
- The pressuremeter test with FHWA (1989) soil strength interpretation equation.
- The SPT method with Liang (2002) correlation charts, currently adopted by the Ohio DOT. These are presented in Tables 3.9 and 3.10, which also provide recommendations for all the other parameters required in the LPILE program.
- The CDOT procedure for estimation of strength and LPILE parameters based on SPT could be used but it is very conservative (i.e., underestimates strength by 50%, see Chapter 5).

The most appropriate soil testing method to determine the cohesionless soil parameters required for the Broms and COM624P methods are:

- The SPT with Liang (2002) correlation provides best soil strength interpretation.
- The pressuremeter test would provide reasonable soil strength interpretation as well.
- The SPT with CDOT correlations methods just for strength parameters (Table 3.2) not for the parameters required in the LPILE program.

Benefits:

The research results have provided several benefits to CDOT. Foremost, the proposed design/analysis approach has been shown to reduce the required drilled shaft length employed in the I-225 sound barrier project from 15.7 ft to 12 ft, yielding about 24% length reduction. Thus, it is anticipated that substantial cost savings can be realized in future CDOT sound barrier wall projects. An equally important benefit is the advancement of a uniform and consistent design/analysis method and acceptance design criteria (factor of safety and permissible movement) across the board for both CDOT engineers and local consultants. This uniformity ensures that less man-hours are needed in deciding on analysis methods. Rather, engineers can focus more on the determination of high quality soil parameters for input into the analysis. The research has provided recommendations for proper geotechnical test methods to characterize pertinent soil parameters needed for both ultimate capacity prediction and p-y curve generation in COM624P or LPILE analyses. The recommended geotechnical test methods would allow CDOT engineers to economize resources in planning out soil testing programs, thus potentially saving costs as well. The research has provided a standard instrumented lateral load test note, which can be used by CDOT engineers to specify a lateral load test in the design/construction plans. For a project that involves a lot of drilled shaft construction, or when unique soil conditions and complex loading combination exist, the lateral load test prior to final design decision could potentially offer cost savings to the project.

TABLE OF CONTENTS

The appendices are only available in electronic format:

http://www.dot.state.co.us/Publications/PDFFiles/drilledshaft2.pdf

LIST OF TABLES

LIST OF FIGURES

1 INTRODUCTION

1.1 Background

The close proximity of residential developments to major highway systems in Colorado has created the need to control the level of noise produced by public motorists. To alleviate this problem, noise barrier walls are increasingly built next to these highways. Sound barriers, sign and signal posts are not heavyweight structures and are subjected to predominantly lateral loads from wind. The Colorado Department of Transportation (CDOT) adopts drilled shafts to support the noise barrier walls and the large overhead signs and signals placed alongside the highways. Drilled shafts are routinely subjected to axial, lateral and moment loads. In the case of cantilever signs and signals, the drilled shafts are also subjected to torsional loads. The geotechnical design of drilled shafts requires that the shafts have adequate embedment length and dimension to ensure adequate margin of safety against ultimate failure (ultimate capacity based design). Furthermore, these shafts should be designed to experience an acceptable level of lateral displacement (service limit based design). Though some of the induced structure (e.g., cantilever signs and signals) displacements are permanent due to the weight of the structure, a larger portion of the induced displacements could be temporary and increase with time due to the influence of repeated wind load cycles.

The Colorado Department of Transportation's geotechnical design practice for drilled shafts may be very conservative and lacking in uniformity. Conservative designs are common when the engineer lacks confidence in the design theory. Design confidence is gained by evaluating data obtained from well-documented instrumented full-scale field load tests. Significant savings to CDOT can be realized if improved and uniform design guidelines and procedures are developed and implemented for future CDOT projects. The current research project on the "Drilled Shaft Design for Sound Barrier Walls, Signs, and Signals, Study No. 80.19" was initiated to re-evaluate and update CDOT design procedures for drilled shafts used to support sound walls, overhead signs and traffic signals. It is expected that this research will result in findings and recommendations to improve CDOT design practice with attendant cost savings and improved safety.

1.2 Objectives of the Study

The objectives of this research study are as follows:

(1) Determine the needs, benefits, potential cost-effectiveness, and justification of identifying improved design methodology for Colorado drilled shafts of sound barrier walls, signs, and signals.

(2) Identify the most accurate approximate design methods to predict the nominal response (ultimate capacity and deformation) of drilled shafts embedded in Colorado typical foundation soil conditions and subjected to typical Colorado loads (lateral, moments, and torsional loads).

(3) Develop a practical procedure to perform instrumented load tests.

1.3 Scope of Work

The research team has carried out the following tasks identified in the research work plan.

a) Identify future candidate construction projects in Colorado for performance of lateral load tests

b) Review, assimilate, and summarize current CDOT practice, and summarize typical soil and rock formations in Colorado

c) Document pertinent literature on the design methodology of drilled shafts for noise barrier walls, overhead signs, and signals

d) Identify and establish the design criteria of drilled shafts for sound barrier walls, overhead signs, and traffic signals

e) Identify and establish the availability of drilled shaft database information in existing literature

f) Recommend design methods and design criteria

g) Perform two lateral load tests and verify the recommended design methods and design criteria with lateral load test results

h) Recommend the appropriate geotechnical test methods for determining soil parameters as related to drilled shaft capacity and deflection predictions

i) Develop a standard note for performing an instrumented lateral load test

j) Develop 3-D FEM (finite element method) modeling details and perform numerical simulations for the two Colorado lateral load tests to gain insight on p-y curves.

k) Establish the needs, benefits, potential cost-effectiveness, and justification

1.4 Outline of the Report

Chapter 2 briefly presents existing lateral ultimate capacity estimate methods, such as the Brinch Hansen method, Broms method, sheet piling method, and caisson program, as well as serviceability analysis methods, such as COM624P (or LPILE) and NAVFAC method, for sound barrier walls foundation design. The design methods for drilled shafts supporting overhead signs and traffic signals are reviewed in Chapter 2 as well. The details of analysis methods are given in Appendix B and Appendix C for lateral and torsional response, respectively. The typical soils and bedrock conditions encountered for sound walls, overhead signs, and traffic signals in Colorado are provided in Chapter 2 as well. More details of the soils and bedrock information of Colorado are given in Appendix A.

The review of foundation design for sound walls, overhead signs, and signals by Colorado Department of Transportation and consultants, including foundation design and geotechnical

investigation, are presented in Chapter 3. Additionally, The AASHTO guidelines and specifications as well as the practice of the Ohio Department of Transportation are reviewed and presented in this chapter.

Evaluation of selected analysis methods for lateral and torsional responses of drilled shafts are documented in Chapter 4. Both hypothetical cases and load test database selected from literature and Ohio's test results are used for evaluation and comparison. The evaluation results support the use of the Broms method with factor of safety of two for sound wall design. The COM624P (or LPILE) program is considered to be a versatile and reliable tool for predicting drilled shaft deflections, provided that representative and accurate p-y curves are used. The resistance factors for LRFD design are also calibrated from the reliability method and fitted to the Allowable Stress Design method. A tentative recommendation on the torsional design method for overhead signs and traffic signal foundation design is also made.

Chapter 5 presents the two lateral load tests and analysis results. Two lateral load tests were conducted on CDOT designed drilled shafts. SPT tests and pressuremeter test results were obtained from test sites. Direct shear tests and triaxial tests were also performed on samples retrieved from the load test sites. The Broms method and COM624P program were used to analyze the lateral load tests with soil parameters determined from these soil testing methods. The comparison of the analysis results indicated that the triaxial test or direct shear test are considered to be the most appropriate soil parameter determination methods for drilled shafts in clay. The pressuremeter test with FHWA (1989) soil strength interpretation equation or SPT method with Liang (2002) correlation charts provide good predictions as well. For sand sites, the SPT method with Liang (2002) correlation charts provides the most appropriate capacity estimate, while direct shear test results provide good match with the measured load-deflection curve at the shaft top. P-y curves based on the strain gages and inclinometer data were also derived for both test sites. The re-designed drilled shafts at the test sites for sound barriers were 25% shorter than the original CDOT design length, thus yielding cost savings.

The FEM modeling techniques for simulating lateral loaded drilled shafts in clay and sand by using ABAQUS were developed in Chapter 6. One lateral load test in Ohio was used to validate

the FEM modeling techniques. The lateral responses of the two load tests in Colorado were simulated by using the developed FEM modeling techniques. P-y curves obtained from the FEM simulation were shown to match with the p-y curves derived from measured strains and deflections.

Finally, the special note for a lateral load test is provided in Chapter 7. The conclusions and recommendations are presented in Chapter 8 and 9, respectively.

2 REVIEW OF ANALYSIS AND DESIGN METHODS, AND SOILS AND BEDROCK IN COLORADO

2.1 Review of Existing Analysis and Design Methods

2.1.1 Lateral Response of Drilled Shafts

The methods for analysis of laterally loaded drilled shafts can be broadly divided into three categories: the elastic theory based approach, the discrete and independent spring based approach, and the finite element based continuum approach. Additional division of various available analysis methods may be made on the basis of the ability of the analysis to provide a complete load-deflection solution or only the ultimate capacity solution. For example, the Broms method is a method that only provides the ultimate capacity solution; whereas, the discrete spring based approach can offer a complete load-deflection solution. Although it is nearly impossible to identify and summarize all published analysis methods for laterally loaded drilled shafts, some of the more prominent and representative analysis methods are briefly reviewed herein and summarized in Table 2.1. A more in-depth description of those reviewed methods is included in Appendix B.

2.1.1.1 Ultimate Capacity Estimation Methods

2.1.1.1.1 Brinch Hansen Method

This method is based on earth pressure theory for c-Φ soils. It consists of determining the center of rotation by taking moment of all forces about the point of load application and equating it to zero. The ultimate lateral resistance can be calculated by equating the sum of horizontal forces to zero. The advantages of this method are its applicability to c- Φ soils and layered system. However, this method is only applicable for short piles (drilled shafts), and a trial-and-error procedure is needed to locate the point of rotation in the calculation.

2.1.1.1.2 Broms Method

Broms method considers piles or drilled shafts as a beam on an elastic foundation. Simplified assumptions have been adopted regarding the ultimate soil reactions along the length of a pile. The rotation point of piles or drilled shafts under lateral load is assumed in different ways for

cohesive soils and cohesionless soils. The Broms method is capable of considering two boundary conditions: one is a free pile head, and the other is a restrained shaft head. Also, the Broms method can handle not only short drilled shafts (piles), but also long drilled shafts (piles). This method however is only suitable for homogeneous soil, which would be either cohesive soils or cohesionless soils. In order to apply the method to layered or mixed soil conditions, an engineers' judgment is needed to determine average (homogenized) soil properties.

2.1.1.1.3 Sheet Piling Method

The Sheet Piling Method is based on the earth pressure theory. It was initially developed for sheet piles embedded in cohesionless soils. For cohesive soils, an assumption on equivalent friction angle has to be made and the cohesion is assumed to be zero. Since it is rather difficult to make any rational assumption about the equivalent friction angle, the sheet piling is not a suggested method for drilled shafts embedded in clays.

To some extent, the hand calculations involved in the application of the sheet piling method are cumbersome. This method is only applicable for short piles embedded in homogenous cohesionless soils. Also, this method is developed for sheet piles, which may exhibit different behaviors than drilled shafts.

2.1.1.1.4 Caisson Program

A CDOT engineer, Michael McMullen, developed the Caisson Program. This program is based on a theory developed by Davidson, et al (1976), which assumes that full plastic strength of the soil is developed in calculating the ultimate capacity. Davidson's method assumes rigid-body motion of the pile and the lateral soil resistance varies linearly with the depth at ultimate load, but reverses direction at the point of rotation of the shaft. The soil strength is based on Equation 9-7 in "Basic Soils Engineering" by B.K. Hough, which in fact was generated for spread footing foundations.

The Caisson Program only applies to homogeneous cohesive or cohesionless soil. The research team encounters some run-time errors when using the Caisson Program to analyze drilled shafts in cohesive soils. The method cannot provide deflection information.

2.1.1.2 Load-Deflection Prediction Methods

2.1.1.2.1 COM624P (LPILE)

The COM624P Program, or the equivalent commercial program, LPILE, has been widely used for decades. The COM624P (LPILE) computer program is based on a numerical solution of a physical model based on a beam on Winkler foundation. The structural behavior of the drilled shafts is modeled as a beam, while the soil-shaft interaction is represented by discrete, non-linear springs. The same concept has been applied to the so-called finite element program, Florida Pier. The Florida Pier program, however, offers the ability to analyze pile group behavior by incorporating an empirical group reduction factor.

The adoption of a beam on Winkler foundation as a physical model may introduce a small amount of inaccuracy because it ignores the interactions between the discrete springs. However, some studies have shown that this error is minor, if the spring characteristics can be deduced to represent the true field behavior. Therefore, the representation of the spring has been developed on the basis of semi-empirical p-y curves, in which p represents the net force acting on the shaft per unit shaft length and y denotes the lateral displacement of the drilled shafts. Soil mechanics principles have been evoked to deduce the theoretical ultimate resistance p, and to estimate the initial stiffness using the subgrade reaction coefficient concept. Nevertheless, the construction of the p-y curves relies on the curve fitting, using the test results of a limited number of full-scale lateral load tests. Correlations with soil properties, shaft diameter, and depth were used to give generality to the recommended p-y curve construction. As a minimum, the friction angle and undrained shear strength from UU tests are needed to represent soil strength parameters for cohesionless and cohesive soils, respectively. Correlations between these strength parameters with the SPT N values have been developed to enable the use of an insitu testing method for improving COM624P analysis results.

2.1.1.2.2 NAVFAC DM-7 Method

NAVFAC DM-7 method is based on Reese and Matlock's non-dimensional solutions for laterally loaded piles with soil modulus assumed proportional to depth (1956). By assuming that soils behave as a series of separate elements, NAVFAC DM-7 method is an elastic method. The

ordinary beam theory can be used to develop the differential equation for a laterally loaded pile (drilled shaft). The differential equation is solved, based upon the development of a mathematically convenient function for the soil reaction p. The soil reaction p is represented by the multiple of the modulus of subgrade reaction and soil deflection. For cohesionless soils, the modulus of subgrade reaction is assumed to be proportional to the depth. The modulus of subgrade reaction is assumed constant in cohesive soils; however, it will be converted to equivalent modulus, which is proportional to the depth for calculation purpose. There are three boundary conditions considered in this method: flexible cap or hinged end condition, rigid cap at ground surface, and rigid cap at elevated position.

The limitations of this method are that the lateral load cannot exceed approximately one-third of the ultimate lateral load capacity and only elastic lateral response can be predicted.

2.1.2 Torsional Response of Drilled Shafts

The analysis methods for torsional response of drilled shafts can be classified into two categories, similar to the lateral responses; namely, on the basis of the method's ability either to provide only ultimate torsion capacity or a complete torsional loads versus torsional twist at the drilled shaft head as well as along the depth of the drilled shaft. A brief review of existing analysis methods for torsional response, including twisting behavior, is given in Table 2.2. A more in-depth discussion of these methods is provided in the Appendix C.

To predict torsional load vs. torsional twist angle, most of the analytical/numerical methods are only concerned with the rotational stiffness at the head of the drilled shafts. The exceptions to this are those developed by O'Neill (1964), Guo and Randolph (1996), who considered the non-linearity of soil behavior and the torque transfer behavior along the length of the pile.

The existing analytical methods for estimating the ultimate torsion capacity of the drilled shafts are summarized in Table 2.3. Most of the methods deal with the torsion loads only; however, Tawfiq (2000) presented a method for combined lateral, overturning, and torsional loads. Empirical equations were used in Tawfiq's approach for determining the interface strength between the soil and the pile.

2.1.3 Finite Element Method

The Florida Pier finite element program is a very powerful software program for analyzing the three-dimensional behavior of drilled shafts subjected to various load combinations (e.g., axial, lateral, torsional, and bending). The soil-drilled shaft interactions however, are characterized by discrete springs, which are similar to the p-y curve concept in the COM624P program for the lateral load response. While the Florida Pier program can handle three-dimensional loads, the need remains to have an appropriate methodology to determine the input for the representative spring behavior. Thus, the Florida Pier program suffers the similar shortcoming as for the COM624P computer program. This is due to the need for more adequate representation of the discrete interaction springs.

A true finite element modeling in the continuum framework can be accomplished by the powerful commercial finite element codes, such as ABAQUS. The drawback of such undertaking is the need to establish modeling techniques, including the constitutive models for the soil and the interface, and the mesh representation. Furthermore, the modeling technique needs to be validated against the actual test data before it can be used for production purposes. Nevertheless, the true continuum based finite element approach should be used for special cases in which further insight may be gained and cost saving realized.

Table 2.1 Summary of Analytical Methods Used to Analyze the Behavior of Laterally Loaded Drilled Shafts

Analytical Method	Assumptions	Description	Advantages	Limitations
Brinch Hansen Method (1961)	Based on the earth pressure theory	Assuming center of rotation, calculates the ultimate capacity	Applicable for c-ϕ soils Applicable for layered system	Applicable only for short piles Requires trial-and-error solution to locate point of rotation
Broms Method (1964)	Pile is equivalent to a beam on an elastic foundation	Gives out the maximum moment, its location, and ultimate lateral resistance (charts are provided)	Easy to calculate	Applicable to homogeneous soil Gives rough estimation
Sheet piling method (AASHTO 1989)	Based on the earth pressure theory	Uses the sheet piling approach to get the ultimate lateral soil pressure		Requires hand calculations Applicable for short piles
Caissons Program		Gives out the ultimate capacity		Cannot provide deflection information Applicable to homogeneous soil Requires computer program

Table2.1 Summary of analytical methods used to analyze the behavior of laterally loaded drilled shaft   Con.

Analytical Method	Assumptions	Description	Advantages	Limitations
NAVFAC DM-7, 1971	For coarse grained soil, E_s increases linearly with depth For stiff to hard clays, E_s is constant with depth	For coarse grained soil, $k_h = \dfrac{fz}{D}$ and for stiff to hard clays constant modulus E_s is converted to equivalent modulus E_s varying linearly with depth and then the deflection is calculated.		Considers lateral load not exceeding 1/3 of the capacity Gives out only elastic solutions
P-Y Method (1986)	The axial load in the pile is constant.	$\dfrac{p}{p_{ult}} = 0.5\left(\dfrac{y}{y_{50}}\right)^{\frac{1}{3}}$	Accounts for the nonlinear behavior of most soils	Continuous nature of soil is not clearly modeled The default curves are limited to the soil types of their original development Computer program is required.

Table 2.2 Summary of Analytical Methods for Torsional Response of Piles/Drilled Shafts

Methods	Description	Equations for Calculation	Advantages	Limitations
O'Neill (1964-a)	• A closed form differential equation solution. • Elastic analysis. • Soil is homogeneous, and it can be cohesive or cohesionless.	$T(z) = T_0 e^{-z\sqrt{\beta\lambda}}$ $\left(\dfrac{T}{\theta}\right)_{pilehead} = \sqrt{\dfrac{\lambda}{\beta}}$	• Estimate the initial torsional stiffness of pile head by simple hand calculation. • The torque transfer along the shaft.	• It's available only for small pile-head loads. • The estimation is very rough
O'Neill (1964-b)	• A discrete method which can handle the non-linearity of soil response	A program TORQUE1	• Predict the torque-twist curve along the shaft rather than shaft head torsional stiffness.	• Some key parameters are unavailable for application.
Poulos (1975)	• Numerical elastic analysis and parametric solutions • Uniform soil and a soil in which shear modulus and pile-soil adhesion increase linearly with depth. • Cohesive soils.	$\phi = \dfrac{T}{G_s d^3} \dfrac{I_\phi}{F_\phi}$	• Charts are available for calculation.	• Unavailable for nonlinear soil response analysis.
Randolph (1981)	• Closed-form elastic solutions • For homogeneous soil and a soil where the stiffness is proportional to depth.	$\dfrac{T_{top}}{G r_0^3 \phi_{top}} = \dfrac{\left(\dfrac{16}{3} + 4\pi \dfrac{1}{r_0} \dfrac{\tanh(\mu l)}{\mu l}\right)}{\left(1 + \dfrac{32}{3\pi\lambda} \dfrac{1}{r_0} \dfrac{\tanh(\mu l)}{\mu l}\right)}$	• A simple assumption makes the closed form solution available. • The governing equation is widely used by other researchers.	• Only suitable for elastic analysis

Table 2.2 Summary of Analytical Methods for Torsional Response of Piles/Drilled Shafts (Con.)

Chow (1985)	• A discrete element approach • Nonhomogeneous soil	$[K_p]\{\psi\} + [K_s]\{\psi\} = \{0\}$	• Complex soil stratification can be considered • Arbitrarily varying pile sections	• For linear soil response
Hache & Valsangkar (1988)	• Mathematical solutions • Nondimensional charts	$\phi_t = \dfrac{T_t L}{(GJ)_p}(I_\phi)$	• Layered soil profile can be considered	• Elastic solution
Guo & Randolph (1996)	• Analytical and numerical solutions. • Non-homogeneous soil	Charts and Program GASPILE	• Vertical non-homogeneity of soil is expressed as a power law • Elastic-perfectly plastic soil is considered • Non-linear hyperbolic stress-strain law of soil is also explored	• Layered soils cannot be handled
Lin (1996)	• A finite element numerical analysis • Investigated the crack of the reinforced concrete pile	A FEM program	The pile's non-linearity is considered	• Complicated • Difficult for practical application
Carter & Kulhawy (1988)	• An approximate linear elastic solution • For rock	$\dfrac{T}{G_r B^3 \phi} = \dfrac{(\frac{2}{3})(\frac{1}{\xi}) + \pi(\frac{D}{B})\frac{\tanh(\mu D)}{\mu D}}{1 + (\frac{64}{3\pi\lambda\xi})(\frac{D}{B})\frac{\tanh(\mu D)}{\mu D}}$	• It's suitable for rock	• An elastic analysis method

Table 2.3 Summary of Estimation Methods for Torsional Ultimate Capacity of Piles/Drilled Shafts

Methods	Description	Equations for Calculation	Advantages	Limitations
FDOT Structural Design Office Method	- Simple torsional load - Soil can be cohesive or cohesionless - Soil is assumed as a rigid plastic material	For cohesionless soil $T_s = (K_0 \cdot \gamma \cdot 0.5L^2) \cdot \pi \cdot D \cdot \tan \delta \cdot 0.5D$ $T_b = W \cdot \tan \delta \cdot 0.33D$	Stratified soil can be considered	Simple torsional loads
Florida District 5 Method	Simple torsional load	$T_b = 0.67 \cdot (W + A_y) \cdot \tan(0.67\varphi) \cdot (D/2)$ Program SHAFTUF determines the side friction.		Needs a program
Modified Florida District 5 Method	- Cohesionless soil - Based on β method	$Q_s = \pi \cdot D \cdot L \cdot f_s, Q_b = 0.67 \cdot (W + A_y) \cdot \tan(\delta)$ $T = Q_s \cdot (D/2) + Q_b \cdot (D/2)$	Easy calculation	Difficult to adopt an appropriate value of β
Tawfiq (2000)	- Combined torsional and lateral loading conditions - Cohesionless soil	A Program is necessary.	Combined loads are considered	Complicated calculation.
Florida District 7 Method	- Cohesive soil - Based on the α method	$T_s = p \cdot L \cdot \sum f_s \cdot D/2$ $T_b = Q_b (0.67 \cdot D)$	Over consolidation ratio is considered	Simple torsional loading.
Colorado DOT	- Cohesive soil - Cohesionless soil	$T_{clay} = \pi D(L - 1.5D)c(D/2) + \pi (D^2/4)c(D/3)$ $T_{sand} = (K\gamma \dfrac{L^2}{2})(\pi D)\mu(\dfrac{D}{2}) + w\mu(\dfrac{D}{3})$	Easy calculation	Simple loads only.

2.2   Colorado Soils and Bedrock

2.2.1 Introduction

Over much of the state, Colorado surficial soils, shallow soils, and bedrock are highly variable due to repeated episodes of mountain building, subsidence, igneous intrusion and extrusion, and glaciation. Within many provinces or trends, the character of soil and bedrock vary within definable limits due to similar geologic history, thus allowing for generalizations of their geotechnical properties. The emphasis in this report is on soil and bedrock conditions likely to affect structures rather than total geologic aspects.

This study concentrates on shallow subsurface conditions of soil and bedrock usually encountered for sound barrier walls, overhead signs, and similar structures along the Urban Front Range Corridor (the Corridor). For our purposes, the Corridor is defined by a combination of geologic/geomorphic and population/transportation factors. From west to east, it covers the far eastern portion of the Rocky Mountains Front Range, the Frontal Hogback, and the valleys and uplands divisions of the Great Plains Western Piedmont Sub-Province. The Corridor extends from approximately Fort Collins on the north, including the Greeley area, to Pueblo on the south, thus capturing the State's dominant population centers along Interstate 25. An outline of the statewide geological environment is also presented including a brief overview of soil and bedrock conditions along other (non-Front Range) important highway corridors.

2.2.2 Summary of Soil and Bedrock Conditions in the Urban Front Range Corridor

The soils and bedrock existing along the Urban Front Range Corridor vary considerably as a result of the geologic processes that formed them. This section provides a brief overview of the soil and bedrock types often found in the Corridor and discusses engineering properties that may affect laterally loaded drilled shafts. More detailed geologic descriptions are presented in Appendix A.

2.2.2.1 Soil Deposits

2.2.2.1.1 General Soil Types

Soils in the Corridor vary from clean sands and gravels to clays and silts. Sands and gravels are commonly encountered near existing and historic river channels including the South Platte River, Cherry Creek, Plum Creek, St. Vrain River, Cache la Poudre River, Arkansas River, and many others. Remains of previous valley floors or alluvial fans can be seen in gravel capped terraces in many areas. Alluvial clays and silts are also occasionally present within the river deposits, although the clay soils are much more common than silt soils. Silt is very often present as a minor constituent in alluvial sands and gravels. Eolian sands and clays are often located east of the major historic rivers, coinciding with the prevailing westerly winds. Sometimes these soils compress upon wetting and may require special design considerations. Significant thicknesses of the residual surficial soils also exist in some areas, although to a lesser extent than alluvial and eolian deposits. Even less common are soils of colluvial (slope wash) origin which often contain the full range of soil types frequently mixed with bedrock fragments. Most sands and gravels typically encountered are rounded to subangular, and clays possess low to high plasticity. Due to the many geologic processes that created the soil deposits in the Corridor, significant variations in material types are common, oftentimes over relatively short distances both horizontally and vertically.

Man-placed fill soils comprised of the full range of natural soil types, and sometimes bedrock fragments, are common along the Corridor. Cuts and fills are an inherent part of highway development and often have significant thicknesses at overpasses and in areas with moderate or greater topographic relief. Fill soils may also be found in old sanitary landfills, old aggregate pits, and in low lying areas that were raised for development to reduce the risk of flooding. In the case of sound barrier walls, berms are sometimes constructed to reduce the height of the wall so a nominal thickness of fill is typical to most sound barrier projects. Typically, fill soils have been placed under relatively controlled circumstances in recent decades, but there are exceptions. It remains the CDOT practice to allow contractors to place construction debris within the right of way outside of the roadway prism defined by a 1:1 outward slope from the edge of the shoulder. These fills are typically uncontrolled.

2.2.2.1.2 Plasticity

The plasticity of fine grained soils in the Front Range Urban Corridor ranges from non-plastic to low plastic silts to very high plastic clay. Silt soils are not encountered very frequently. Most of the clay possesses medium plasticity, with plasticity indexes in the range of 15 to 30. Liquid limits are most often below 50, but higher liquid limits and plasticity indexes are occasionally observed. Liquid limits greater than approximately 70 are rare. Medium to high plasticity clays have the potential to be expansive when wetted. The swell potential depends on many factors including moisture content, dry unit weight, mineral composition, particle size gradation, and Atterberg Limits. Where swelling soils exist, it is likely that required caisson depths to resist uplift forces will control the design instead of lateral loading conditions. Of course, both conditions would need to be checked.

2.2.2.1.3 Moisture Content and Ground Water

The Moisture contents of soils in the Corridor usually range from slightly moist to wet below the ground water table. Dry soils, defined for our purposes as not having visible moisture, are encountered occasionally. Saturated soils exist in areas of poor surface drainage, below the ground water elevation, and sometimes several feet above the ground water table due to capillary action in fine grained soils. Depths to ground water are highly variable, and localized perched water conditions frequently exist. Generally, however, the ground water table near permanent flowing water channels is likely to be at approximately the same level as the water surface. Ground water elevations rise further away from the river or creek and often correlate with the ground surface topography, but the ground water surface is sometimes highly variable.

2.2.2.1.4 Consistency or Density

The consistency and density of cohesive and cohesionless soils, respectively, vary considerably. Cohesive soil consistency runs the gamut of the generally accepted classifications from very soft to hard, and cohesionless soils also vary over the entire density range from very loose to very dense. Most cohesive soils encountered in the Corridor typically are medium (UC strength of 0.5 to 1.0 tsf or SPT of 4 to 8) to very stiff (UC of 2.0 to 4.0 tsf or SPT of 15 to 30). The consistency tends to vary inversely with moisture content; relatively dry cohesive soils are stiffer

than soils with greater moisture. Most cohesionless soils range from medium dense (SPT of 10 to 30) to dense (SPT of 30 to 50).

2.2.2.1.5 General Distribution of Near Surface Geomaterials

The foregoing discussion categorizes soil types based on whether they are cohesive or cohesionless. In reality, many soils in Colorado do not conform neatly into one category or the other; they have cohesive and frictional components. It is assumed that most soils with greater than 70% passing the #200 sieve in Colorado will behave largely in a cohesive manner, and those with fewer than 30% fines will behave largely in a frictional manner. The estimated proportions of geomaterials likely to be encountered near the ground surface in the more populated areas of the Front Range Urban Corridor at sound barrier wall, overhead sign, or signal projects are presented in the Table 2.4 to provide a general idea of the typical soil distribution. Silts are fine grained soils, having little cohesion and are not commonly encountered in the Urban Corridor.

Table 2.4 Typical Soil Distribution

Material Type	USCS Symbols Included	Fines Content (%<#200)	Estimated Distribution(%)
Clay, silt	CL, CH, ML, MH	>65	20[a]
Sand, gravel	SW, SP, GW, GP, SC, SM SC, etc.	<35	20[b]
Intermediate soils	SC, SM, CL, CH, MH	35-65	60[c]

a. Silt soils are a minor percentage.

b. Gravel soils are a small percentage.

c. A majority (est. 75%) of these soils are clay.

d. Estimated total distribution of soils based on USCS criteria is 65% clay (and silt) and 35% sand (and gravel).

The research team was hesitant to provide estimated distributions in the above table because of the great difficulty in selecting and evaluating an appropriate data set. Consequently, these

estimates are primarily based on representative values deemed reasonable by several local consulting and CDOT geotechnical engineers who provided their opinions. USGS maps (see references) were also reviewed. The values presented in the table should not be considered absolute, but are presented to provide a relative indication of the frequency of occurrence along the Corridor and to help identify which soil conditions should be targeted for future lateral load tests. A review of exploratory boring logs and laboratory data conducted for several CDOT and Geocal, Inc. projects indicate that the above estimated distributions are reasonable. It is important to bear in mind that any particular project could have several soil types, or it could have only one general type of soil. Therefore, it is critical that site specific subsurface investigations be conducted.

2.2.2.2 Bedrock

2.2.2.2.1 Generalized Distribution

Except for transitional zones where bedrock is very highly weathered, the interface between soil and bedrock is usually fairly well defined along the Corridor. A major unconformity (period of non-deposition and/or erosion) which is due to uplift along the mountain front has separated younger soil from older bedrock. The bedrock units in the Corridor are distributed into four major settings (arranged as younger to older for the age of their generally included units):

1. Early Tertiary (Paleocene) coarse sandstone and conglomerate units, the youngest bedrock, are primarily limited to the central part of the Corridor forming major exposures in the Monument Highlands.

2. For valleys and uplands of the Western Plains Piedmont (the dominant portion of the Corridor), upper Late Cretaceous sedimentary rocks are intermittently exposed through soil cover throughout the northern and southern parts and comprise most of the bedrock likely to be encountered in foundations.

3. The mountain front belt includes a wide age range (Triassic to Pennsylvanian) of diverse sedimentary rocks that are exposed in a variably wide and locally intermittent band immediately east of the mountains. Jurassic to lower Late Cretaceous age shale and sandstone-dominant, tilted strata are intermittently well exposed along the narrow Frontal Hogback and as flatter lying outcrops in the Arkansas River valley near Pueblo.

4. Pre-Cambrian igneous and metamorphic rocks are exposed pervasively in mountainous areas along the west margin of the Corridor.

2.2.2.2.2 Common Bedrock Types within the Corridor

Most drilled shafts are likely to be constructed where upper Late Cretaceous sedimentary rocks exist (Item 2 in section 2.2.2.2.1) which includes most of the Denver metro area, Fort Collins, Greeley, Boulder, Colorado Springs, and Pueblo areas. Major bedrock units include the <u>Denver, Arapahoe, & Lower Dawson Formations</u> and the <u>Laramie Formation, Fox Hills Sandstone, and Pierre Shale.</u> Other bedrock types (items 1, 3, and 4 above) are discussed in Appendix A of this report.

2.2.2.2.2.1 Denver, Arapahoe, and Lower Dawson Formations

The <u>Denver, Arapahoe, & Lower Dawson Formations</u> encompass a broad, arc-shaped band sweeping from northern Denver around the Monument Highlands with the general arrangement being <u>Denver Formation</u> dominant to the north (under most of the Denver metropolitan area), <u>Arapahoe Formation</u> in the center, and <u>Lower Dawson Arkose</u> to the south (around Colorado Springs). These units, although sometimes separately mapped, are largely age equivalent and interfinger with each other over long distances.

The <u>Denver Formation</u> predominantly consists of claystone/shale, over most of the Denver area, with thinner interbeds of siltstone, weakly to well cemented sandstone, and infrequent conglomerate. Claystone/shale, as well as tuffaceous sandstone, are well noted for having major vertical and horizontal zones with high to very high swell potential; non-sandy claystone is frequently highly plastic when saturated. Claystone clays and ash-derived sandstone clays are montmorillonite rich (frequently termed "bentonitic") often including seams of nearly pure bentonite. Where unweathered, the formation includes a blue-green-gray claystone (and sandstone in some areas) locally known as the "Denver Blue". The "Denver Blue's" upper surface is not a stratigraphic horizon, but rather an irregular weathering/alteration zone that is often transitional. The bluish color has been observed to change to a predominantly grayish color after exposure to air.

The Arapahoe Formation is generally coarser than the Denver Formation. The two are frequently mapped as Denver-Arapahoe Undifferentiated in the Denver area. The formation is generally described as well stratified, interbedded claystone/shale, siltstone, sandstone, and conglomerate. A well-developed lower Arapahoe conglomerate is frequently only weakly cemented and is a significant aquifer. Conglomerate and sandstone units have variable low to moderate swell potential; siltstone and claystone/shale have moderate to high swell potential.

Lower Dawson Arkose also tends to be well interbedded with layers of conglomerate, coarse sandstone, shale, and silty fine sandy shale (termed "mudstone"). The coarser units usually have moderately well graded quartz and feldspar sands with granitic pebbles ("arkose"); local coal beds are noted. Clay rich and clay-dominant zones have moderate to very high swell potential and moderate to high plasticity, particularly in the Austin Bluffs area north of Colorado Springs.

2.2.2.2.2.2 Laramie Formation, Fox Hills Sandstone, and Pierre Shale

Laramie Formation, Fox Hills Sandstone, and Pierre Shale formations occur in two broad situations: (1) intermittently exposed in moderately dipping beds east of the mountain front (immediately east of the Frontal Hogback) from Ft. Collins to Denver and (2) with thin soil mantles in gently dipping and near flat lying units in the Louisville area and along Interstate 25 between Colorado Springs and Pueblo.

The Laramie Formation is dominated by thinly bedded shale and siltstone with common hard to friable sandstone interbeds, lesser thin hard conglomerate, and lignitic to sub-bituminous coal beds. The formation is sandier in the lower portion. Most Laramie clays are dominantly kaolinitic with usually low to moderate swell potential; the middle third tends to be montmorillonitic with resulting high swell potential. The sandstones vary from weakly to well cemented.

Foxhills Sandstone units are cross-bedded and quartz sand-dominant. Relatively thin interbeds of claystone/shale, mudstone, and coal occur throughout. The sands are generally weakly cemented and friable; they are important aquifers with medium to high permeability, particularly north of Denver.

The Pierre Shale is a very thick, claystone/shale-dominant formation with numerous thin bentonite beds throughout. The bedrock units are almost always suspect for moderate to very high swell potential, medium to high plasticity, and low slope stability, nearly everywhere they are encountered along the Corridor. Thin sandstone interbeds occur throughout the formation. Significantly thick sandstone members are present in several areas at different stratigraphic positions. Hard limestone masses (butte formers in outcrop) occur in the middle portion to the south. To the south, the middle portion also contains appreciable gypsum content that may affect sulfate-susceptible cement.

2.2.2.2.3 Depth to Bedrock

Depths to the most common bedrock units are highly variable and depend on geologic processes that have occurred in an area and sometimes man's activities in the form of cut/fill operations. There is a large area of near surface bedrock in the Monument Highlands between southern Denver and northern Colorado Springs. Bedrock predominates the near surface geomaterials closer to the Rocky Mountain Front Range at the western edge of the Urban Front Range Corridor. In other areas of the Corridor, bedrock may exist near the surface or could be much deeper beneath alluvial deposits, sometimes in the range of 80 to 100 feet. Generally, however, bedrock is likely to be encountered within the upper 50 feet of geomaterials at most sites. Bedrock is intermittently located within the upper few feet in many areas of the overall Corridor.

An estimated percentage of surficial geomaterials likely to be comprised of bedrock at a sound barrier, sign, or signal project in populated areas along the Corridor is on the order of 10 to 15 percent. Even within the population centers of the Corridor, bedrock is estimated to occur much more frequently than 15 percent of the projects when the total length of typical sound barrier, overhead sign, and traffic signal caisson depths is considered. It is important to note that the upper portion of geomaterials along a caisson provides the greatest resistance to lateral loads,

although this is a function of pier diameter. Overhead sign foundations have the greatest depths because of the loading conditions on this type of structure, with typical depths in the range of 17 to 24 feet according to CDOT standard plans. Bedrock is very often encountered within the upper 25 feet; however, depths to bedrock are highly variable as discussed above.

2.2.2.2.4 Bedrock Hardness

The most common bedrock types in the Corridor, discussed in Section 1.2.2.2.2, are sedimentary deposits that have been heavily overconsolidated by as much as 1,000 feet of overburden that subsequently eroded to the present day terrain. The previous overburden pressure, degree of weathering, and amount of cementation of sandstone or conglomerate, are the key factors that largely determine the hardness of the bedrock. Unconsolidated, undrained shear strengths in the <u>Denver Formation</u> range from 3 ksf to 30 ksf, and shear strengths in the Denver Blue range from 8 ksf to more than 30 ksf (Hepworth & Jubenville, 1981). Standard penetration test results generally range from about 30 to 80 for the non-Denver Blue bedrock, although some highly weathered areas may have SPT values in the teens. Denver Blue bedrock normally has SPT blow counts of at least 80. Denver Blue claystone/sandstone bedrock typically has blow count values in the range of 50/8” to 50/2”, and sometimes this is the first 6 inches of a drive that would normally not be recorded for a SPT. SPT refusal also occurs. Bedrock hardness varies from very low strength to moderate strength according to International Society of Rock Mechanics classification criteria. The weaker bedrock is better described in terms of soil consistency terminology in the range of very stiff to hard and tends to behave similar to heavily overconsolidated clay.

Another CDOT study, “Improvement of the Geotechnical Axial Design Methodology for Colorado’s Drilled Shafts Socketed in Weak Rocks” (July 2003), dealing with axial drilled shaft capacity has yielded some useful data on the bedrock strength of the metro Denver area. As part of this study, Osterberg load cell tests (O-cell), pressure meter testing, and coring with subsequent unconfined compression testing was performed on the weaker brown claystone and the harder, gray “Denver Blue” claystone/sandstone. O-cell tests at two sites with relatively weak bedrock (SPT ranging from about 30 to 60) indicated ultimate caisson end bearing values on the order of 50 ksf, and three O-cell tests in the much harder bedrock indicated ultimate end

bearing values greater than approximately 250 ksf. Pressure meter tests conducted indicated unconfined strengths in the general range of 10 ksf to 20 ksf for the weaker bedrock and 50 ksf to greater than 150 ksf for the harder bedrock. Unconfined compression (UC) tests on the weaker bedrock generally ranged from 5 ksf to 20 ksf. UC tests on the relatively hard bedrock indicated strengths ranging from 50 ksf to 300 ksf; the higher values are from well cemented, clayey sandstone bedrock.

3 CURRENT DESIGN PRACTICE BY THE COLORADO DOT, AASHTO, AND THE OHIO DOT

Lateral load design procedures for drilled shafts used to support sound barrier walls, overhead signs, and traffic signals in Colorado are presented in this chapter. It was found that CDOT engineers and engineering consultants generally do not use the same procedures to design these foundations. CDOT Staff Bridge engineers prefer to use ultimate strength methods, whereas the consultants were found to prefer the p-y method of analysis in the form of the commercially available computer program LPILE, which is an upgraded and more user friendly version of COM624P. CDOT practice has been to design the various types of structures (sound walls, overhead signs, and traffic signals) with different design methodologies; whereas, the consultants apply the p-y method, and sometimes finite element methods, to nearly all laterally loaded structures. Typically, geotechnical design parameters are provided by geotechnical engineers, and structural engineers perform the detailed analyses and designs based on the parameters provided. Consequently, structural engineers usually take the lead role in the design process. Drilled shafts are nearly always designed to bear in the soils that exist (or will exist in the case of fill areas) at the structure location; no special effort is made for the shafts to bear in bedrock or other dense or hard geomaterials.

3.1 Current Sound Barrier Walls Practice in Colorado

3.1.1 Overview

3.1.1.1 CDOT Practice

Several methods have been used by CDOT to design sound barrier wall foundations, and the method selected largely depends on the designer's preference. Structural designs are performed by Staff Bridge engineers based on geotechnical parameters provided by the CDOT geotechnical group. The level of effort invested by CDOT to design foundations for a sound wall project depends on the length of wall that will be built. Larger projects would likely have a site specific design performed, but smaller projects might simply use details from a previous design.

There are no official CDOT Standard Plans for sound barrier walls, although some designs have been used at several sites. A design prepared for a sound wall along I-225 between Parker Road and Iliff Avenue has become somewhat of a pseudo-standard in that most new CDOT sound barrier projects have borrowed this design. The wall varies in height from 14 to 18 feet. The drilled shaft foundations have diameters of 2'6" and are 16'8" deep with typical center to center spacing of 23'4". Closer spacing of drilled shafts at 7'4" occurs at pilaster locations where the wall height is increased for aesthetic reasons. These drilled shafts are also 16'8" long below the bottom of the wall. The design allows for up to 2 feet of unbalanced, unreinforced soil backfill on a side, and can accommodate permanent ground slopes of 3 (horizontal) to 1 (vertical) from the wall down. Up to ten feet of unbalanced, geosynthetically reinforced soil is also allowed.

3.1.1.2 Consultants Practice

In the consulting side, several practicing structural engineers employed by consulting firms in Colorado, ranging from small to very large multi-national companies, were interviewed to gather the information presented in this section. These consultants have performed design services for numerous CDOT projects. Engineering consultants practicing in Colorado overwhelmingly use the computer program LPILE in their analyses of sound barrier wall foundations. Some engineers perform an ultimate strength analysis (such as Broms Method or Sheet Pile Method) in addition to the LPILE analysis, and a small number might perform finite element analyses depending on the magnitude of the sound wall project. Consultants generally perform location specific foundation designs due to the absence of any formal CDOT standard. As with the CDOT design practice, the foundation designs are performed by the structural engineers based on geotechnical parameters provided by geotechnical engineering consultants.

3.1.2 Foundation Design
Methods Used By CDOT

CDOT designers have stated that ultimate strength methods are preferred because a traditional factor of safety can be applied and deflection limits have not been established for deflection (or serviceability) based methods. Design loads are based on the *AASHTO Guide Specifications for Structural Design of Sound Barriers, 1992*, and according to Appendix C of that document, pile (drilled shaft) design is "to be determined by a structural analysis procedure based upon accepted

theories." Procedures used in the past for structural design of sound barrier wall foundations include the sheet piling method presented in the AASHTO guide and Broms Method. A Fortran spreadsheet program called "Caisson" developed internally by CDOT Staff Bridge has also been used. The program is based on Davidson's work related to subgrade reaction theory.

Deflections are calculated using LPILE Version 1, COM624P, or procedures in NAVFAC documents, although no limiting deflections have been established. It appears that ¼ inch of deflection at the ground line is considered to be a non-issue, and deflections of ½ inch have been considered acceptable.

Methods Used By CDOT Consultants

Many consulting engineers have been using COM624P and LPILE for more than a decade. The consultants concur with CDOT engineers that there are no well established deflection limits for drilled shafts; however, each has established their own design criteria. Discussions of the LPILE program, ultimate strength analysis, and finite element methods are presented.

Drilled shafts for sound walls are typically at least 18 inches in diameter, but are more likely to be in the 24 to 30 inch range in diameter. Foundation depths vary and are dependent on the spacing of the shafts. Typical sound wall foundations may be 10 to 15 feet deep and spaced at 15 to 20 feet intervals. One diameter size and one drilled shaft length are typically selected for an entire project, although differing embedment lengths may be provided for large projects with a sufficient amount of geotechnical data to adequately identify variations of the subsurface materials.

3.1.2.1 Loads

3.1.2.1.1 Loading Criteria Used by CDOT Engineers

CDOT structural engineers use the loads provided in Section 2 of the AASHTO Guide Specifications for Structural Design of Sound Barriers(1992), regardless of which method is used to design the foundation drilled shafts. The AASHTO document states that sound barrier shall be designed for wind speeds based on a 50-year mean recurrence interval. For Colorado, this corresponds to a wind speed of 80 mph for most of the state, but in some areas (near the Front Range and in Boulder County) wind speeds up to 100 mph are used by CDOT.

Wind exposure C has typically been used by CDOT for sound barrier design. Exposure C is prescribed by AASHTO for open terrain with scattered obstructions and for sound barriers located on bridge structures, retaining walls, or traffic barriers. The corresponding design pressure for the wall face is usually 27 psf, but may range from 20 psf to 40 psf depending on the wall height and geographic location. The calculation to determine the wind pressure includes a gust factor consisting of a 30 percent increase in the wind velocity.

In 2000, CDOT adopted the Load and Resistance Factor Design (LRFD) method for all structures including sound barrier walls. Working Stress Design (WSD) and Load Factor Design (LFD) were used in the past. The design is typically controlled by wind loading because the vertical loads are light and seismic acceleration coefficients are relatively low.

3.1.2.1.2 Loading Criteria Used by Consulting Engineers

Consulting engineers perform their designs based on the same AASHTO loading criteria that CDOT engineers use. The reader should refer to Section 3.1.2 for the loading criteria.

A main difference between CDOT and consultant design loads appears to exist with the selection of an appropriate wind exposure level. Consultants are more apt to use exposure B classifications which are less severe than exposure C that CDOT has typically used. Exposure B1 is for urban and suburban areas having numerous closely spaced buildings (such as single family homes) located a distance extending at least 1500 feet in the prevailing upwind direction. Exposure B2 is defined as more open terrain than exposure B1 and not meeting the requirements of exposure B1. It appears that exposure B2 is more likely to be selected for sound barrier design by consultants than exposure B1. Corresponding wind pressures are more likely to be around 20 psf for exposure B2, but will depend on the wind velocity and wall height. The typical exposure C wind pressure is 27 psf, but may range from 20 to 40 psf.

3.1.2.2 Design Methods

3.1.2.2.1 Design Methods Used by CDOT Engineers

3.1.2.2.1.1 Sheet Pile Method

The sheet piling method is included in Appendix C of the AASHTO Guide Specifications for Structural Design of Sound Barriers (1992), and is based on U.S.S. Steel Sheet Pile Design analysis. Performing a design using this method involves a trial and error procedure to find an appropriate shaft embedment length that results in moment equilibrium of the system. Charts are used to determine active and passive earth pressure coefficients depending on the friction angle of the soil and slope geometry. Overturning is resisted by the calculated allowable net horizontal ultimate lateral soil pressure which is equal to the passive pressure on one side of a pile minus the active pressure on the other side. The upper six inches of supporting soil is neglected in the analysis.

3.1.2.2.1.2 Broms Method

Broms Method has been used by CDOT engineers to design sound barrier foundations. This method of lateral analysis and design for drilled shafts is discussed in Appendix B. Broms made simplifying assumptions about the soil reactions along the length of a pile to estimate the pile's lateral response. To perform a design using the Broms Method, soils are classified as either cohesive or cohesionless. Consequently, a cohesion value for cohesive soils is necessary and a friction angle is required for cohesionless soils. Appropriate coefficients of lateral subgrade reaction are also needed to determine whether the piles behave as short (rigid) or long (flexible) piles. Overall factors of safety (based on load factors divided by resistance factors) in the range of 2 to 3 are typically applied by CDOT to the design procedure.

3.1.2.2.1.3 Caisson Program

The "Caisson" program was used to design the I-225 sound barrier foundations discussed in Section 3.1.1.1. The program is based on the theory developed by Davidson, et al (1976), assuming that full plastic strength of the soil is developed for calculating the ultimate capacity. The soil strength is based on the Equation 9-7 in "Basic Soils Engineering" by B.K. Hough, which was generated for footing foundation.

The program can only apply to homogeneous cohesive or cohesionless soil. The program, however, cannot be run correctly for cohesive soil conditions. The method cannot provide deflection information.

3.1.2.2.1.4 LPILE/COM624P

As previously mentioned, CDOT has used LPILE and/or COM624P computer programs to check the deflections of sound barrier foundations designed using one of the above ultimate strength methods. CDOT uses LPILE version 1.0 or COM624P. Specific parameters required for the analysis are discussed in the Section 3.1.2.3.1.2 for geotechnical parameters and a more detailed description of more recent versions of the LPILE software are discussed in Section 3.1.2.2.2 under the consultant design practices.

3.1.2.2.2 Design Methods Used by Colorado Consulting Engineers

3.1.2.2.2.1 LPILE Computer Program

Nearly all of the engineering consultants interviewed were using a recent version of the LPILE program, and most were using the latest version, LPILE Plus 4.0. One company prefers a finite element approach, but occasionally uses COM624P. Ensoft, Inc distributes the LPILE software. LPILE Plus 4.0 can be used to perform the structural design of the drilled shaft, but many of the consultants use other software packages for this task. The program is capable of analyzing scenarios with a number of boundary conditions, loading combinations, sloping ground surface, layered soils, user input p-y curves, and can generate extensive tabular and graphical outputs. A particularly useful output graph shows pile length vs. pile-head deflection. Emphasis in this report is on the soil-structure interaction capabilities of the program.

The program models the soil-structure interaction of laterally loaded piles and drilled shafts using p-y curves generated by the computer program that are based on published recommendations for various types of soils. Soil types that can be analyzed by the program are called 1) Soft Clay, 2) Stiff Clay with Free Water, 3) Stiff Clay without Free Water, 4) Sand, 5) Linear Interpolation (user specified p-y curve), 6) Vuggy Limestone (strong rock), 7) silt (with cohesion and internal friction), 8) API Sand, and 9) Weak Rock. Soil types 1, 3, and 4 are most likely to be used in Colorado for sound barrier walls. Soil Type 2, Stiff Clay with Free Water, is

intended to be used where stiff clay is the top soil layer with water existing above the ground line (e.g. lakes, ponds, rivers), so its use may not be appropriate for sound wall foundations in Colorado. However, it appears that some engineers may have used Soil Type 2 on occasion to model clay soils at depth below the ground water table, even though this would not be appropriate. Sedimentary bedrock most likely to be encountered in Colorado at a typical project is modeled as hard clay using Soil Type 3. As mentioned elsewhere, soft soils of Soil Type 1 are fairly uncommon, but they may exist at a site. Geotechnical parameters required as input to the program are discussed in Section 3.1.2.3.2.2.

Deflection limits established by a designer are somewhat arbitrary and are based on the individual's engineering judgment. Most designers cited one inch of deflection at the ground line under service loading conditions as a maximum, and all were comfortable with ½ inch of deflection at the shaft top. Others stated that deflections greater than one inch may be acceptable in some situations. Deflection at the bottom of the shaft is normally checked to ensure that it is a very low number nearly equal to zero.

A deflection limit at the top of sound barrier walls, not the top of caisson, equal to the wall height divided by 120 (or 0.833% of the height) was established for the T-REX project by the design build contractor team. (T-REX is a $1.7 billion highway and LRT project currently being designed and constructed for 19 miles of I-25 and I-225 in metro-Denver). This criterion was selected based on aesthetic considerations, not structural concerns. Ground line deflections are typically less than one inch using this criterion, but occasionally are slightly greater than one inch. Deflection estimates for the T-REX project often include a load caused by retained soil.

A plot of pile head displacement vs. pile length is easily generated by the recent versions of the LPILE program to identify a shaft length at which greater embedment length results in very small increases in deflection at the shaft head. This procedure is employed by nearly all of the consulting engineers in their analysis and design.

Sensitivity studies are sometimes performed to gain additional confidence in the design by varying the geotechnical parameters. Some designers have applied a global factor of safety to

the design load to evaluate the deflections. Changing the factor applied to the load can create a curve of the shaft deflection vs. applied lateral load at the ground line. If the service load plots at or close to a point on the curve where relatively small increases in the load result in large increases in deflection, then the foundation design can be modified until acceptable results are achieved.

3.1.2.2.2.2 Ultimate Strength Methods

As discussed above, most engineering consultants use the LPILE computer program to design sound barrier wall foundations. Some engineers, however, also check minimum caisson embedment lengths using the sheet pile method or other moment equilibrium calculations. One engineer stated that he has used Broms method for ultimate capacity analysis.

3.1.2.2.2.3 Finite Element Methods

Few consulting engineers routinely use finite element methods to analyze laterally loaded foundations and sometimes use the method to analyze sound wall foundations. It appears that finite element analysis for sound barrier foundations is performed in a small minority of cases. One large engineering consulting firm is very comfortable using the Florida Pier program for larger structures, but they will very likely begin using the newer version of the program called FB Pier for routine design of all types of structures. Reportedly, FB Pier is much more user friendly, simpler, and quicker than the previous version. Companies using finite element method computer programs also have the capability of using LPILE or COM624P.

3.1.2.3 Geotechnical Investigations

3.1.2.3.1 CDOT Geotechnical Investigations

3.1.2.3.1.1 Field Investigation and Laboratory Testing

CDOT uses the *AASHTO Standard Specification for Highway Bridges, 1996 with Interims 1997, 1998, and 1999*. Section 5.3.3 of the AASHTO standards recommends that wall borings be spaced at intervals of 100 feet, although the interval may be increased or decreased depending on geologic conditions. Review of several CDOT engineering geology sheets for sound barrier wall projects indicated that CDOT's practice is to space borings at intervals of 100 ft. to 300 ft. with the most common interval being about 200 ft. along the length of the wall. This coincides with

the information that the CDOT Geology group provided early in the study. For longer walls, the spacing of geotechnical bore holes is often increased. In mountainous terrain or other potentially highly variable geologic regions, borings are sometimes made more frequently than the typical 200 feet intervals. Borehole depths are typically about two times the wall height, which is consistent with the AASHTO standards. If unusual conditions exist, such as soft soils, boring depths may be lengthened.

Most of CDOT's borings for geotechnical investigations are advanced by either solid or hollow stem auger drilling. CDOT also has capability to core bedrock materials or use a continuous sampling system for soils; however, these methods are rarely used for sound barrier wall projects. The typical field sampling and testing procedure used is the SPT method. CDOT has performed penetration testing using a nominal 2-inch inside diameter California spoon sampler that is commonly used by local geotechnical consultants, although this procedure is rarely used by CDOT for sound barrier investigations. CDOT's drill rigs have automatic hammers via a chain mechanism that ensures the appropriate drop height for each blow. The split spoon sampler is used to obtain samples at approximately 5 feet intervals.

Laboratory testing includes soil index properties, gradations and Atterberg Limits. Occasionally, unconfined compression (UC) tests may be performed on cohesive soil samples as needs arise; however, it would be rare for UC testing to be performed specifically for sound barrier projects. Any UC tests would be performed on samples obtained with the continuous sampling system or Shelby tubes pushed into soft soils.

3.1.2.3.1.2 Geotechnical Design Parameters
Specific recommendations are provided depending on the Staff Bridge designer's method(s) of analysis. Recommendations may include the coefficient of lateral subgrade reaction, design values for cohesion or friction angle, unit weight, and/or specific LPILE input parameters (e.g. ε_{50}, soil modulus). Lateral design parameters are provided for the entire length of shaft, and there may or may not be a reduction or elimination of capacity in the upper several feet of the shaft. One geotechnical memorandum that was reviewed recommended neglecting the upper 5 feet of clay soils for lateral load resistance. There are no rigid procedures established by CDOT

for determining the geotechnical parameters; rather, geotechnical engineers use their experience and engineering judgment to select appropriate design values. SPT test results are the primary parameter used by CDOT Geotechnical Engineers to provide lateral load geotechnical design criteria.

3.1.2.3.1.2.1 Friction Angle and Cohesion

Empirical correlations between SPT values and friction angle of cohesionless soils or unconfined compressive strength of cohesive soils are used. There are many references that the geotechnical engineer might use for this purpose including various FHWA publications, textbooks, or technical articles. It is necessary for the engineer to make a determination as to whether a soil will be treated as cohesive or cohesionless.

Angle of internal friction (ϕ) correlations with SPT results such as those proposed by Peck, Hanson & Thornburn, Meyerhof, or Sowers are used for cohesionless soils. Relationships proposed by others are generally very similar to these values. Corrections to the N-value for overburden pressure are usually not performed. Table 3.1 provides typical values.

Table 3.1 SPT Correlations for Cohesionless Soils

N per ft.	Density Description	Phi angle		
		Peck, Hanson &Thornburn	Meyerhof	Sowers
0-4	Very loose	<28	<30	26-30
4-10	Loose	28-30	30-35	28-33
10-30	Medium	30-36	35-40	30-38
30-50	Dense	36-41	40-45	35-44
>50	Very Dense	>41	>45	>42

CDOT geotechnical engineers generally use the relationships between unconfined compressive strength and SPT of cohesive soils shown in Table 3.2.

Table 3.2 SPT Correlations for Cohesive Soils

N per ft.	UC (TSF)	Consistency
0-2	0.0-0.25	Very Soft
2-4	0.25-0.5	Soft
4-8	0.5-1.0	Medium
8-16	1.0-2.0	Stiff
16-30	2.0-4.0	Very Stiff
>30	>4.0	Hard

3.1.2.3.1.2.2 Coefficient of Lateral Subgrade Reaction

The coefficient of lateral subgrade reaction, k_h, is used in a Broms Method of analysis to determine if a pile or drilled shaft is short or long. Values for this parameter have typically been based on procedures developed at the former geotechnical engineering consulting firm of Chen and Associates. The parameters are summarized in an unpublished, undated draft document by F. H. Chen that seems to be fairly well circulated in the local geotechnical engineering community. Other references such as Terzaghi's published data are sometimes used in the engineer's assessment of this parameter. The coefficients of lateral subgrade reaction of cohesive soils are tabulated in Table 3.3. For cohesive soils k_h is constant with depth, but k_h increases linearly for cohesionless soils. The constant of horizontal subgrade reaction, n_h, is used for cohesionless soils to represent the increase of k_h with depth. Table 3.4 provides the constants of horizontal subgrade reaction for cohesionless soils. Note that the values presented are for a one foot diameter pier and must be corrected by dividing by the diameter for other size shafts. Also note that Chen did not differentiate between dry or moist cohesionless soils and submerged soils. The geotechnical engineer must exercise judgment.

Table 3.3 Coefficients of Lateral Subgrade Reaction of Cohesive Soils

Cohesive Soil Consistency	k_h (tcf)	
	Terzaghi	Chen
Soft		25
Medium Stiff		50
Stiff	75	100
Very Stiff (Medium Hard)	150	200
Hard	300	400

Table 3.4 Constant of Horizontal Subgrade Reaction of Cohesionless Soils

Cohesionless Soil Density	n_h (tcf)		
	Terzaghi		Chen
	Moist	Submerged	
Very Loose			7
Loose	7	4	21
Medium	21	14	56
Dense	56	34	74
Very Dense			92

As discussed in Chapter 2, there is a fair chance that bedrock may be encountered within the typical drilled shaft length for sound barrier foundations approximately 16 feet long. Bedrock may be significantly harder than as described in the above tables. Reportedly, the maximum value of k_h given by the CDOT geotechnical group for hard to very hard bedrock is 500 tcf. Claystone and sandstone bedrock are typically treated as cohesive soils with k_h remaining constant with depth.

3.1.2.3.1.3 LPILE/COM624P Parameters

The CDOT geotechnical engineers provide LPILE parameters when the structural engineer requests them. Geotechnical parameters include effective total unit weight, soil modulus

constant (k), undrained shear strength (c_u), internal friction angle (φ), and the strain at 50% of the maximum stress (ε_{50}).

Recommendations for c_u and φ are based on the previously discussed correlations relating the parameters to SPT N-values. Unit weight values are also based on SPT results and the engineer's experience. The soil modulus parameter, k, has sometimes been assumed to be the same as the coefficient of lateral subgrade reaction, k_h, discussed in the previous section; the values presented by Chen are typically provided. It must be noted that the soil modulus parameter required as an input to LPILE is different from the coefficient of lateral subgrade reaction concept used by Terzaghi, Broms, and others. Values for ε_{50} are obtained from the LPILE User's Manual based on the average undrained shear strength which is taken to be equal to half of the unconfined compressive strength obtained through correlation with the SPT.

3.1.2.3.1.4 Ground Water

Any ground water that may exist at a site is not specifically factored into the geotechnical recommendations. Friction angles or cohesion values provided to the structural designer are in large part based on the SPT values for a given soil layer and the SPTs are generally assumed to reflect the effects of ground water conditions. Ultimate strength design parameters are therefore considered not greatly affected by the presence of ground water. LPILE parameters and analyses, however, are dependent on the location of the ground water table. Logs of exploratory borings are provided to the structural engineer and they apply the ground water condition when appropriate. Typically, there is no conservative assumption made that the ground water level will increase in the future. In summary, it appears that ground water levels are not a major design factor for the CDOT design procedures.

3.1.2.3.2 Consultant Geotechnical Investigations

Geotechnical engineering consultants nearly always work as subconsultants to the transportation design firm and structural engineers perform the actual foundation design.

3.1.2.3.2.1 Field Investigation and Laboratory Testing

Geotechnical engineering consultants generally space borings at intervals similar to those used by CDOT. The most common interval is about 250 ft. along the length of the wall, but intervals as great as 500 ft. have been used. Borings are rarely spaced at intervals less than 200 feet, although boring spacing of 100 feet intervals has been used. The actual spacing may depend on the anticipated geologic conditions, the proximity of other structure borings, and the needs of the prime consultant. Borehole depths are typically about 20 feet, but boring depths may be lengthened if expansive or soft soils exit. If high swelling soils are suspected, drilling depths on the order of 30 feet are likely. Borings are also lengthened to extend through any proposed cut areas that would be removed by grading operations.

Bore holes for consultant geotechnical investigations are advanced by either solid or hollow stem auger drilling. Some drill rigs used by consultants have automatic hammers, but manual hammers are frequently used as well. Samples are taken at approximately 5 feet intervals.

The typical field sampling and testing procedure is by penetration testing using a nominal 2-inch inside diameter California spoon sampler. The procedure is very similar to the SPT procedure (ASTM D1586) except that the blow counts for the different diameter sampler are recorded as the first 12 inches of the drive. The California sampler is typically seated into the hole with a few light blows of the hammer prior to recording the blow counts. Penetration testing using the nominal 1-3/8 inch inside diameter standard split spoon is often used when cohesionless granular soils are encountered. It is local practice to consider the blow counts achieved with both methods to be equivalent. A small number of geotechnical consultants, believed to consist of two national firms, use a Dames & Moore ring sampler having an internal diameter of 2.42 inches and an outside diameter of 3.25 inches. Because the blow counts achieved with this sampler are much greater than a standard spoon size, the consultants periodically use a standard spoon to obtain SPT data. Push tube samples are regularly obtained in overburden materials by one company, but this type of sampling is not considered to be standard practice for the area. Shelby tubes may be used if soft soils are encountered, but they are not typically considered for use.

The predominant local practice of using California samplers was developed primarily to obtain samples suitable for swell testing. California liner samples are also used to obtain relatively undisturbed (according to local practice) samples suitable for natural unit weight and unconfined compression testing. Brass liners 4 inches long fit snugly inside the barrel, and a typical California barrel can accommodate four liners for a total of 16 inches. Normally, only the liner near the tip of the barrel is saved, although two liners are saved if a material transition is noted. A minority of consultants routinely save two liners nearest the tip of the barrel.

Laboratory testing typically includes natural moisture content and unit weight determinations, gradations, Atterberg Limits, swell tests, and unconfined compression (UC) tests on cohesive soil samples. Unit weight, swell testing, and UC testing are conducted on California samples extruded from the brass liners. The Dames & Moore ring sampler can also provide samples for these tests.

3.1.2.3.2.2 Geotechnical Design Parameters

Specific geotechnical recommendations are provided to the structural engineer depending on his or her method(s) of analysis. Recommendations may include the coefficient of lateral subgrade reaction, design values for cohesion or friction angle, unit weight, and/or specific LPILE input parameters (e.g. ε_{50}, soil modulus). Generally, soil resistance is neglected in the upper three feet of shafts for sound barrier wall foundations to account for weakening of soils due to frost action or moisture increases. Consulting geotechnical engineers, like their CDOT counterparts, use their experience and engineering judgment to select appropriate geotechnical design parameters. Like CDOT engineers, consultants rely heavily upon SPT results, but laboratory testing plays a more prominent role in consultant practice.

3.1.2.3.2.2.1 Friction Angle and Cohesion

Empirical correlations between SPT values and friction angle of cohesionless soils or unconfined compressive strength of cohesive soils discussed in Section 3.1.2.3.1.2 for the CDOT practice are also used by consultants and are not repeated here. Many consultants use UC test results to aid in evaluating an appropriate cohesion value, although cohesion may be estimated solely based on

SPT. Many geotechnical engineers evaluate all of the data available and provide design parameters based on both SPT data and laboratory data.

It is most common to use half of the laboratory UC strength for cohesion, and this value for cohesion may be provided as a design parameter. Less frequently, the geotechnical engineer may provide somewhat lower values than half of the peak UC strength because some of the observed peak strength may be due to a frictional component of the specimen and to account for possible loss of strength if the soils become wetted. It is recognized that laboratory UC test results can be heavily influenced by the moisture content of the sample.

3.1.2.3.2.2.2 Coefficient of Lateral Subgrade Reaction

It appears that geotechnical consultants also widely use values for the coefficient of lateral subgrade reaction, k_h, based on either the Terzaghi typical values or the historic Chen and Associates parameters. This parameter is discussed in detail in Section 3.1.2.3.1.2 and is not repeated since the CDOT and consulting geotechnical engineers appear to be providing similar values. This value may be provided, with some adjustment for geometry, to structural engineers that will perform finite element analyses.

3.1.2.3.2.3 LPILE Parameters

LPILE parameters are provided by geotechnical engineers when the structural engineer requests them. Geotechnical parameters include effective total unit weight, soil modulus constant (k), undrained shear strength (c_u), internal friction angle (φ), and the strain at 50% of the maximum stress (ε_{50}). Values of each parameter may be provided for a particular soil type or values may be provided for depth intervals below the ground surface if conditions are uniform. It is normally left to the structural engineer to identify the locations with the most critical subsurface conditions based on the boring logs and geotechnical parameters provided.

Recommendations for c_u and φ are based on the previously discussed correlations relating the parameters to SPT N-values or unconfined compressive strength. Unit weight values are likely to be based on results of laboratory testing on California liner samples, SPT results, and the

engineer's experience. Laboratory results are likely to be weighted more heavily than SPT data in the evaluation to determine the unit weight.

The soil modulus constant, k, is provided in accordance with the LPILE User's Manual based on estimates of the undrained shear strength which might be based on laboratory UC tests and SPT data. Like in CDOT practice, the k parameter has sometimes been assumed to be the same as k_h discussed previously, although it appears that most geotechnical engineering consultants recognize the difference between the parameters.

The LPILE User's Manual is used along with the results of UC tests and SPT data to establish appropriate values for ε_{50}. There seem to be two schools of thought on this subject; one school relies on the laboratory data, and the other bases the recommendation for ε_{50} on the recommendations in the user's manual. Strains observed in samples of Colorado geomaterials obtained with the California sampler are often higher than those recommended in the software documentation, particularly for the harder clays and bedrock.

3.1.2.3.2.4 Ground Water

Ground water that may exist at a site is not specifically factored into the geotechnical recommendations that will be used for an ultimate strength analysis. Values for cohesion and friction angle are not typically adjusted to reflect any ground water condition. The coefficient of lateral subgrade reaction may vary for sands as presented in section 3.1.2.3.1.2.

LPILE parameters and analyses, however, are dependent on the location of the ground water table. Geotechnical recommendations for effective unit weight or submerged soil modulus parameter k for sands are provided if ground water exists at a site. Some geotechnical engineers may recommend that the subsurface soils below the water table be modeled as Soil Type 2, stiff clay with water, although this would only be appropriate if permanent standing water exists above the ground line. Typically, there is no conservative assumption made that the ground water level will increase in the future.

3.2   Overhead Signs Practice in Colorado

3.2.1 CDOT Design Procedure Using Standard Plans

CDOT engineers use standard drawings based on AASHTO documents for routine design of overhead sign structures and their foundations. Standard Plan No. S-614-50, Sheets 1 through 14 provide structural details, as well as foundation dimensions and details. The standard plans are available for download on CDOT's web site. The drawings provide a procedure to determine the required sign post diameter based on the proposed wind loading and geometry of the structure.

Foundation designs shown in the Standard Plans were developed using the Broms Method. Several documents are referenced as design information on Sheet 1 of drawing S-614-50 including the following:

> "Standard Specification for Structural Supports for Highway Signs, Luminaires, and Traffic Signals" (1994 AASHTO), (Static Signs Only).

> "Standard Specification for Structural Supports for Highway Signs, Luminaries, and Traffic Signals" (2001 AASHTO), (Dynamic Signs Only).

> "Fatigue-Resistant Design of Cantilevered Signal, Sign, and Light Supports" (NCHRP Report 412, 1998) (Static Signs Only).

> Subsection 17.4, Signs, in the Staff Bridge Branch Design Manual.

Notes on the standard plans indicate that an 80 mph wind speed is the standard design speed for Colorado, with a few exceptions. A 90 mph wind design speed is to be used for sign locations within 4 miles of the base of the foothills along the front range of the eastern slope, and a 100 mph wind speed is used in Boulder County.

Sign geometry inputs required to use the design tables include the sign panel height and length, height above the base plate to the center of the sign and mast arm, and span distance. For bridge sign structures, the design is based on a sign height of 15 feet, but sign heights of 10, 12, and 14

feet may be selected for cantilever signs. The total area of all signs attached to a sign bridge and the span length are used to find the pipe post diameter. Pipe outside diameters range between 12.75 inches and 24 inches. Infrequently, proposed signage dimensions exceed the limits of the standard, and specific designs must be performed.

Drilled shaft foundation dimensions tabulated on Sheet No. 14 of Standard Plan S-614-50 are selected based on the outside pipe diameter of the sign post. Diameters range from 36 to 48 inches, and caisson depths vary from 13 to 24 feet (29 feet for dynamic cantilever sign). Diameters are dictated by the required anchor bolt patterns. Vertical reinforcement of the caissons consists of 13 to 24 #8 bars.

Typically, a geotechnical investigation is not performed by CDOT for design of overhead signs. The design is based on a set of soil parameters as follows (CDOT Standard Plan No. S-614-50):

Soil unit weight = 100 pcf

Soil cohesion = 500 psf

Soil friction angle = 28 degrees

When the following soil conditions (listed in the Standard drawings) are encountered, engineers need to be contacted for further investigation.

(a) Soils have high organic content or consists of saturated silt and clay
(b) The site won't support the drilling rig
(c) Foundation soils are not homogeneous
(d) Firm bedrock is encountered.

3.2.2 Consultant Design Practice

Consultants also use CDOT Standard Plan S-614-50 to design foundations for overhead signs. Many consultants consider the standard drawings to be sufficiently conservative to forego drilling exploratory borings at the sign foundation locations. However, some consultant designers will perform geotechnical investigations at specific sign locations if it is not near other

structure borings. If a proposed sign foundation is more than about 100 feet away from another boring, a soil boring might be made to confirm that the geotechnical conditions meet or exceed the minimum strength characteristics noted on the standard plans as discussed in the previous section. Caisson dimensions shown on the standard drawings are typically used even if higher strength soils are identified.

Design for signs larger than those included in the design standard will typically be done by consultants using the LPILE program, finite element methods, and/or other procedures discussed in Section 3.1 for sound barriers. LPILE seems to be the most prevalent design method with various finite element software programs being the second most common choice.

Geotechnical design parameters are determined in the same manner as for sound barrier walls discussed in Section 3.1 and are not repeated here. Geotechnical consultants will typically recommend that the upper 3 to 5 feet of soil be neglected in the structural analysis.

3.3   Traffic Signals Practice in Colorado

3.3.1 AASHTO Design Criteria

There are no definite design criteria for foundation in *AASHTO Standard Specifications for Structural Supports for Highway Signs, Luminaries and Traffic Signals (4th Edition, 2001)*. Mostly, the design of drilled shafts shall be based on *Standard Specifications for Highway Bridges*. In *AASHTO LRFD Bridge Design Specifications*, the allowable horizontal movement at drilled shaft head is specified as 1.5 inch for bridge foundations and the drilled shaft head should be fixed into a foundation cap.

The design loads have been described in chapter 2 of the *AASHTO Standard Specifications for Structural Supports for Highway Signs, Luminaries and Traffic Signals (4th Edition, 2001)*. The AASHTO standard specifications also suggest the use of Broms method for the design of drilled shaft under lateral loads.

3.3.2 CDOT Design Practice

CDOT Standard Plan Nos. S-614-40 (7 sheets) and S-614-40A (5 sheets – Alternate Design) are used for the routine installation of traffic signal structures and their foundations. Structural details, as well as foundation dimensions and details are provided in the standard plans available for download on CDOT's web site. The drawings prescribe caisson dimensions based on the signal mast arm length.

Foundation dimensions shown in the Standard Plans were developed based on AASHTO "Standard Specification for Structural Supports for Highway Signs, Luminaires, and Traffic Signals" (4th Edition, 2001). A design wind velocity of 100 mph and one 12 ft. lane for truck induced gust loading were used for the design.

Design parameters appear on the CDOT standard drawings. Overturning analyses were performed based on Broms procedure as discussed in the AASHTO code. Torsion was also analyzed using a sliding wedge theory for granular soils and cohesive resistance for clayey soils.

Drilled shaft foundation dimensions are shown on Sheet No. 6 of Standard Plan S-614-40. Caisson diameters are dictated by the anchor bolt pattern and range from 36 to 54 inches for mast arm lengths of 30 to 75 feet. Required caisson depths vary from 12 to 20 feet. Vertical reinforcement of the caissons consists of 11 to 23 #9 bars. For the alternate traffic signal installation, foundation details are shown on Sheet No. 4 of Standard Plan S-614-40A. 36-inch diameter caissons are required, and they are 14 feet long for cohesionless soils and 18 feet long for cohesive soils.

Geotechnical investigations are rarely, if ever, performed by CDOT for design of traffic signals. The design is based on a set of soil parameters as follows (CDOT Standard Plan No. S-614-40):

> Soil unit weight = 110 pcf
> Soil cohesion = 750 psf
> Soil friction angle = 30 degrees

Safety factors used by CDOT for flexure and torsion design are:

Flexure Factor of Safety (FS) = 3.0

Torsion FS: FS = 1.5 (Dwg. S-614-40)

FS = 1.25 (Dwg. S-614-40A)

The low safety factors for torsion were chosen by CDOT to prevent torsion from needlessly controlling drilled shaft depths based on field observations indicating that the vast majority of traffic signals performed well. The very few unsuccessful foundation installations were due to installing signal foundations in saturated clay soils with high ground water tables.

When the following soil conditions (listed in the Standard drawings) are encountered, engineers need to be contacted for further investigation.

a) Signals will not be installed within the roadway prism
b) Soils have high organic content or consists of saturated silt and clay
c) The site won't support the drilling rig
d) Foundation soils are not homogeneous
e) Firm bedrock is encountered

3.3.3 Consultant Design Practice

Consultants also use the CDOT standard drawings for traffic signals. We are not aware of any situations where site specific designs or geotechnical investigations were conducted for traffic signals on CDOT projects. Site specific investigations for some cities and counties have been performed by consultants, and the procedures discussed in Section 3.1 were used for design.

3.4 AASHTO Specification

The AASHTO and Ohio DOT design criteria of drilled shaft for supporting sound barrier walls, overhead signs, and traffic signals are presented in this chapter. Suggested design criteria based

on this review are then summarized. Specifically, the analysis methods, loads specifications, tolerable deflection at the drilled shaft top, and factor of safety will be covered.

The AASHTO loads specifications for sound barrier walls were reviewed in section 3.1.2. The design pressure on wall face could range from 20 psf to 40 psf, with a typical design value of 27 psf. The sound barrier wall height in Colorado typically varies from 14 to 18 feet, while the typical spacing of drilled shaft ranges from 7'4'' to 23'4''. Therefore, the force applied to the drilled shaft head can be approximated from the multiplication of wind pressure and the tributary wall area. The maximum, typical, and minimum lateral loads applied to the drilled shaft head are therefore 16.8 kips, 11.3 kips, and 2 kips, respectively. The moment due to each lateral load is the load multiplied by half of the wall height.

The design method for lateral response of drilled shaft specified in the *AASHTO Guide Specifications for Structural Design of Sound Barriers* (2002) is sheet piling method taken from the U.S.S. Steel Sheet Piling Design Manual. The sheet piling method is one of several ultimate strength methods. The details of the sheet piling method are reviewed in Section 3.1.2.2.1.1 and Appendix B.

As to the tolerable deflection of drilled shaft and Factor of Safety, there are no specifications in *AASHTO Guide Specifications for Structural Design of Sound Barriers* (1989, 2002 interim). However, in the *AASHTO LRFD Bridge Design Specifications (2ⁿᵈ Edition, 1998 with 2003 interim)*, the allowable horizontal movement at drilled shaft head is specified as 1.5 inch for bridge foundations.

3.5 ODOT Design Practice

In Ohio DOT practice, the standard foundation for sound barrier walls is a single 30 inch diameter drilled shaft. The design load is calculated based on an 80 mph wind velocity producing a uniform pressure of 25 psf over the tributary area of the wall.

The ODOT design criterion is based on the tolerable deflection at the top of the wall to be 1% of the wall height. The computer program COM624P is usually used as the design method since the design criterion is based on the serviceability, i.e., tolerable wall deflection.

Liang (1997) developed design charts for both 1% and 1.5% wall height as allowable deflections at wall top. Table 3.5 to Table 3.8 are reproduced in this report for both cohesive soil and cohesionless soil deposits. It should be noted that the design tables were based on correlations between COM624P input parameters and SPT N values. The SPT blow count was assumed to be corresponding to 60% energy efficiency, hence the subscript 60 shown in the tables. The blow count number should be adjusted for overburden pressure to standard practice of 1 tsf. Table 3.9 and Table 3.10 provide the updated correlations based on a more extensive sensitivity study on the enhanced lateral load test database (Liang 2002).

Table 3.5 Design Chart for Cohesive Soil (Allowable Deflection 1.0% of Wall Height)

	Post Spacing (feet)				Group	N_{60}	0-2	2-4	4-8	8-16	16-32
						S_u (psi)	0-1.74	1.74-3.47	3.47-6.94	6.94-13.89	13.89-27.78
	8 and under	Over 8 Thru 12	Over 12 Thru 16	Over 16 Thru 24		ε_{50}	>0.02	0.02	0.01	0.007	0.005
						k_s (pci)	<30	30	100	300	1000
						γ_{sat} (pcf)	100-120	110-130	110-130	120-135	130-145
B A R R I E R	12 and less	10 and less	8 and less	6 and less	I	Level	14.0	13.5	7.5	5.5	4.0
						5:1	14.5	14.5	8.0	5.5	4.0
						4:1	15.0	14.5	8.0	5.5	4.0
						3:1	15.5	15.5	8.0	6.0	4.0
						2:1	16.0	16.0	8.5	6.0	4.0
	Greater than 12 thru 16	Greater than 10 thru 14	Greater than 8 thru 12	Greater than 6 thru 10	II	Level	19.5	18.0	10.0	8.0	5.5
						5:1	20.0	19.5	10.5	8.0	5.5
H E I G H T						4:1	20.5	20.0	11.0	8.0	5.5
						3:1	21.0	21.0	11.0	8.5	5.5
						2:1	22.0	21.5	11.5	8.5	5.5
	Greater than 16 thru 20	Greater than 14 thru 20	Greater than 12 thru 16	Greater than 10 thru 14	III	Level	23.0	23.0	14.0	10.0	7.0
						5:1	25.0	25.0	15.5	10.0	7.0
						4:1	25.0	25.0	15.5	11.0	7.5
						3:1	26.0	26.5	16.0	11.5	7.5
(FT)						2:1	27.0	26.5	17.0	11.5	7.5
			Greater than 16 thru 20	Greater than 14 thru 20	IV	Level	*	*	21.0	13.5	9.0
						5:1	*	*	24.0	14.5	9.0
						4:1	*	*	28.0	14.5	9.5
						3:1	*	*	29.0	15.0	9.5
						2:1	*	*	*	15.0	10.0

Table 3.6 Design Chart for Cohesive Soil (Allowable Deflection 1.5% of Wall Height)

Post Spacing (feet)				Group	N_{60}	0-2	2-4	4-8	8-16	16-32
					S_u (psi)	0-1.74	1.74-3.47	3.47-6.94	6.94-13.89	13.89-27.78
8 and under	Over 8 Thru 12	Over 12 Thru 16	Over 16 Thru 24		ε_{50}	>0.02	0.02	0.01	0.007	0.005
					k_s (pci)	<30	30	100	300	1000
					γ_{sat} (pcf)	100-120	110-130	110-130	120-135	130-145
B	12 and less	10 and less	8 and less	6 and less	I — Level	12.5	12.5	7.0	5.0	4.0
A					5:1	13.5	13.5	7.5	5.0	4.0
R					4:1	13.5	13.5	7.5	5.0	4.0
R					3:1	14.0	14.0	8.0	5.0	4.0
I					2:1	14.5	15.0	8.0	5.5	4.0
E	Greater than 12 thru 16	Greater than 10 thru 14	Greater than 8 thru 12	Greater than 6 thru 10	II — Level	17.0	17.0	9.5	7.5	5.0
R					5:1	18.5	18.5	10.0	8.0	5.0
					4:1	19.0	18.5	10.5	8.0	5.0
					3:1	19.5	19.0	10.5	8.0	5.0
					2:1	20.0	20.0	11.0	8.5	5.5
H	Greater than 16 thru 20	Greater than 14 thru 20	Greater than 12 thru 16	Greater than 10 thru 14	III — Level	21.5	21.0	13.5	9.5	6.5
E					5:1	23.0	23.0	14.5	10.0	7.0
I					4:1	23.5	23.0	14.5	10.0	7.0
G					3:1	25.0	24.0	15.0	10.5	7.0
H					2:1	25.5	24.5	16.0	11.0	7.0
T			Greater than 16 thru 20	Greater than 14 thru 20	IV — Level	*	*	19.0	13.0	9.0
					5:1	*	*	20.5	14.0	9.0
(FT)					4:1	*	*	21.0	14.5	9.0
					3:1	*	*	22.0	15.0	9.5
					2:1	*	*	24.0	15.0	10.0

Table 3.7 Design Chart for Cohesionless Soil (Allowable Deflection 1.0% of Wall Height)

Post Spacing (feet)				Group	N_{60}	2-4	4-10	10-20	20-30	30-50	50-60
					Φ	25-32	27-35	30-38	32-40	34-43	36-44
8 and under	Over 8 Thru 12	Over 12 Thru 16	Over 16 Thru 24		k_s (pci) AWT	<25	25	90	90	225	250
					k_s (pci) BWT	<20	20	60	60	125	140
					γ_{moist} (pcf) L	104 to 108	108 to 112	115 to 120	120 to 125	124 to 128	128 to 130
					γ_{moist} (pcf) U	114 to 118	120 to 124	122 to 130	128 to 132	130 to 145	140 to 145
12 and less	10 and less	8 and less	6 and less	I	Level	9.0	9.0	7.0	6.0	5.5	5.0
					5:1	9.0	9.0	7.5	6.5	6.0	5.5
					4:1	9.5	9.5	7.5	7.0	6.5	6.0
					3:1	9.5	9.5	8.0	7.5	7.0	6.5
					2:1	10.5	10.5	8.5	8.0	7.5	7.0
Greater than 12 thru 16	Greater than 10 thru 14	Greater than 8 thru 12	Greater than 6 thru 10	II	Level	10.5	10.5	8.5	8.0	8.0	6.5
					5:1	11.0	10.5	9.0	9.0	8.5	7.0
					4:1	11.5	11.0	9.5	9.0	8.5	7.5
					3:1	12.0	11.5	10.0	9.5	9.0	8.0
					2:1	13.0	13.0	11.0	10.0	10.0	8.5
Greater than 16 thru 20	Greater than 14 thru 20	Greater than 12 thru 16	Greater than 10 thru 14	III	Level	12.5	12.0	10.0	9.0	9.0	9.0
					5:1	13.5	12.5	11.0	10.5	9.5	9.5
					4:1	13.5	13.0	11.5	10.5	10.0	10.0
					3:1	14.5	13.5	12.0	10.5	10.0	10.0
					2:1	15.5	15.5	13.0	11.5	11.0	11.0
		Greater than 16 thru 20	Greater than 14 thru 20	IV	Level	*	*	14.0	13.5	11.5	11.0
					5:1	*	*	18.0	16.0	13.0	13.0
					4:1	*	*	20.0	17.5	14.0	14.0
					3:1	*	*	23.0	21.0	16.0	16.0
					2:1	*	*	*	23.0	20.0	17.0

Leftmost column (vertical): BARRIER HEIGHT (FT)

Table 3.8 Design Chart for Cohesionless Soil (Allowable Deflection 1.5% of Wall Height)

Post Spacing (feet)				Group	N$_{60}$		2-4	4-10	10-20	20-30	30-50	50-60
					Φ		25-32	27-35	30-38	32-40	34-43	36-44
					k$_s$ (pci)	AWT	<25	25	90	90	225	250
						BWT	<20	20	60	60	125	140
8 and under	Over 8 Thru 12	Over 12 Thru 16	Over 16 Thru 24		γ$_{moist}$ (pcf)	L	104 to 108	108 to 112	115 to 120	120 to 125	124 to 128	128 to 130
						U	114 to 118	120 to 124	122 to 130	128 to 132	130 to 145	140 to 145
12 and less	10 and less	8 and less	6 and less	I	Level		8.0	8.0	6.5	6.0	5.5	5.0
					5:1		8.0	8.0	7.0	6.5	6.0	5.5
					4:1		8.5	8.5	7.0	7.0	6.0	6.0
					3:1		9.0	8.5	7.5	7.0	6.5	6.5
					2:1		10.0	9.5	8.0	7.5	7.0	6.5
Greater than 12 thru 16	Greater than 10 thru 14	Greater than 8 thru 12	Greater than 6 thru 10	II	Level		9.5	9.5	8.0	7.5	7.5	6.5
					5:1		10.5	10.0	8.5	8.0	8.0	7.0
					4:1		11.0	10.5	9.0	8.5	8.0	7.5
					3:1		11.5	11.0	9.5	9.0	8.5	7.5
					2:1		12.5	12.0	10.0	9.5	9.0	8.0
Greater than 16 thru 20	Greater than 14 thru 20	Greater than 12 thru 16	Greater than 10 thru 14	III	Level		11.5	11.0	9.5	9.0	8.0	8.0
					5:1		12.5	11.5	10.0	10.0	8.5	8.5
					4:1		13.0	12.0	10.5	10.5	9.0	8.5
					3:1		13.5	13.0	11.0	10.5	9.5	9.0
					2:1		14.5	14.5	12.0	11.5	10.0	9.5
		Greater than 16 thru 20	Greater than 14 thru 20	IV	Level		15.5	14.0	12.0	11.0	10.5	10.5
					5:1		19	16.0	13.5	12.5	11.0	11.0
					4:1		20.5	17.5	14.0	13.0	12.0	11.5
					3:1		24.0	19.5	15.0	14.0	12.5	12.0
					2:1		*	30.0	19.0	16.0	14.0	13.0

BARRIER HEIGHT (FT)

Table 3.9 Correlation of Cohesionless Soil for Predicting Lateral Deflection

N_{60}		2 to 4	4 to 10	10 to 20	20 to 30	30 to 50	50 to 60
ϕ		25 to 35	30 to 38	33 to 41	35 to 43	37 to 45	39 to 48
k_s lb/in^3	A.W.T.	< 25	25	90	90	225	250
	B.W.T.	< 20	20	60	60	125	140
γ_{moist} pcf	Min.	104 to 108	108 to 112	115 to 120	120 to 125	124 to 128	128 to 130
	Max.	114 to 118	120 to 124	122 to 130	128 to 132	130 to 145	140 to 145

Table 3.10 Correlations of Cohesive Soil for Predicting Lateral Deflection

N_{60}	0 to 2	2 to 4	4 to 8	8 to 16	16 to 32	32 to 64
S_u (psi)	0 to 1.88	1.88 to 3.75	3.75 to 7.53	7.53 to 15.00	15.00 to 30.00	30.00 to 55.6
ε_{50}	> 0.02	0.02-0.01	0.01 to 0.007	0.007 to 0.005	0.005 to 0.004	0.004 to 0.002
k_s(lb/in^3)	< 30	30	100	500	1000	2000
γ_{sat} (pcf)	100 to 120	110 to 130	110 to 130	120 to 135	130 to 145	140 to 145

4   COMPARISON AND EVALUATION OF ANALYSIS METHODS

Existing analysis methods for drilled shafts under lateral loads were first evaluated on the basis of several assumed hypothetical conditions involving relatively uniform soil deposits with typical soil properties and typical shaft dimensions and embedment lengths. This was intended to provide a basis of comparison of the results of various analysis methods.

In addition to hypothetical cases, a database was established from the review of existing open literature as well as from numerous lateral load tests previously conducted by the principal investigators for the ODOT. The compiled database was limited to contain only drilled shafts with the dimensions of typical drilled shafts currently in use by CDOT. Efforts were also made to compile a limited database for torsional load tests. Based on comparisons between the results of existing analysis methods and load test databases complied for this study, appropriate analysis methods were recommended for analysis and design of drilled shafts subjected to lateral and/or torsional loads.

The effects of loading rate, cyclic degradation, and ground water on soil stiffness and strength are also summarized based on pertinent literature review. This discussion is intended to provide qualitative understanding of the possible implications of transient wind loads.

Calibrations of resistance factors for the Broms method are also presented. The recommended factor of safety of two seemed to yield a similar resistance factor as determined from reliability based calibration using a target reliability index of 2.5.

4.1   Hypothetical Cases

For the purpose of comparing predictions made by various existing analysis methods, several hypothetical cases involving uniform soil profile and typical soil properties together with typical drilled shaft dimensions are assumed. The selected typical properties for clay, sand, and rock are summarized in Table 4.1, along with the drilled shaft properties.

Table 4.1 Assumed Properties of Sand, Clay, Rock, and Drilled Shafts in a Comparison Study for Hypothetical Cases

Properties	Sand (Medium Dense)	Clay (Medium Stiff)	Rock (Limestone)	Drilled Shaft
γ (pcf)	110	110	156	150
E (ksf)	700	150	1.0E6	5.2E5
ν	0.3	0.5	0.3	0.2
G (ksf)	269	50	3.8E5	2.17E5
ϕ (Degree)	30	0	40	
δ (Degree)	20	0	30	
C_u (ksf)	0	0.75	200	
k_s (pci)	25	100		
ε_{50}		0.009		

Note: γ=unit weight; E= Young's Modulus; ν= Poisson's ratio; G= shear modulus; ϕ= friction angle; δ= friction angle between shaft and soils; C_u= undrained shear strength; k_s = modulus of horizontal subgrade reaction; ε_{50}= strain at half of the maximum principal stress difference.

4.1.1 Lateral Response of Drilled Shafts

Fig. 4.1 provides a schematic diagram of the hypothetical case of laterally loaded shafts, depicting the soil profile, the drilled shaft dimensions, and the location of applied lateral loads. As indicated in the figure, two soil profiles are studied, one is a clay deposit and the second one is a sand deposit. The methods of analysis investigated include Broms method, sheet piling method, Caisson program, and the COM624P program. The Brinch Hansen method and the NAVFAC DM7 method were not evaluated for these hypothetical cases because these two methods were not considered in the initial course of the study; however, they will be evaluated with existing lateral load test database.

The calculated results from these analysis methods are tabulated in Table 4.2 which includes both ultimate lateral capacity and maximum moment. The comparison of capacity estimates is also presented in Fig. 4.2. It is noted that the methods used by CDOT (i.e., the sheet piling method and the caisson program) were not applied to the case of cohesive soil deposit due to the

fact that these methods were not intended for such soil types. For the sandy soil profile studied, it can be seen that the sheet piling method and COM624P program tend to give relatively lower estimates of the ultimate capacity compared to the Broms method and Caisson program's predictions.

Table 4.2 Summary of Calculated Lateral Capacities and Maximum Moments of Drilled Shafts in Hypothetical Cases

Soils		Methods			
		Broms Method (Ultimate)	COM624P (At deflection 2.4")	Sheet piling Method (Isolation Factor = 2)	Caisson program (Ultimate)
Sand	Lateral Capacity (kips)	55.7	32	40	55.8
	Maximum Moment (kip -ft)	806	549	NA	899
Clay	Lateral Capacity (kips)	24.8	16	NA	NA
	Maximum Moment (kip -ft)	360	239	NA	NA

4.1.2 Torsional Response of Drilled Shafts

For the torsional response of the drilled shaft, four hypothetical soil profiles depicted in Fig. 4.3 are used for comparing five different analysis methods listed in Table 4.3. The calculated ultimate torsion capacities are summarized in Table 4.3, while the torsional stiffness defined as torsion divided by twist angle is shown in Table 4.4. The comparison of torsional capacity estimates in a bar chart is also presented in Fig. 4.4. It can be seen that the CDOT method tends to predict the highest value of ultimate torsion capacity for all the cases investigated. On the other hand, the difference of the estimated torsional stiffness among other methods is very small, roughly within 25% for the simple soil profiles investigated. This is not surprising because most of these methods are based on similar theoretical basis.

Table 4.3 Comparison of Ultimate Torsional Capacity Estimated by Various Methods in Hypothetical Cases

Soil Profiles	Torsional Capacity (kips-ft)				
	Florida Structures Design Office (sand)	Modified Florida District 5 Method (sand)	Florida District 7 Method (clay)	Florida District 5 Method	Colorado Dept. of Trans. (sand & clay)
Sand	25.4	52	30.3^2	26.1^3	91.8
Clay	N/A	N/A	44.2	44.2^3	85.9
Sand over Rock	30.2^1	60.6^1	N/A	N/A	N/A

Note: [1]: The method was initially developed for cohesionless soils.
[2]: The method was initially developed for cohesive soils.
[3]: The side resistance is the same with Florida District 7 Method.

Table 4.4 Comparison of Calculated Torsional Stiffness at Shaft Head in Hypothetical Cases

Soil Profiles	Torsional Stiffness (T_t/ϕ_t, 10^4 kips-ft)				
	Poulos (1975)	Randolph (1981)	Chow (1985)	Hache & Valsangkar (1988)	Carter& Kulhawy (1988)
Sand	4.9	5.6	5.9	6.2	N/A
Clay	1.3	1.4	1.3	1.1	N/A
Rock only	297	249	N/A	N/A	249

4.2   Load Test Database

4.2.1 Selected Lateral Load Test Database

There are quite a few lateral load test data available in the literature, such as Florida DOT's database compiled by University of Florida. However, only a small part of the existing test data is related to the shaft diameter between 20 inches and 36 inches and shaft length between 6 feet

and 30 feet, which are the dimensions commonly found in the CDOT sound wall foundation practice. After searching the available test data, only 3 lateral load tests with 7 tested drilled shafts in clay are selected from the ODOT Database, and one test with 5 tested drilled shafts conducted in sand by Bhushan et al. (1981) is selected. To enlarge the database for drilled shaft tests in sand, drilled shafts with 42 inch and 48 inch diameters are also included.

Table 4.5 provides a brief summary of the content of the selected database for lateral load tests in clay. The details of the database for drilled shafts in clay are presented in Appendix D, including soil profiles, SPT N values, the correlated soil parameters for analysis, and the measured load-deflection data. The test shafts information and relevant soil properties for the database for sand are given in Table 4.6 and Table 4.7, respectively.

Table 4.5 Selected Database for Lateral Response of Drilled Shafts in Clay

No.	Project Name	Depth of Shaft (L) in ft	Diameter of Shaft (D) in inches	Predominant Soil Type
1	I-70 (Columbus, OH), Shaft 1	9.5	30	Clay
2	I-70 (Columbus, OH), Shaft 2	9.5	30	Clay
3	I-90 Sound Barriers, Shaft 2	12	30	Clay
4	I-90 Sound Barriers, Shaft 3	8'-8"	30	Clay
5	I-90 Sound Barriers, Shaft 4	8'-5"	30	Clay
6	I-90 Noise Wall, Shaft 1 (P101)	12	30	Clay
7	I-90 Noise Wall, Shaft 2 (P100)	10	36	Clay

Note: All the tests were conducted in Ohio.

Table 4.6 Selected Database for Lateral Response of Drilled Shafts in Sand

Pier Number	Diameter(ft)	Embedded Length(ft)	Test Site	Concrete Modulus (psi)	Reinforcement
1	3.5[1]	17	A	3000000	NA
4	2	18	B	4330000	14 #11 bars
5	3	18	B	4330000	14 #11 bars
6	3	18	C	4330000	14 #11 bars
7	4	18	C	4330000	14 #11 bars

Note [1]: Piers were constructed with a 5-ft diameter bell near the bottom 2 ft.

Table 4.7 Test Site Information for Drilled Shafts in Sand

Test Site	Soil Type	Depth (ft)	Total Unit Weight (pcf)	Friction Angle (degree)	Relative Density (%)
A	sand (SP-SM)	0-8	105	38	55
	sand (SP-SM)	8~15	110	40	67
	silty sand (SM)	0-3	105	36	77
B	silty sand (SM) w/gravelly layers	3~18	105	42	88
	silty sand (SM)	0-6	105	36	38
C	silty sand (SM) w/gravelly layers	6~18	105	42	92

4.2.2 Torsional Load Test Database

There is a dearth of torsional load test data available in the open literature. Table 4.8 provides a brief summary of the existing torsional load test results collected under this research effort. The most recent torsional load tests on drilled shafts were reported by Tawfiq (2000). It appears that

the geotechnical community can benefit from more torsional load test results. Pertinent test data, including soil properties and drilled shaft dimensions are compiled in Table 4.9. It should be noted that other than Tawfiq (2000b), all other test data are related to small-size model piles. Thus, one needs to be cautious in interpreting analysis and test results.

Table 4.8 Compilation of Existing Data for Torsional Response of Piles/Drilled Shafts

Investigator	Test Description	Pile	Soil	Available Data
Stoll (1972)	• The first field torsion load tests. • 2 piles • Simple loads	• Steel pipe piles filled with concrete. • Length: 57ft. and 68 ft. • 10.75 in.-OD, 0.25 in.-wall	Clay	• 2 pile head torque-twist curves.
Poulos (1975)	• Model pile tests • Simple loads	• Solid aluminum piles • Length: 6 - 20 in. • Diameter: 0.5 - 1.5 in.	Kaolin clay	• 4 pile head torque-twist curves.
Dutt (1976)	• Model pile tests • Simple loads	• Soft aluminum pipe piles • 1.9 in. OD-0.1 in. wall, Circular • 2.0 in.-0.125 in. wall, Square • Length: 5 ft.	Sand	• 4 pile head torque-twist curves. • 3 torque distribution along pile curves. • 3 torque transfer versus twist curves.
Tawfiq (2000a)	1 Scaled model tests 2 Simple loads and combined loads	3 Concrete piles 4 Diameter: 4 in. 5 Length: 20 in.	Sand	6 6 pile head torque-twist curves.
Tawfiq (2000b)	• 3 Full scaled field tests • Combined lateral, overturning and torsional loads	• Reinforced concrete piles • Diameter: 4 feet • Length: 20 feet	Sand	• 3 pile head torque-twist curves.

Table 4.9 Summary of Soil and Drilled Shaft Information of the Available Torsional Load Test Results from Literature

Properties / Tests		Pile Information				Soil Information				
		Type	1	2	3	Type	4	5	6	7
			γ (pcf)	L (ft)	D (in.)		γ (pcf)	C (psf)	ϕ	δ
Tawfiq (2000), Full-Scale Field Tests	#1	Drilled shaft	140	20	48	Sand	125	0	30	30
	#2	Drilled shaft	140	20	48	Sand	125	0	30	27
	#3	Drilled shaft	140	20	48	Sand	125	0	30	21
Dutt (1976), Model Tests	#1	Circular aluminum pipe pile	162	5	1.9	Dense Sand	107	0	43	28
	#2		162	5	1.9	Loose sand	96	0	39	25
Stoll (1972), Field Tests	A-3	Pipe pile filled with concrete	150	57	10.75	Clay	120	500	0	0
	V-4		150	68	10.75	Clay	120	800	0	0
Poulos (1975), Model Tests	#1	Solid aluminum pile	162	1.65	1.0	Clay	110	124	15	15
	#2		162	0.83	1.0	Clay	110	343	15	15
	#3		162	0.98	0.75	Clay	110	232	15	15

Note: 1 – Unit weight of pile; 2 – Pile length; 3 – Pile diameter;

4 – Unit weight of soil; 5 – Cohesion of soil; 6 – Friction angle of soil; 7 – Friction angle between soil and pile.

4.3   Evaluation of Analysis Methods with Load Test Data

4.3.1 Lateral Load Test Results

The database established in section 4.2 is used for evaluating the accuracy of various analysis methods. A comparison of the results is presented in this section.

4.3.1.1 Hyperbolic Curve Fit

Usually, the lateral load tests do not reach the stage of complete soil failure; therefore, the ultimate lateral capacity is not directly available from test results. Kulhawy and Chen (1995) developed a hyperbolic curve fit technique to simulate the non-linear load-deflection behavior and to predict the ultimate capacity of piles (drilled shafts). The hyperbolic equation in terms of the lateral load (H) and the lateral deflection (δ) can be expressed as follows:

$$H = \frac{\delta}{a + b\delta} \tag{4.1}$$

where a and b are curve fitting constants. The ultimate lateral load capacity can be calculated as $H_h = 1/b$.

4.3.1.2 Ultimate Capacity Estimation - Clay

The analysis methods used to estimate ultimate lateral capacity of drilled shafts in clay include Broms method and Brinch Hansen method. The Caisson program and Sheet piling method were not evaluated, since they were intended only for the analysis of drilled shafts embedded in sand. The undrained shear strength of cohesive soils which were correlated from SPT N values by using Table 3.6 and then averaged with the weighted average on the basis of the soil layer thickness, together with lateral loading conditions, are summarized in Table 4.10.

Table 4.10 Parameters Used in the Calculation of Lateral Response of Drilled Shafts in Cohesive Soils.

Parameters / Tests	Cohesion (psi)	Embedded Length (ft)	Load Arm (ft)*	Diameter (inch)
I70 Sound Barriers, Columbus OH, Shaft 1	23	9.5	0	30
I70 Sound Barriers, Columbus OH, Shaft 2	23	9.5	0	30
I-90 Sound Barriers, Shaft P 100	18.7	10	0	36
I-90 Sound Barriers, Shaft P 101	18.7	12	0	30
I-90 Sound Barriers, 12ft Shaft 2	22.6	12	10	30
I-90 Sound Barriers, 8ft Shaft 1	22.2	8.7	10	30
I-90 Sound Barriers, 8ft Shaft 2	22.1	8.4	10.1	30

Note: * Load Arm: the length between load point and ground line.

The comparisons between the Broms method, the Brinch Hansen method, and the load test results using the hyperbolic curve fit technique, are summarized in Table 4.11. A bar chart showing measured capacity over predicted capacity for these six cases is presented in Fig. 4.5.

In the cases when the load arm is zero feet, Broms method provides a very close estimate with the test results, except for one case. On the other hand, the Brinch Hansen method provides larger predicted capacities than the test results. Generally, the Broms method provides more conservative and safer capacity estimates than Brinch Hansen method.

In the cases when the load is applied 10 feet above ground level, both the Broms and the Brinch Hansen methods yield similar prediction results. The range of the ratio (the measured results over the predicted results) is 2.1 to 2.5. This means that these two methods tend to yield relatively conservative estimates for the load test cases with 10 feet load arm.

Table 4.11 Summary of Calculated Lateral Capacity of Drilled Shafts in Cohesive Soils

Methods / Soils		Col. 1 Load Test (hyperbolic fit) H_h	Col. 2 Broms Method	Col. 3 Brinch Hansen Method	Col. 1 /Col. 2	Col. 1 /Col. 3
I70 Sound Barriers, Columbus OH, Shaft 1	Lateral Capacity (kips)	92	90	120	1	0.77
I70 Sound Barriers, Columbus OH, Shaft 2	Lateral Capacity (kips)	>60[1]	90	120	NA	NA
I-90 Sound Barriers, Shaft P 100	Lateral Capacity (kips)	78	73	99.8	1.1	0.78
I-90 Sound Barriers, Shaft P 101	Lateral Capacity (kips)	85	123	129.6	0.7	0.66
I-90 Sound Barriers, 12ft Shaft 2	Lateral Capacity (kips)	161	67	67.6	2.4	2.4
I-90 Sound Barriers, 8ft Shaft 1	Lateral Capacity (kips)	71	34	34.9	2.1	2.0
I-90 Sound Barriers, 8ft Shaft 2	Lateral Capacity (kips)	70	28	32.5	2.5	2.2

[1]: The measured load-deflection curve does not appear highly nonlinear, hyperbolic fit method can not make accurate estimation.

4.3.1.3 Ultimate Capacity Estimation - Sand

The analysis methods for estimating the ultimate capacity of drilled shafts in sand include the Broms method, the Brinch Hansen method, the Caisson program, and the Sheet piling method. The average soil friction angles, which are weight averaged from the friction angles shown in Table 4.7, are summarized in Table 4.12

The predicted lateral capacities using various analysis methods are summarized in Table 4.13. The normalized ratios based on the measured vs. predicted values are also presented in the table. Additionally, a bar chart showing the measured capacity over predicted capacity for the five cases in Table 4.13 is presented in Fig. 4.6. It seems that all analysis methods yield lower capacity values than the actual measured capacities. The Broms method appears to predict the lowest lateral capacities compared to other methods. On the other hand, the Brinch Hansen method appears to yield the highest predicted capacities compared with other methods.

Table 4.12 Parameters Used in the Calculation of Lateral Response of Drilled Shafts in Cohesionless Soils (After Bhushan et al., 1981)

Parameters / Tests	Φ (Degree)	Embedded Length (ft)	Load Arm (ft)	Diameter (inch)
Pier 1	39	17	0	42
Pier 4	41	18	0	24
Pier 5	41	18	0	36
Pier 6	40	18	0	36
Pier 7	40	18	0	48

Table 4.13 Summary of Calculated Ultimate Lateral Capacity of Drilled Shafts in Cohesionless Soils

Tests	Load Test (kips)	Capacity (kips)				Normalized Ratio			
		Broms Method	Sheet Piling	Caisson	Brinch Hansen	Broms Method	Sheet Piling	Caisson	Brinch Hansen
Pier 1	337	190	199	200	247	1.8	1.7	1.7	1.6
Pier 4	316	102	165	150	283	3.1	1.9	2.1	1.1
Pier 5	325	177	248	230	346	1.8	1.3	1.4	0.9
Pier 6	307	177	211	230	269	1.7	1.5	1.3	1.1
Pier 7	342	260	282	300	299	1.3	1.2	1.1	1.1

Note: Normalized Ratio = Measured Capacity over Predicted Capacity.

4.3.1.4 Load-Deflection Prediction - Clay

The ability of COM624P (LPILE) and NAVFAC DM-7 to predict the load-deflection curve for laterally loaded shafts in clay is evaluated and the comparison plots are shown in Fig. 4.7 through Fig 4.13 for each of seven load tests. The soil parameters used in COM624P are interpreted from the SPT correlation method and summarized in Appendix D. The subgrade reaction coefficients used in NAVFAC DM-7 method are correlated from Chen's correlation discussed in Section 2.1.1.2.2.

For the cases with a zero foot load arm, the NAVFAC DM-7 predictions tend to either match with test results or to be larger than measured in the initial linear part of the load-deflection curve. The COM624P prediction, on the other hand, shows good agreement with the measured load-deflection curves and yields safer results in the non-linear part of the load-deflection curve.

For the cases where a 10 foot load arm was involved, the NAVFAC DM-7 predictions seem to agree well with the initial part of the measured load-deflection. The COM624P, on the other hand, does not seem to be able to provide good matches for these three cases. The predicted deflection, however, is larger than measured, and therefore, it is on safe side.

In general, it seems that NAVFAC DM-7 can yield a good prediction on the linear part of the load-deflection response for the drilled shafts in clay, but it cannot capture the non-linear behavior. The COM624P, however, does provide a fairly reasonable, but somewhat conservative, prediction of the load-deflection behavior of all seven cases. It is particularly true that COM624P tends to over predict the deflections for the drilled shafts subjected to combined lateral loads and moments.

4.3.1.5 Load-Deflection Prediction - Sand

The ability of COM624P (LPILE) and NAVFAC DM-7 to predict the load-deflection behavior of drilled shafts in sand was investigated and a comparison of the results are plotted in Fig. 4.14 through Fig 4.18. The soil parameters used in COM624P were interpreted from SPT and CPT test by Bhushan et al. (1981), and they are shown in Table 4.7. The subgrade reaction coefficients used in the NAVFAC DM-7 method are obtained from Chen's correlation.

The NAVFAC DM-7 method yields larger deflections than those predicted by the COM624P method or those actually measured, particularly in the elastic portion. COM624P prediction shows good agreement with the initial portion of the measured load-deflection curves. However, it overestimates the deflections in the nonlinear portion of the curve. The COM624P nevertheless provides fairly reasonable, but somewhat conservative, predictions of the load-deflection behavior of all five cases.

4.3.1.6 Permissible Deflection at Drilled Shaft Head - Clay

To establish a sense of linkage between the shaft deflection and shaft capacity, the capacity values predicted by COM624P according to different permissible deflection criteria (e.g., 0.6 inch, 1 inch, and 1.5 inch), are presented in Table 4.14. The factor of safety calculated on the basis of the ratio between the deflection based capacity and the actual test capacity is also shown in the table. Additionally, a chart showing measured capacities over predicted capacities at these three permissible deflections is presented in Fig. 4.19. From Table 4.14, one can see that the Factor of Safety ranges from 1.2 to 1.8, for the cases where the load arm equals 0 feet, and from 3.3 to 4.7 for the cases with a 10 foot load arm, respectively. For the 1.5 inch permissible deflection at the shaft head (ground level), the factor of safety is more than 1.2. It seems that the 1.5 inch permissible deflection is safe from the load capacity point of view. However, if the relationship between the deflection at shaft top and the deflection at the wall top is assumed to be linear as shown in Fig. 4.20, then the 1.5 inch deflection at the shaft head would result in the deflection at wall top to be 3.3 inch for typical drilled shafts with 15 feet of length supporting 18 ft high noise wall. The allowable deflection at wall top should be determined from the input of structural engineers. Without this input from structural engineers, it seems prudent to adopt a more conservative criterion of 1 inch permissible deflection at the drilled shaft head (ground level).

Table 4.14 Summary of Calculated Lateral Capacity of Drilled Shafts by COM624P with Different Permissible Deflections in Cohesive Soils

Methods / Soils	Load Test (hyperbolic fit) H_h	COM624P		COM624P		COM624P	
		0.6 inch	F.S.	1 inch	F.S.	1.5 inch	F.S.
I70, Columbus OH, Shaft 1	92	52	1.8	59	1.6	66	1.4
I70, Columbus OH, Shaft 2	>60	52	NA	60	NA	66	NA
I-90, Shaft P 100	78	54	1.4	60	1.3	67	1.2
I-90, Shaft P 101	85	57	1.5	66	1.3	72	1.2
I-90, 12ft Shaft 2	161	38	4.2	44	3.7	49	3.3
I-90, 8ft Shaft 1	71	17	4.2	19	3.7	21	3.4
I-90, 8ft Shaft 2	70	15	4.7	18	3.9	20	3.5

Note: F.S. = Ratio of hyperbolic fit capacity over prediction

4.3.1.7 Permissible Deflection at Ground Level - Sand

Following the same path of investigation as in the previous section, the capacity values predicted by COM624P corresponding to different permissible deflection criteria are summarized in Table 4.15. Also shown are the calculated Factor of Safety based on the ratio between the deflection based capacities and the actual test data. Additionally, a chart showing measured capacities over predicted capacity at these three permissible deflections is presented in Fig. 4.21. From Table 4.15, one can see that the F.S. ranges from 3.3 to 7 for 0.6 inch permissible deflection, from 2.7 to 4.5 for 1 inch permissible deflection, and from 2.3 to 3.4 for 1.5 inch permissible deflection, respectively. For 1.5 inch permissible deflection at the shaft top (ground level), the factor of safety is more than 2.3. Again, it seems that a permissible deflection of 1.5 inches will correspond to an adequate factor of safety from the drilled shaft capacity point of view. However,

based on the same argument as before, it seems prudent to recommend a more conservative permissible deflection at the drilled shaft head (ground level) to be 1.0 inch.

Table 4.15 Summary of Calculated Lateral Capacity of Drilled Shafts by COM624P with Different Permissible Deflections at Ground Level in Cohesionless Soils

Methods Soils	Load Test (hyperbolic fit) H_h	COM624P		COM624P		COM624P	
		0.6 inch	F.S.	1 inch	F.S.	1.5 inch	F.S.
Pier 1	337	88	3.8	115	2.9	133	2.5
Pier 4	316	45	7	70	4.5	93	3.4
Pier 5	325	76	4.3	102	3.2	130	2.5
Pier 6	307	72	4.3	95	3.2	120	2.6
Pier 7	342	105	3.3	128	2.7	150	2.3

Note: F.S. = Ratio of hyperbolic fit capacity over predicted

4.3.2 Torsional Load Test Results

The database presented in Section 4.2.2 does not contain sufficient information on the torque-twist relationships; therefore, the evaluation will be focused on ultimate torsional resistance at the top of the drilled shafts. It is important to note that the dimensions of the drilled shafts or piles of the torsional load tests in the database are smaller than the dimensions of the drilled shafts used in CDOT practice.

The comparisons between the estimated torsion capacity from various analysis methods and the test results for the tests conducted in sand are tabulated in Table 4.16. A bar chart showing the measured torsional capacity over the predicted torsional capacity is presented in Fig. 4.22. Similar comparisons for the tests conducted in cohesive soils are summarized in Table 4.17 and Fig. 4.23. In most cases, Florida DOT's various methods tend to under-predict the capacity; on the other hand, the CDOT's method tends to over-predict the torsion capacity.

Table 4.16 Comparison between Estimated Torsional Capacity and Test Results in Cohesionless Soils

Tests		Capacity				Normalized Ratio		
		Test results	Florida Struct. Design Office	Modified Florida District 5 Method	Colo. Dept. of Trans.	Florida Struct. Design Office	Modified Florida District 5 Method	Colo. Dept. of Trans.
Tawfiq (2000), Full-Scale Drilled Shaft Tests (kip * ft)	#1(dry)	490	207.8	341.2	646.2	0.42	0.70	1.32
	#2 (polymer slurry)	480	183.7	325	570	0.38	0.68	1.19
	#3 (bentonite slurry)	280	137.8	269.1	430	0.49	0.96	1.54
Dutt (1976), Model Tests (lb * ft)	#1 pile in dense sand	13.3	8.9	20.9	187	0.67	1.60	14.06
	#2 pile in loose sand	7.5	8.1	18.9	171.6	1.08	2.52	22.9

Note: Normalized Ratio = Predicted Capacity over Measured Capacity.

Table 4.17 Comparison between Estimated Torsional Capacity and Test Results in Cohesive Soils

Tests		Capacity			Normalized Ratio	
		Test results	Florida District 7 Method	Colorado Dept. of Trans.	Florida District 7 Method	Colorado Dept. of Trans.
Stoll (1972), Field Tests (kip-ft)	A-3	21.5	14.4	35.2	0.67	1.64
	V-4	38.5	27.4	67.4	0.71	1.75
Poulos (1975), Model Tests (lb-ft)	#1	1.375	1.2	2.1	0.87	1.53
	#2	1.62	1.326	2.68	0.82	1.65
	#3	0.67	0.6	1.26	0.90	1.88

Note: Normalized Ratio = Predicted Capacity over Measured Capacity.

4.4   Recommended Methods of Analysis and Design

4.4.1 Lateral Response of Drilled Shafts

4.4.1.1 Ultimate Capacity Based Design - Clay

For the design of drilled shafts in clay, we suggest the use of the Broms method. The Broms method is considered to provide a more accurate and safer prediction than the Brinch Hansen method. The calculation steps involved in the Broms method are fairly straight forward as well.

A design Safety Factor of two is recommended based on the discussion in Section 4.3.1. The lateral loads applied to sound walls, overhead signs, and traffic signals, usually produce the accompanying moments. For example, the applied wind load on sound walls can be assumed to concentrate at the mid height of the wall, and then the load arm is 7 to 9 feet for 14 to 18 feet

high walls. The last three cases in Table 4.11 are very similar to these situations, and the Broms method prediction is about ½ of the measured ultimate capacity. If a Factor of Safety of two is applied to Broms method, the actual Factor of Safety will be about 4. Thus, we can adopt a relatively low factor of safety; however, the value can not be too low, since the first four cases in Table 4.11 indicate that Broms method may over predict in some cases.

4.4.1.2 Ultimate Capacity Based Design - Sand

The comparisons in section 4.3.1 do not provide conclusive evidence regarding the accuracy of several capacity estimate methods for laterally loaded drilled shafts in sand. Therefore, for consistency, the Broms method is suggested. It should be noted that the test data in sand for this study comes from only one reference. Thus, it warrants the adoption of a safer prediction method (Broms method) until more extensive database becomes available for further evaluation.

The design Safety Factor of two is recommended based on the discussion in Section 4.3.1. If a Factor of Safety of two is applied to Broms method, the actual Factor of Safety based on load test data will range from 2.6 to 6.2, with an average F.S. of 3.9.

4.4.1.3 Service Limit Based Design - Clay

For drilled shafts embedded in clay, COM624P (LPILE) computer program is recommended for predicting the load-deflection response. The NAVFAC DM-7 method can only predict the initial linear part of the load-deflection behavior; therefore, it is not recommended.

Without additional input from structural engineers, a permissible deflection of 1.0 inch at the drilled shaft head is recommended. It should be emphasized that this conclusion was derived from drilled shaft response, not from structural consideration of sound walls. It is the structure engineers' decision according to sound wall structure details.

It is noted that the Broms method may result in larger design length than the COM624P (LPILE) design value, if a relatively high permissible deflection (say 1.5 inch) is adopted. Therefore, the design embedment length of drilled shaft should be controlled by the longer length determined by the Broms method and the COM624P (LPILE) results.

4.4.1.4 Service Limit Based Design - Sand

Similar to the recommendation on drilled shafts in clay, COM624P (LPILE) is recommended for predicting the load-deflection response of drilled shafts in sand. The NAVFAC DM-7 method can only predict the initial linear part of the load-deflection behavior; therefore, it is not recommended. The permissible deflection at drilled shaft head (ground level) is recommended to be 1.0 inch from drilled shaft performance viewpoint. Furthermore, the design embedment length of drilled shafts in sand should be controlled by the longer length determined by Broms method and COM624P (LPILE) program.

4.4.2 Torsional Response of Drilled Shafts

For the torsional response of drilled shafts, the dimensions of the drilled shafts in the existing test data do not match the dimensions of the drilled shafts used by CDOT. Nevertheless, according to the analysis presented in Section 4.1 for the hypothetical cases and Section 4.3.2 for actual torsional load test cases, Florida DOT's various methods tend to provide safer capacity prediction. On the other hand, the CDOT's method tends to over-predict the torsional capacity. At this stage, due to the lack of relevant test data, Florida Structures Design Office Method (FSDOM) and Florida District 7 Method are tentatively recommended for the torsional design of drilled shafts in cohesionless and cohesive soils, respectively, if soil investigation would be made.

The reasons for the over-prediction of the CDOT method can be summarized as follows. In granular soils, the major difference between FSDOM method and CDOT method is the determination of coefficient of earth pressure. FSDOM method use K_0, coefficient of earth pressure at rest, while CDOT method has the coefficient of earth pressure K calculated to be ηK_0, in which η is the ratio of volume of slice over the volume of a planer wedge (Refer Section 2.1 of Appendix C for detail). In the calculation of η, simplification was involved by assuming a large value of L/R, in which L is the length of shaft and R is the radius of shaft. The error introduced from this simplification should increases as the L/R decreases. However, the results for the Dutt model test in Table 4.16 for cohesionless soil do not support this statement. Specifically, the L/R ratios for the Tawfiq test are 10 and the L/R ratios for the Dutt model test are about 60 while the normalized ratios for the Tawfiq test are reasonable and the normalized ratios for the Dutt model

test are unreasonable. Accordingly, the error must come from something other than the L/R ratio; perhaps from the frictional resistance.

The coefficient of friction between the soil and the concrete was taken as $\tan(\varphi)$ assuming that the caisson body was rough enough to trap soil along its perimeter to promote the frictional resistance of soil-on-soil. If this is not the case, such as the reduction of friction due to the use of drilling mud, then a lesser value such as $\tan(2/3*\varphi)$ could be used. In fact, $\tan(2/3*\varphi)$ was already utilized for the calculation of the torsional capacity of the bentonite slurry constructed drilled shaft of Tawfiq's test, shown in Table 4.16. The over-prediction by CDOT method for this case, therefore, might imply a need for further investigation on the determination of K since the coefficient of friction and K are the two most influential factors in the estimation of torsional capacity. Additionally, the CDOT method will probably over-predict the total torsional resistance in mixed soils if the torsional resistances from the cohesive and cohesionless components can be added by superposition.

In cohesive soils, the soil's cohesive value was used as bond strength at the soil-to-concrete interface for predicting torsional resistance. In fact, the bond strength at this interface may not be as good as the soil's cohesive value or, as previously stated, the drilling mud may have a tendency to reduce the friction developed at the pile-to-soil interface and this may warrant further investigation.

In fact, CDOT's current design procedure does not require soil strength investigation for signs and signals. Instead, they rely on a minimum friction angle of 30 degree for granular soils, a minimum cohesion of 750 psf for cohesive soils, and a minimum unit weight of 110 pcf for all soils. A factor of safety of 1.25 and the CDOT torsion design method are used. It is not able to conclude whether or not the selected minimum soil strength parameters are reasonable without a wide range of investigation on Colorado soil strength in this study. However, according to CDOT's current practice, there are no torsional failures reported and the selected soil parameters are really based on soft clay and loose sand. Therefore, the current practice should be ok, even on conservative side. It is recommended to perform SPT testing at the location of the major signs and signals so that a more rational design could be utilized and a cost saving can be expected.

4.5 Other Considerations

4.5.1 Loading Rate Effect

Some literature exists pertaining to the effect of loading rate on the strength of the soils. The current understanding of the undrained shear strength of cohesive soils as affected by the loading rate is summarized herein. However, it is important to note that additional research is needed before any conclusion can be drawn regarding the effect the loading rate has on the lateral response of drilled shafts.

The standard strain rate of 0.5% to 1% per hour is considered as the strain rate in the laboratory monotonic tests (Lefebvre and LeBoeurf, 1987). Sheahan et al (1996) found that the strain rate is insignificant in affecting the undrained shear strength of cohesive soils for the rate ranging from 0.05% to 0.5% per hour. Here, we can assume that typical monotonic load testing in the lab is about 1% per hour. Sheahan et al (1996) also observed that the average failure strain for the Boston blue clay is about 3.7%. Thus, it could be assumed that the typical failure strain of cohesive soils is about 3%. From Lefebvre and LeBoeuf's study (1987), they observed that there is a 7% to 14% increase in the undrained shear strength per log cycle of strain rate increase, with an average of 10% strength increase as a conservative estimate. This increase in shear strength is linear over five log cycles of strain rate.

Consider that the drilled shafts supporting the noise wall are subjected to 3 seconds of wind gust. If the soil surrounding the shaft is to fail in three seconds during gust, then the strain rate to failure is 3600% per hour by assuming a failure strain of 3%, a roughly 3.5 log cycles of strain rate increase compared to a laboratory shear strain rate. Thus, one can conclude that the undrained shear strength of cohesive soils determined by standard laboratory tests would be increased by about 35% for the gust induced failure.

Concerning the loading rate effect on the strength of cohesionless soils, a review of literature is summarized in Table 4.18. It appears that with exception of Whitman and Healy (1962) experimental results, other researchers have indicated rather small increase in the apparent strength increase of cohesionless soils due to increase in loading rate. According to Whitman and

Healy, the effective friction angle of the cohesionless soils appears to be uninfluenced by the rate of loading. The undrained shear strength increase in saturated loose sand due to high loading rate can be attributed to slower pore pressure increase than that during the normal loading rate. Until more definite experimental findings suggest differently, the research team believes that the loading rate effect due to a gust may not be an important consideration for dry sand or saturated dense sand. There might be small benefits if one considers an apparent increase in undrained shear strength in loose cohesionless soils due to gust loading.

Table 4.18 Test Results of Strain Rate Effect on Strength of Cohesionless Soils

Investigator	Soil	Confining pressure	Loading velocity	The effect on strength	
				Drained	Undrained
Casagrande and Shannon (1948)	Sands	30-90 kPa	0.2 meters/sec.	Increased 10%	
Seed and Lundgren (1954)	Dense saturated sands	200 kPa	1.0 m/s		Increased 15-20%
Whitman and Healy (1962)	Dense and loose sand	70 kPa	0.5 m/s	Increased 10%	Increased 100%
				Friction angle is largely independent of strain rate	
Lee et al. (1969)	Loose and dense dry sand	100-1470 kPa	0.22 m/s	Increased 20% for dense sand at high confining pressure, 7% for loose sand and low confining pressure on dense sand	
Yamamuro and Lade (1993)	Dense sands	34 MPa	$1.33 \times 10^{-7} - 2.29 \times 10^{-5}$ m/s	Increased 2%	Increased 7%

4.5.2 Cyclic Loading Degradation

Some researchers have looked into the effects of cyclic loading on the drilled shaft lateral response. It has been found that the repeated loading degrades the clay structure, changes the pore water pressure, and decreases the stiffness and strength of the soil. In sand and normally

consolidated clays, the cyclic pore water pressures developed are usually positive and hence it can be directly linked to the cyclic degradation (Matasovic, et al. 1995). However, in overconsolidated clays, negative pore water pressure may develop at the beginning of cyclic loading, despite the fact that degradation of soil stiffness and strength may occur simultaneously (Matasovic, et al. 1995). For cohesive soils, the undrained strength degradation caused by undrained cyclic loading can be recovered due to drainage after cyclic loading, combined with returning to the original effective stress, except for sensitive clay and peat (Yasuhara, 1994). Poulos (1982) found that the effect of cyclic degradation is more severe for stiff soils than for soft soils. It is important to note that additional research is necessary before any conclusion can be drawn.

From the above brief literature review, one can see that strength and stiffness degradation of both cohesive and cohesionless soils due to cyclic loading may be important; but, currently we lack a comprehensive understanding, particularly in relation to laterally loaded drilled shafts. Certainly, more in-depth research in this subject area is warranted. Without further investigation, the recommended design methods should still work fine. Because the Broms method is conservative, as discussed in section 4.4.1, the actual factor of safety is larger than the recommended value of two in the design. Cyclic degradation is expected to occur more in cohesive soils and in the upper portion of the soil layer. However, the soil resistance in the upper 1.5 diameters of the shaft was not considered in the Broms method. Thus, this will take care of any degradation. Furthermore, for sound wall, the main lateral force is wind force which may increase the cohesive soils' undrained strength due to high loading rate. The loading rate effect may also offset the degradation from cyclic loading.

4.5.3 The Effect of Soil Saturation

For sand, it is not necessary to consider the effect of saturation since the sand friction angle does not vary with water content significantly. Bhushan and Askari (1984) observed that an increment less than 10% of deflection resulted from saturating the sand.

In clay, for capacity estimation, the water content effect can be considered by using the highest possible elevation of water at the site and then using saturated strength parameter for soil under

the water table and in-situ strength for water above water table. For serviceability design, the same soil parameters can be selected as that done in capacity prediction, and then use the appropriate p-y curve criteria (above or below water table) by using COM624P (LPILE).

4.5.4 The Effect of Moment Arm

During the course of this study, it was observed that all the prediction methods, including the Broms method, the Brinch Hansen method, and the COM624P program, provide very conservative capacity estimates for shafts with large applied moments, as shown in Table 4.11 and Figs. 4.11 through 4.13. It would be of great savings, if the conservatism can be accounted for in the design. We believe that the "pull-push" effect on shaft under large applied moment might result in vertical soil friction on two side of the shaft with opposite direction and thus providing additional resistance to the applied moment at the shaft head. The scenario is illustrated in Fig. 4.23. This pull-push effect can be quantified by measuring or analyzing the moments resulting from vertical soil resistance. Either strain gages at the top portion of shaft or friction measurement device can be used to measure this effect in future lateral load tests.

4.5.5 Calibration of Resistance Factors for Lateral Design of Drilled Shafts

4.5.5.1 Resistance Factors for Drilled Shafts in Clay

In order to convert from Allowable Stress Design (ASD) to Load Resistance Factor Design (LRFD) for the lateral design of drilled shafts supporting sound walls, it is required to calibrate resistance factors either by reliability method or by fitting to the ASD method. The reliability method is a statistical approach, which requires the statistics on soil strength variations and load variations. Fitting to the ASD method is an approach to choose resistance factors that will, on average, result in the same factors of safety as would from ASD.

The calibration of resistance factors for the calculation of the lateral capacity of drilled shafts in clay will be presented here. First, the reliability method will be used to calibrate the resistance factors, then, fitting to the ASD method will be used to obtain resistance factors. The resistance factors from both calibration methods will be compared at the end of this section.

4.5.5.1.1 Reliability Method

4.5.5.1.1.1 Resistance Statistics

There are at least two kinds of uncertainties on resistance, one is the variation in the capacity prediction model, and the other one is the uncertainties involved in the soil parameters determination. For both uncertainties, two variables are required: one is the bias factor (λ) which is equal to the measured value over predicted value, and the other one is the coefficient of variance (COV) which is equal to the standard deviation over mean value.

In order to obtain the resistance statistics of the Broms method, a database including the measured lateral capacity and the predicted capacity by the Broms method is necessary. The lateral load tests conducted in Ohio for sound wall design is chosen as the database. Table 4.19 shows the lateral load test results for drilled shafts in clay and predicted capacity by the Broms method. The bias factor, λ_{RB}, is also included. The mean of the bias factor, shown in Table 4.19, is 1.63.

Table 4.19 Database on Measured and Predicted Lateral Capacities in Clay

Shaft	Measured	Broms' Method	λ_{RB}
1	92	90	1
2	78	73	1.1
3	85	123	0.7
4	161	67	2.4
5	71	34	2.1
6	70	28	2.5

The value of the coefficient of variance on the prediction model, COV_{RB}, could be estimated using a rule-of-thumb, known as the "six sigma" rule. The use of the "six sigma" rule involves three simple steps. The first step is to estimate the most likely value of the property (V_{est}), which usually is the mean value, the lowest conceivable value (V_{min}), and the largest conceivable value (V_{max}). Then, in the second step, one could use the "six sigma" rule to estimate the value of the standard deviation (σ):

$$\sigma = \frac{V_{max} - V_{min}}{6} \tag{4.2}$$

The third step is to calculate the coefficient of variance (COV) by:

$$COV = \frac{\sigma}{V_{est}} \tag{4.3}$$

Therefore, the COV_{RB} of the bias factors is 0.18 according to the "six sigma" rule outlined above.

The uncertainties involved in determining the soil parameters lie in the test procedures and interpretation methods. In this case, SPT test was used to estimate the shear strength of clay. The study by Orchant et al. (1988) on the variation of SPT test, shown in Table 4.20, is adopted for determining the COV of the SPT test. The value of 0.45 is chosen for COV of SPT test for conservative reasons. The bias factor for the SPT test is assumed to be 1.0 since no database is available. Because of the lack of data for estimating the variation on SPT result interpretation, the uncertainty in this aspect is ignored for this calibration. Therefore, the bias factor on soil parameter determination, λ_{RS}, is assumed as 1.0 and the coefficient of variance on soil parameter determination, COV_{RS}, is chosen as 0.45.

Table 4.20 COVs for Various In-Situ Tests (After Orchant et al., 1988)

Test	COV Equipment	COV Procedure	COV Random	COV Total	COV Range
SPT	0.05-0.75	0.05-0.075	0.12-0.15	0.14-1.0	0.15-0.45
MCPT	0.05	0.10-0.15	0.10-0.15	0.15-0.22	0.15-0.25
ECPT	0.03	0.05	0.05-0.10	0.07-0.12	0.05-0.15
VST	0.05	0.08	0.10	0.14	0.10-0.20
PMT	0.05	0.12	0.10	0.16	0.10-0.20

After the bias factors and COVs are obtained, they should be combined into one value to represent the total uncertainties as follows:

$$\lambda_R = \lambda_{RB} \cdot \lambda_{RS} \tag{4.4}$$

$$COV_R = \sqrt{COV_{RB}^2 + COV_{RS}^2} \tag{4.5}$$

in which, λ_R is the bias factor on resistance side, and COV_R is the coefficient of variance on resistance side. Therefore, for this calibration study, $\lambda_R = 1.63$ and $COV_R = 0.48$.

4.5.5.1.1.2 Load Statistics

For sound wall design, only the wind load is considered as a lateral load. The bias factor for the wind load (live load), λ_L, is assumed as 1.0 due to the lack of load information. The COV of wind load, COV_L, is chosen as 0.18 from Nowak (1992)'s study on bridge loads as shown in Table 4.21. The load factor for wind load, γ_L, is 1.4 according to AASHTO specification (2003).

Table 4.21 Statistics for Bridge Load Components (After, Nowak, 1992)

Load Component	Bias, λ	COV
Dead Load		
Factory-made	1.03	0.08
Cast-in-place (CIP)	1.05	0.10
Asphaltic wearing surface	1.00	0.25
Live Load (w. dynamic load allowance)	1.1-1.2	0.18

4.5.5.1.1.3 Target Reliability Index

For drilled shaft design, the target reliability index, β_T, could range from 2.5 to 3.0 according to Table 4.22. For this calibration study, both 2.5 and 3.0 will be used for evaluation.

Table 4.22 Values of Target Reliability Index β_T (Barker, et al. 1991)

Foundation Type	β_T
Spread Footings	3.0 to 3.5
Drilled Shafts	2.5 to 3.0
Driven Piles (group)	2.0 to 2.5

4.5.5.1.1.4 Calculation of Resistance Factors

Based on the above obtained variables, the resistance factors, Φ, for lateral capacity based design of drilled shafts supporting sound walls by using the Broms method can be obtained from the following equation:

$$\phi = \frac{\dfrac{\lambda_R \gamma_L}{\lambda_L} \sqrt{\dfrac{1+COV_L^2}{1+COV_R^2}}}{\exp\{\beta_T \sqrt{\ln[(1+COV_L^2)(1+COV_R^2)]}\}}$$
(4.6)

The calibrated resistance factors are provided in Table 4.23.

Table 4.23 Resistance Factors for Drilled Shafts in Clay by Using Reliability Method

Target Reliability Index β_T	Resistance Factor Φ
2.5	0.62
3.0	0.48

4.5.5.1.2. Fitting to ASD

The values of resistance factors can also be determined by "fitting" the value of Φ to the conventional factor of safety that would be used in allowable stress design. The resistance factor estimated by fitting to the ASD can be calculated from the following equation.

$$\phi = \frac{\gamma_D(Q_D/Q_L)+\gamma_L}{FS(1+Q_D/Q_L)} = \frac{\gamma_L}{FS}$$
(4.7)

in which Q_D = dead load, Q_L= live load, FS = factor of safety. In this case, the dead load is not involved; thus, it is simplified to its final expression shown in Equation 4.7. The recommended factor of safety for sound wall design is 2.0. Finally, the resistance factor is 0.7 by using fitting to the ASD method, which is larger than the resistance factor obtained from the reliability method for a target reliability index of 2.5 by 11%. If a factor of safety equal to 3 is chosen, the fitted resistance factor is 0.47, which is almost the same as the one obtained by the reliability method for a target reliability index of 3, as shown in Table 4.24.

Table 4.24 Values of Φ Calculated Using Fitting to ASD Method

Factor of Safety	Resistance Factor, Φ	Compare with Reliability Method
2.0	0.7	+11%
3.0	0.47	0%

4.5.5.2 Resistance Factors for Drilled Shafts in Sand

Similar to the calibration work done in the previous section for drilled shaft in clay, the same procedure is followed to calibrate the resistance factors for drilled shafts in sand. Table 4.25 provides calculated bias factors based on Bhushan et al. (1981)'s test data. The mean value of the bias factor is 1.94.

Table 4.25 Database on Measured and Predicted Lateral Capacities in Sand

Shaft	Measured	Broms Method	λ_{RB}
1	337	190	1.8
2	316	102	3.1
3	325	177	1.8
4	307	177	1.7
5	342	260	1.3

The value of the coefficient of variance on the prediction model, COV_{RB}, is 0.15 by using the "six sigma" rule.

Similar to the previous section, the bias factor on soil parameter determination, λ_{RS}, is assumed as 1.0 and the coefficient of variance on soil parameter determination, COV_{RS}, is chosen as 0.45.

After the bias factors and COVs are obtained, they should be combined into one value to represent the total resistance uncertainties, resulting in $\lambda_R = 1.94$ and $COV_R = 0.47$.

The values for load statistics are the same as before. The calibrated resistance factors are shown in Table 4.26 for a target reliability index of 2 and 3. Similar to the procedure used before for clay, the resistance factors based on fitting to ASD method are shown in Table 4.27.

Table 4.26 Resistance Factors for Drilled Shaft in Sand by Using Reliability Method

Target Reliability Index β_T	Resistance Factor Φ
2.5	0.75
3.0	0.59

Table 4.27 Values of Φ Calculated Using Fitting to ASD Method

Factor of Safety	Resistance Factor, Φ	Compare with Reliability Method
2.0	0.7	-7%
3.0	0.47	-20%

The above two calibration examples for drilled shafts in clay and sand presented the procedure to calibrate the resistance factors for drilled shaft design by using the reliability method and fitting to the ASD method. Although some assumptions were involved in the determination of resistance statistics and load statistics, the reliability method provides comparable results with the fitting to the ASD method. The resistance factor could be chosen from Tables 4.23, 4.24, 4.26, and 4.27 for drilled shafts in clay and sand, respectively.

P

10 ft

Case 1: 15' sand

Case 2: 15' clay

15 ft

2.5 ft
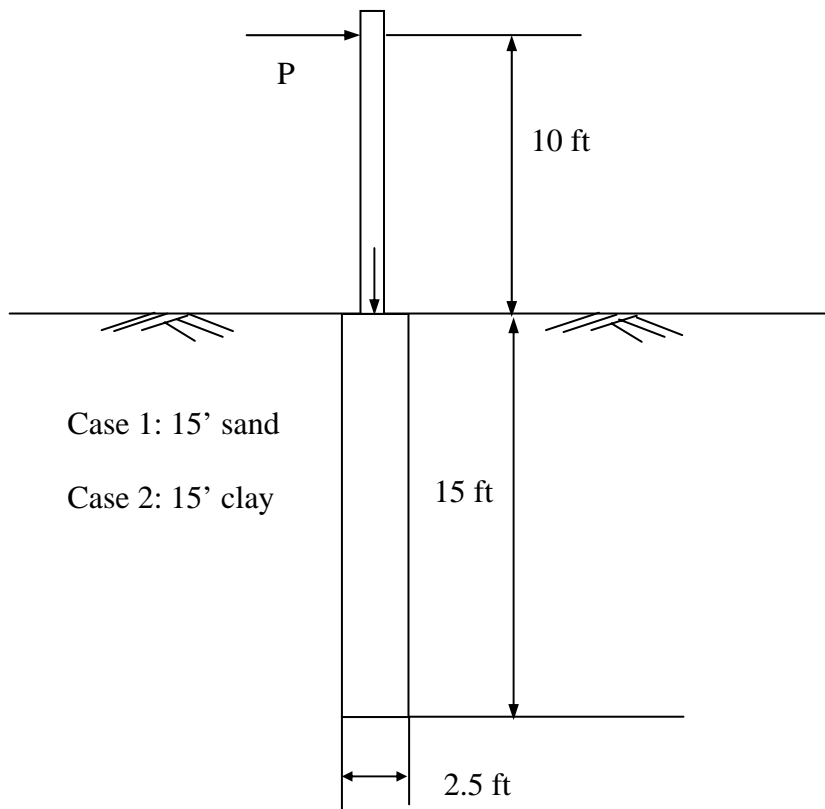
Figure 4.1 Schematic representation of soil profile and drilled shaft dimensions for lateral response in hypothetical cases
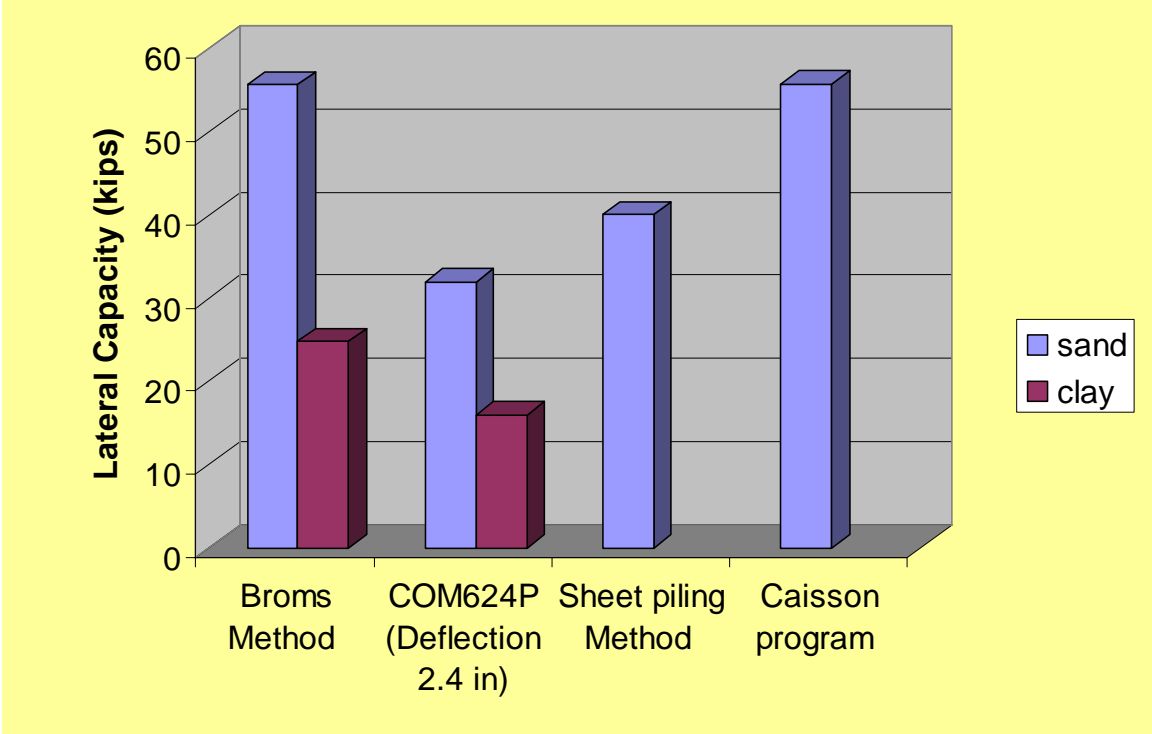
Figure 4.2 Comparison of calculated lateral capacities for hypothetical cases
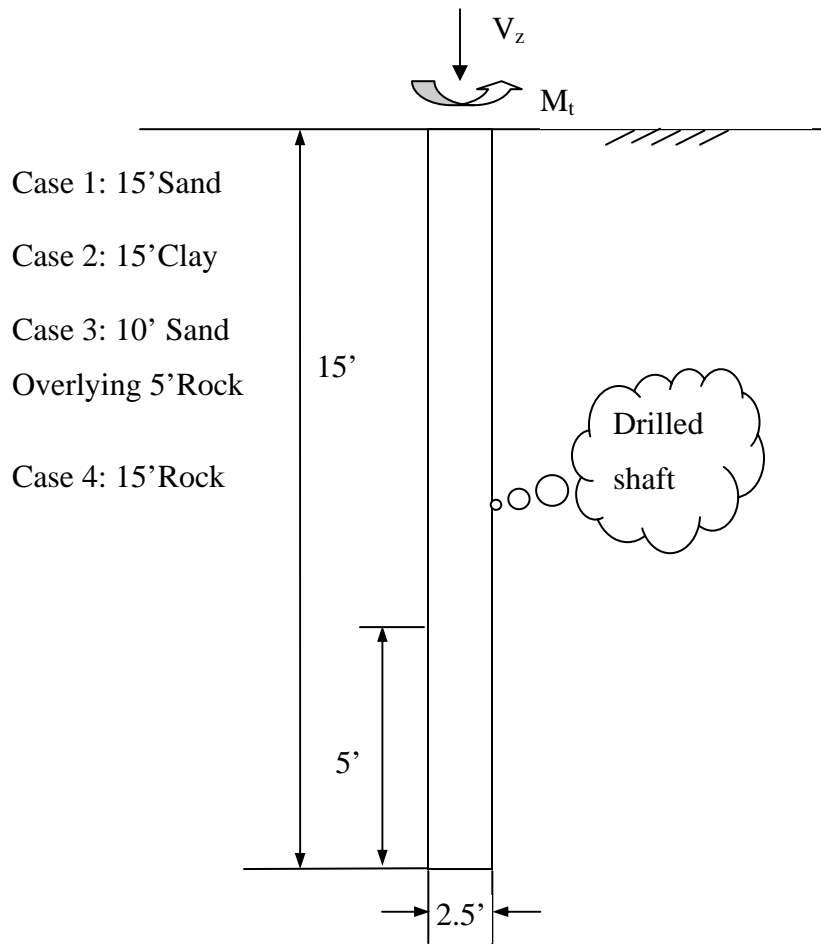
Figure 4.3 Assumed soil profiles and drilled shaft dimensions for torsional responses in hypothetical cases
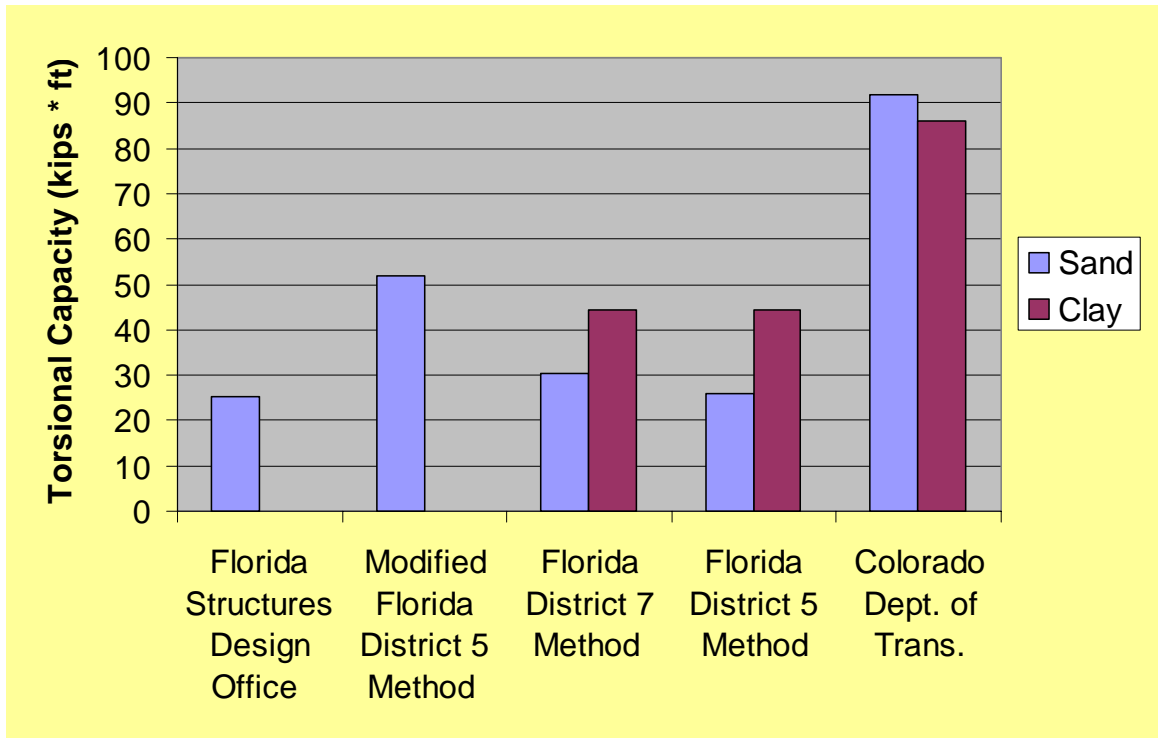
Figure 4.4 Comparison of calculated torsional capacity for hypothetical cases
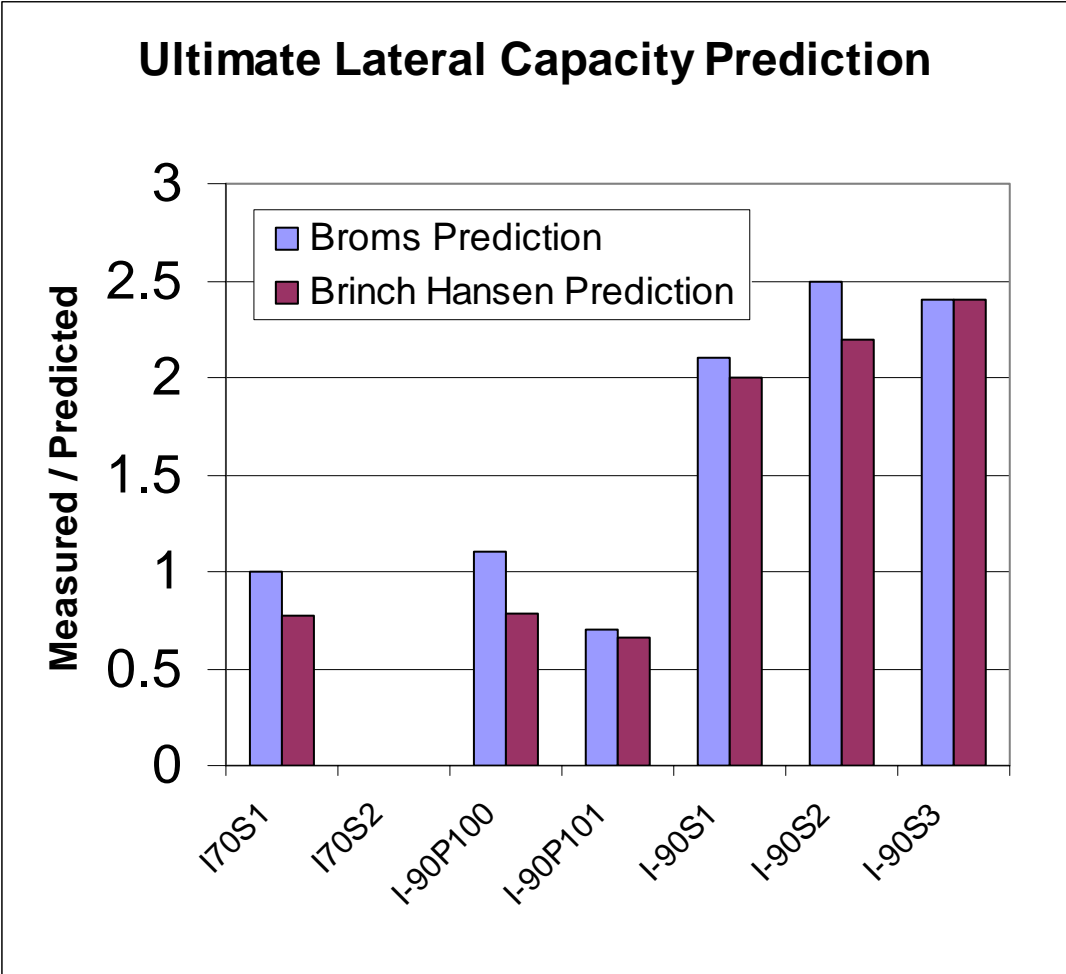
Figure 4.5 Measured over-predicted capacities of drilled shafts in clay based on load test database
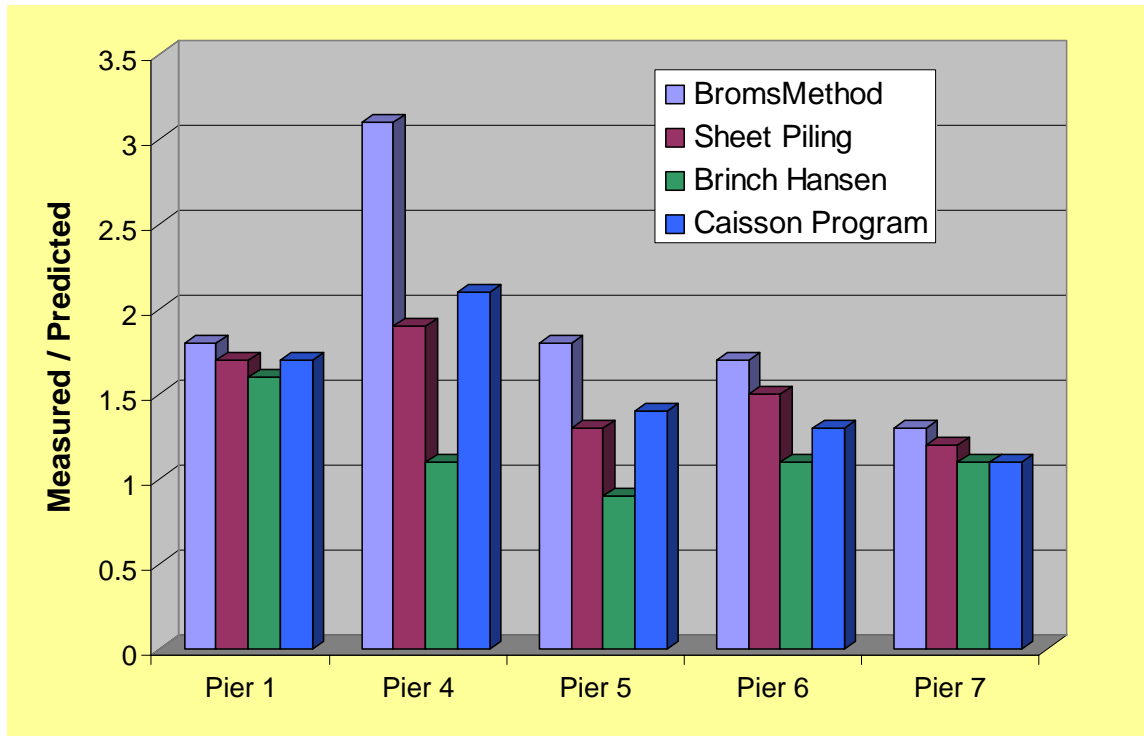
Figure 4.6 Measured over-predicted capacities of drilled shafts in sand based on load test database
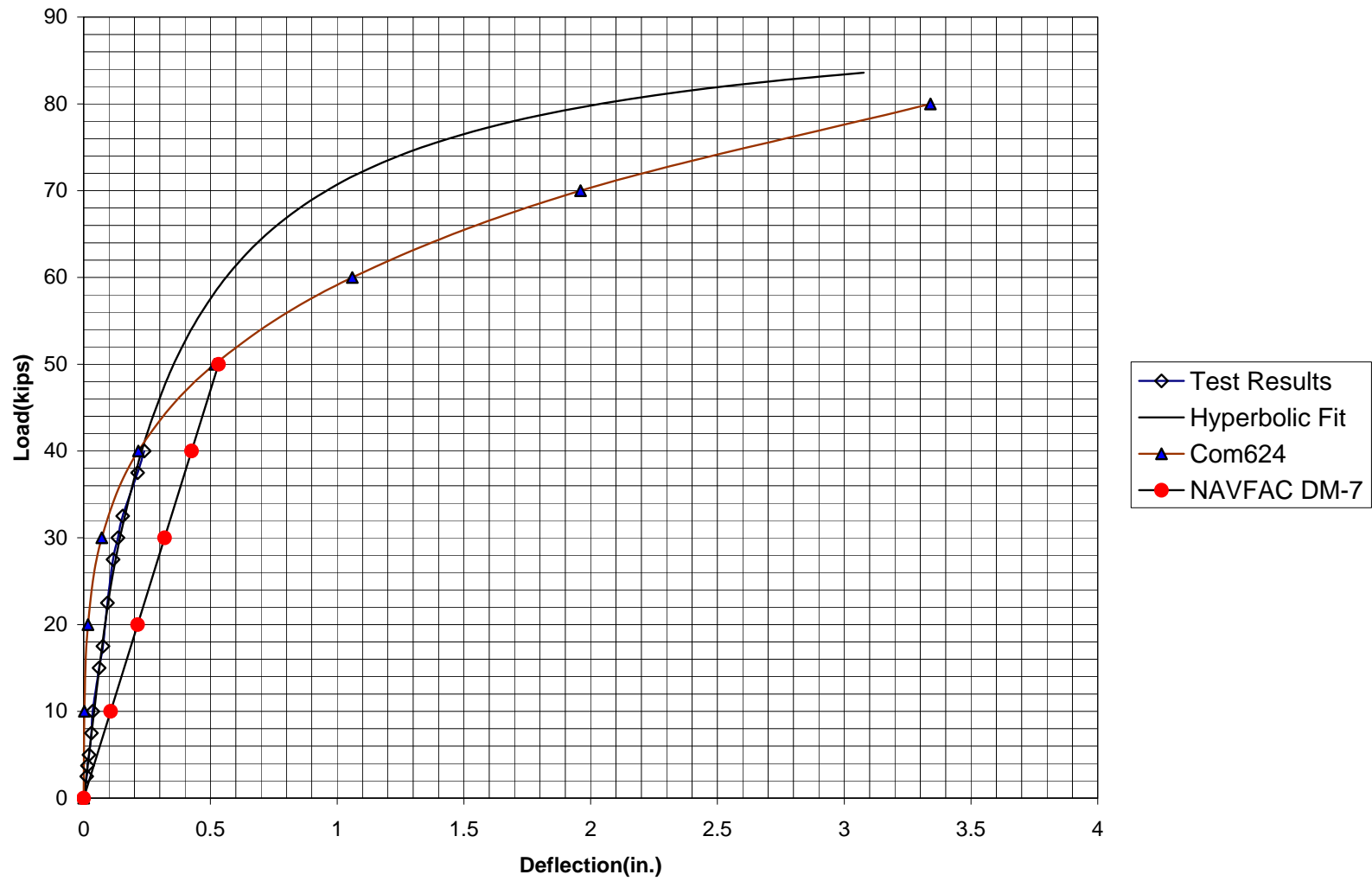
Figure 4.7 I-70 sound barriers, Columbus OH, shaft 1, lateral load-deflection curves
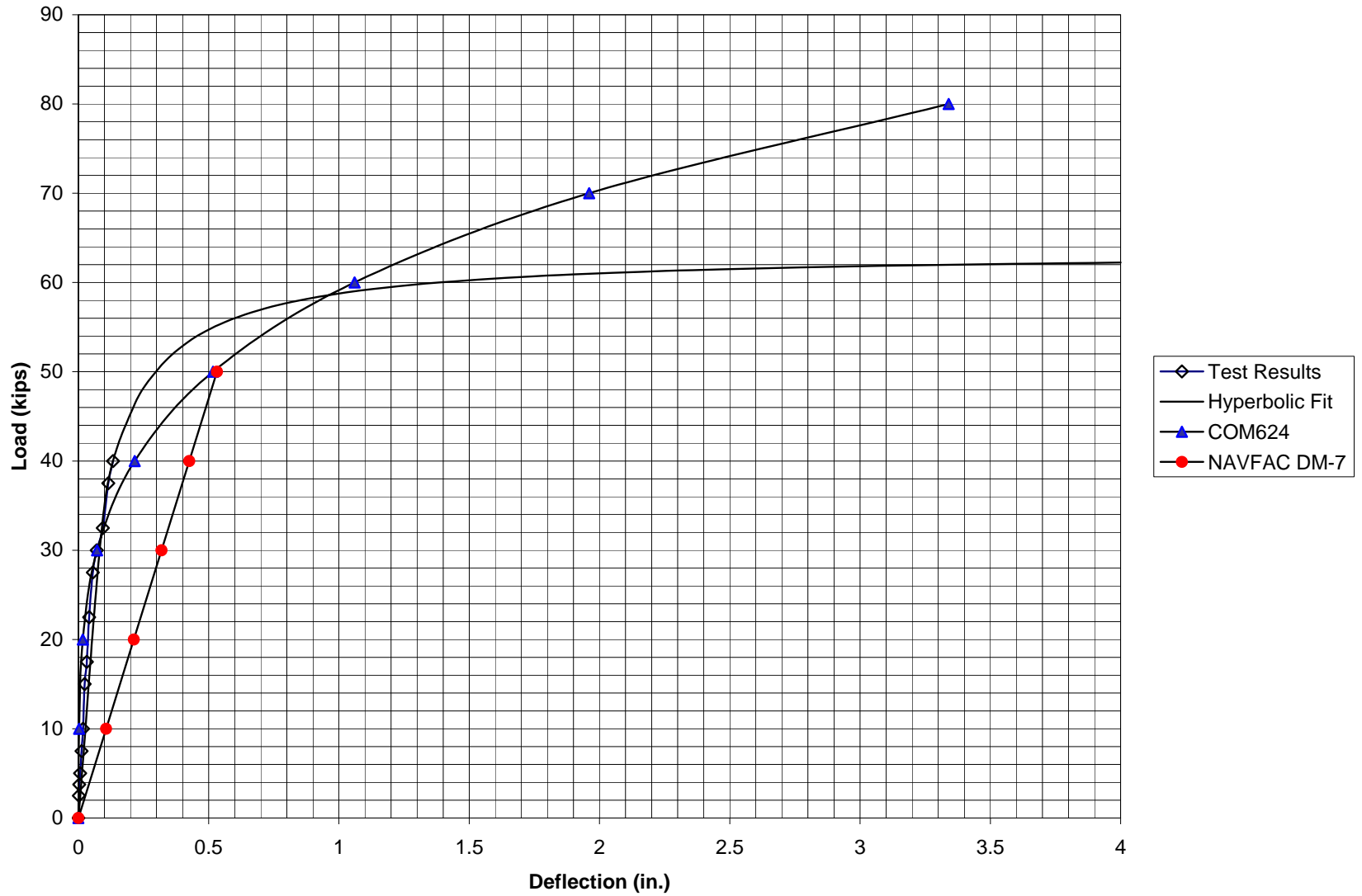
Figure 4.8 I-70 sound barriers, Columbus OH, shaft 2, lateral load-deflection curves
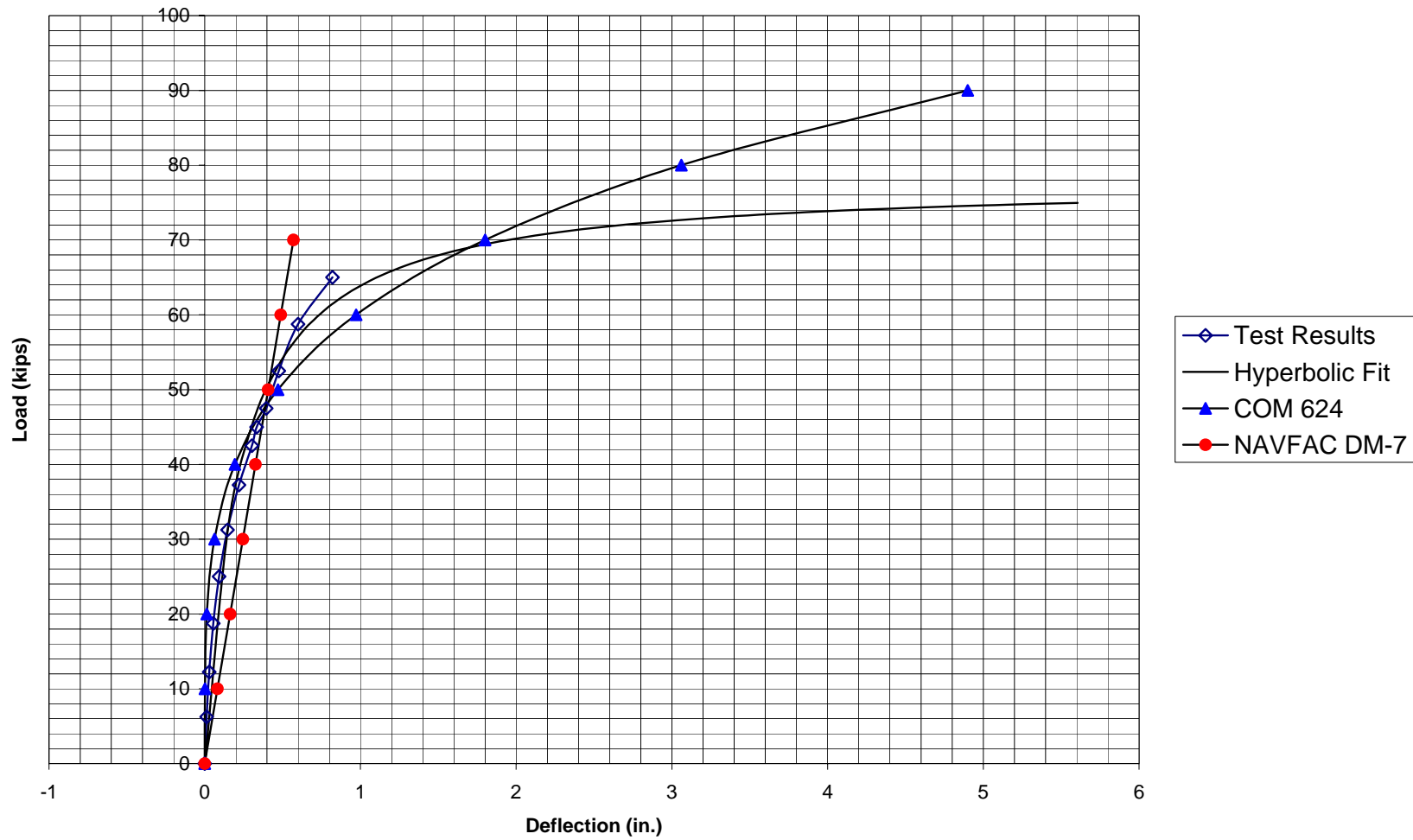
Figure 4.9 I-90 sound barriers, shaft 100 lateral load-deflection curves
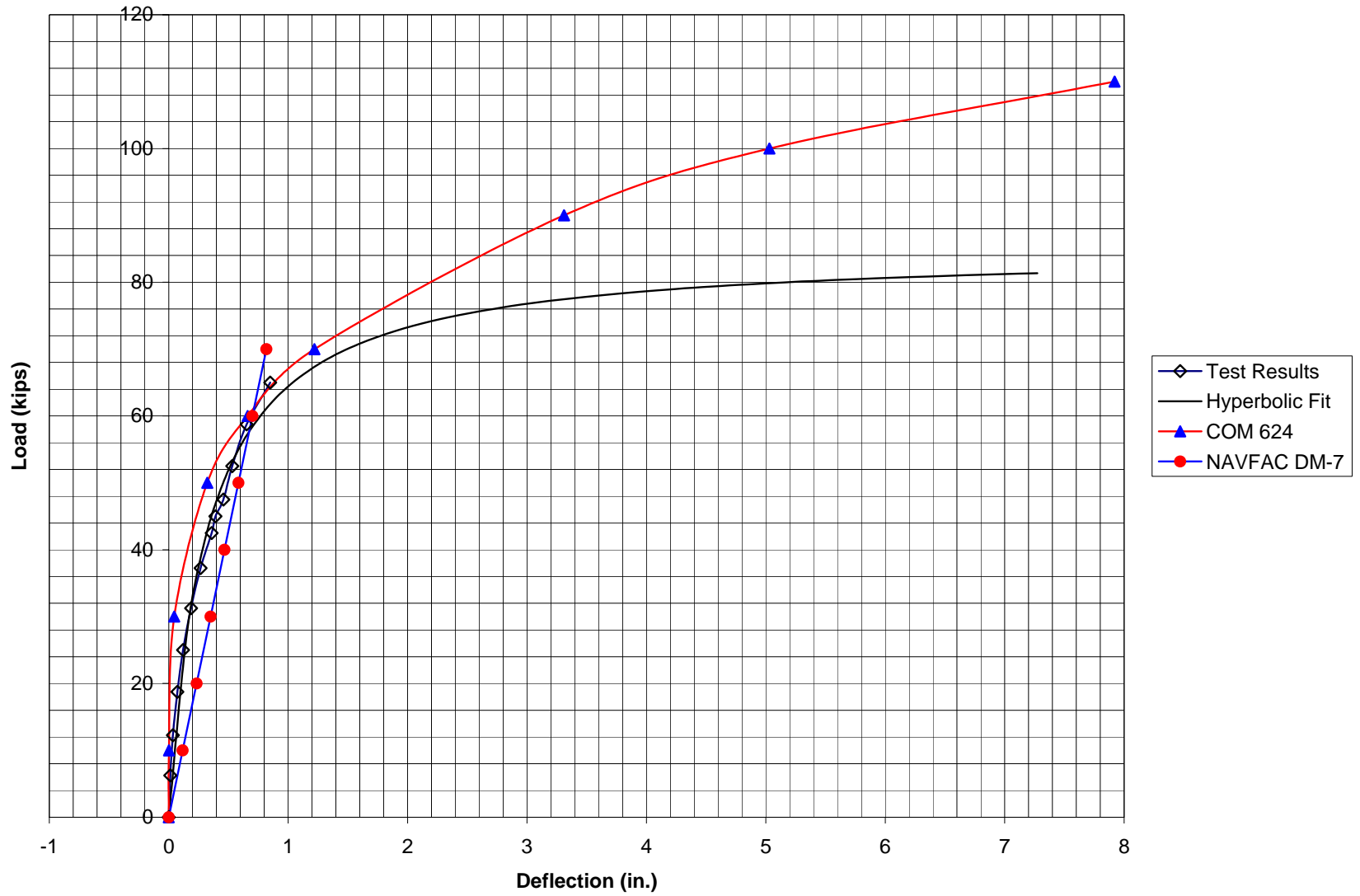
Figure 4.10 I-90 sound barriers, shaft 101, lateral load-deflection curves
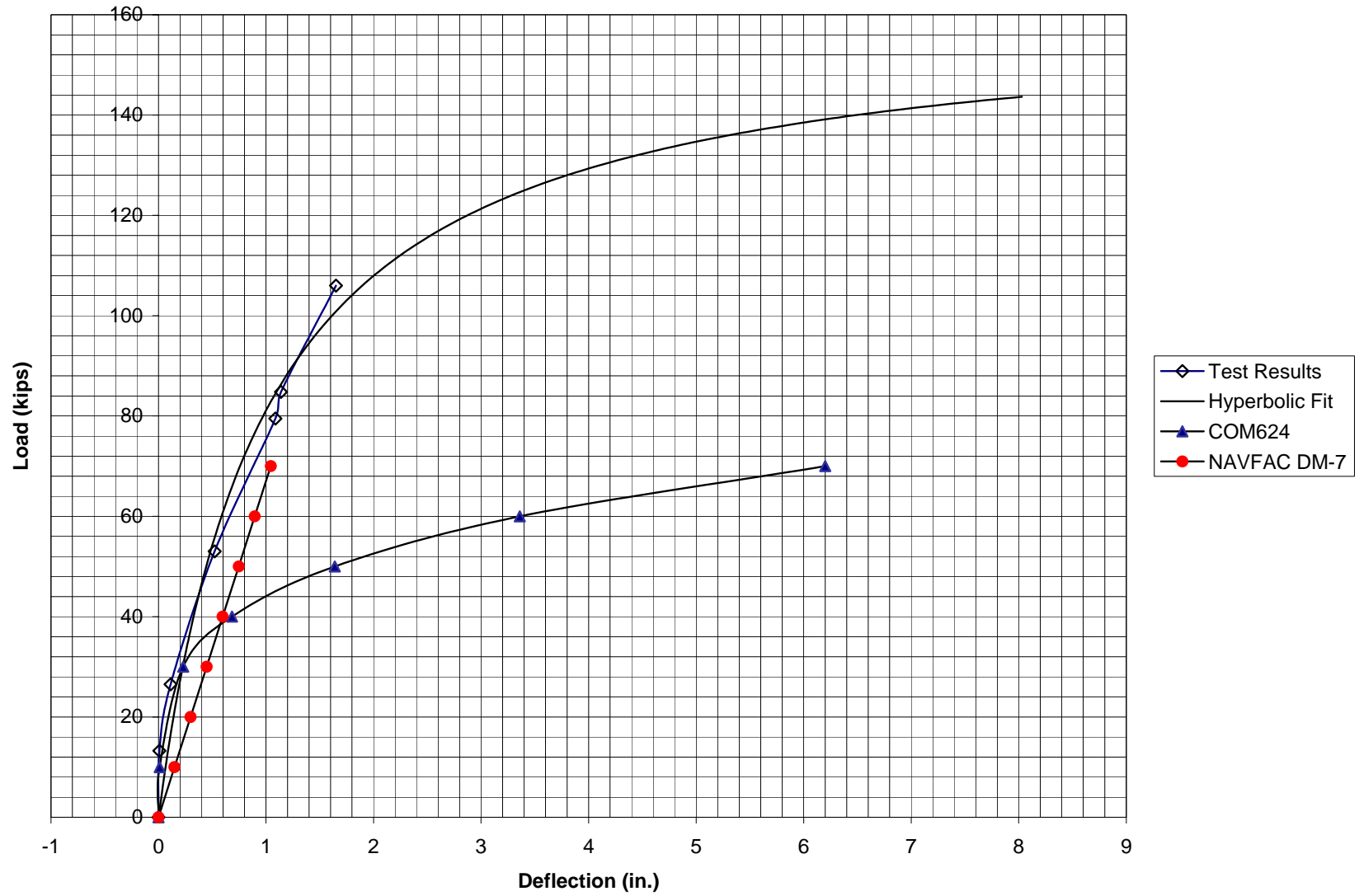
Figure 4.11 I-90 sound barriers, 12 ft depth, shaft 2, lateral load-deflection curves
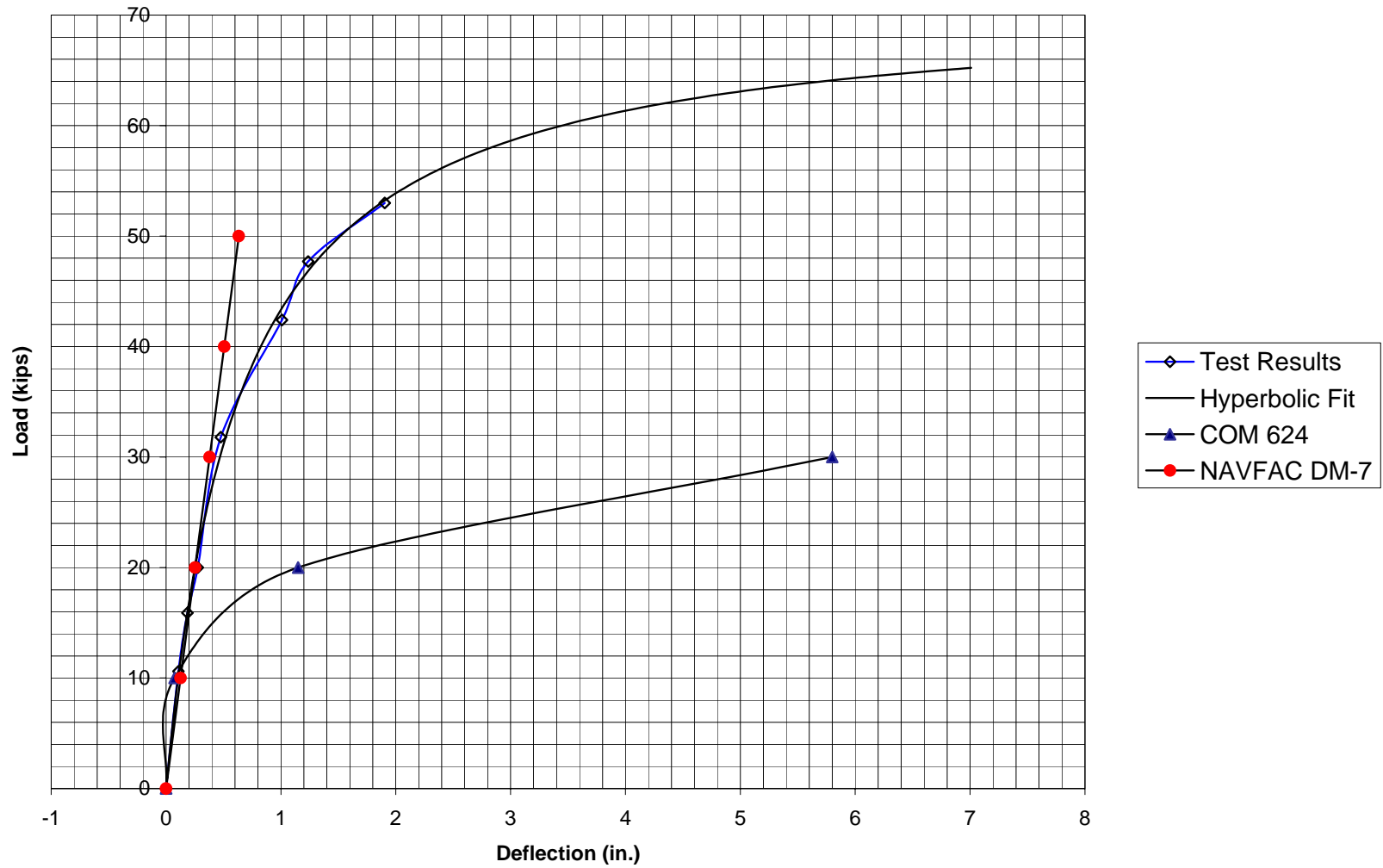
Figure 4.12   I-90 sound barriers, 8 ft depth, shaft 1 lateral load-deflection curves
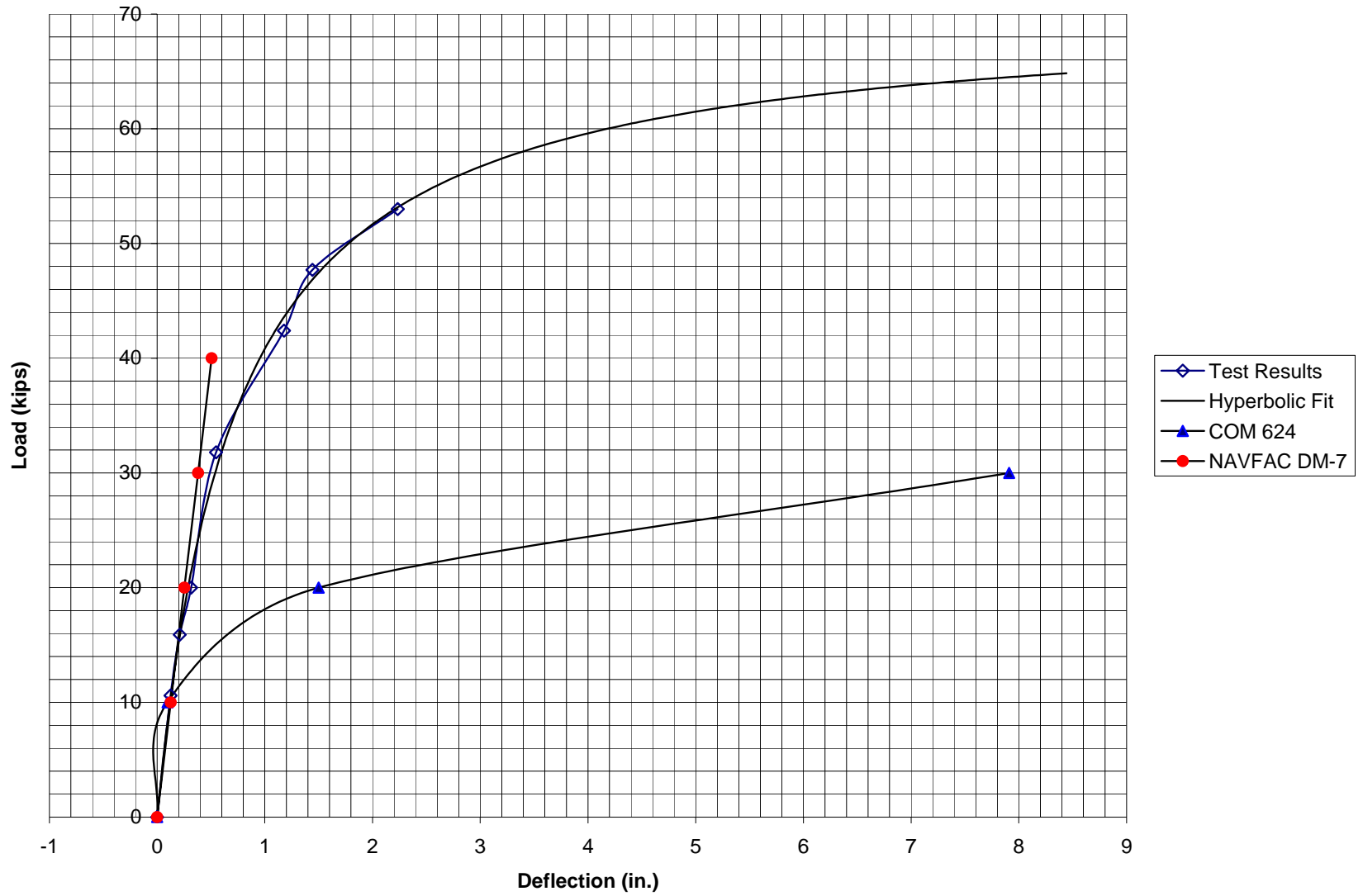
Figure 4.13   I-90 sound barriers, 8 ft depth, shaft 2 lateral load-deflection curves
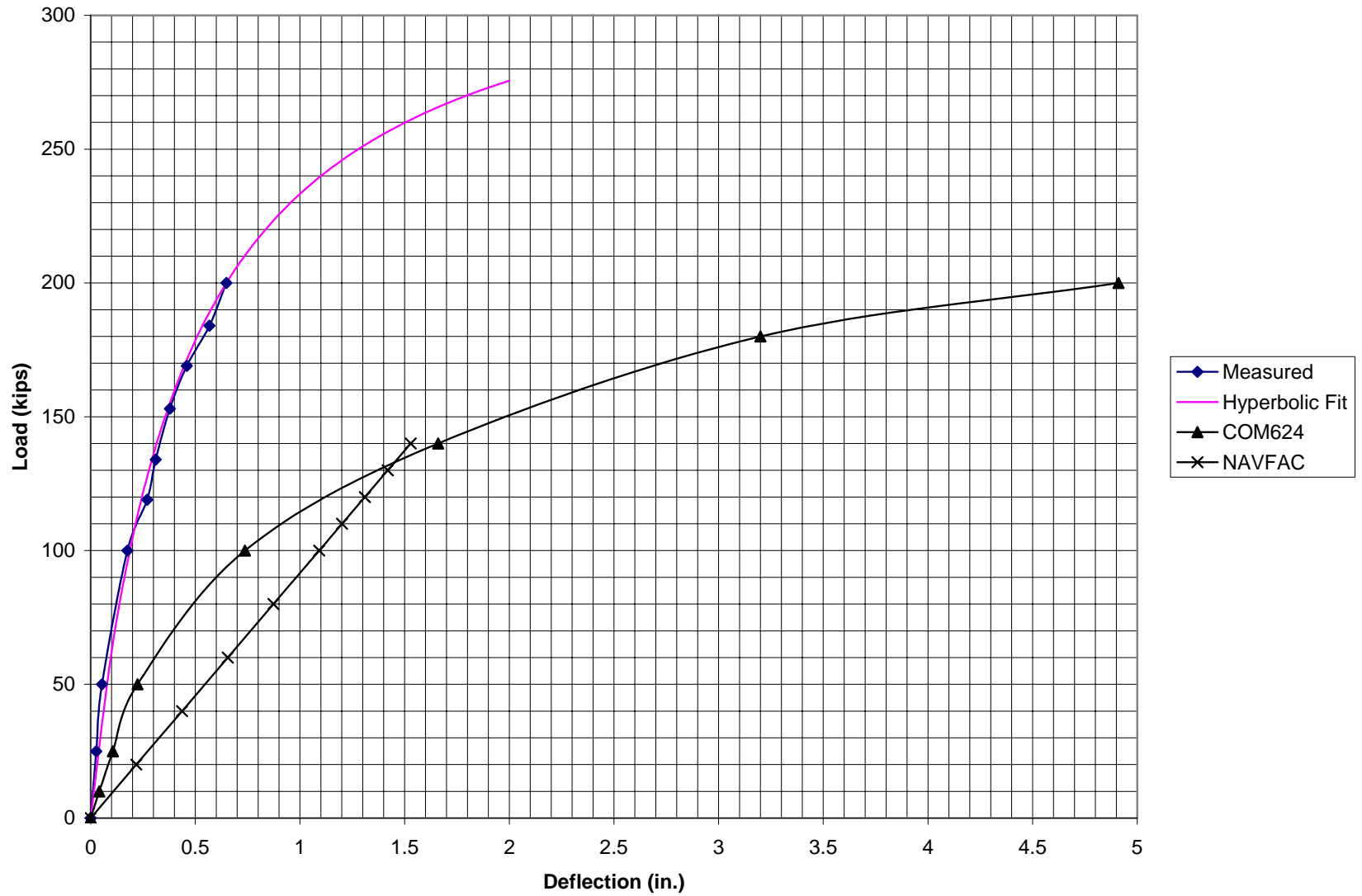
Figure 4.14   Bhushan et al. (1981), pier 1 lateral load-deflection curve
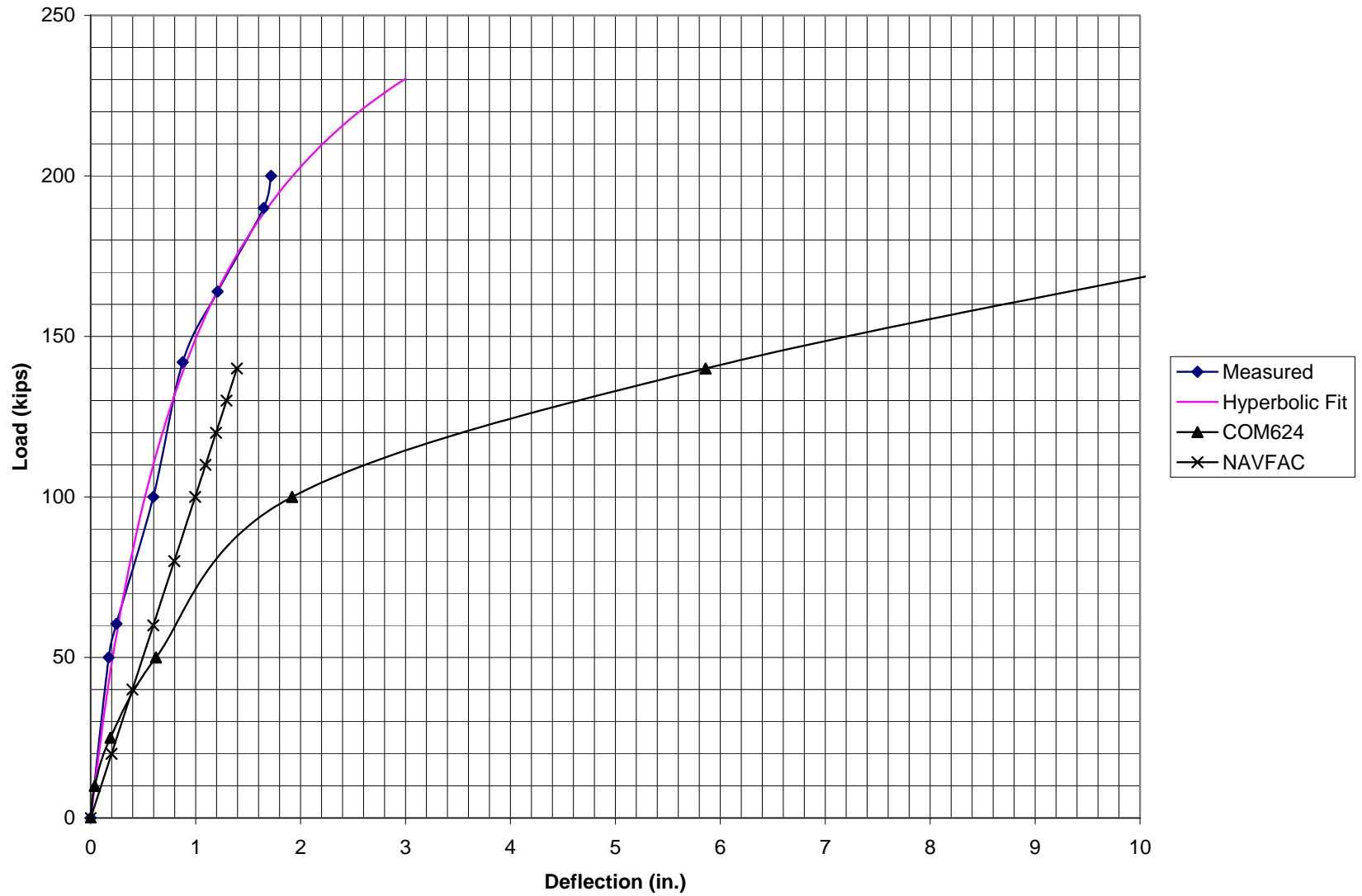
Figure 4.15   Bhushan et al. (1981), pier 4 lateral load-deflection curve
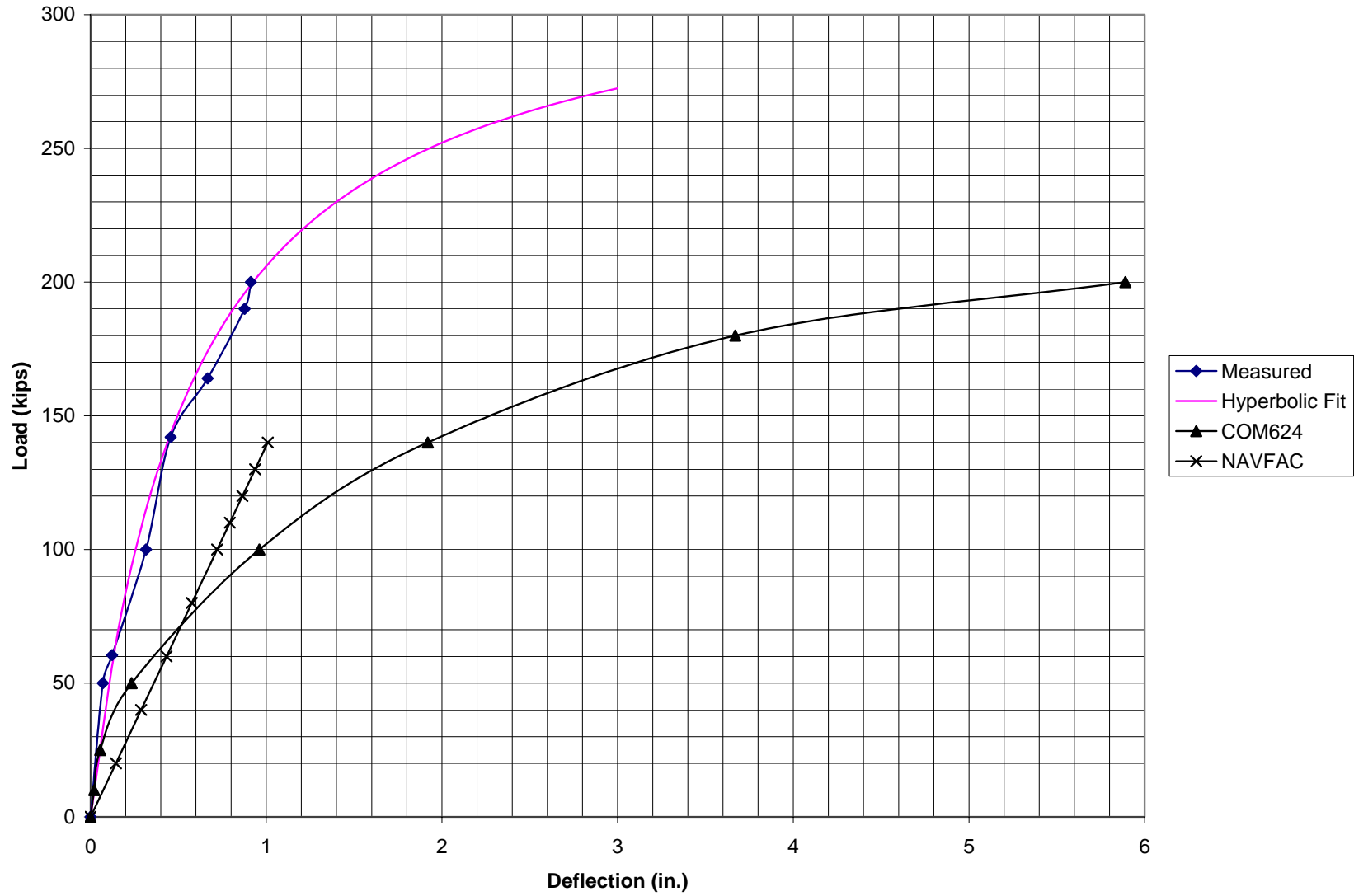
Figure 4.16   Bhushan et al. (1981), pier 5 lateral load-deflection curve
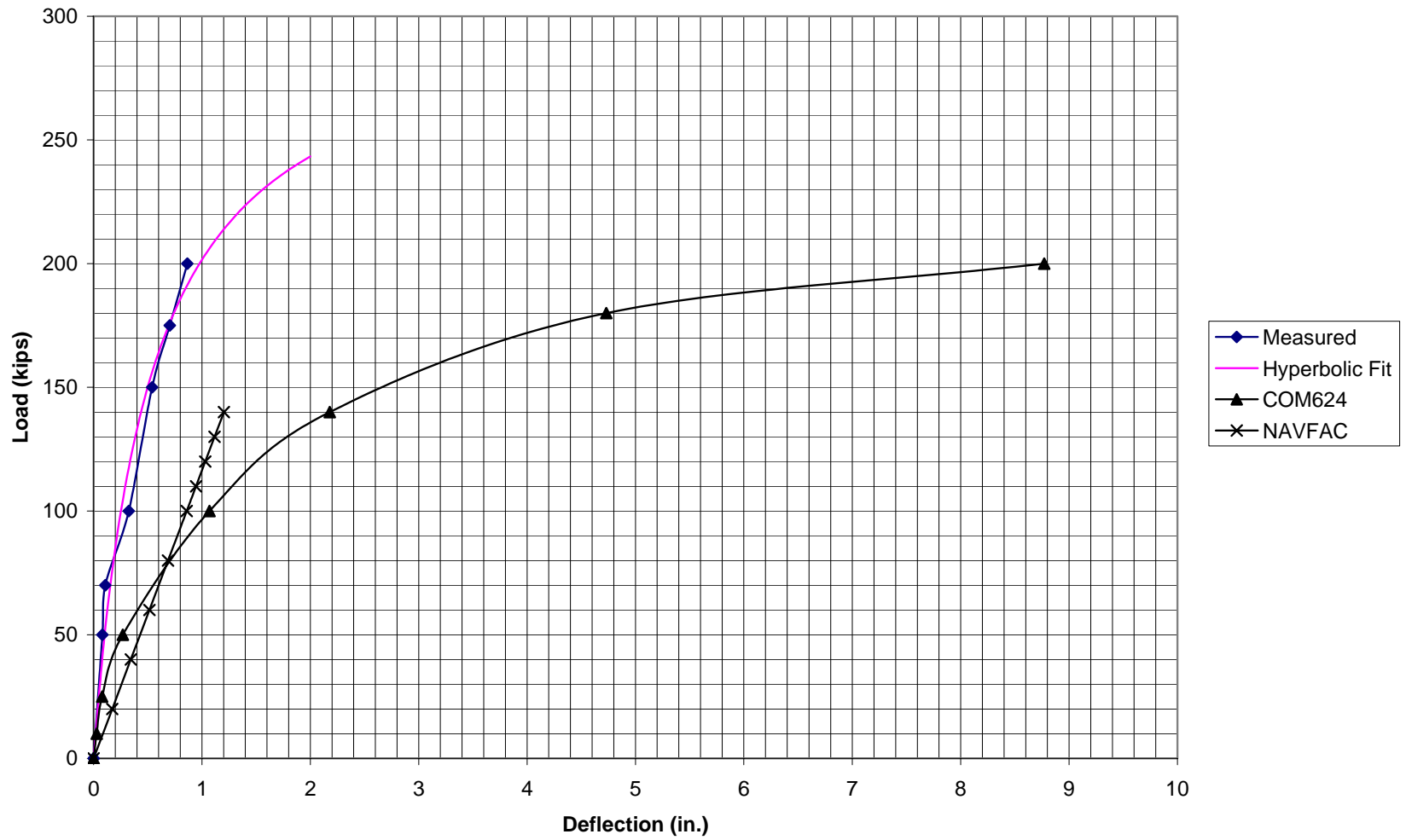
Figure 4.17   Bhushan et al. (1981), pier 6 lateral load-deflection curve
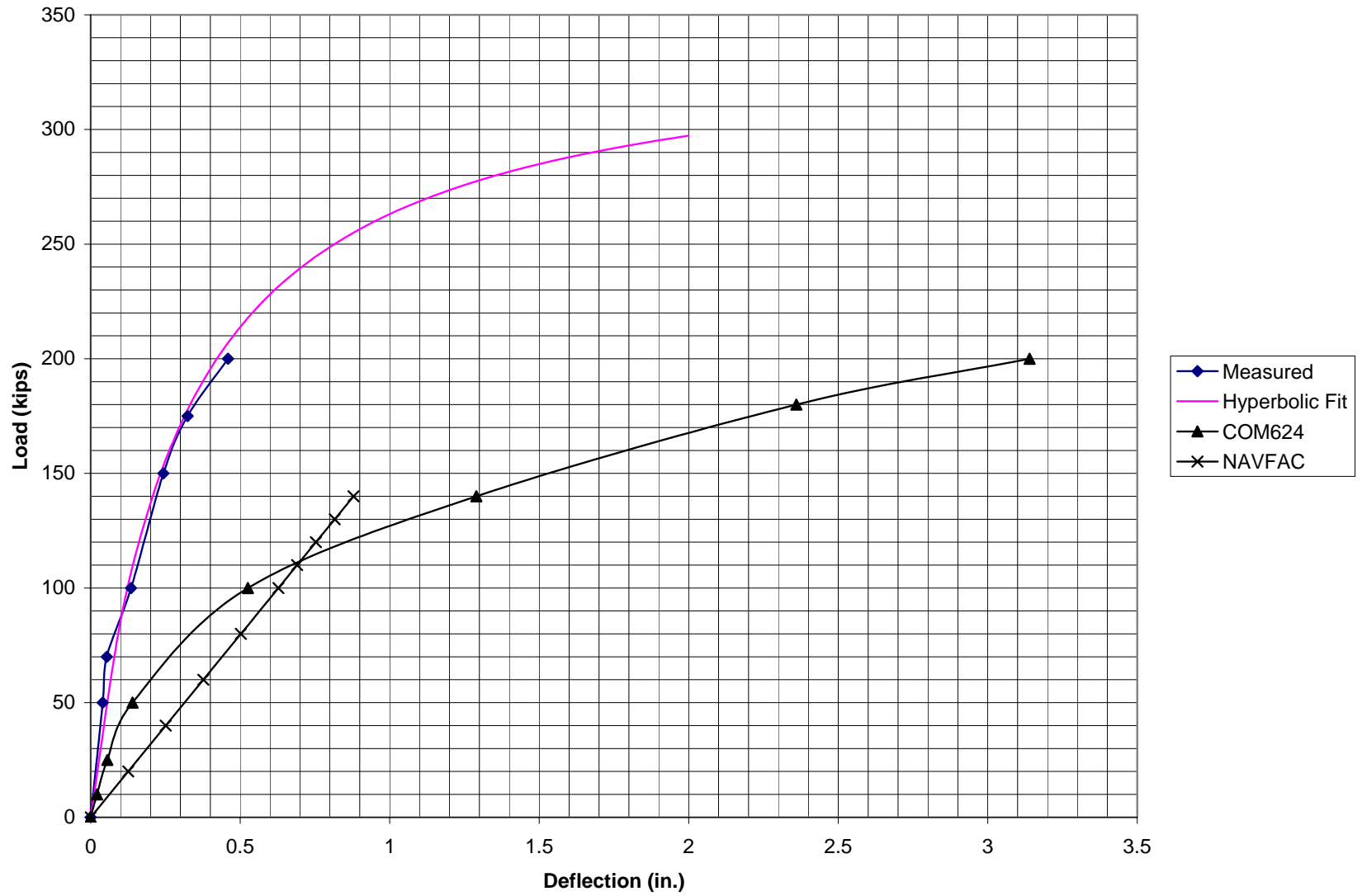
Figure 4.18   Bhushan et al. (1981), pier 7 lateral load-deflection curve
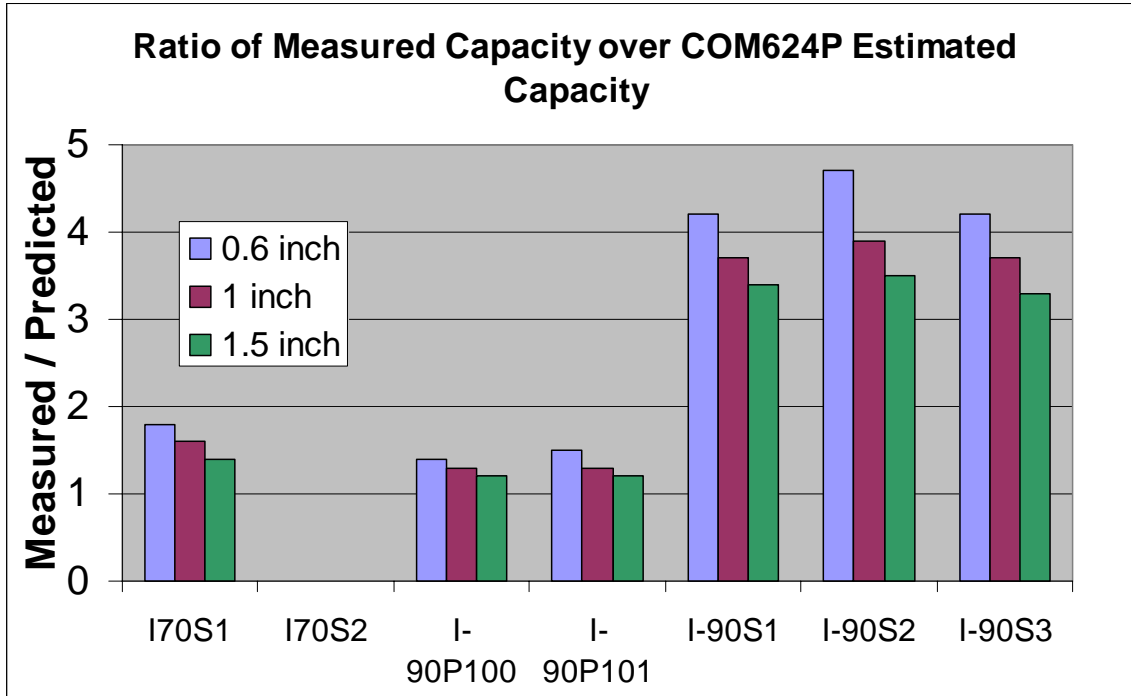
Figure 4.19 Measured over-predicted capacities of drilled shafts in clay at various permissible deflections
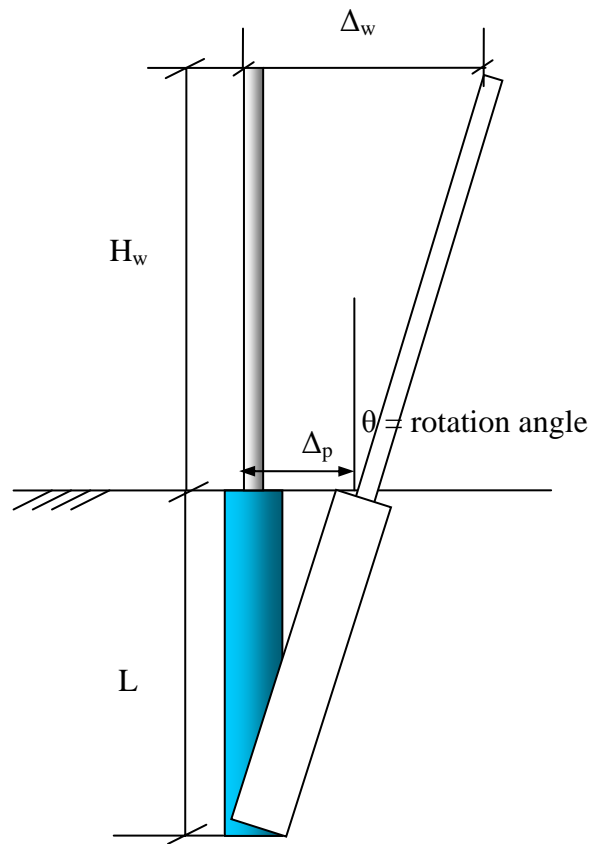
Figure 4.20 The assumed drilled shaft and sound wall deflection under lateral load
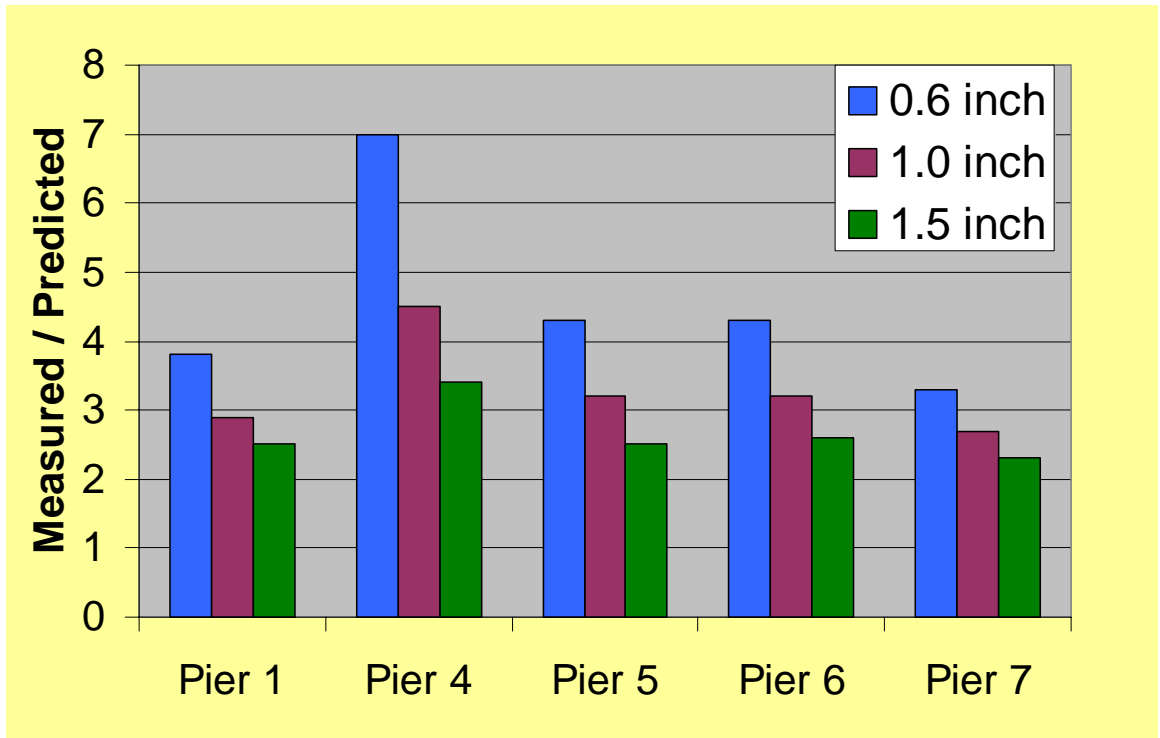
Figure 4.21 Measured over-predicted capacities of drilled shafts in sand at various permissible deflections
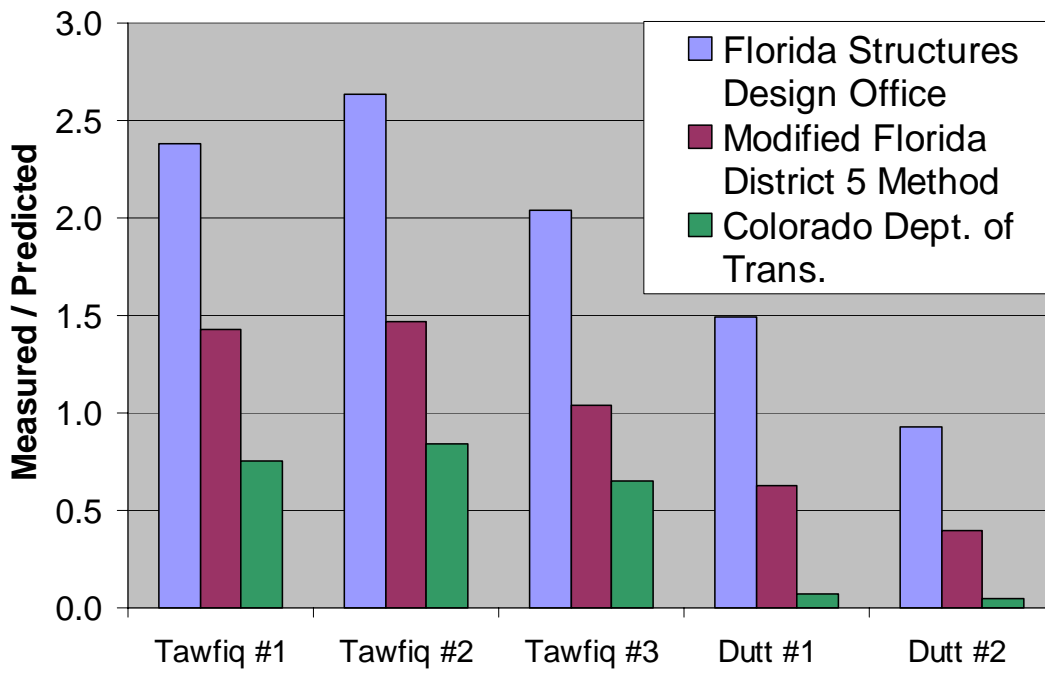
Figure 4.22 Measured over-predicted torsional capacities of drilled shafts in sand
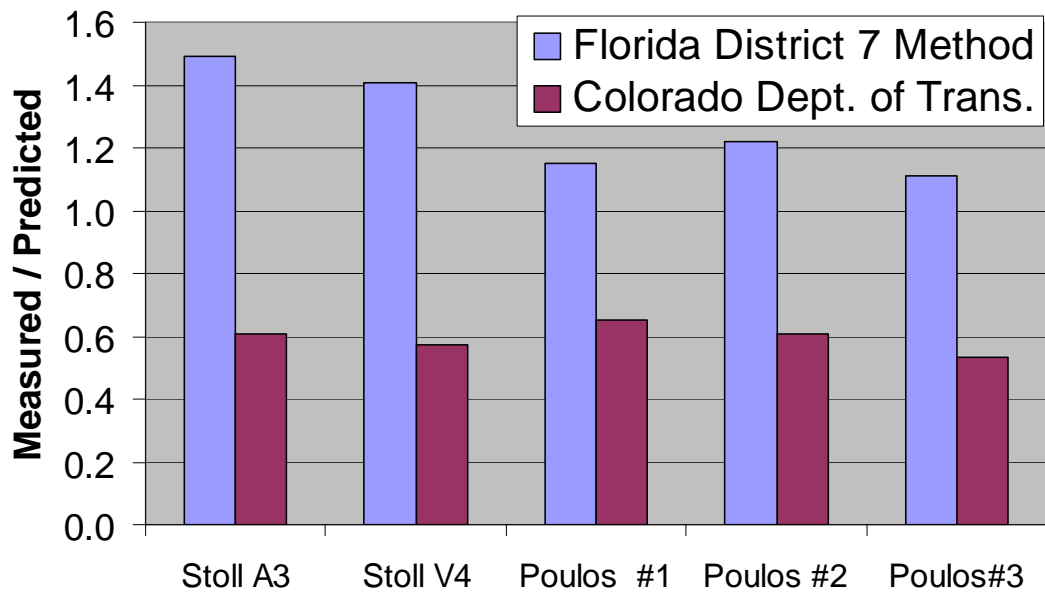
Figure 4.23 Measured over-predicted torsional capacities of drilled shafts in clay

M

P

Vertical Soil
Resistance

Lateral
Soil
Resistance
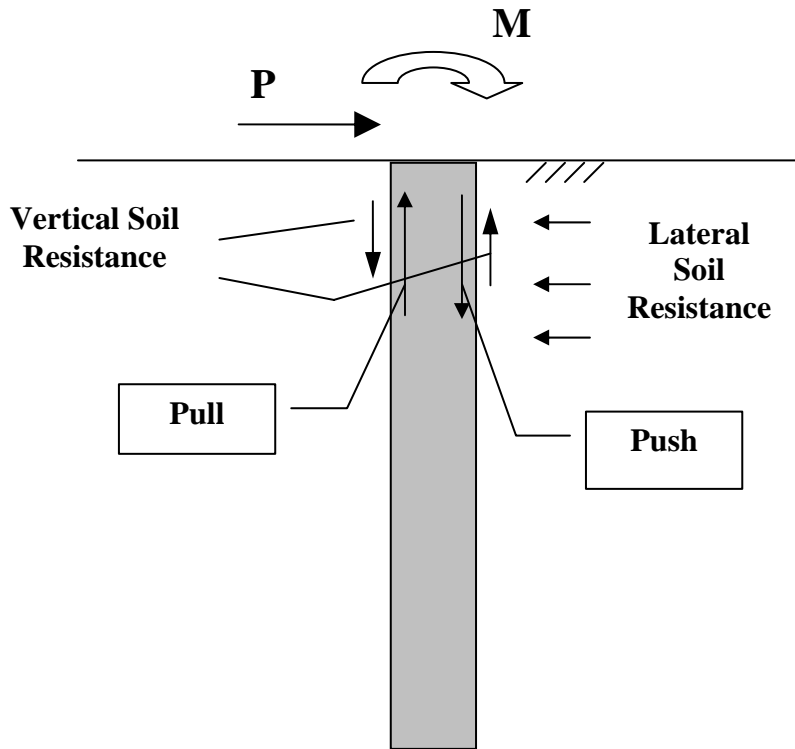
Pull

Push

Figure 4.24 The mechanism of pull-push effect

5 LATERAL LOAD TESTS ON DRILLED SHAFTS AND ANALYSIS OF TEST RESULTS AT SELECTED NOISE WALL SITES NEAR DENVER, COLORADO

5.1 Project Description

This research project required the research team to perform two lateral load tests on drilled shafts used to support noise walls. The first lateral load test was conducted on June 11, 2003 near I-225 and 6th Avenue. The second lateral load test was conducted on test shafts drilled near I-225 and Iliff Avenue. The design consultant used the current CDOT practice to design the drilled shaft foundations. The load test data allowed an evaluation of the current CDOT design approach as well as the recommended analysis methods proposed in this research.

5.2 Subsurface Conditions

5.2.1 Introduction

This section presents the geotechnical investigation results and geotechnical design parameters from the four soil borings advanced at the two proposed test sites for the purpose of lateral load analysis for this research project. The project includes two lateral load test sites; near I-225 and 6th Avenue and near I-225 and Iliff Avenue. The purpose of the geotechnical site investigation was to determine the geotechnical profile, to characterize the physical properties of the materials at the site, and to perform pressuremeter testing (this data was utilized to develop geotechnical recommendations necessary to evaluate the lateral load capacity of the test shafts). The field investigation was needed to compare design results using the geotechnical data with the lateral load test results. The plan view of the locations of the soil borings and the summary of the field and laboratory test results is shown in Figs. 5.1a and 5.1b. The logs of borings are presented in Figs. 5.2a thru 5.2d.

A total of four borings were drilled using a CME-75 drill rig utilizing 7-½ inch hollow stem auger (HSA). Borings 1 and 2 were drilled near the I-225/6th Avenue site while Borings 3 and 4

were drilled near the I-225/Iliff Avenue site. Standard penetration tests (SPT) were performed at selected intervals in Borings 1 and 3. Shelby tube samples were collected at selected intervals in Borings 2 and 4. Results of the field investigation and laboratory testing are included in Chapter 7. One-inch diameter PVC piezometers were installed in Borings 1 and 3 in order to monitor groundwater levels. Gradation analyses and Atterberg limits tests were performed for classification purposes on representative soil samples retrieved from the borings.

5.2.2 Site Conditions & Geotechnical Profile

5.2.2.1 I-225 near 6th Avenue

At the lateral load test site located near I-225 and 6th Avenue, man-placed fill consisting of stiff silty clay was encountered to a depth of approximately 6.5 feet below the original ground surface (OGS). Native materials consisting of soft to medium stiff silty clay and loose silty sand were encountered below the fill to a depth of approximately 22 feet, where bedrock was encountered. Bedrock was encountered at an elevation of approximately 5420.5 feet and consisted of firm claystone. Bedrock was encountered to the maximum depth of investigation of approximately 26.5 feet below OGS, which corresponds to an elevation of approximately 5416 feet. Groundwater was encountered at an elevation of approximately 5431 feet.

5.2.2.2 I-225 near Iliff Avenue

At the lateral load test site located near I-225 and Iliff Avenue, native materials consisting of loose to medium dense silty sand were encountered below the OGS to a depth of approximately 19 feet, where bedrock was encountered. Bedrock was encountered at an elevation of approximately 5618 feet and consisted of firm to medium hard sandstone with interbedded claystone lenses. Bedrock was encountered to the maximum depth of investigation of approximately 25 feet below OGS, which corresponds to an elevation of approximately 5612 feet. Groundwater was encountered at an elevation of approximately 5622.5 feet.

Based on results of the geotechnical site investigation, the CDOT geotechnical engineer recommended the material properties presented in Table 5.1 to be used in the lateral load analysis of the drilled shafts using LPILE or similar software. CDOT also recommended that the lateral resistance for the top five feet of silty clay fill at the 6th Avenue site should be neglected to account for desiccation cracks in the material for the design of structures.

Table 5.1: CDOT Recommended Material Properties for Lateral Load Analysis Using LPILE.

Lateral Load Test Site	Elevation (feet)	Internal Friction Angle (degrees)	Cohesion c(psf)	Modulus of Horizontal Subgrade Reaction k_h(pci)	Strain at ½ the Maximum Principal Stress Difference, ε_{50} (in/in)	Total Unit Weight γ (pcf)
	Below 5442	0	1200	75	0.007	110
I-225/6th Avenue	Below 5436	0	800	35	0.015	110
	Below 5426	30	0	20	--	115
	Below 5420	0	3,000	500	0.005	130
I-225/Iliff Avenue	Below 5637	30	0	25	--	115
	Below 5618	0	4,000	500	0.005	130

5.3   Lateral Load Test and Analysis at I-225 near 6th Avenue

5.3.1 Field Installation of Instruments and Drilled Shafts Construction

The planned fieldwork consisted of instrumenting the two test drilled shafts which are to be used as part of the noise barrier wall foundations at this site, denoted as Test Shafts #1 and #2. The location of the test shafts is shown on the attached plans in Fig. 5.1a. The instrumentation consisted of inclinometer tubes to measure the lateral movement with depth during the load testing, vibrating wire sister bar strain gages, tilt meters, and dial gages as shown in Fig. 5.3a and 5.3b. A complete list of the required instrumentation for the lateral load test is summarized in Table 5.2, and the detailed plan of instrumentation and instrument elevations are attached in Chapter 7. The reinforcement details of the test drilled shafts are shown in Fig. 5.3e. E.L. Robinson Engineering and Geocal, Inc. personnel installed the instrumentation. The test shafts were instrumented and constructed on June 9, 2003.

Table 5.2. Table of Instrumentation Used for Lateral Load Test.

Type of Instrument	Sister Bar (each)	Load Cell (each)	Inclinometer Tube (ft.)	Tilt meter	Dial Gages
Test Shaft # 1 16 ft. Deep	10	1	25	2	2
Test Shaft # 2 16 ft. Deep	10		25	2	2
Total Quantity	20	1	50	4	4

Arrangements were made with the CDOT Project Engineer to facilitate the installation of the instruments. This included mounting the vibrating wire strain gages to the main steel rebar, installing the inclinometer tubes in the holes, and supervising the installation of the test shafts.

Pictures showing the installation of the instruments and the drilled shafts construction are shown in Figs. 5.4 thru 5.9.

5.3.2 Preparation and Setup for the Lateral Load Test

Detailed drawings of the testing devices and schematics of the test setup were discussed with all parties involved. An agreement on the testing setup and methodology was reached as shown in the attached drawings in Chapter 7. Hamon Contractors built the reference beams and setup the 1.5-inch diameter Dywidag rods and all jacking devices under the supervision of the research team.

The contractor began constructing the drilled shafts by drilling the hole to the plan bottom elevation with a 30-inch auger, and then drilled the 6 feet deep 12-inch diameter sub-bottom hole below the bottom of the drilled shaft. The inclinometer was then lowered into the hole to the bottom of the 12-inch diameter sub-bottom hole and sand was poured to fill around it in the 6 feet portion below the base of the shaft. The 30-inch diameter, 3-foot long casing was then installed, followed by the instrumented cage. The 10 feet long W14x109 was then installed in position as shown in the installation pictures. After installation of all the test shaft elements, the

concrete was poured in the hole to the top of the steel casing, which was approximately 1 foot above ground elevation. The same methodology was performed at Test Shaft # 2.

On June 10, 2003, the contractor installed the reference beams and setup the jacking devices as shown in the pictures in Figures 5.10 and 5.11. The Dywidag rods were assembled and installed in position.

The loading devices including a 60 Ton jack, a 100 Ton load cell, and special readout devices were provided by the contractor. The devices were calibrated before shipping to the site. The jack, load cell, special bearing plates, dial gages, and tilt meters were all installed on the day of testing (i.e. 6/11/2003). The picture in Fig. 5.12 shows the testing devices and equipment setup. The strain gages were attached to the data acquisition just before the test started and initial readings were collected. The calibration factors for the sister bar strain gages and tiltmeters are shown in Chapter 7. A schematic of the location and serial number of each gage are provided in Chapter 7. Two sets of initial readings were taken from the inclinometers in Test shafts #1, and #2 before any load was applied. Pictures showing the preparation and setup for the load test are shown in Figs. 5.13 and 5.14. Fig. 5.15 shows a general view of the load test.

5.3.3 Lateral Load Test Procedure

The lateral load test was performed in increments of loading and unloading as shown below. One cycle of loading was performed according to the following sequence:

Load cycle 1: (Loads are in Kips)

Loading: 5, 10, 15, 20, 30, 40, 50, 60, 75, and 90.

Unloading: 47, 22, and 0

The strain gages were connected to the CR10X Campbell Scientific Data logger. The strain readings were taken for each load increment during the time the load was applied, and stored in the computer for later processing.

The lateral movement (deflection) of the drilled shafts was measured using the SINCO slope indicator device. The deflection was measured every two feet along the depth of each shaft. The measurements were taken for the following loads (in Kips):

Load cycle 1: (Loads are in Kips)

Loading: 5, 10, 15, 20, 30, 40, 50, 60, 75, and 90.

Furthermore, the deflection at the top of the drilled shafts was measured using dial gages. The load applied to the drilled shafts was measured using the load cell. The rotation at the top of the shafts and at the jacking point was measured using vibrating wire tilt meters. Figs. 5.16 thru 5.18 shows the test being conducted.

The CDOT Project Engineer provided the concrete compressive strength test results on the day of testing. Two cylinders from each test shaft were tested. The average compressive strength in test shafts was 4510 psi.

CDOT Engineers supervised the lateral load test, and gave their recommendations on the load applied. The lateral load applied was stopped at 90 kips because the two shafts were production shafts and a considerable amount of nonlinear deflection had occurred.

5.3.4 Lateral Load Test Results

The measured load-displacement relationships at the top of the shafts, as measured using the dial gages, are shown in Figs. 5.19 and 5.20 for shafts No. 1 and No. 2, respectively. The deflections of the drilled shafts, as measured by the inclinometer probe, versus depth of the shaft, are shown in Figs. 5.21 and 5.22 for shafts No. 1 and No. 2, respectively. Moreover, the deflection of the drilled shafts at the point of load application, as measured by the inclinometer probe, versus applied lateral load are shown in Figs. 5.23 and 5.24 for shafts No. 1 and No. 2, respectively.

The measured strains vs. depth (measured from jacking point) in test shaft No. 1 at the tension side and the compression side are shown in Figs. 5.25 and 5.26, respectively. The measured angle of tilt in degrees vs. the applied lateral load from the tiltmeters mounted at the jacking point and at top of concrete is shown in Fig. 5.27.

For test shaft #2, the measured strains vs. depth (measured from jacking point) at the tension side and the compression side are shown in Figs. 5.28 and 5.29, respectively. The measured angle of

tilt in degrees vs. the applied lateral load from the tiltmeters mounted at the jacking point and at top of concrete is shown in Fig. 5.30.

5.3.5 Interpretation of Soil Parameters

CDOT has commissioned Knight Piesold, LLC to conduct laboratory tests on soil samples retrieved from two load test sites. The laboratory test program included soil classification tests, direct shear tests, and triaxial tests. In addition to index testing, the in-situ water content and in-place densities of the soils at the test sites were also determined.

The direct shear tests were performed on silty clay samples in an undrained condition, with an increased shear strain rate. Samples with in-situ water content as well as samples with full saturation (S = 100%) were tested. The samples were subjected to vertical stresses that are consistent with in-situ effective overburden stress, thus ensuring close duplication of in-situ confining stress conditions. The peak shear stress at failure was used to represent the shear strength under undrained loading. The interpreted shear strength parameters for the cohesive silty clay are provided in Table 5.3 for both unsaturated (in-situ water content) and fully saturated conditions. The simplified soil profile at the 6th Avenue test site is shown in Fig. 5.31.

The CU triaxial tests were performed on cohesive silty clays as well. The consolidation pressures selected in the triaxial tests were consistent with the in-situ effective overburden stresses. During undrained shearing, the loading rate was increased to about 1% per minute of axial strain rate. The samples were either tested under the initial water content condition or after being fully saturated by backpressure saturation. The interpretation of the shear strength under undrained shear, as reported by the consultant, is based on the total stress based Mohr Circle and the assumption that the failure plane corresponds to the peak shear stress of the Mohr Circle. For fully saturated samples, this approximation would result in higher interpreted shear strength than the Mohr Coulomb's shear strength. For unsaturated samples, the interpreted shear strength by the consultant may be conservative, since the effective stress based Mohr Circle may be larger in size than that the total stress based Mohr Circle. The best estimate of shear strength by the Knight Piesold's Laboratory Report is summarized in Table 5.3, in which different tests are not performed at the same exact depth but in what seems to be the same soil layer.

Table 5.3 Shear Strength (Undrained Shearing) from Pressuremeter and Lab Tests

Soil Layers (ft)	Sample ID	Pressuremeter		Direct Shear Test		Triaxial Shear Test	
		S_u, G&A (psi)	S_u, FHWA (psi)	Unsaturated (psi)	Saturated (psi)	Unsaturated (psi)	Saturated (psi)
0-2.5	2-A					18.3	
2.5-4.5	2-AA	22.2	16.2	15	5.6	18.3	8.6
4.5-6.5	2-B						
6.5-10	2-C	12.5	8.8	13.7	8.2	14.7	4.5
10-12.5	2-D					9.4	11.9
12.5-16	2-E	15.3	10.9			11.7	

Pressuremeter tests were performed at the 6th Avenue site and the Iliff Avenue site by the URS in Denver. The report prepared by the URS corporation contains the pressuremeter test results, along with interpreted soil parameters. For the cohesive silty clay site at the 6th Avenue test site, the undrained shear strength, interpreted by URS consultant who employing Gibson and Anderson (1961)'s procedure from pressuremeter tests, are presented in Table 5.3. The undrained shear strength interpreted by using FHWA (1989)'s equation is also included in Table 5.3. FHWA's interpretation equation is provided in Equation 5.1.

$$S_u = 0.25(p_l - p_0)^{0.75} \tag{5.1}$$

in which, p_l = limit pressure; p_0 = in-situ initial horizontal pressure.

From a comparison of the interpreted shear strength in Table 5.3, one may conclude that the saturation of cohesive soil samples will definitely result in reduction in shear strength, compared to that obtained from partially saturated samples. The difference between the direct shear and triaxial test results is unpredictable, due to different stress conditions and strength interpretation between these two methods. Finally, the interpreted undrained shear strength from the pressuremeter test by using Gibson and Anderson (1961) method appears to be larger than those determined from laboratory tests and pressuremeter test interpreted by using FHWA's equation. As often is the case, different test methods have resulted in different shear strength parameters. It

is of interest to compare the elastic modulus of soils obtained from pressuremeter and those from triaxial test. For pressuremeter test, three types of elastic modulus based on the portion of test data used for interpretation, E_{inital} based on initial part of test curve, E_{reload} based on reload portion of pressure-volume change curve, and E_{unload} based on using unload portion of pressure-volume change curve, as shown in Fig. 5.32, can be achieved. Table 5.4 presents the modulus from the pressuremeter test and the triaxial test. It can be seen that the modulus interpreted from the initial portion of PM test curve is the smallest one. On the other hand, the unload portion of PM test curve provides largest estimation of modulus of soils.

Table 5.4 Elastic Modulus (psi) of Soils from Pressuremeter Test and Triaxial Test

Layers (ft)	$E_{initial}$	E_{reload}	E_{unload}	$E_{triaxial}$
0-2.5	2919	9174	16680	4140
2.5-4.5	2919	9174	16680	3320
4.5-6.5	2919	9174	16680	3320
6.5-10	723	1529	1946	1614
10-12.5	723	1529	1946	789
12.5-16	1015	2919	5282	3474

5.3.6 Analysis of Load Test

Fig. 5.19 and 5.20 show that the two test shafts at the 6th Avenue test site have almost same lateral response. However, shaft #1 appeared more deflection than shaft #2, which means shaft #1 can represent a worse situation for these two shafts. Therefore, shaft # 1 is used for analysis. The analysis is carried out using Broms method and Brinch Hansen method for ultimate capacity and the COM624P computer program for load-deflection curves. The synthesized shear strength parameters are summarized in Table 5.5. The strength correlated from the SPT correlation chart developed by Liang (2002) and the CDOT suggested soil strength in Table 5.1 are also included. It can be seen that the soil strength suggested by CDOT geotechnical engineer is around half of that from lab test on soil under in-situ conditions. The averaged soil strength parameters are presented in Table 5.6 for five analysis cases: SPT Liang Case based on Liang (2002) SPT correlations, SPT CDOT Case based on CDOT geotechnical engineer recommended soil parameters, Unsaturated Case based on lab determined strength for unsaturated (in-situ)

condition, PM (Su,G&A) Case based on pressuremeter determined undrained strength from Gibson and Anderson method, and PM (Su, FHWA) Case based on pressuremeter determined undrained strength by using FHWA (1989) equation. It is noted that the unit weight takes into account the situation of ground water table.

Table 5.5. Interpreted Shear Strength Parameters

Soil Layers (ft)	Sample ID	SPT Liang Case		Unsaturated Case	SPT CDOT Case
		N values	Strength (psi)	Strength (psi)	Strength (psi)
0-2.5	2-A	12[*]	11.3[*]	18.3	8.3
2.5-4.5	2-AA	12	11.3	15	8.3
4.5-6.5	2-B	15	14	14.4[*]	8.3
6.5-10	2-C	9	8.5	13.7	5.6
10-12.5	2-D	4	3.75	9.4	5.6
12.5-16	2-E	8	7.53	11.7	5.6

Note *: No direct test results, linear interpolation from adjacent soil layers was used.

Table 5.6. Average Strength in psi for Broms Method

Unsaturated Case	SPT Liang Case	SPT CDOT Case	PM (S_u, G&A) Case	PM (S_u, FHWA) Case
13.6	9	6.7	17.3	12.3

For COM624p computer analysis, it is necessary to input additional soil parameters other than just the strength parameters. To this end, the correlation charts developed by Liang (2002) based on SPT N values were used to create the input parameters as shown in Table 5.7. For the SPT CDOT Case, the suggested parameters are used for analysis, as shown in Table 5.1.

The calculated lateral capacities using the Broms method and the Brinch Hansen method are presented in Table 5.8 for five strength cases: SPT Liang case, unsaturated case, SPT CDOT case, PM (S_u, G&A) case, and PM (S_u, FHWA) case. It should be noted that the estimated capacities shown in Table 5.8 are geotechnical capacities. The ratios between the measured capacities and

the predicted capacities are also tabulated in Table 5.8. It can be seen that, in general, both Broms method and Brinch Hansen method predict comparable capacities and they are on the safe side, with the ratio of the measured vs. the predicted ranges from 1.2 to 2.7 for the unsaturated case, SPT Liang case, SPT CDOT case, and PM (S_u, FHWA) case. It can also be observed that the prediction with the CDOT geotechnical engineer suggested soil parameters yields most conservative results. On the other hand, the pressuremeter test strength parameters interpreted from Gibson and Anderson method would result in unsafe prediction of the lateral capacity of the test shaft. This is not surprising, as the Gibson and Anderson method interpreted strength parameters are much higher than SPT or laboratory determined strength parameters.

Table 5.7 Other Soil Parameters

Soil Layers(ft)	Sample ID	Φ	ε_{50}	γ_d (pcf)	γ_{wet} (pcf)	k_s (pci)
0-2.5	2-A	0	0.006	87.9	106	500
2.5-4.5	2-AA	0	0.006	96.8	120	500
4.5-6.5	2-B	0	0.005	NA	119[*]	500
6.5-10	2-C	0	0.007	95.2	117	500
10-12.5	2-D	0	0.01	97.8	122	100
12.5-16	2-E	0	0.007	100.9	126	500

Note *: No lab test result is available; the average value of the two adjacent layers is adopted. k_s is the static modulus of horizontal subgrade reaction (K_h).

Table 5.8 Calculated Lateral Capacity of Drilled Shaft #1 in CDOT Test in Clay

Strength Case	Capacity (kips)		Measured/Predicted	
	Broms Method	Brinch Hansen Method	Broms Method	Brinch Hansen Method
SPT Liang	71	70	1.9	1.9
Unsaturated	108	101	1.3	1.3
SPT CDOT	53	50	2.5	2.7
PM (S_u, FHWA)	98	114	1.4	1.2
PM (S_u, G&A)	137	158	0.99	0.85

Note: The ultimate lateral capacity of Shaft #1 is 135 kips.

The COM624P computer analysis was carried out based on different strength cases. The predicted load-deflection curves at the shaft head are compared with the measured in Fig. 5.33 for SPT and lab strength parameters, and in Fig. 5.34 for pressuremeter tests. For a close-up view of the accuracy of prediction for the working load condition, the initial portion of the load-deflection curves in Figs. 5.33 and 5.34 are re-plotted in Figs. 5.35 and 5.36. It can be seen that at the working load of 20 kips, the COM624P predicted deflection is very close to the measured, if the laboratory determined strength parameters for unsaturated samples are used. The SPT correlated soil parameters by using Liang (2002) correlation can still yield a very reasonable prediction at 20 kips of lateral load. The soil parameters suggested by the CDOT geotechnical engineer tend to provide a conservative prediction. Also, the NAVFAC method predicts too much deflection. The pressuremeter method, if undrained strength is interpreted from FHWA equation, can also provide reasonable prediction of the drilled shaft deflection response. On the other hand, the pressuremeter method, if the undrained strength is interpreted from Gibson and Anderson (1961) or from direct conversion into p-y curves, cannot provide a reasonable prediction.

The loads correspond to three values of drilled shaft deflections (i.e., 0.6 inch, 1 inch, and 1.5 inch) and are extracted from the predicted load-deflection curves for six (6) strength cases, which are tabulated in Table 5.9. The measured ultimate lateral capacity using the hyperbolic curve fit

method is used to determine the ratio between the measured ultimate capacity and the predicted load at different permissible deflection values. These ratios are tabulated in Table 5.9 under the heading of F.S., as they represent the margin of safety from the measured ultimate capacity. From this table, one can see that the recommended permissible deflection of 1.0 inch would yield an equivalent factor of safety between 2.4 to 4.8, for soil parameters interpreted from SPT, laboratory tests, and pressuremeter test by using FHWA's interpretation for undrained strength. On the other hand, the equivalent factor safety based on 1.0 inch permissible deflection is 1.9, if the soil parameters are interpreted from the pressuremeter tests by using Gibson and Anderson (1961) method was employed by URS consultant. This equivalent factor of safety is considered to be unacceptable.

Table 5.9 Calculated Lateral Capacity and Factor of Safety (F.S.) of Drilled Shaft #1 by COM624P with Different Permissible Deflections at Ground Level in CDOT Test in Clay

Methods / Cases	COM624P		COM624P		COM624P	
	0.6 inch	F.S.	1 inch	F.S.	1.5 inch	F.S.
SPT Liang	35	3.9	41	3.3	46	2.9
Unsaturated	47	2.9	57	2.4	65	2.1
SPT CDOT	24	5.6	28	4.8	31	4.4
PM (S_u,FHWA)	45	3.0	54	2.5	57	2.4
PM (S_u, G&A)	57	2.4	70	1.9	80	1.7
PM (p-y)	96	1.4	NA		NA	

Note: The ultimate lateral capacity of Shaft 1 is 135 kips. The PM (p-y) analysis is based on the p-y curves calibrated directly from the p-$\Delta V/V_0$ curve of pressuremeter test.

A numerical algorithm has been developed by Liu and Liang (2004) for deriving p-y curves using the strain and deflection data measured during lateral load tests. The p-y curve at the 24-inch depth derived by this method is shown in Fig. 5.37. The existing stiff clay p-y curve criteria with strength parameters determined by lab and SPT correlations are used to generate p-y curves shown in Fig. 5.37(a). Similarly, the pressuremeter test data is used to generate p-y curves shown in Fig. 5.37(b). The load test data derived p-y curve is much stiffer than other approaches.

The predicted load-deflection curve is compared with the actual measured for shaft #1 in Fig. 5.38. The match at the working load range is excellent.

Based on the analysis performed in this section, the following observations may be made.

1. The Broms method, when used with SPT correlated in-situ strength or laboratory determined shear strength for in-situ (unsaturated) samples, yield reasonable F.S. for this load test result.

2. The use of shear strength from the CDOT geotechnical engineer recommendation would yield high F.S. due to conservative approach to strength interpretation.

3. The COM624P computer program, when used with SPT correlated soil parameters or laboratory determined strength for in-situ (unsaturated) water content, appears to be capable of predicting shaft deflection at the working load of 20 kips.

4. The use of the pressuremeter test, if the strength parameters are interpreted by using FHWA (1989)'s equation, would provide reasonable prediction on capacity and lateral deflection of the shaft. However, if the strength parameters are interpreted by using Gibson and Anderson (1961)'s procedure, the pressuremeter method would result in an unsafe prediction of ultimate lateral capacity for the 6th Avenue test shafts. Furthermore, the drilled shaft deflection cannot be predicted accurately using soil parameters interpreted from the Gibson and Anderson (1961) method or the p-y curves directly derived from pressuremeter test.

5.3.7 Re-Design of Drilled Shafts

The recommended design methods and design criteria are applied to determine the drilled shaft length for the 6th Avenue site. The design procedure is as follows. First, the Broms method and a safety factor of two are used to determine the drilled shaft length. Next, the COM624P computer program is used to determine if the deflection of the designed drilled shaft under the design load exceeds the permissible deflection of 1.0 inch. If the deflection is under the permissible deflection, the design drilled shaft length will be final. Otherwise, if deflection criterion controls, then COM624P computer program should be run to determine the shaft length such that the design load would not result in more than 1.0 inch shaft head deflection.

5.3.7.1 Calculation of Design Load and Load Point

The design load on the sound barrier walls in CDOT can be calculated by multiplying the tributary area (shaft spacing multiplied by the wall height) with design wind pressure. The

typical shaft length in CDOT is about 16'8'', and diameter is 2.5 feet. The spacing of drilled shaft varies from 7 to 24 feet. The sound barrier wall height ranges from 14 to 18 feet. The wind pressure on sound barrier wall is about 20 to 40 psf, with typical pressure of 27 psf. The load on a single drilled shaft is therefore calculated as following:

$P_{maximum}$ = 24ft * 18ft * 40psf =17.3 kips,

$P_{minimum}$ = 7ft * 14ft * 20psf = 2 kips,

$P_{typical}$ = 18ft * 24ft * 27psf = 12 kips.

The average load point is about 9 feet above the ground, by assuming that the wind pressure is uniformly distributed on the wall. Thus, the design load of 17.3 kips and the load arm of 9 feet are used in this design.

5.3.7.2 Selection of Soil Parameters

These parameters were summarized in Section 5.3.6. The unsaturated soil strength parameters from lab test results are used.

5.3.7.3 Determination of Drilled Shaft Length by the Broms Method

A spreadsheet was created to perform the calculation according to Broms method and the adopted F.S. of 2. Through several trials, the 12-foot drilled shaft embedment length is selected for the site. The iterative process for the determination of shaft length can be easily accomplished in the spreadsheet by changing the 'Embedded Length L=' value and the weighted average shear strength. Although 11 feet of embedded shaft length was calculated to be able to provide 19 kips resistance load, it was decided to use the 12-foot shaft length to accommodate the possible effect of ground water fluctuation. The spreadsheet calculation is given in Appendix E.

5.3.7.4 Check the Deflection with COM624P.

COM624P is used to calculate the deflection of the 12-foot drilled shafts under the design load. The soil parameters used for the COM624P computer analysis is the unsaturated soil strength case discussed in Section 5.3.6. The 17.3 kips lateral load applied at 9 feet above ground is used as wind load. The analysis results give the deflection of 0.2 inches at the drilled shaft head (ground level). This value is less than the permissible 1.0 inch deflection. The predicted load-deflection curve from COM624 is shown in Fig. 5.39.

5.3.7.5 The Final Design

Based on above calculations and analysis results, a 12-foot embedment length of drilled shaft with a 30-inch diameter is recommended. This, when compared to the 15.7-foot original design drilled shaft length, would yield about 24% length reduction.

5.4 Lateral Load Test and Analysis at I-225 near Iliff Avenue

5.4.1 Field Installation of Instruments and Drilled Shafts Construction

The work consisted of building and instrumenting two non-production test shafts with the same geometry as the shafts tested at I-225 near 6th Avenue. The test shafts were denoted as Test Shaft North and Test Shaft South. The locations of the test shafts are shown in Fig. 5.1b. The same instrumentation plan was used as in I-225 near 6th Avenue test shafts. Figs. 5.3c and 5.3d show the as-built instrumented shafts. The instrumentation used was as per Table 5.2. Additional details of instrumentation plans and details are shown in Chapter 7. The reinforcement details of the test shafts are shown in Fig. 5.3e. Instrumentation was installed by E.L. Robinson Engineering and Geocal, Inc. personnel. The test shafts were instrumented and constructed on March 29, 2004.

Pictures showing the installation of the instruments and the drilled shafts construction are shown in Figs. 5.40 thru 5.45.

5.4.2 Preparation and Setup for the Lateral Load Test

Detailed drawings of the testing devices and schematics of the test setup were discussed with all parties involved. An agreement on the testing setup and methodology was reached as shown in the attached drawings in Figs. 5.3c and 5.3d. Castle Rock Construction Company built the reference beams and setup the 1.5" diameter Dywidag rods and all jacking devices under the supervision of the research team.

The contractor began constructing the drilled shafts by drilling the hole to the plan bottom elevation with a 30" auger, and then drilled the 6 feet deep portion below the bottom of the

drilled shaft. The inclinometer was then lowered in the hole, and gravel was poured to fill around it in the 6 feet portion below base of the shaft. The instrumented cage was then lowered in the hole, followed by the 8 feet long W14x109 which was then installed in position and welded to several of the #9 bars as shown in the pictures of installation. After installation of all the test shaft elements, the concrete was poured in the hole to the ground elevation. The same methodology was performed at Test Shaft North.

On March 31, 2004, the contractor completed the setup of the reference beams and the jacking devices as shown in the pictures in Figures 5.46 and 5.47. The Dywidag rods were assembled and installed into position the same day.

The loading devices included a 60-Ton jack with pressure gage rented from VSL, a 100-Ton load cell, and special readout device rented from Geokon, Inc. The devices were calibrated before shipping to the site. The jack, load cell, special bearing plates, dial gages, and tilt meters were all installed on the day of testing (i.e. 4/1/2004). A schematic in Fig. 5.3d shows the testing devices and equipment setup. The strain gages were attached to the data acquisition just before the test started and initial readings were collected. The calibration factors for the sister bar strain gages and tiltmeters are shown in Chapter 7. A schematic of the location and serial number of each gage are provided in Chapter 7. Two sets of initial readings were taken from the inclinometers in North and South Test Shafts #1, and #2 before applying any load to the shafts. Pictures showing the preparation and setup for the load test are shown in Figs. 5.48 through 5.50. Fig. 5.51 shows a general view of the load test.

5.4.3 Lateral Load Test Procedure

The lateral load test was performed in increments of loading and unloading as shown below. Two cycle of loading were performed according to the following sequence:

Load cycle 1: (Loads are in Kips)

Loading: 3, 8, 13, 18, 25, 35, 45, 55, and 65.

Unloading: 0

Load cycle 2: (Loads are in Kips)

Loading: 25, and 35.

Unloading: 0

The strain gages were connected to the CR10X Campbell Scientific Data logger. The strain readings were taken for each load increment during the time the load was applied and stored in the computer for later processing.

The lateral movement (deflection) of the drilled shafts was measured using the SINCO slope indicator device. The deflection was measured every two feet along the depth of each shaft. The measurements were taken for the following loads (in Kips):

Load cycle 1: (Loads are in Kips)

Loading: 3, 5, 8, 13, 25, 35, 45, 55, and 65.

Load cycle 2: (Loads are in Kips)

Loading: 25, and 35.

Furthermore, the deflection at the top of the drilled shafts was measured using dial gages. The load applied to the drilled shafts was measured using the load cell. The rotation at the top of the shafts and at the jacking point was measured using vibrating wire tiltmeters. Figs. 5.51 thru 5.53 shows the test being conducted.

Geocal, Inc. Engineers provided the concrete compressive strength on the day of testing. Two cylinders were tested, and the average compressive strength in the test shafts was 4700 psi.

CDOT Engineers supervised the lateral load test, and gave their recommendations on the load applied. The picture in Fig. 5.54 shows the CDOT Engineers with the researchers.

5.4.4 Lateral Load Test Results

The measured load-displacement relationships at the top of the shafts, as measured using the dial gages, are shown in Figs. 5.55 and 5.56 for the North and South test shafts, respectively. The deflection of the drilled shafts at the point of load application, as measured by the inclinometer probe, versus applied lateral load are shown in Figs. 5.57 and 5.58 for the North and South, respectively. The deflections of the drilled shafts, as measured by the inclinometer probe, versus depth of the shaft, are shown in Figs. 5.59 and 5.60 for test shafts North and South, respectively.

The measured strains vs. depth in Test Shaft North at the tension side and the compression side are shown in Figs. 5.61 and 5.62, respectively. The measured angle of tilt in degrees vs. the applied lateral load from the tilt meters mounted at the jacking point and at top of concrete is shown in Fig. 5.63.

For Test Shaft South, the measured strains vs. depth at the tension side and the compression side are shown in Figs. 5.64 and 5.65, respectively. The measured angle of tilt in degrees vs. the applied lateral load from the tilt meters mounted at the jacking point and at top of concrete is shown in Fig. 5.66.

The load-displacement curve for the North Shaft (Fig. 5.56) exhibits excessively large movement when the applied load exceeded 55 kips. A closer look at the deflection vs. depth plot (Fig. 5.59) reveals that the breakage of shaft structure had occurred at the bottom of the H-Beam, contributing to sudden and abnormal movement. A postmortem investigation of the structurally failed drilled shaft has shown cracking and spalling of concrete at the bottom of the H-Beam due to insufficient bond between the H-Beam and concrete. The poor bond could be attributed to small clearance between the H-Beam and reinforcement bars, which prohibited proper consolidation and compaction of concrete as well as facilitated trapping of water. Since the current study was to evaluate geotechnical lateral capacity of drilled shafts, the subsequent analyses in this report focused on the South Shaft.

5.4.5 Interpretation of Soil Parameters

CDOT has commissioned Knight Piesold, LLC to conduct laboratory tests on soil samples retrieved from the I-225 and Iliff Avenue load test site. The laboratory test program includes soil classification tests and direct shear tests. The in-situ water content and in-place densities of the soils at the test sites were also determined.

The direct shear tests were performed on silty sand samples under consolidated drained conditions. Samples with in-situ water content as well as samples with full saturation (S = 100%) were tested. The interpreted shear strength parameters for the silty sand are provided in Table

5.10 for both samples 4A which is unsaturated (in-situ water content) and 4B which is fully
saturated. The simplified soil profile at the Iliff Avenue test site is shown in Fig. 5.67.

Table 5.10 Shear Strength (Drained) from Pressuremeter, SPT, and Lab Tests

Soil Layers (ft)	Sample ID	Pressuremeter		SPT	Direct Shear Test	
		C' (psi)	Φ'	N values	C' (psi)	Φ' (degree)
0-4		9.7	34	13		
4-6	4A			8	2.3	41.1
6-9	4A	5.6	28	10	2.3	41.1
9-15	4B	11	27	7	0.7	39.5
15-15.7				7		

Pressuremeter tests were also performed at the Iliff Avenue site by the URS in Denver. The
report prepared by the URS contains the pressuremeter test results, along with interpreted soil
parameters. For the silty sand site at the Iliff Avenue, the drained cohesions and friction angles,
interpreted by the URS consultant from pressuremeter tests, are presented in Table 5.10.
Additionally, SPT N values are provided in Table 5.10. The elastic modulus of sands interpreted
from pressuremeter test are tabulated in Table 5.11.

Table 5.11 Elastic Modulus (psi) of Sands from Pressuremeter Test

Depth (ft)	$E_{initial}$	E_{reload}	E_{unload}
4	1112	5421	13483
9	1293	4309	7923
14	2224	7645	15290

From a comparison of the interpreted shear strength in Table 5.10, one may conclude that
saturation of cohesionless soil samples (4B) will not result in much reduction in shear strength,
compared to that obtained from unsaturated samples (4A). The interpreted friction angles from
the pressuremeter test appear to be smaller than those determined from laboratory tests. As often
is the case, different test methods have resulted in different shear strength parameters.

5.4.6 Analysis of Load Test

The two test shafts at the Iliff Avenue site, North Shaft and South Shaft, exhibited different lateral response when the applied lateral load exceeds 18 kips. The test configuration of the two shafts was the same and they were embedded in the same site. Therefore, the softer response of the North Shaft may be caused by the defects of the shaft itself. The South Shaft will be selected for capacity analysis since the main concern in this research is the soil capacity rather than the shaft capacity.

The analysis of the test shaft at the Iliff Avenue test site is carried out using Broms method for ultimate capacity and the COM624P computer program for load-deflection curves. The synthesized shear strength parameters are summarized in Table 5.12, in which the friction angles correlated from the SPT correlation chart developed by Liang (2002) and suggested by CDOT in Table 5.1 are also included. The averaged soil strength parameters are presented in Table 5.13 for four analysis cases: SPT correlation by Liang (2002), SPT suggested by CDOT, pressuremeter determined strength, and direct shear test determined friction. It is noted that the unit weight takes into account the situation of ground water table. The ground water table was at 15 feet below the ground surface. The averaged effective unit weight based on lab testing on in-situ density is 0.067 pci.

Table 5.12 Interpreted Shear Strength Parameters at Sand Site

Soil Layers (ft)	Pressuremeter		SPT		Direct Shear Test	
	$C^{'}$ (psi)	$\Phi^{'}$	Φ, CDOT (degree)	Φ, Liang (degree)	$C^{'}$ (psi)	$\Phi^{'}$ (degree)
0-4	9.7	34	30	36	2.3	41.1
4-6	9.7	34	30	31	2.3	41.1
6-9	5.6	28	30	33	2.3	41.1
9-15	11	27	30	29	0.7	39.5
15-15.7	11	27	30	29	0.7	39.5

Table 5.13 Average Friction Angle (Degree) for Broms Method

SPT Liang Case	SPT CDOT Case	PM Case	Direct Shear Case
32	30	30	40.4

For COM624p computer analysis, it is necessary to input additional soil parameters other than just the strength parameters. To this end, the correlation charts developed by Liang (2002) based on SPT N values were used to create the input parameters as shown in Table 5.14.

Table 5.14 Other Soil Parameters at Sand Site

Soil Layers(ft)	γ_d (pcf)	γ_{wet} (pcf)	k_s (pci)
0-4	105.0	120	90
4-6	105.0	120	25
6-9	105.0	120	90
9-15	106.4	116	25
15-15.7	106.4	116	20

The calculated lateral capacities using the Broms method are presented in Table 5.15 representing four strength cases: SPT Liang Case, SPT CDOT Case, Direct Shear Case, and PM Case. It should be noted that the estimated capacities shown in Table 5.15 are geotechnical

capacity. The ratios between the measured capacity and the predicted capacities are also tabulated in Table 5.15. It can be seen that, in general, most of the strength cases provide safe and good prediction, especially SPT Liang Case which provides the most accurate estimate. On the other hand, direct shear case over predict capacity by 36%. It may be due to that the sample during testing was not the same as field condition, resulting in higher friction angle.

Table 5.15 Calculated Lateral Capacity of South Shaft in CDOT Test in Sand

Strength Case	Broms Method (kips)	Measured/ Predicted
SPT Liang	91	1.05
SPT CDOT	84	1.14
PM	84	1.14
Direct Shear	131	0.73

Note: The ultimate lateral capacity of South Shaft is 96 kips.

The COM624P computer analysis was carried out for different strength cases. The predicted load-deflection curves at the shaft head are compared with the measured in Fig. 5.68. It can be seen that at the working load of 20 kips, the COM624P predicted deflection by direct shear case, SPT Liang case, and PM case is very close to each other. In general, the load-deflection curves predicted by all the cases are softer than that from the measured.

The loads correspond to three values of drilled shaft deflections (i.e., 0.6 inch, 1 inch, and 1.5 inch) and are extracted from the predicted load-deflection curves for four (4) strength cases which are tabulated in Table 5.16. The measured ultimate lateral capacity using the hyperbolic curve fit method is used to determine the ratio between the measured ultimate capacity and the predicted load at different permissible deflection values. These ratios are tabulated in Table 5.16 under the heading of F.S., as they represent the margin of safety from the measured ultimate capacity. From this table, one can see that the recommended permissible deflection of 1.0-inch would yield an equivalent factor of safety between 2.3 to 3.7, for soil parameters interpreted from SPT, PM or laboratory tests.

Table 5.16 Calculated Lateral Capacity and Factor of Safety (F.S.) of Drilled Shafts by COM624P with Different Permissible Deflections at Ground Level in CDOT Test in Sand

Methods / Cases	COM624P 0.6 inch	F.S.	COM624P 1 inch	F.S.	COM624P 1.5 inch	F.S.
Direct Shear	30	3.2	42	2.3	54	1.8
SPT Liang	26	3.7	36	2.7	45	2.1
PM	24	4.0	32	3.0	41	2.3
SPT CDOT	18	5.3	26	3.7	34	2.8

Note: The ultimate lateral capacity of South Shaft is 96 kips.

Using the Liu and Liang (2004) methodology, the p-y curve at the 30-inch deep derived from strain and deflection data of load test is plotted in Fig. 5.69. The p-y curves calculated from existing p-y curve criteria and soil parameters by various methods are also plotted in Fig. 5.69. It can be seen that measured p-y curve is stiffer than those from existing p-y criteria. The predicted load-deflection curve based on the measured p-y curve matches the actual load-deflection curve well, as shown in Fig. 3.70.

Based on the analysis performed in this section, the following observations can be made.

1. The Broms method, when used with SPT correlated in-situ strength or pressuremeter test interpreted strength, yield a very good estimate on capacity for this load test result.
2. The use of shear strength from direct shear test results would over predict capacity by 36% using Broms method.
3. The COM624P computer program, in general, when used with soil parameters determined by SPT correlations, pressuremeter test interpreted soil strength, or laboratory determined strength for in-situ condition, appears to provide a conservative prediction.
4. The derived p-y curve from strain and deflection data works well for sand test site. However, more gages at the top portion of shaft are necessary in order to derive high quality p-y curves.

5.4.7 Re-Design of Drilled Shafts

The recommended design methods and design criteria are applied to determine the drilled shaft length for the Iliff Avenue site. The design procedure is as follows. First, the Broms method and a factor safety of two are used for determining the drilled shaft length. Next, the COM624P computer program is used to determine if the deflection of the designed drilled shaft under the design load exceeds the permissible deflection of 1.0 inch. If the deflection is under the permissible deflection, the design drilled shaft length will be final. Otherwise, if deflection controls, then COM624P computer program should be run to determine the shaft length such that the design load would not result in more than 1.0 inch shaft head deflection.

5.4.7.1 Calculation of Design Load and Load Point

The design load on the sound barrier walls in CDOT can be calculated by multiplying the tributary area (shaft spacing multiplied by the wall height) with design wind pressure. Similar to the calculation done in section 5.3.7.1, the design load of 17.3 kips and the load arm of 9 feet will be used in this design.

5.4.7.2 Selection of Soil Parameters

The soil parameters were summarized in Section 5.4.6. The soil strength parameters correlated from the SPT N values using Liang's (2002) correlation chart were used.

5.4.7.3 Determination of Drilled Shaft Length by the Broms Method

A spreadsheet was created to perform the calculation according to Broms method and the adopted F.S. of 2. Through several trials, the 12 foot drilled shaft embedment length is selected for the site. The iterative process for the determination of the shaft length can be easily accomplished in the spreadsheet by changing the 'Embedded Length L=' value and the weighted average friction angle. The spreadsheet calculation is given in Appendix E.

5.4.7.4 Check the Deflection with COM624P.

COM624P is used to calculate the deflection of the 12 foot drilled shafts under the design load. The soil parameters used for the COM624P computer analysis is the SPT Liang Case discussed in Section 5.4.6. The 17.3 kips lateral load applied at 9 feet above ground is used as wind load.

The analysis results give the deflection of 0.9 inch at the drilled shaft head (ground level). This value is less than the permissible 1.0-inch deflection. The predicted load-deflection curve from COM624 is shown in Fig. 5.71.

5.4.7.5 The Final Design

Based on above calculations and analysis results, a 12 foot embedment length of drilled shaft with 30 inch diameter is recommended. This, when compared to the 15.7 foot original design drilled shaft length, would yield about 24% in length reduction.

Test Hole Locations

$1453{+}00$

$1454{+}00$

¢ I–225 (N of 2nd Ave) —

5450

5440

5430

5420

5410
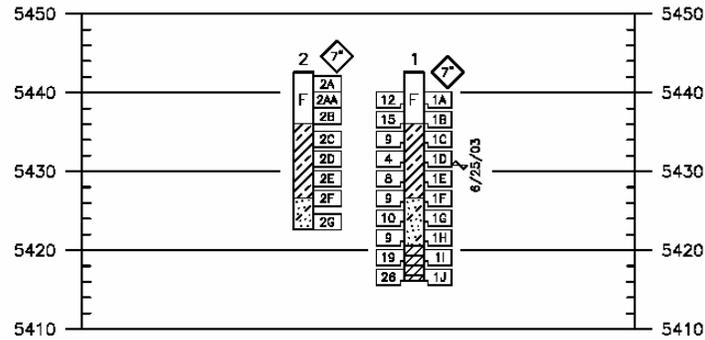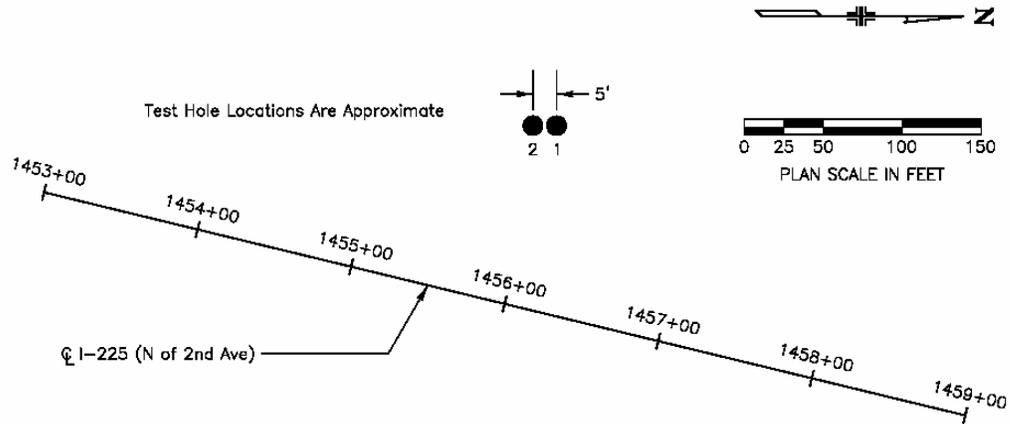
SUM		
Sample Number	Depth (feet)	Cl...
		Corps of Engrs. or Visual
2A	0.5–2.5	Silty Clay
2AA	2.5–4.5	Silty Clay
2C	7.5–9.5	Silty Clay
2D	10.0–12.0	Silty Clay
2E	12.5–14.5	Silty Clay
4A	5.0–7.0	Silty Sand
4B	10.0–12.0	Silty Sand

Figure 5.1a Location of test shafts and test borings

Test Hole Locations Are Approxim[...]

¢ I-225 (S of Iliff Ave)

1274+00   1275+00   [...]

5650

5640

5630

5620

5610

TY[...]

| F | Fill – Silty Clay |
| Silty Clay |
| Silty Sand |
| Claystone Bedrock |
| Sandstone Bedrock |

TEST BORING

3" Hole Size

Blows per foot * 30,[...] 1A Sample Number
R = Refusal on SPT

50/0.1   Water Level
50 Blows in 0.1 ft

Core Recovery 50   *Standard
R.Q.D. 25   Penetration Test
(AASHTO T 206–8[...]
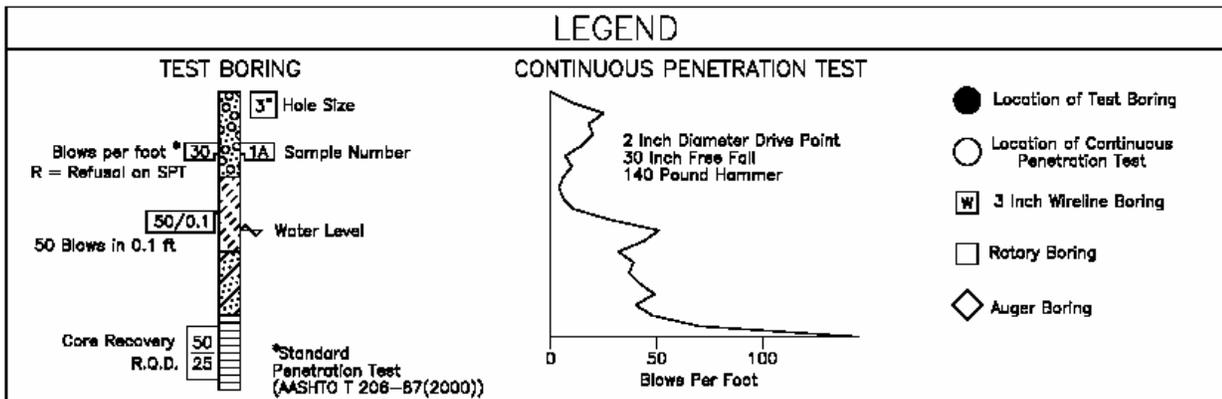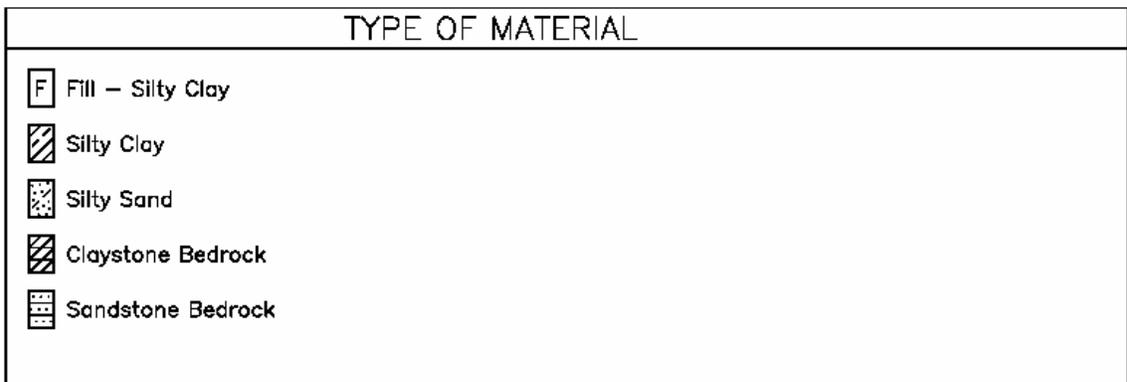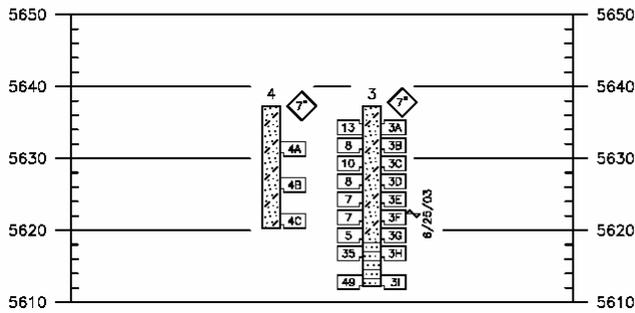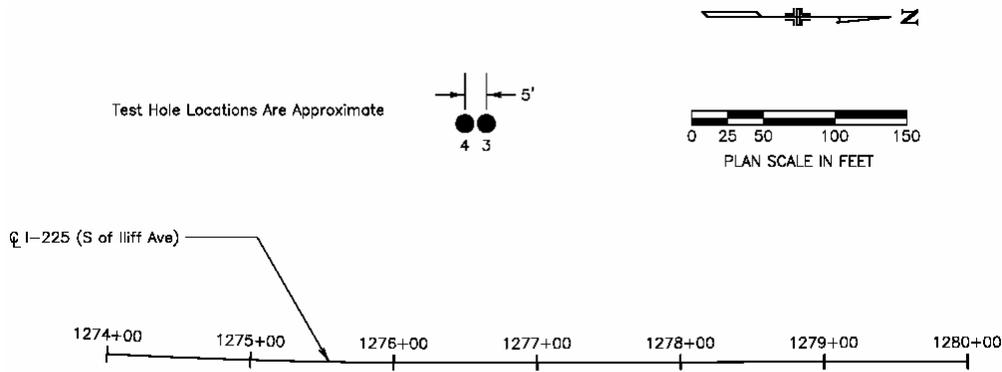
Figure 5.1b Location of test shafts and test borings
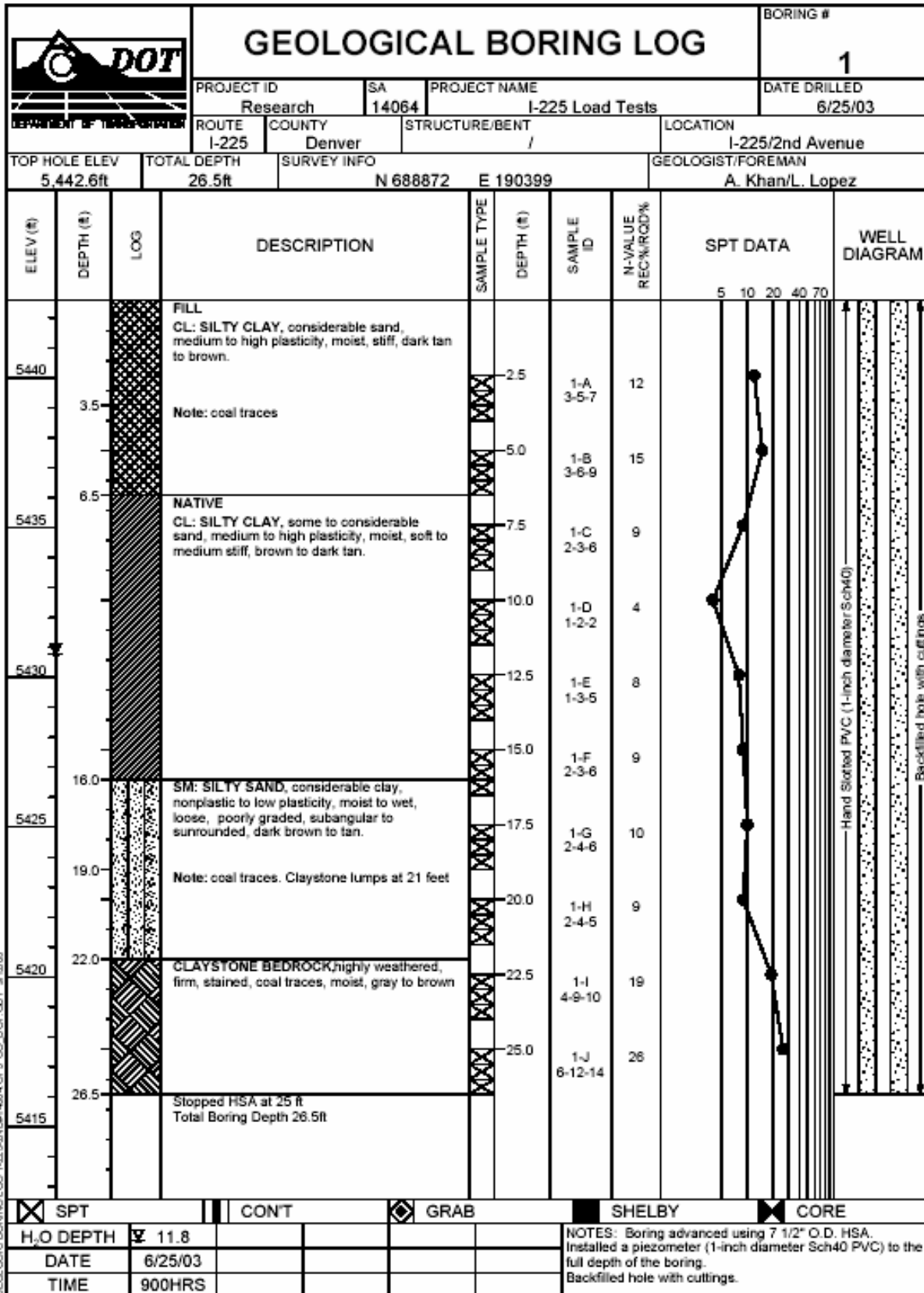
Figure 5.2a Test borings 1
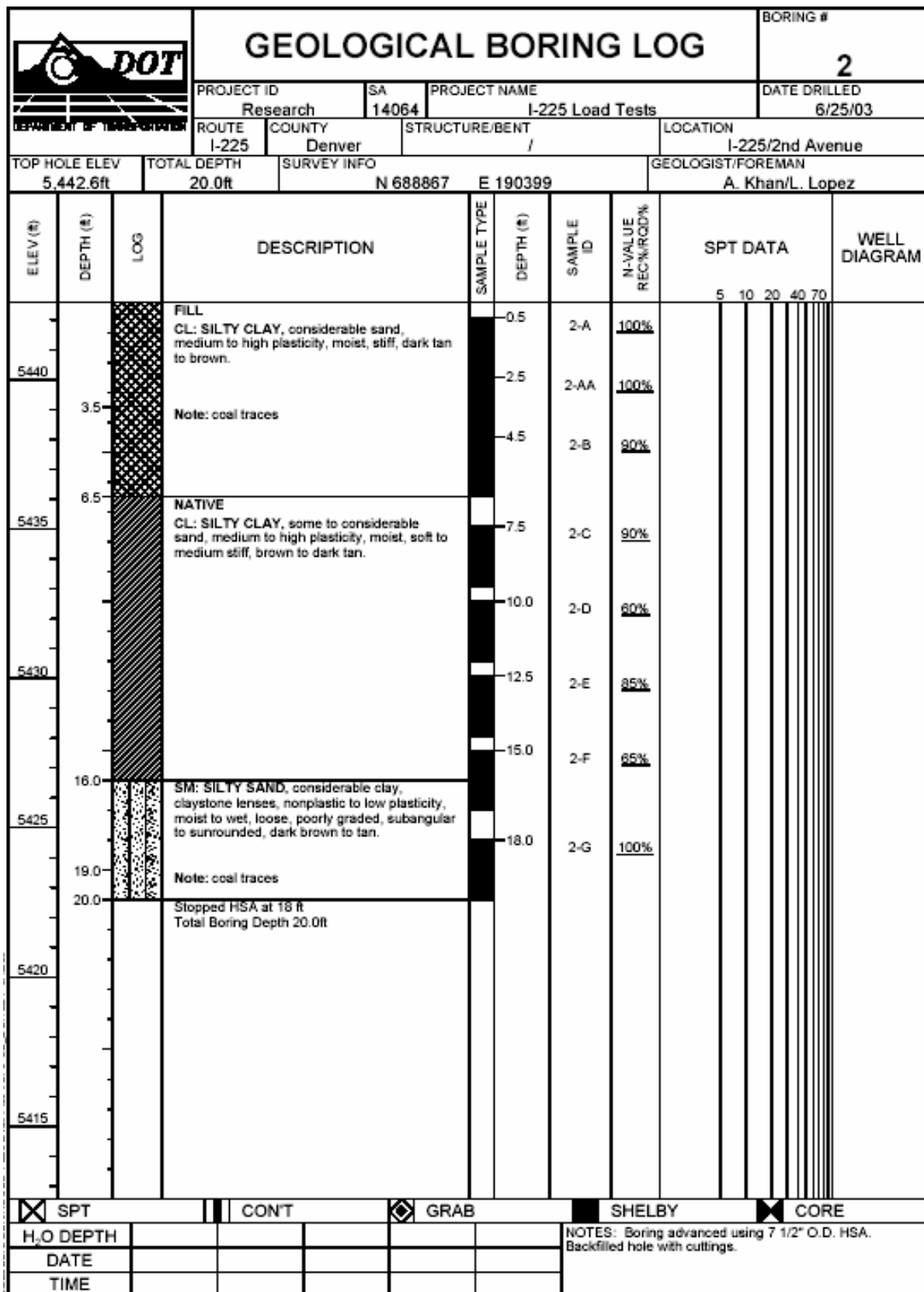
Figure 5.2b Test borings 2
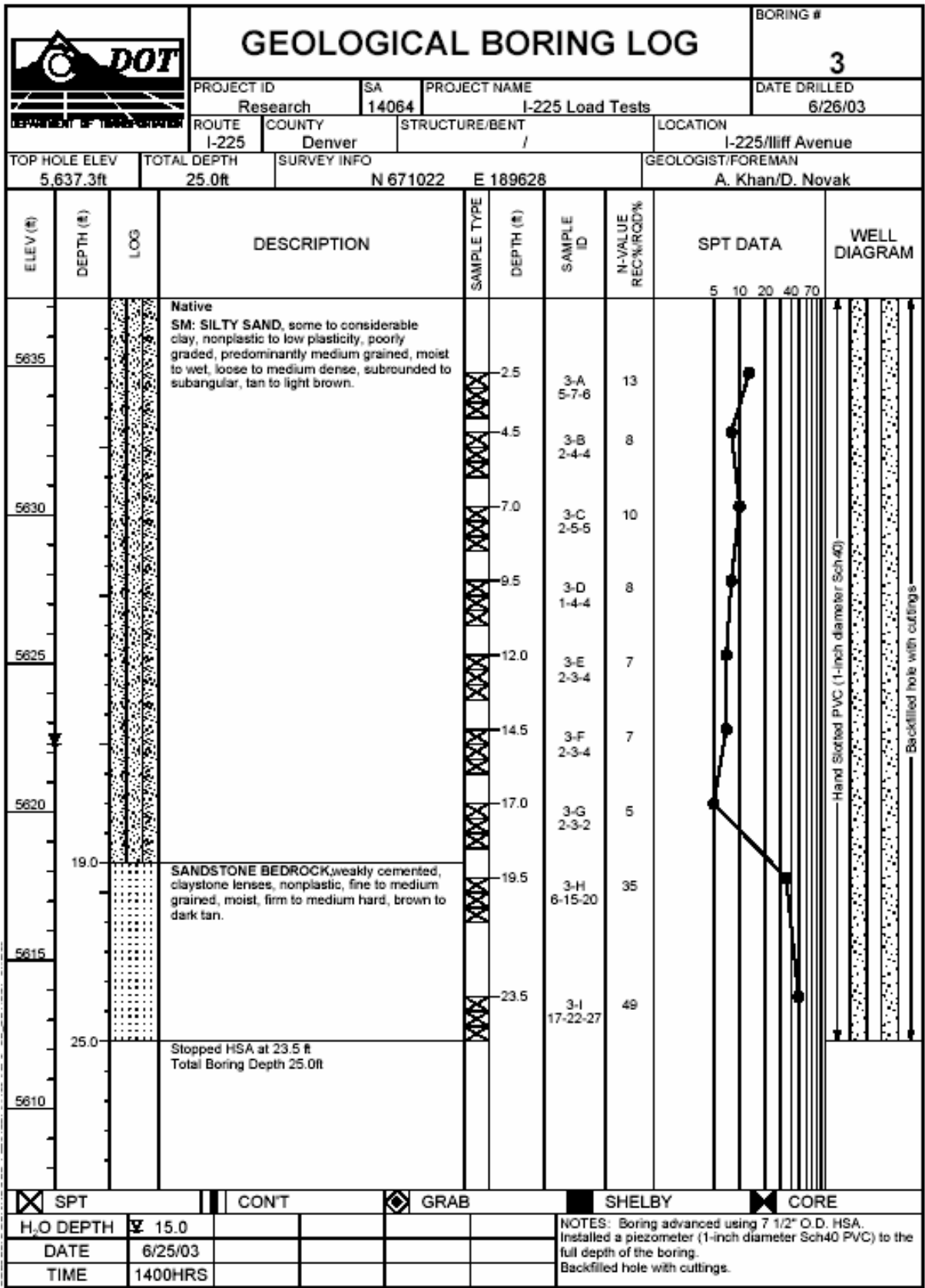
Figure 5.2c Test borings 3
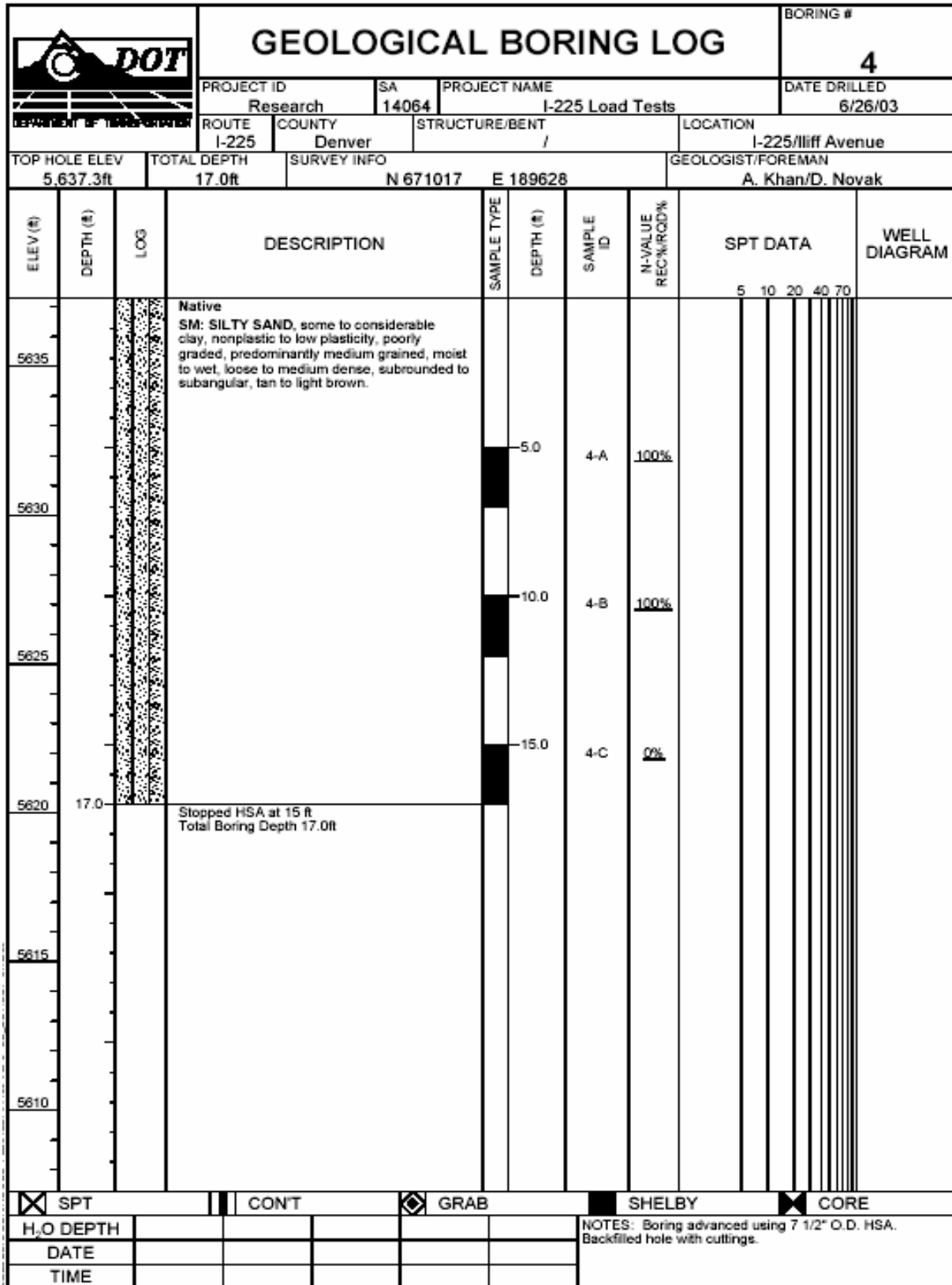
Figure 5.2d Test borings 4

2 - ℓ12"x12"x1"

C10x30

C10x30

DIAL GAGE
TYP.

HANGING BEAM
TO CARRY THE
DIAL GAGE

3'-0" CASING
¼" THICK, 30" DIA.
TYP.

SISTERBAR
VIBRATING WIRE
STRAIN GAGE
TYP.
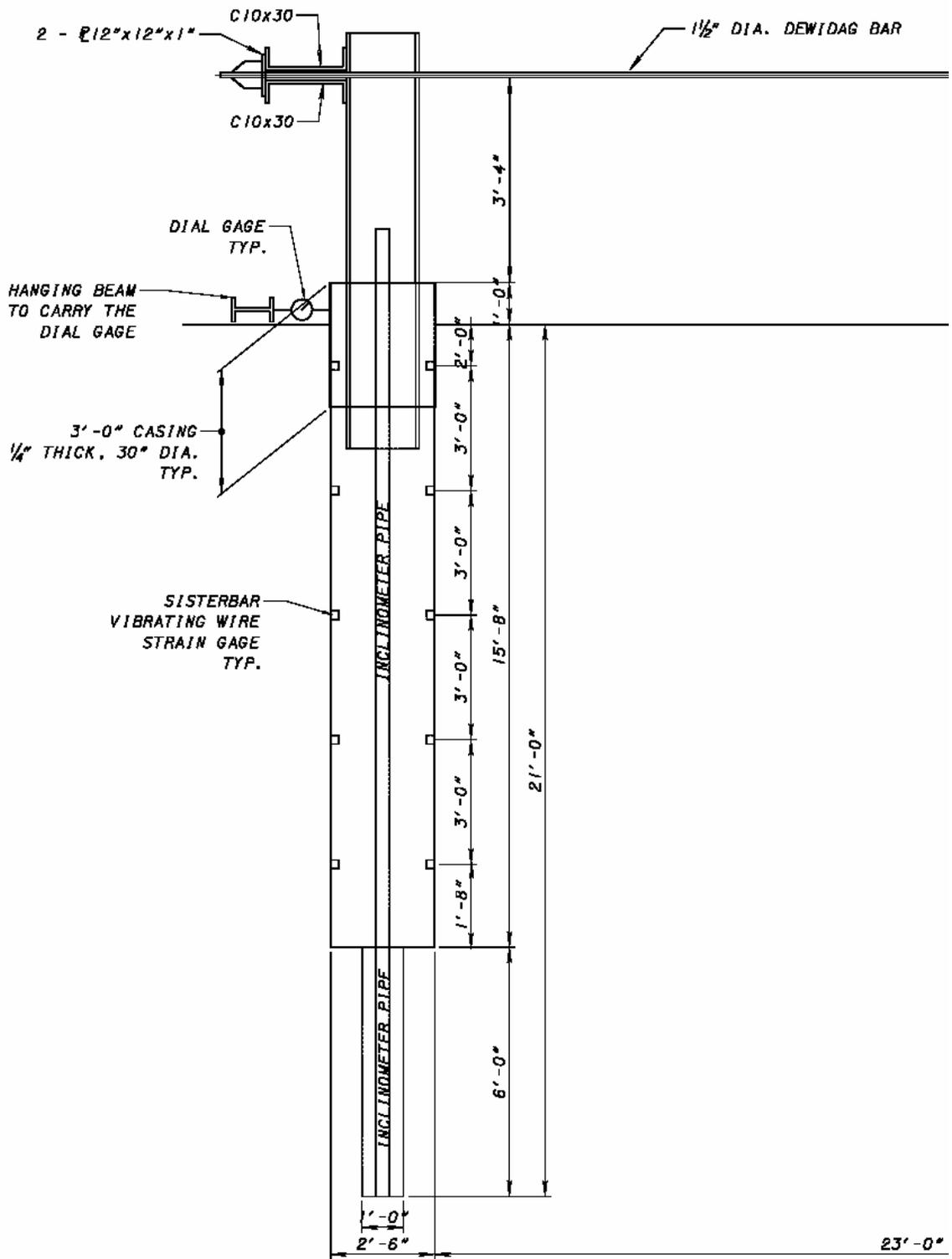
Figure 5.3a Location of instruments at test shaft 1
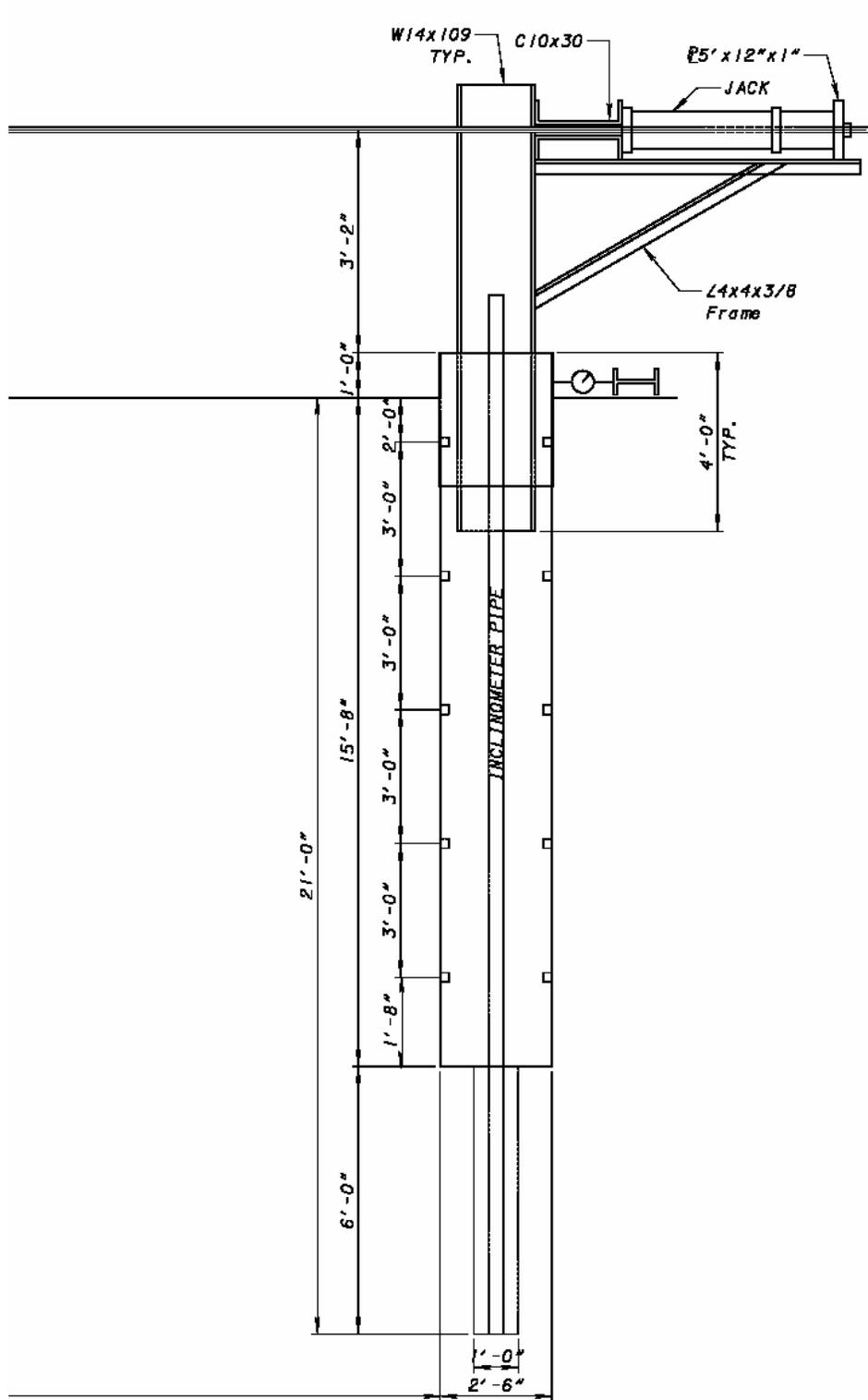
Figure 5.3b Location of instruments at test shaft 2
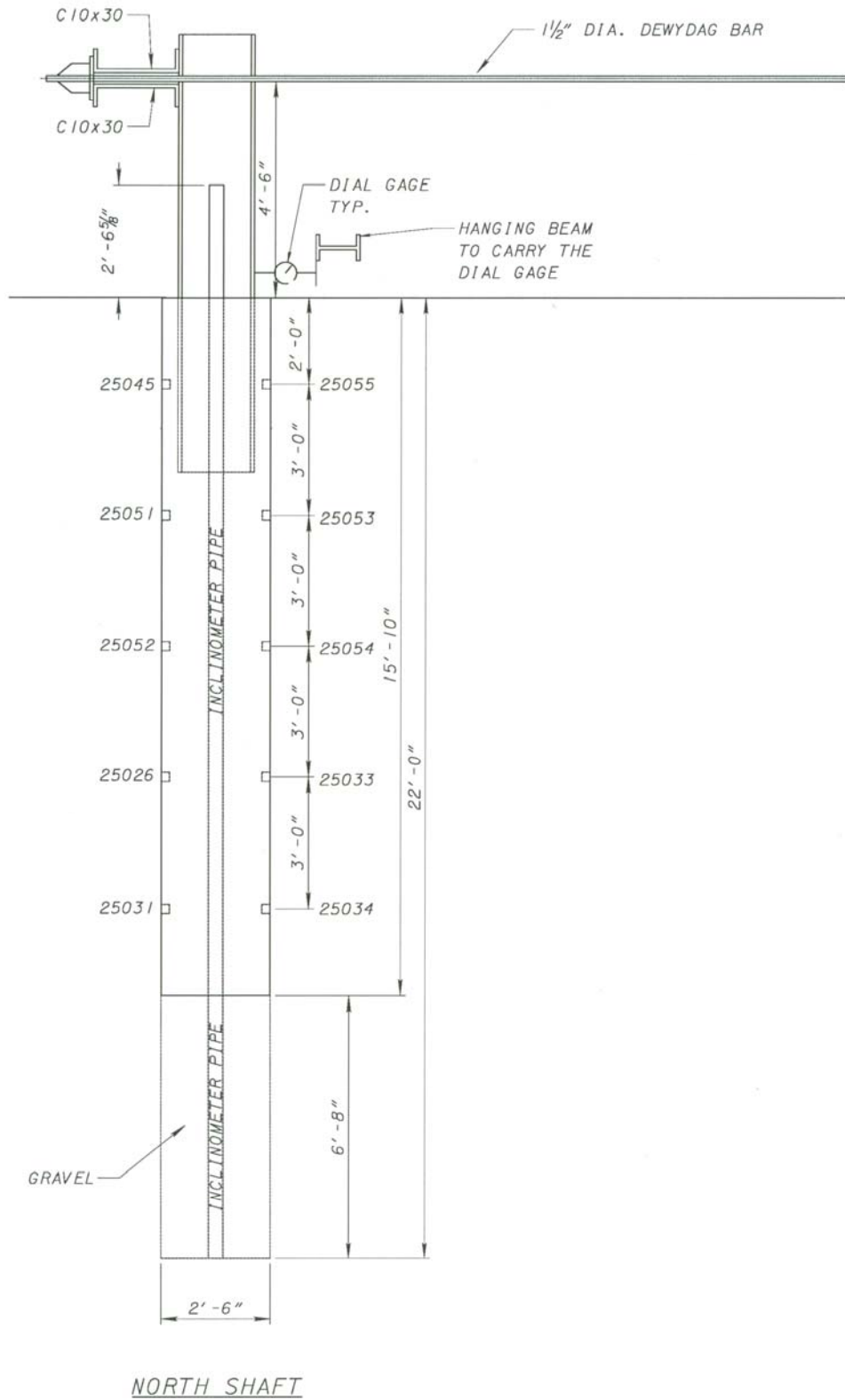
Figure 5.3c Location of instruments at test shaft North (Iliff Ave)
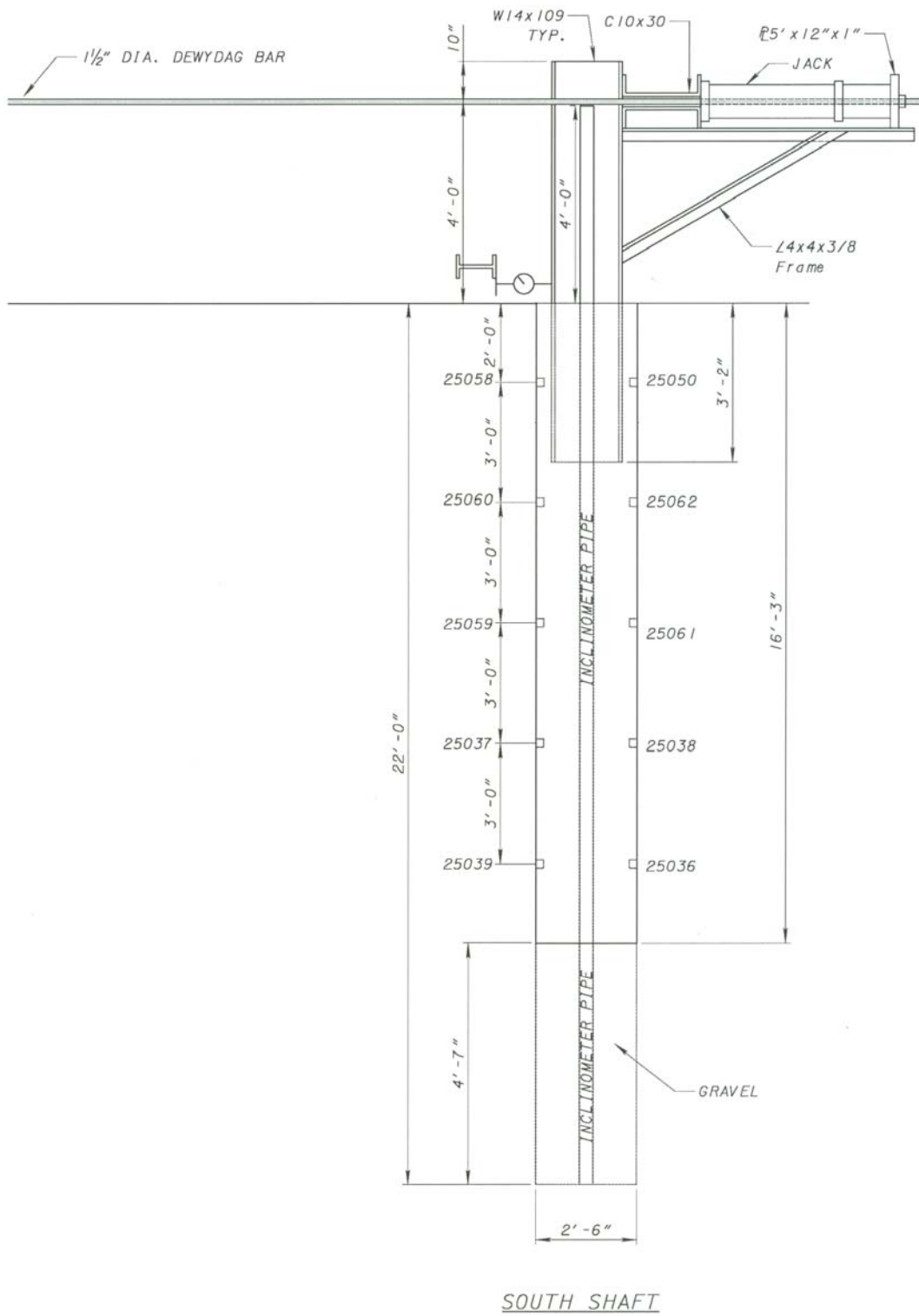
Figure 5.3d Location of instruments at test shaft South (Iliff Ave.)

2'-6"∅ Caisson
16'-8" deep where
indicated on the
layout.

#8 (Proj.
5'-0")

#8 bundles (Proj.
5'-0" and 8'-0")
(Typ.)
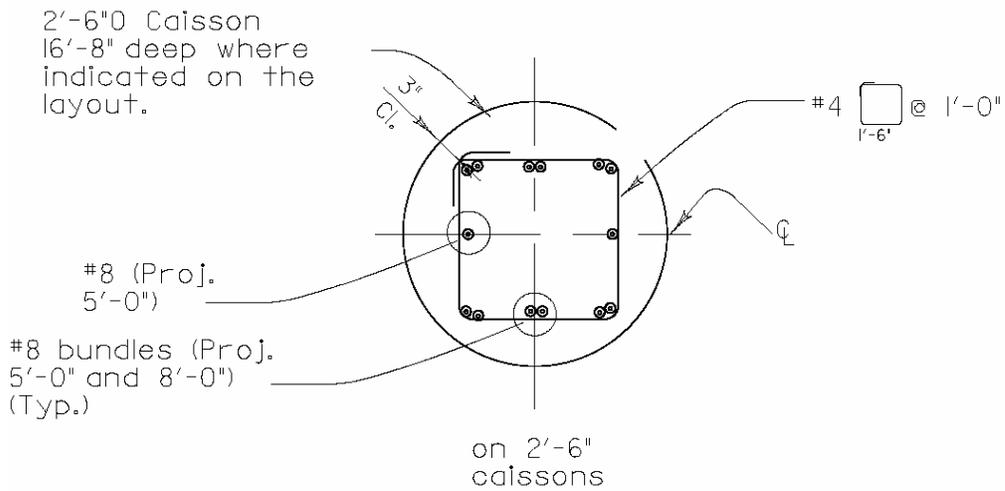
Reinforcement of test drilled shafts at 6th Avenue (clay site)

2'-6"∅ Caisson
16'-8" deep where
indicated on the
layout.

#9 Rebar

#9 Rebar
(Typ.)
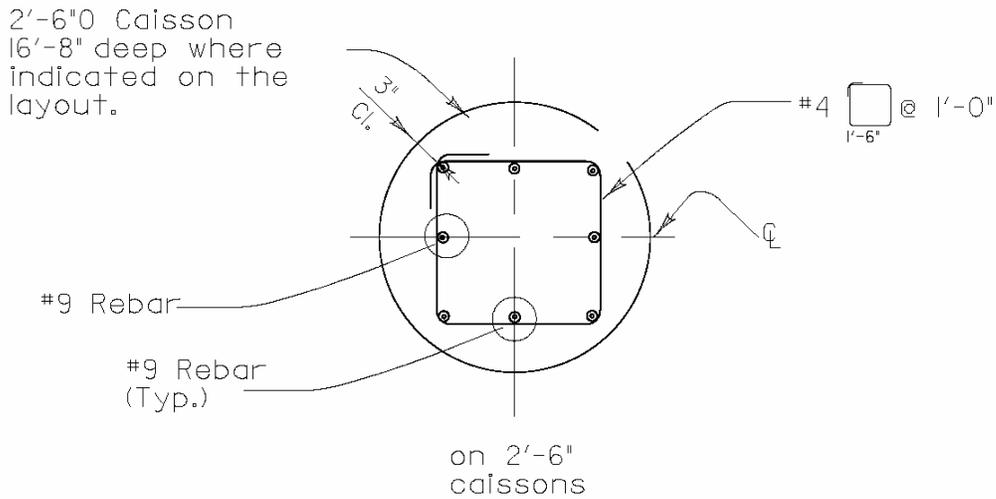
Reinforcement of test drilled shafts at Iliff Avenue (sand site)

Figure 5.3e Reinforcement of drilled shafts at both test sites

Figure 5.4 Installation of gage on steel cages

Figure 5.5a Inclinometer assembly

Figure 5.5b Inclinometer installation in the hole

Figure 5.6 Pouring sand to fill around the bottom 6' of the inclinometer tube

Figure 5.7 Instrumented cage transferred to the hole

Figure 5.8 Drilled shafts installed and ready for concrete

Figure 5.9 Pouring concrete in the hole

Figure 5.10 Picture showing the installation of the testing devices

Figure 5.11 Picture showing the installation of the testing devices

Figure 5.12 Picture showing the jacking devices

Figure 5.13 Setup of measuring devices at shaft 2 (South)

Figure 5.14 Setup of measuring devices at shaft 1 (North)

Figure 5.15 General view of the load test

Figure 5.16 Running the test and watching the instruments

Figure 5.17 Picture showing opening behind the shaft during the test

Figure 5.18 Picture showing data collection devices used in the test

CDOT-Lateral load test Shaft 1 - CLAY
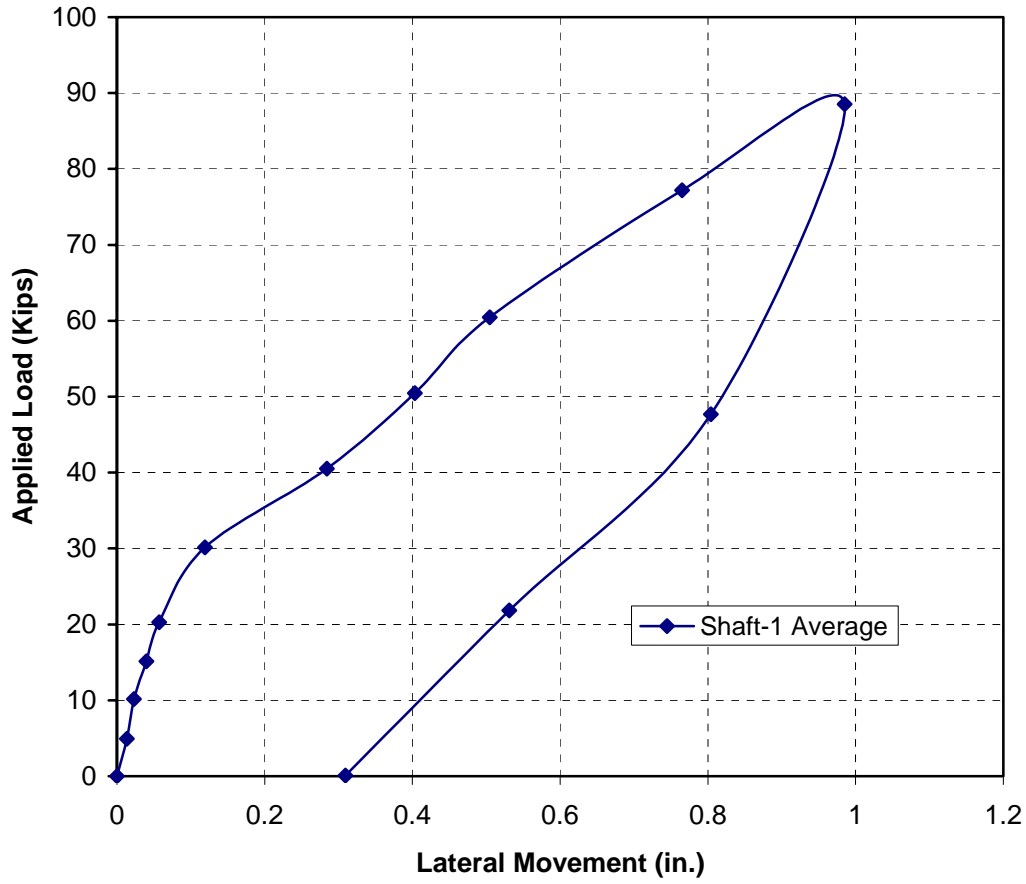
Figure 5.19 Load-deflection curve at the top of test shaft #1 from dial gages

CDOT-Lateral Load Test Shaft 2 - CLAY
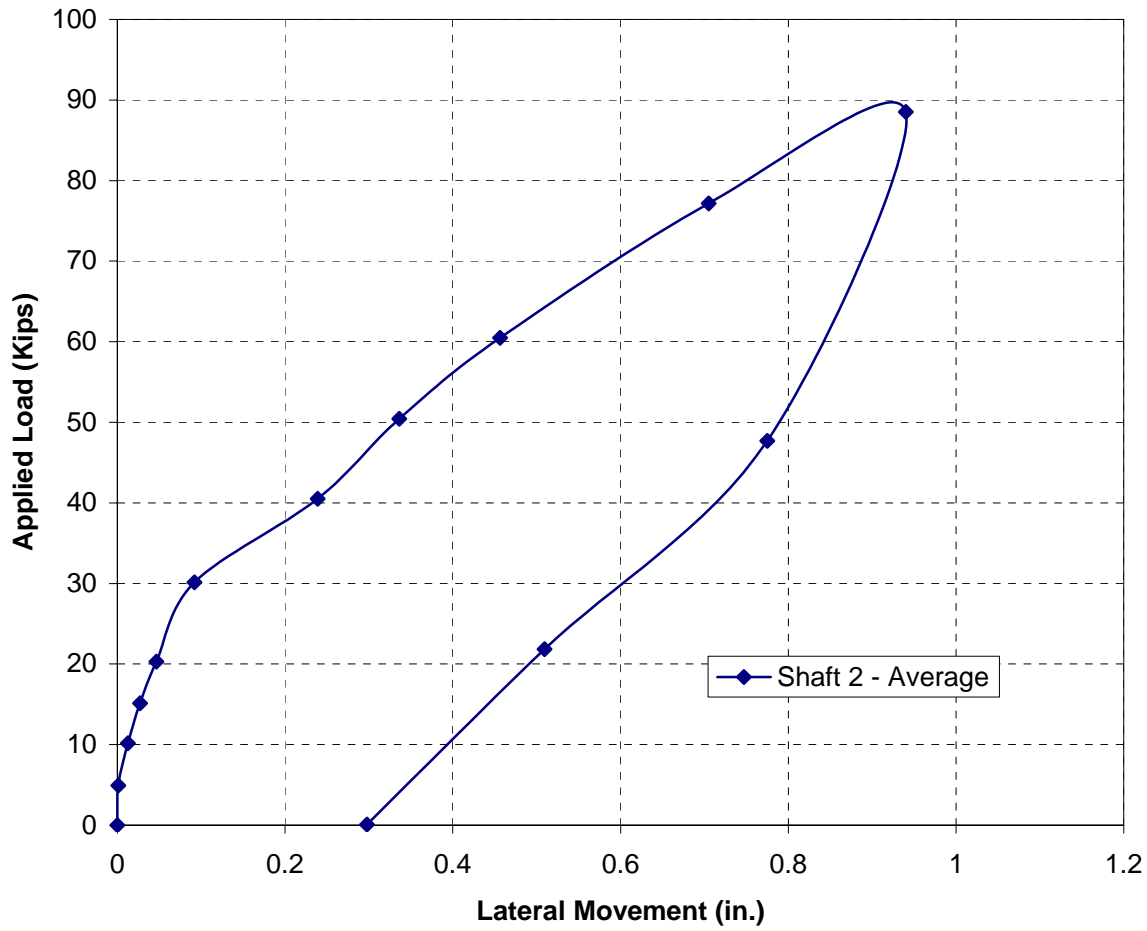
Figure 5.20 Load-deflection curves at the top of test shaft #2 from dial gages

CDOT-Lateral load test Shaft 1 - CLAY
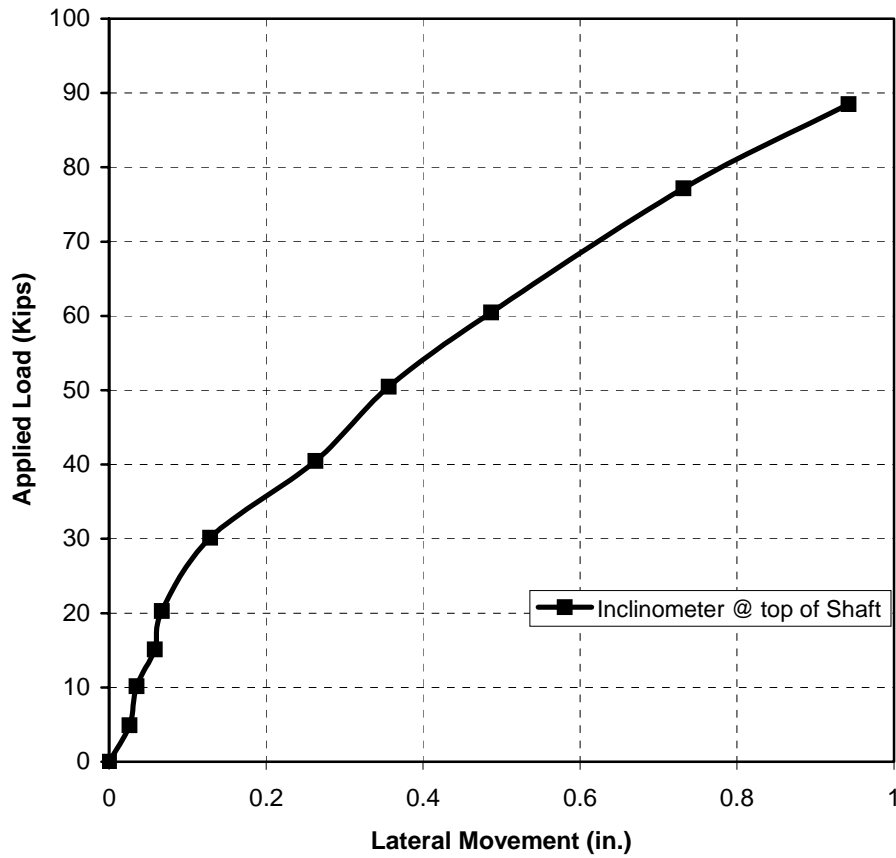
Figure 5.21 Load-deflection curve at the top of test shaft #1 from inclinometer

CDOT-Lateral load test Shaft 2- CLAY
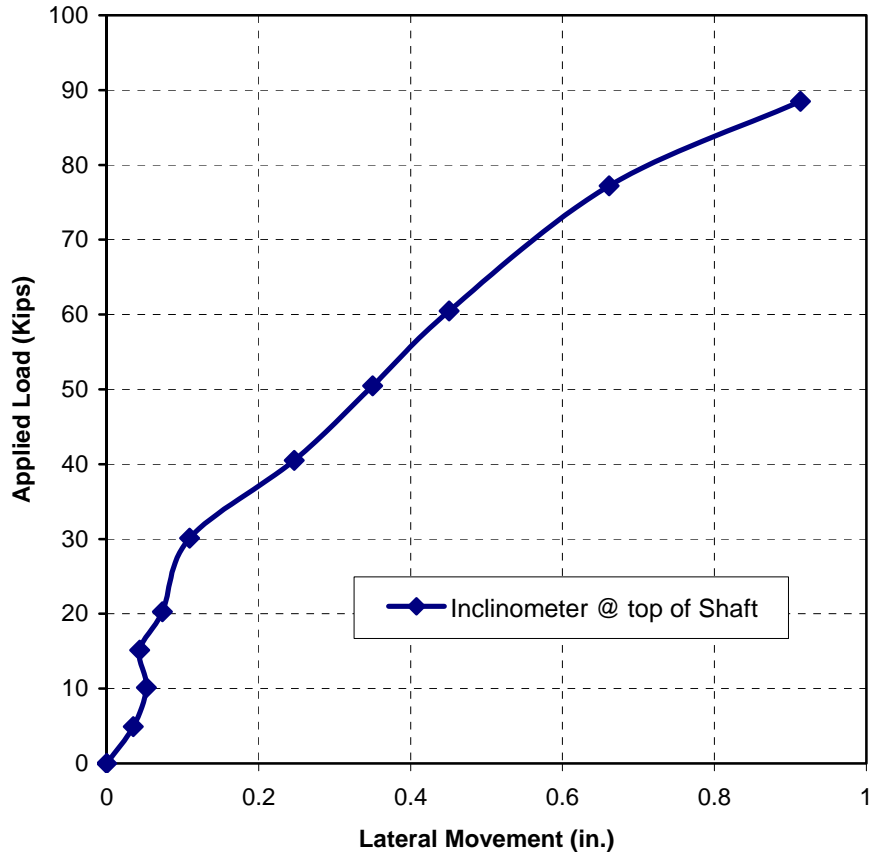
Figure 5.22 Load-deflection curve at the top of test shaft #2 from inclinometer

CDOT-LATERAL LOAD TEST SHAFT #1 - CLAY
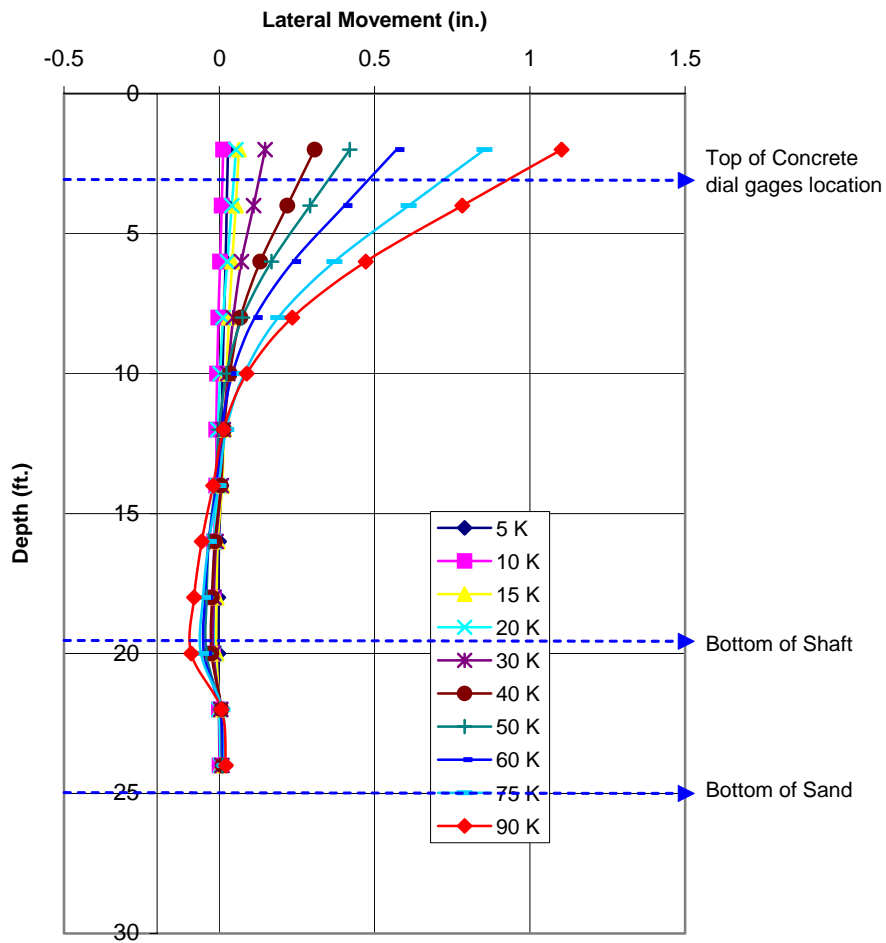
Figure 5.23. Load-deflection curve along the depth of test shaft #1 from inclinometer
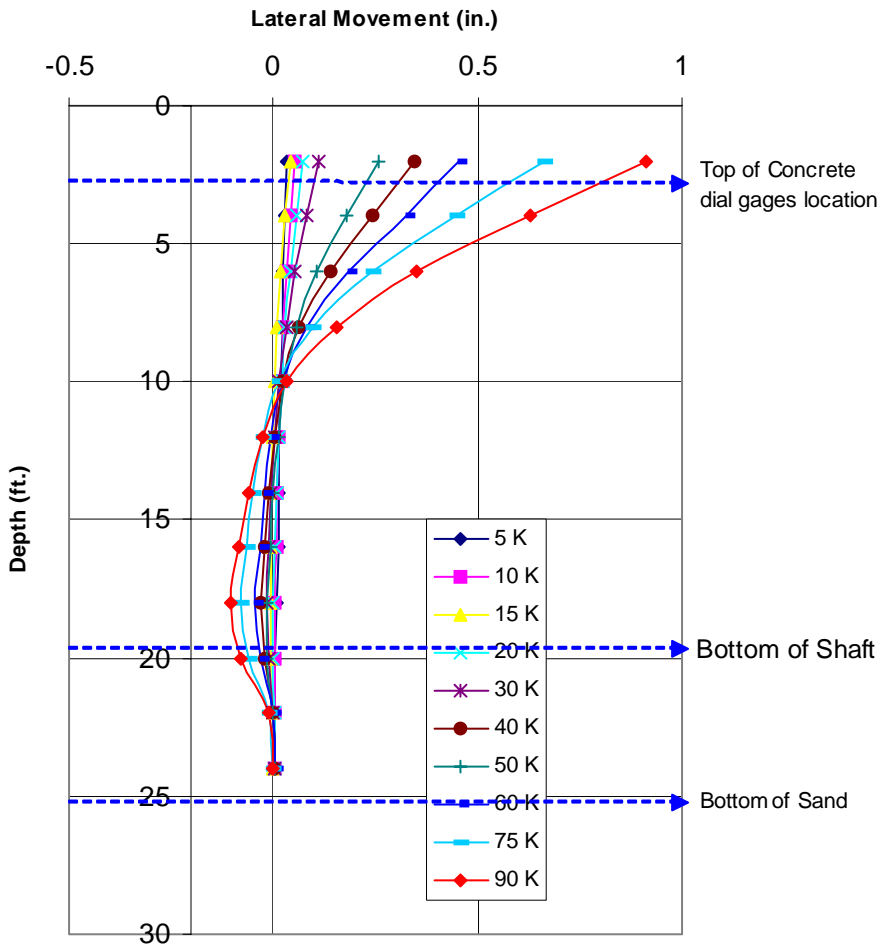
Figure 5.24 Load-deflection curves along the depth of test shaft #2 from inclinometer

CLay Site: Shaft-1
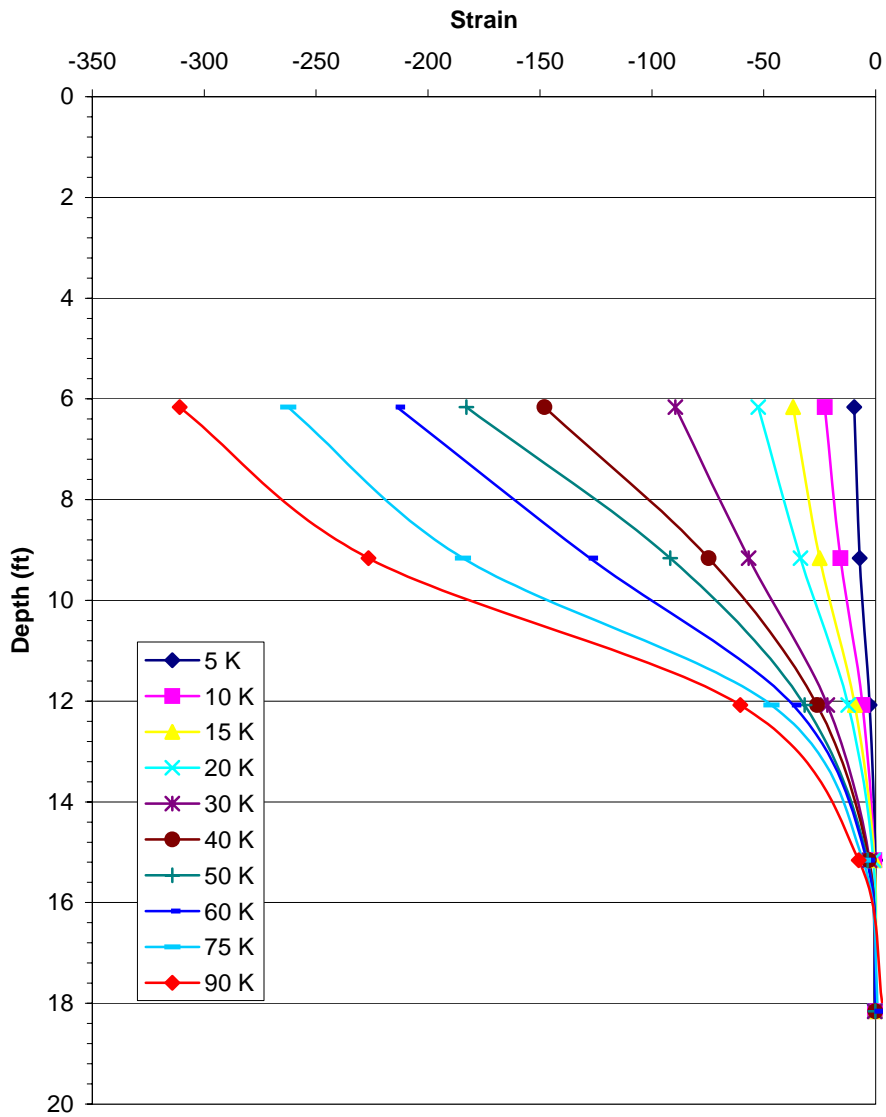
Strain

Figure 5.25. Test shaft #1, strain vs. depth on compression side

Figure 5.26. Test shaft #1, strain vs. depth on tension side

Figure 5.27. Test shaft #1, measured angle of tilt
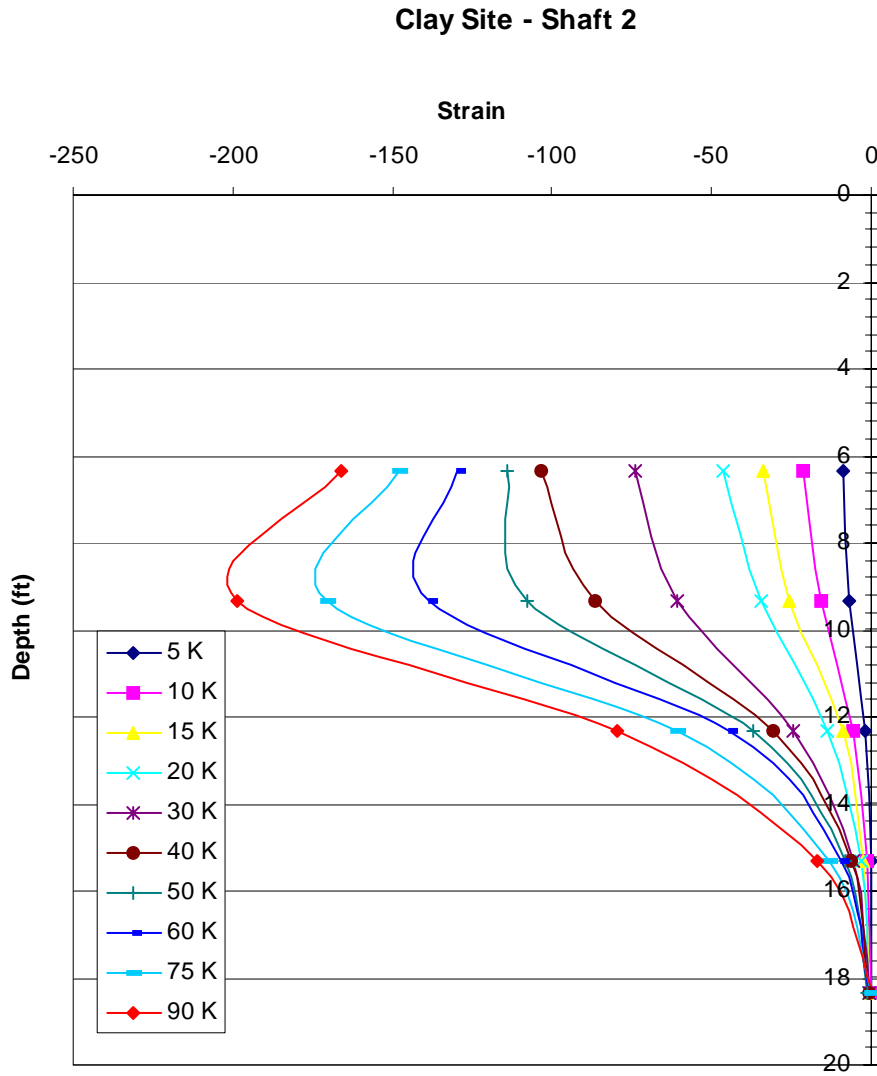
Clay Site - Shaft 2

Figure 5.28. Test shaft #2, strain vs. depth on compression side

Clay Site - Shaft 2
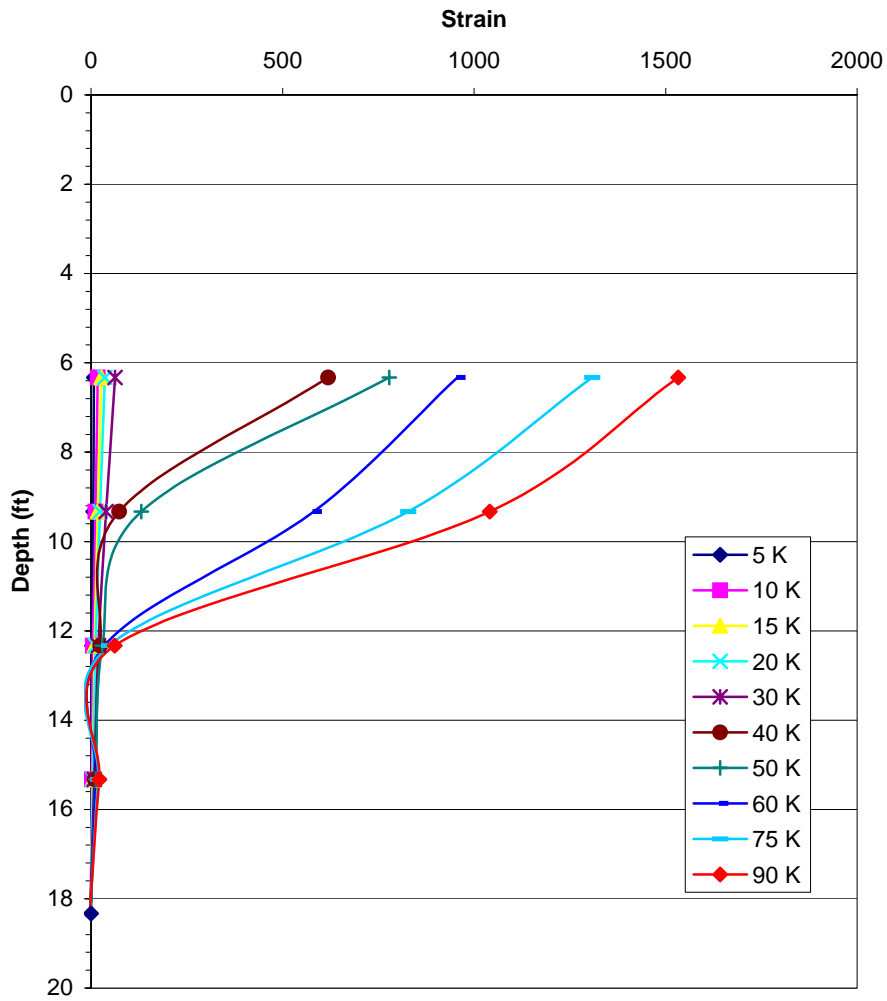
Figure 5.29. Test shaft #2, strain vs. depth on tension side
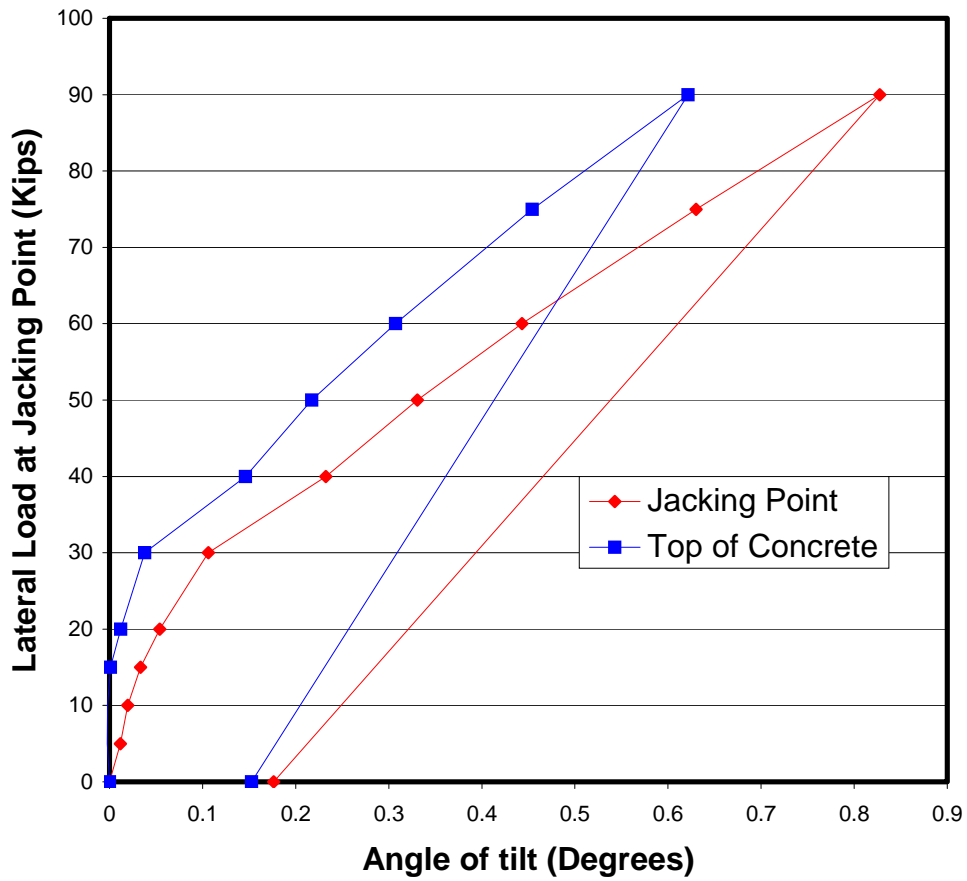
Figure 5.30. Test shaft #2, measured angle of tilt
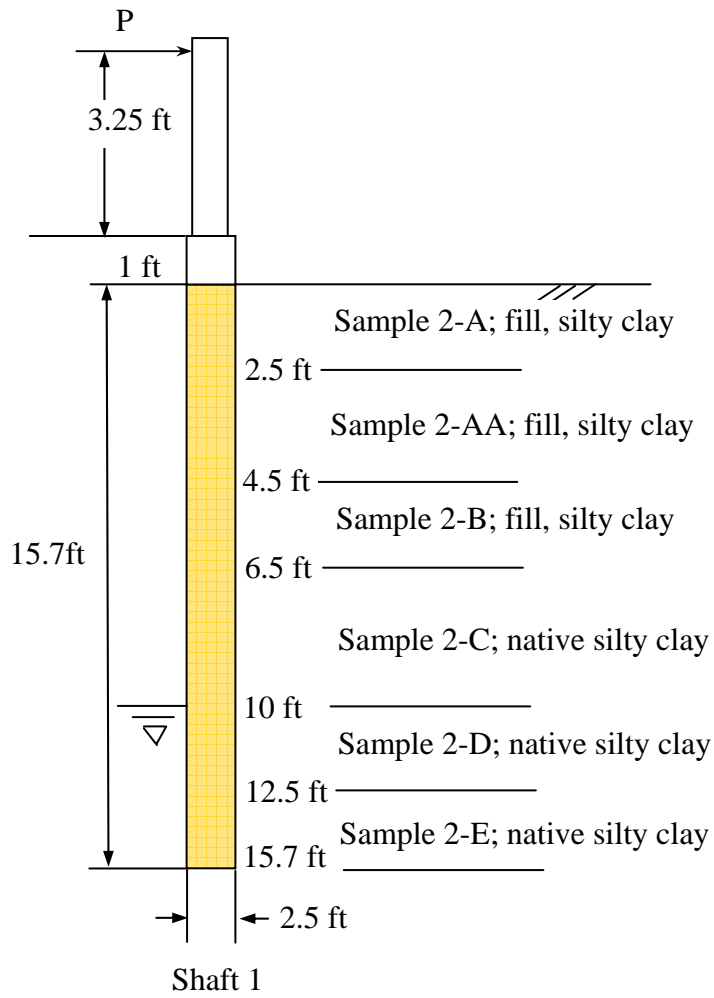
Figure 5.31 The shaft setup and soil profile interpreted for analysis at clay site
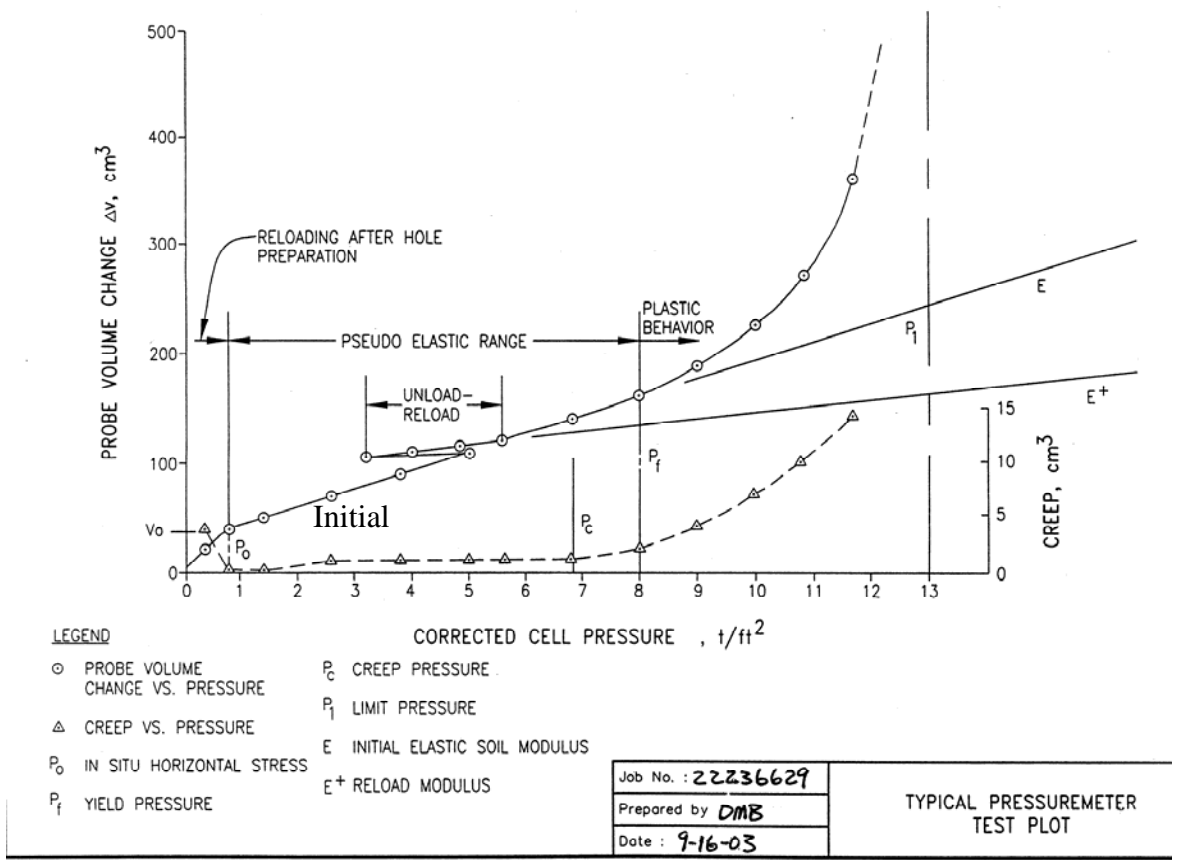
Figure 5.32 Typical pressuremeter test plot
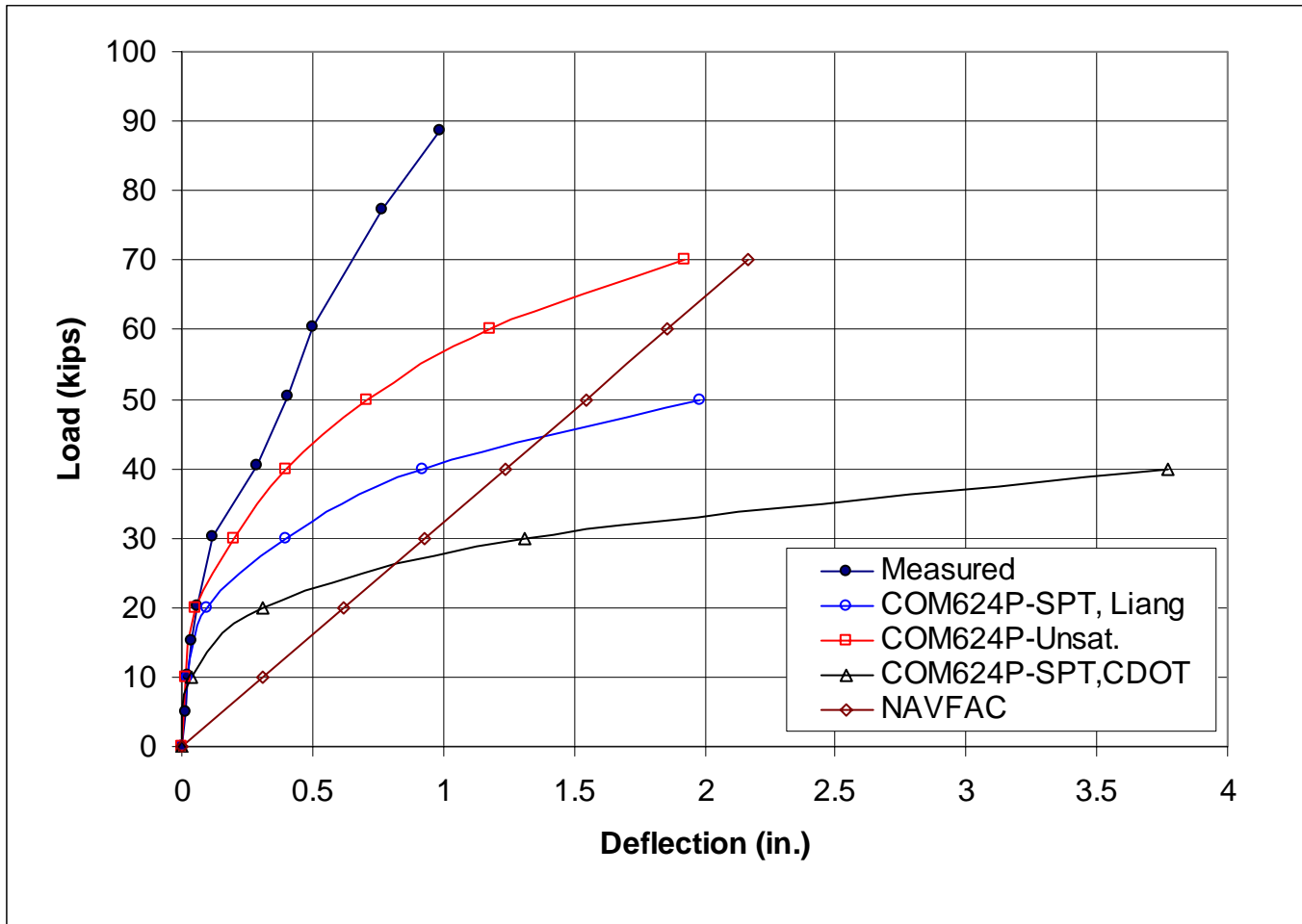
Figure 5.33. Lateral load-deflection curves based on SPT and lab test results for CDOT test in clay, shaft # 1
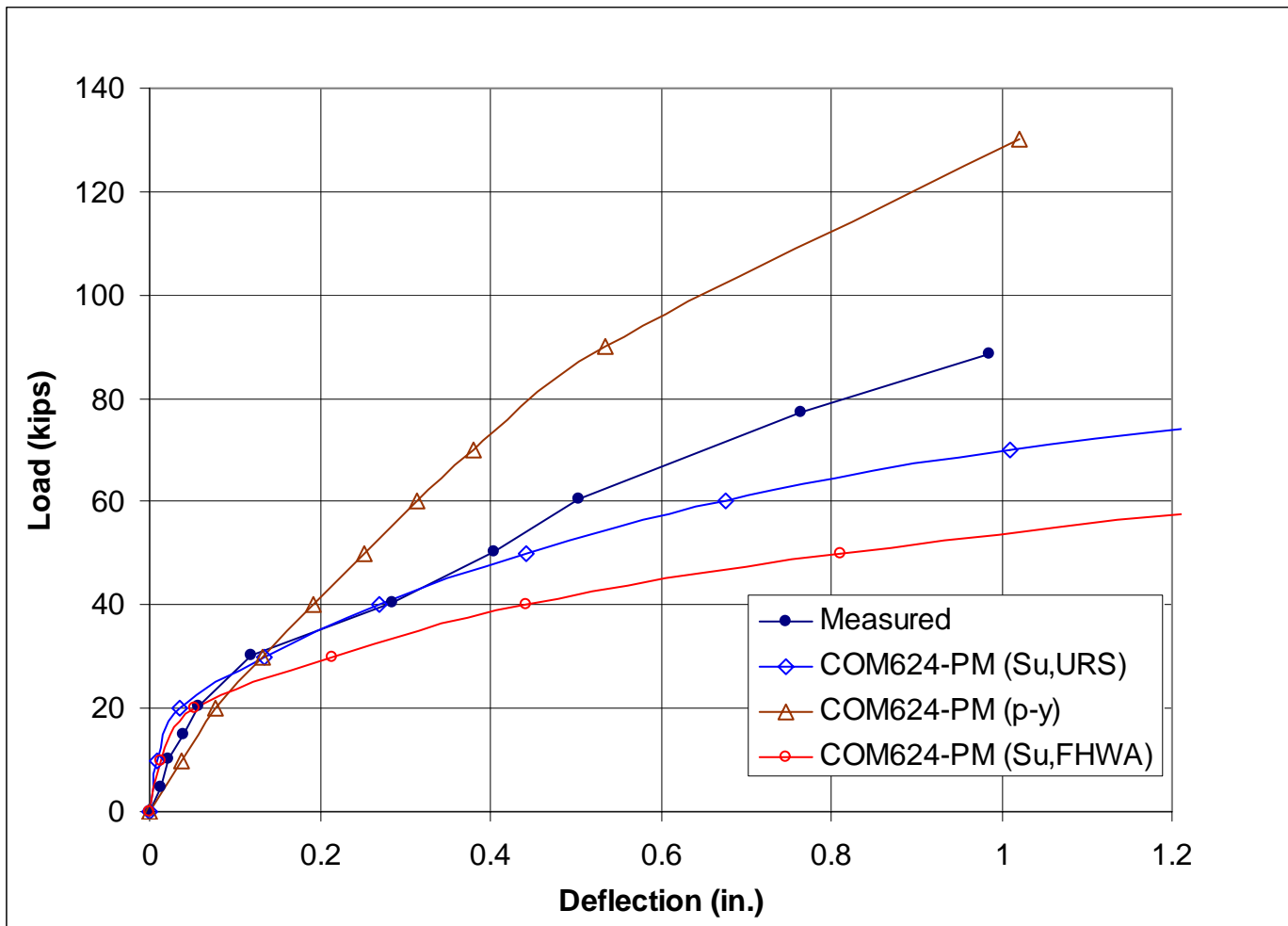
Figure 5.34. Lateral load-deflection curves based pressuremeter test results for CDOT test in clay, shaft # 1
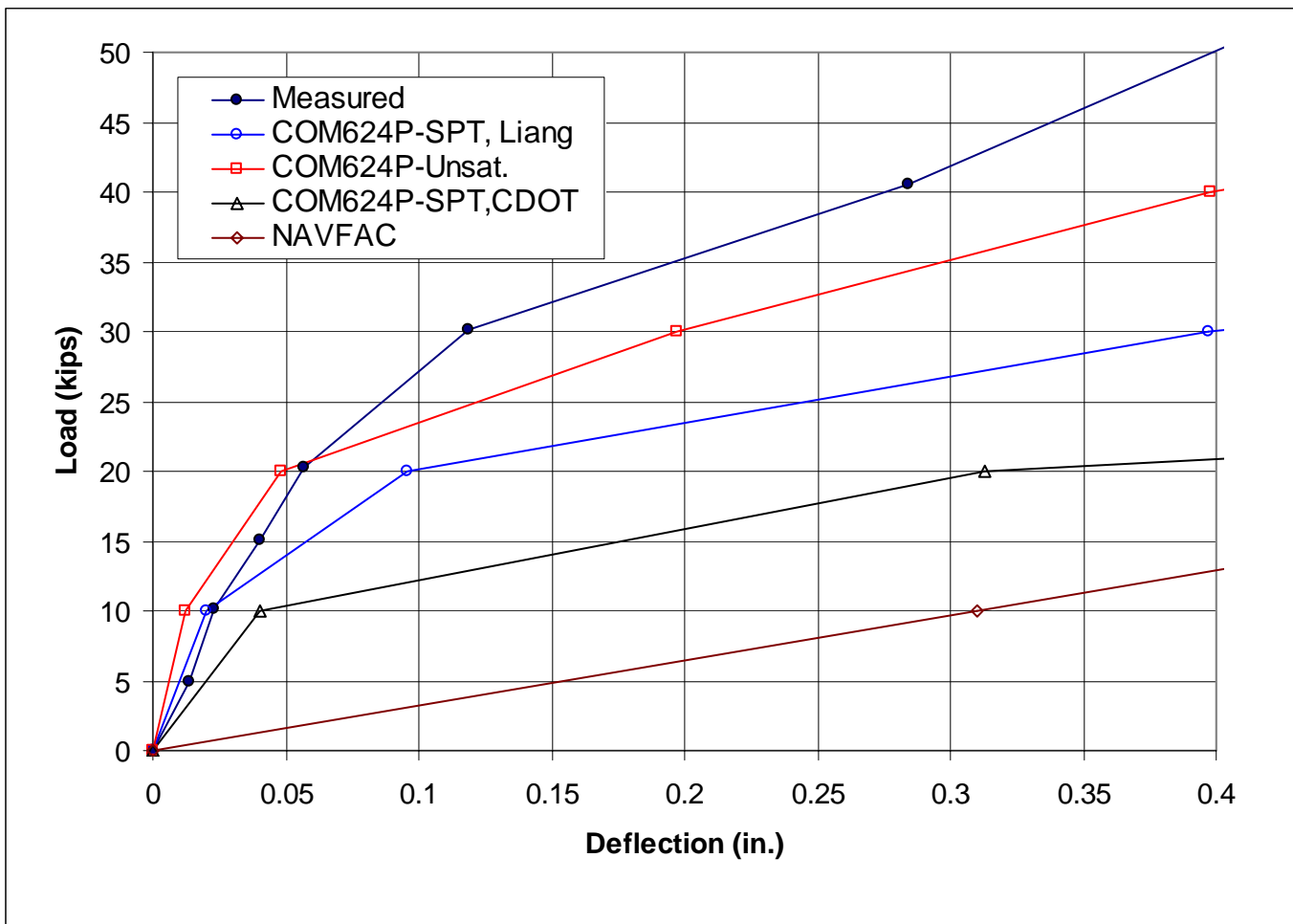
Figure 5.35. Zoomed load-deflection curves based on SPT and lab test results for CDOT test in clay, shaft # 1
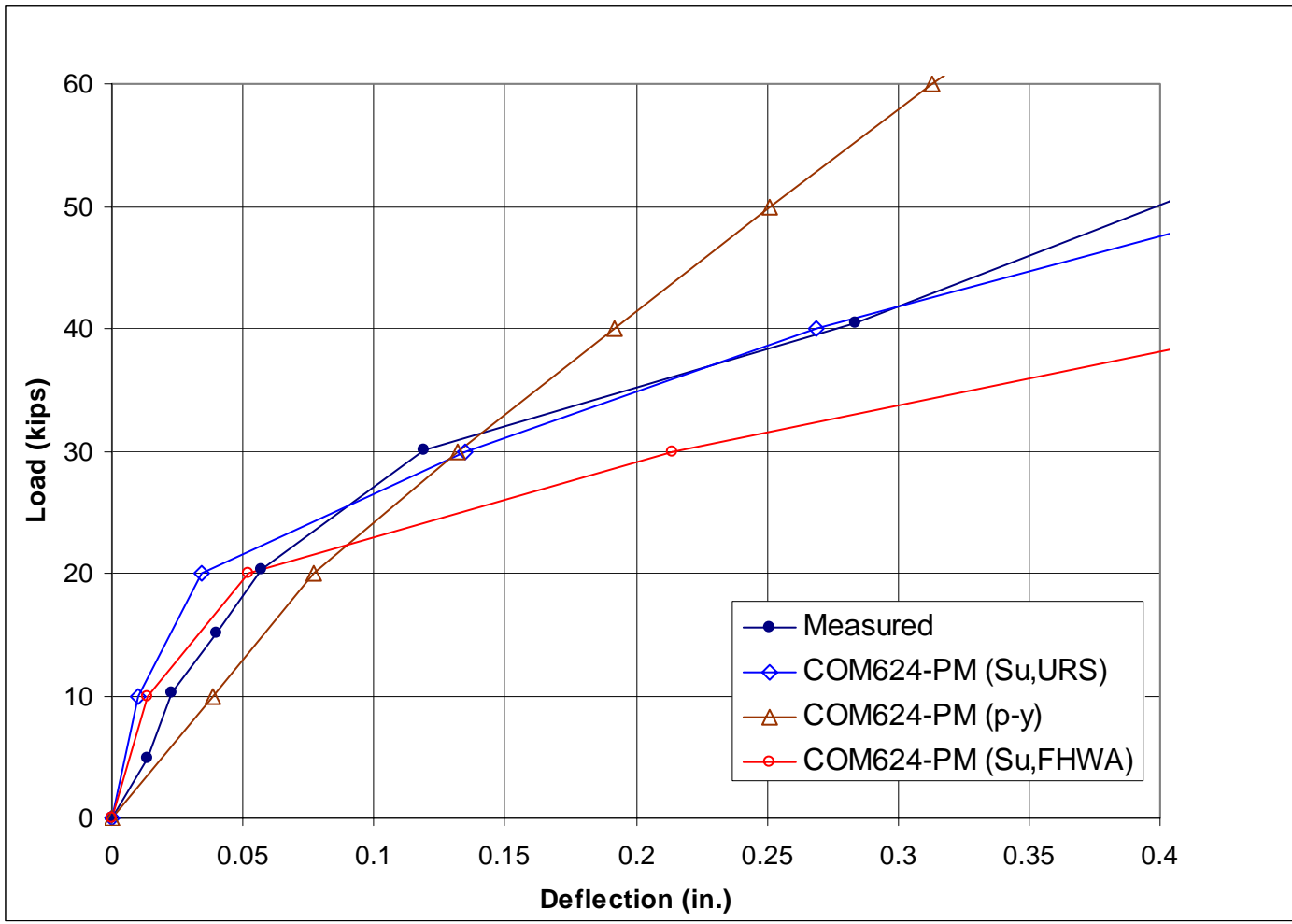
Figure 5.36. Zoomed load-deflection curves based on pressuremeter test results for CDOT test in clay, shaft # 1
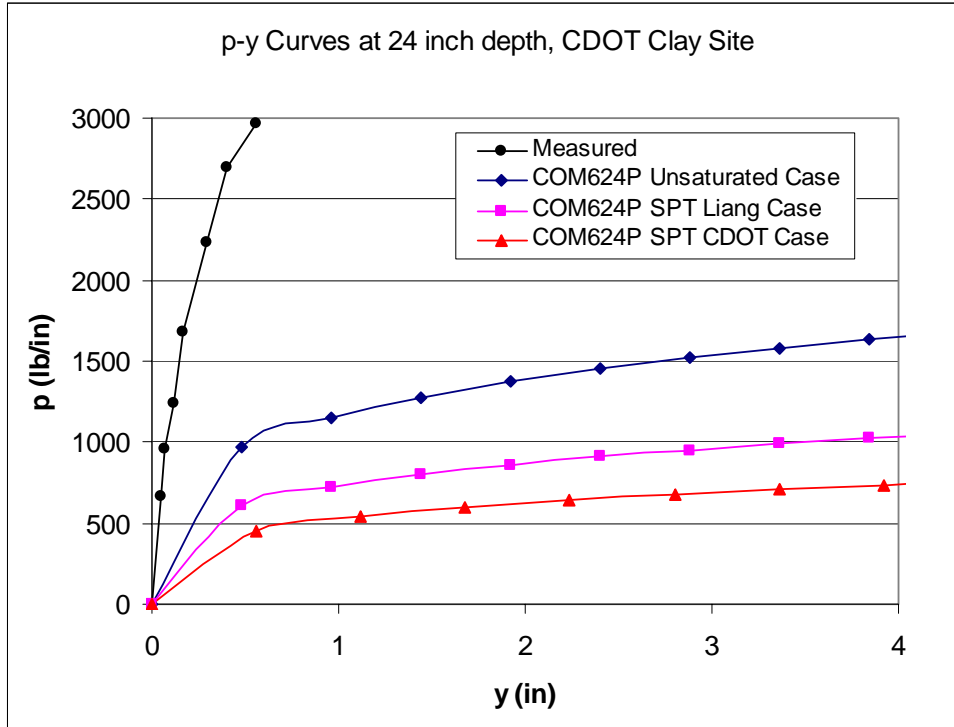
(a) p-y curves from SPT and lab test determined soil parameters
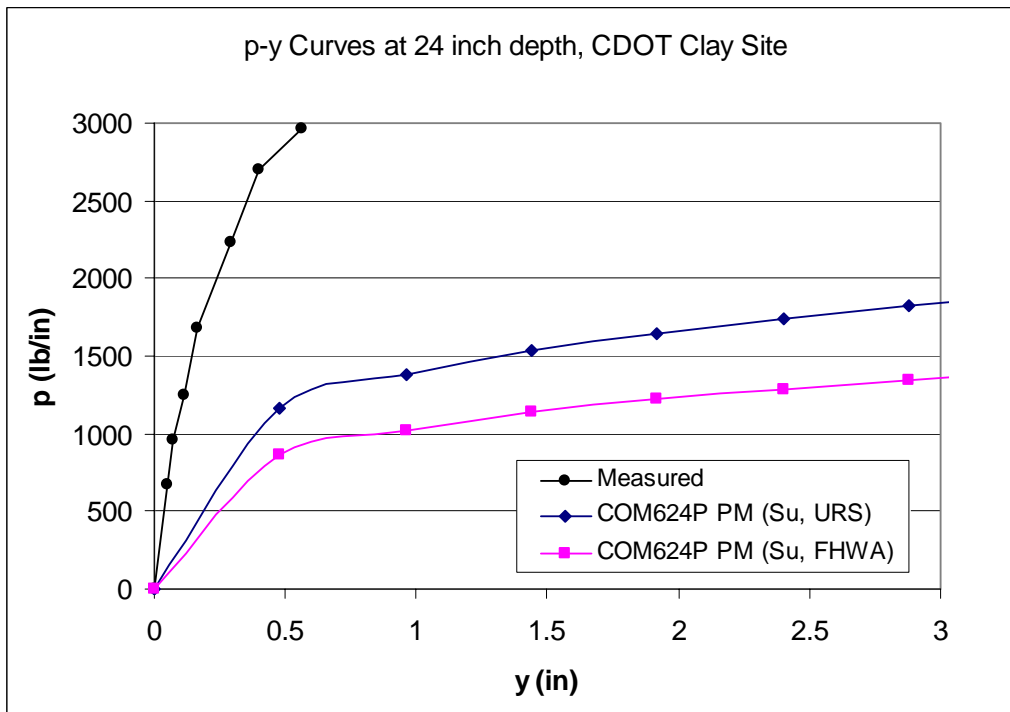
(b) p-y curves from pressuremeter determined soil parameters

Figure 5.37 P-y curves derived by strain and deflection data versus by (a) Lab and SPT soil parameters, and (b) pressuremeter data
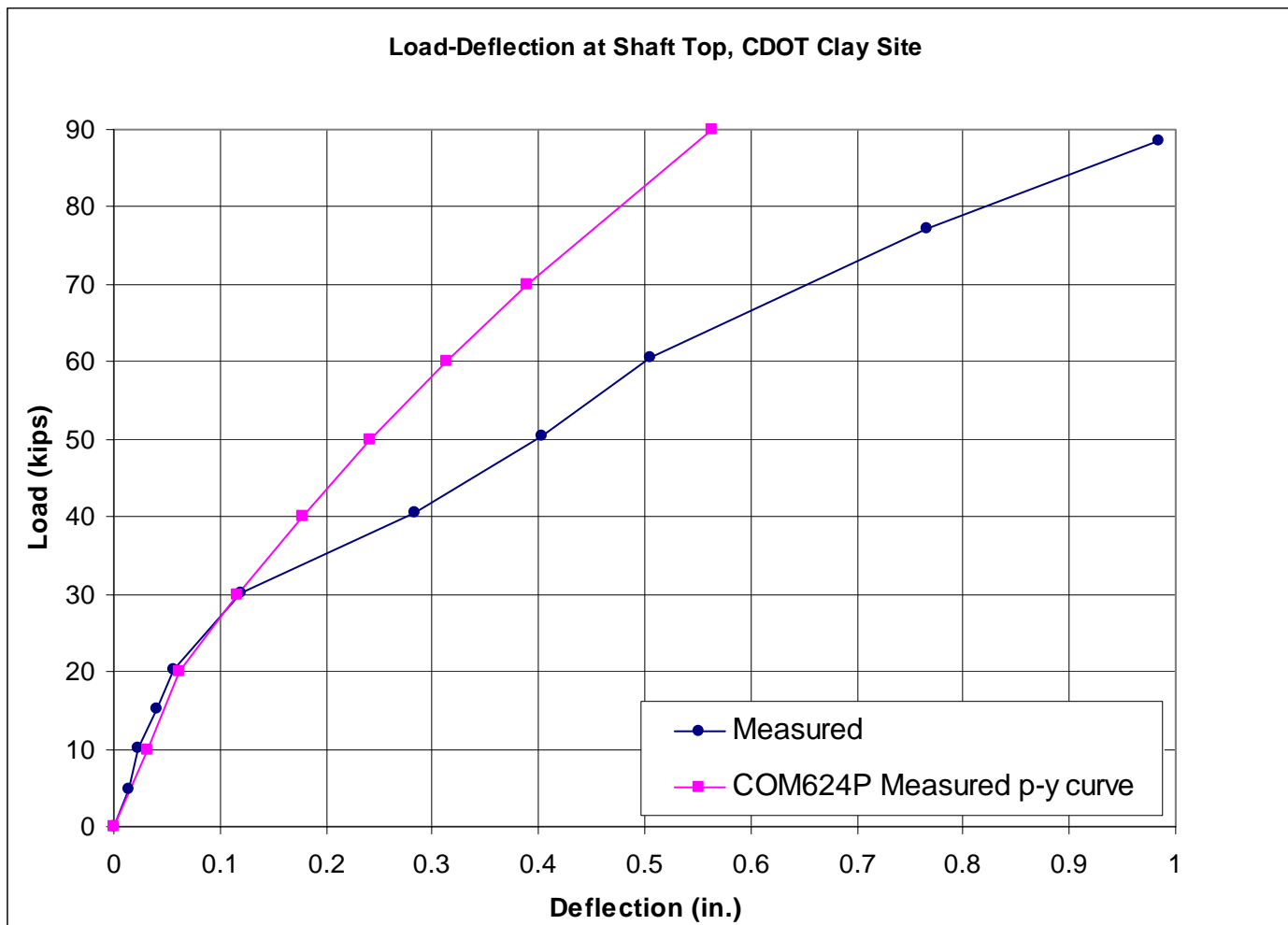
Figure 5.38 Back analysis of load-deflection from measured p-y curves
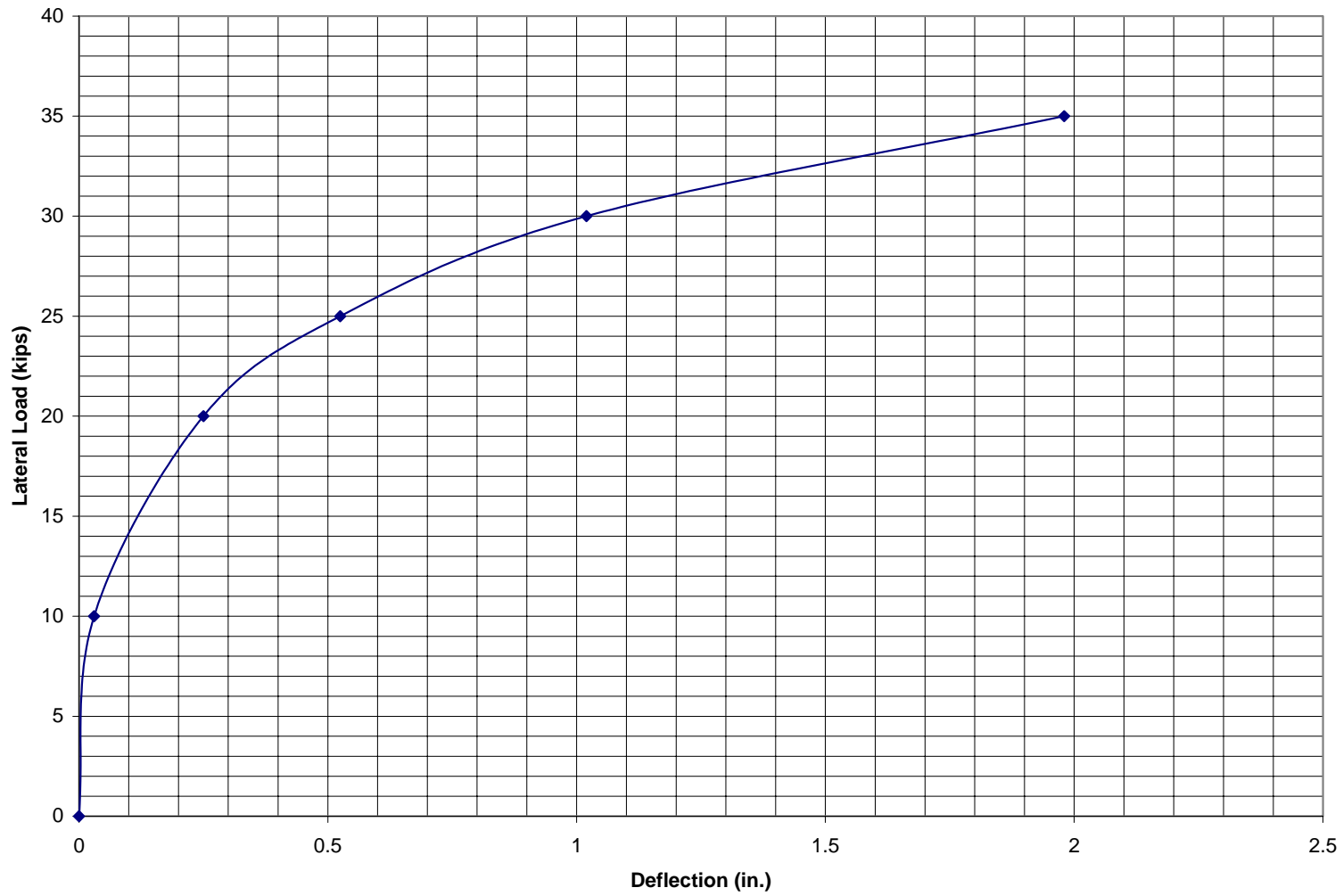
Figure 5.39 Load-deflection curve of new design for CDOT test at clay site

Figure 5.40 Installation of gage on steel cages

Figure 5.41a Inclinometer assembly

Figure 5.41b Inclinometer installation in the hole

Figure 5.42 Pouring sand to fill around the bottom 6' of the inclinometer tube

Figure 5.43 Instrumented cage transferred to the hole

Figure 5.44 Drilled shafts installed and ready for concrete

Figure 5.45 Pouring concrete in the hole

Figure 5.46 Picture showing the installation of the testing devices

Figure 5.47 Picture showing the installation of the testing devices

Figure 5.48 Picture showing the jacking devices

Figure 5.49 Setup of measuring devices at shaft 2 (South)
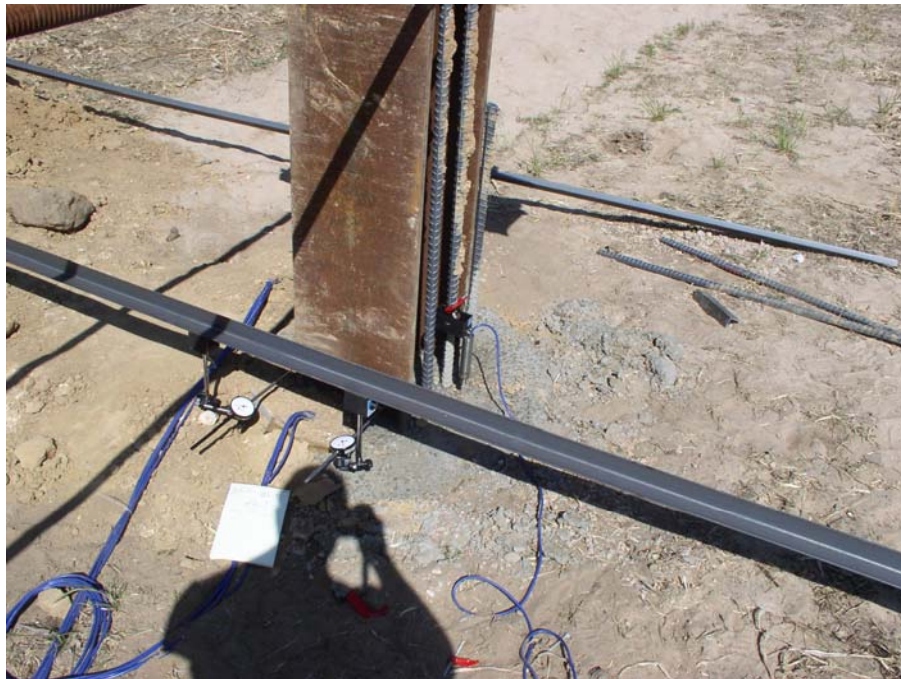
Figure 5.50 Setup of measuring devices at shaft 1 (North)

Figure 5.51 General view of the load test

Figure 5.52 Running the test and watching the instruments

Figure 5.53 Picture showing opening behind the shaft during the test

Figure 5.54 Picture showing CDOT Engineers with the Research team

Northern Shaft (Deflection vs. Applied load)
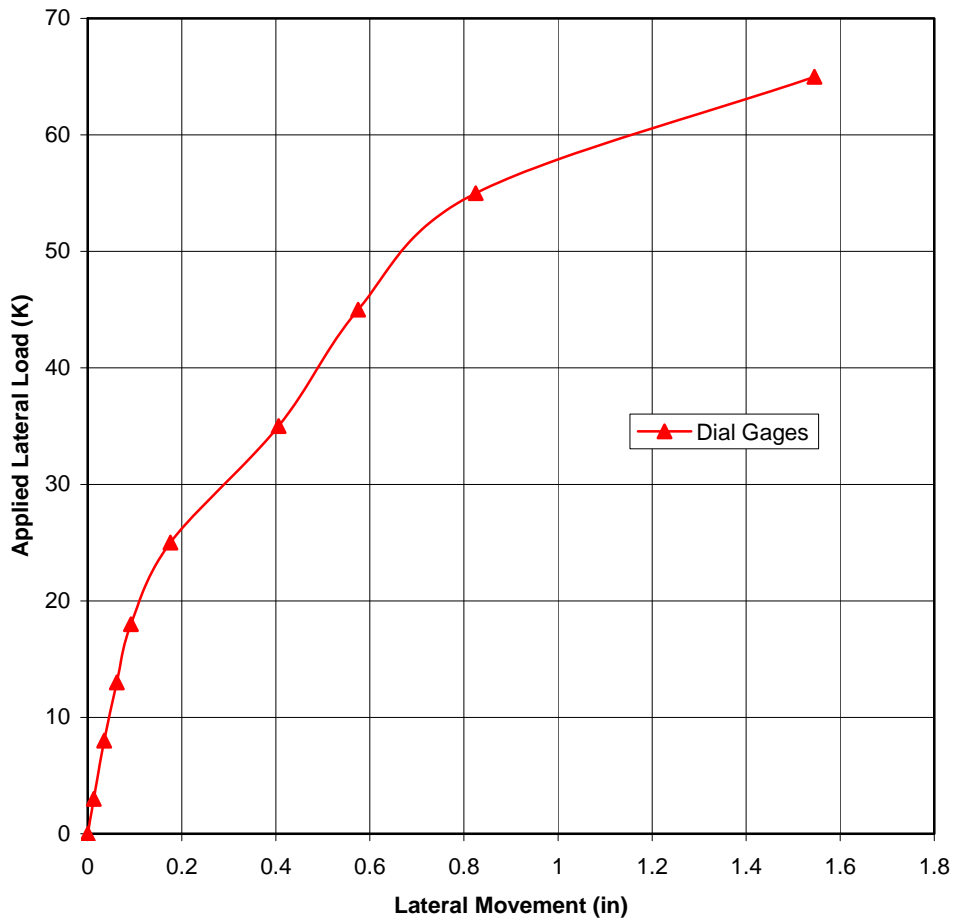
Figure 5.55 Load-deflection curve at the top of test shaft North from dial gages

Southern Shaft (Deflection vs. Applied load)
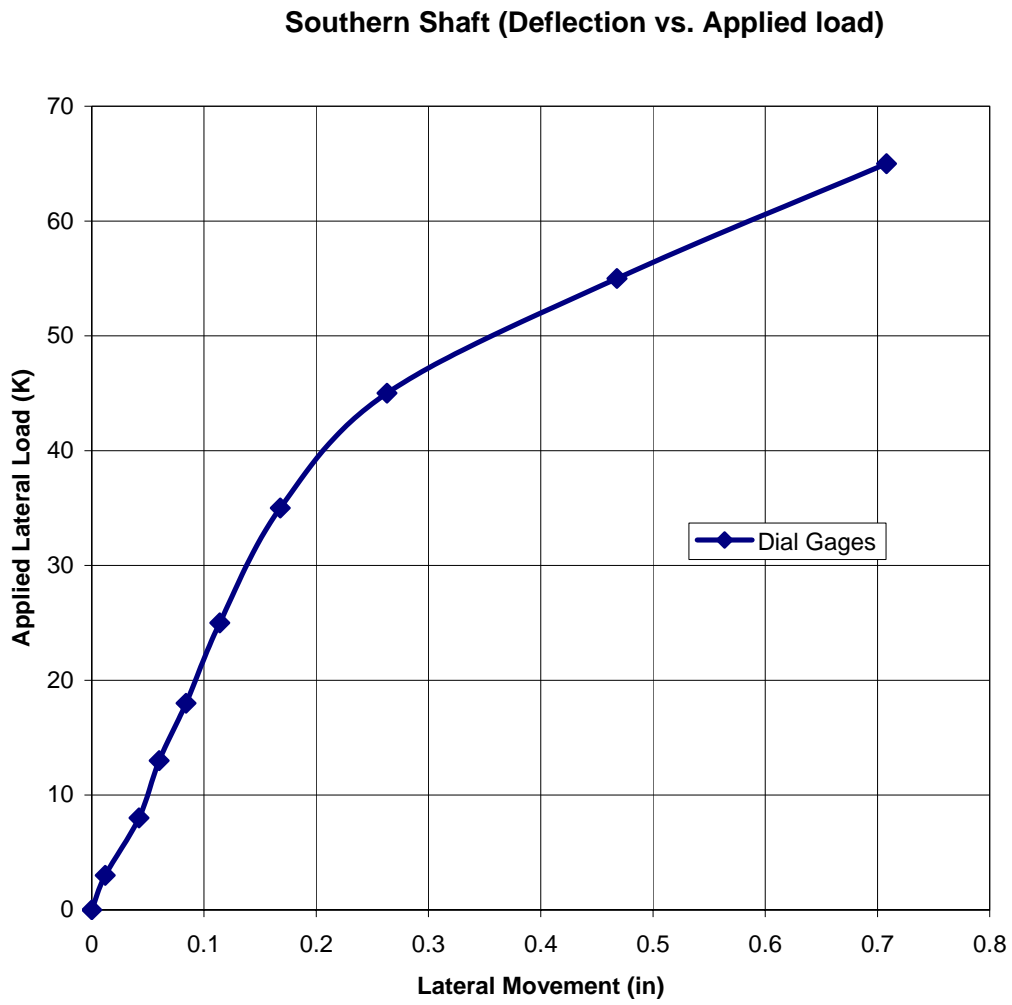
Figure 5.56 Load-deflection curves at the top of test shaft South from dial gages
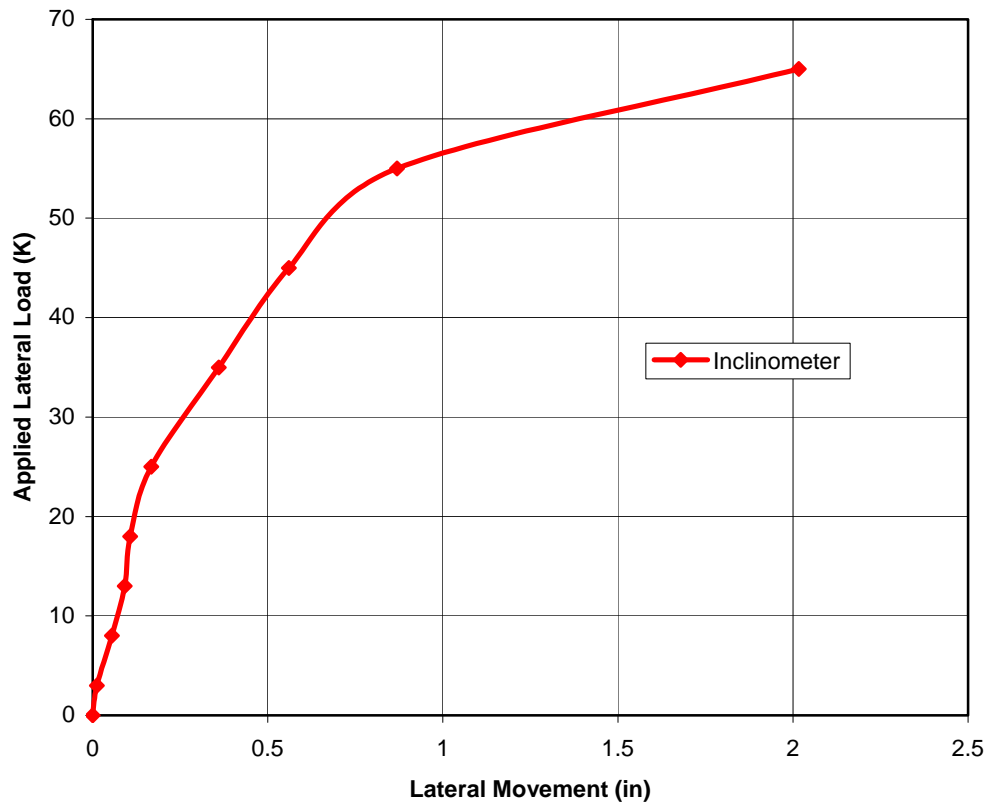
Figure 5.57 Load-deflection curve at the top of test shaft North from inclinometer
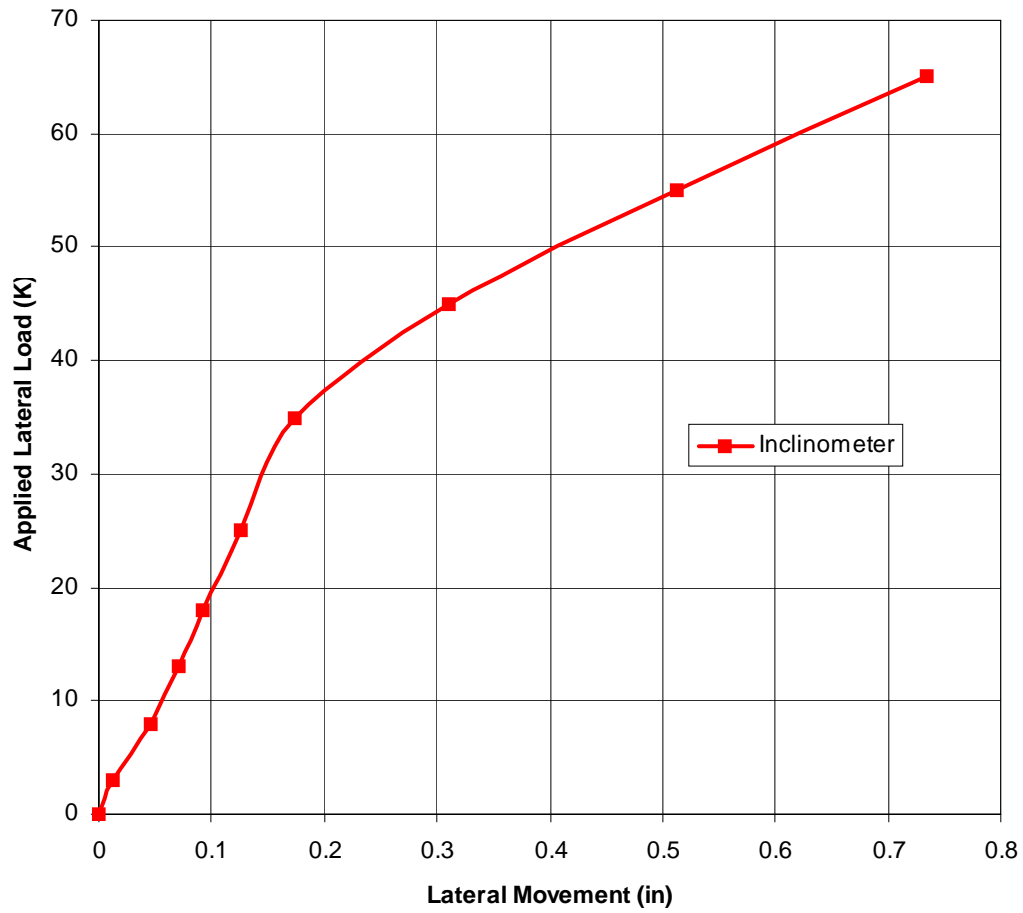
Figure 5.58 Load-deflection curve at the top of test shaft South from inclinometer
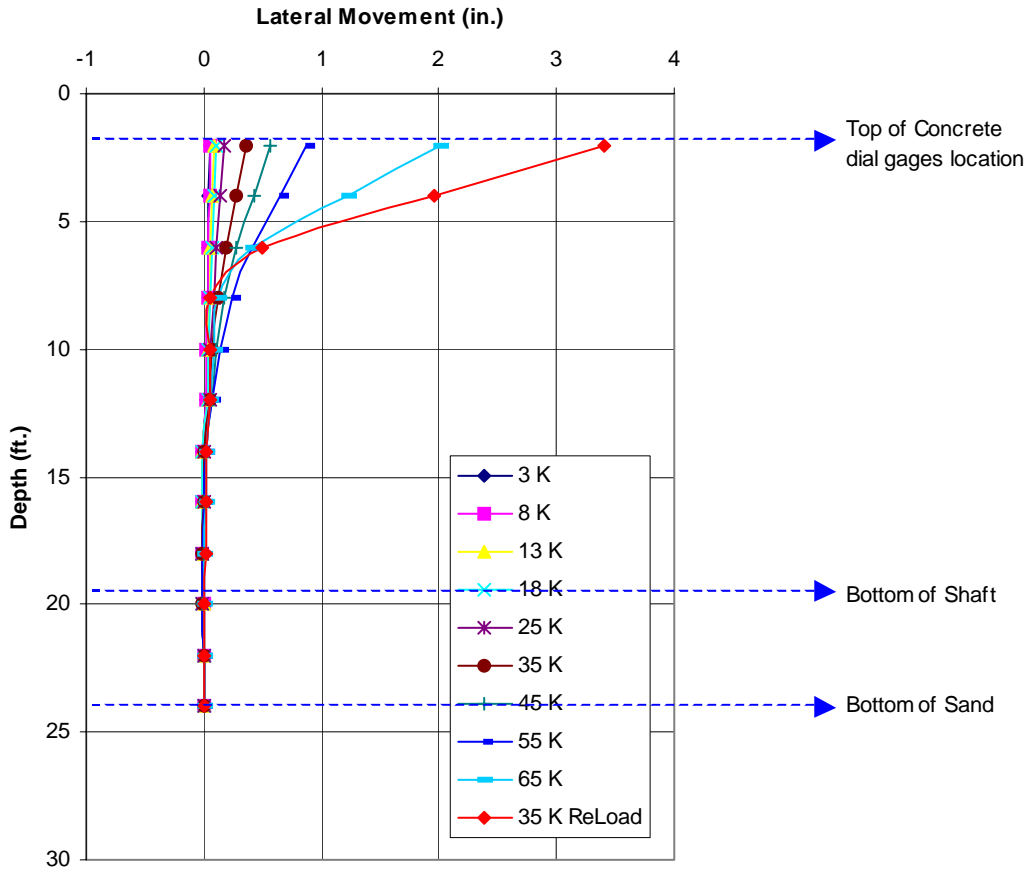
Figure 5.59. Load-deflection curve along the depth of test shaft North from inclinometer
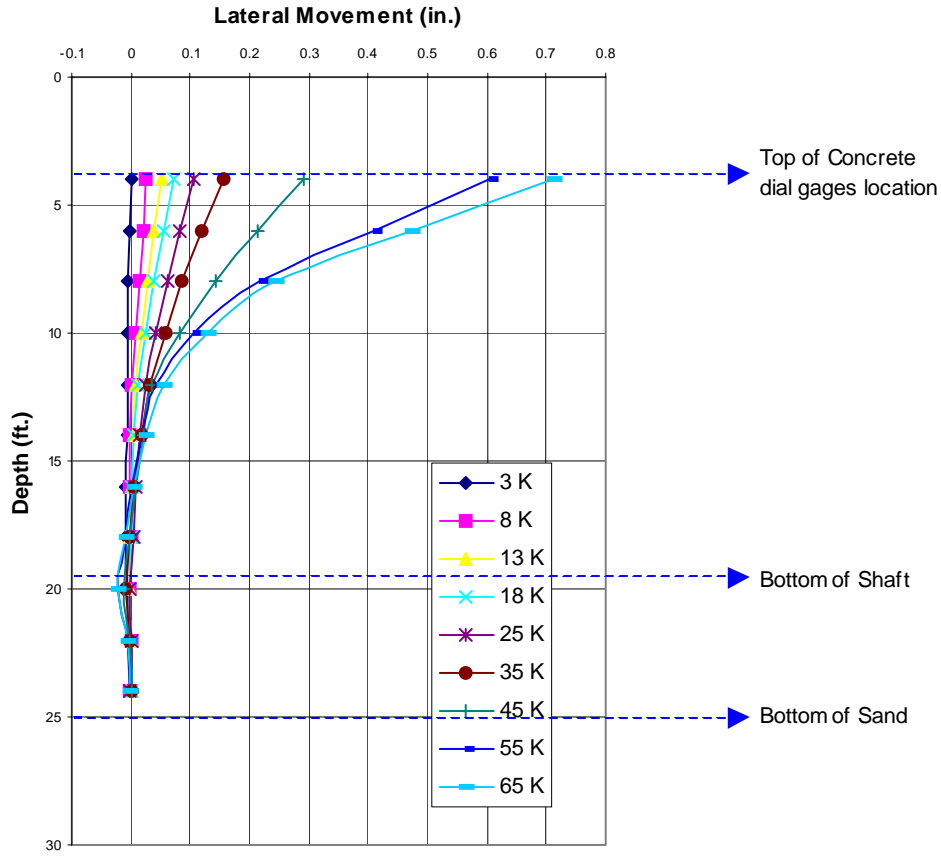
Figure 5.60 Load-deflection curves along the depth of test shaft South from inclinometer

Figure 5.61. Test shaft North, strain vs. depth on compression side

Figure 5.62 Test shaft North, strain vs. depth on tension side

Sandy Site - Northern Shaft

Distance from jacking point to top of concrete is 54"
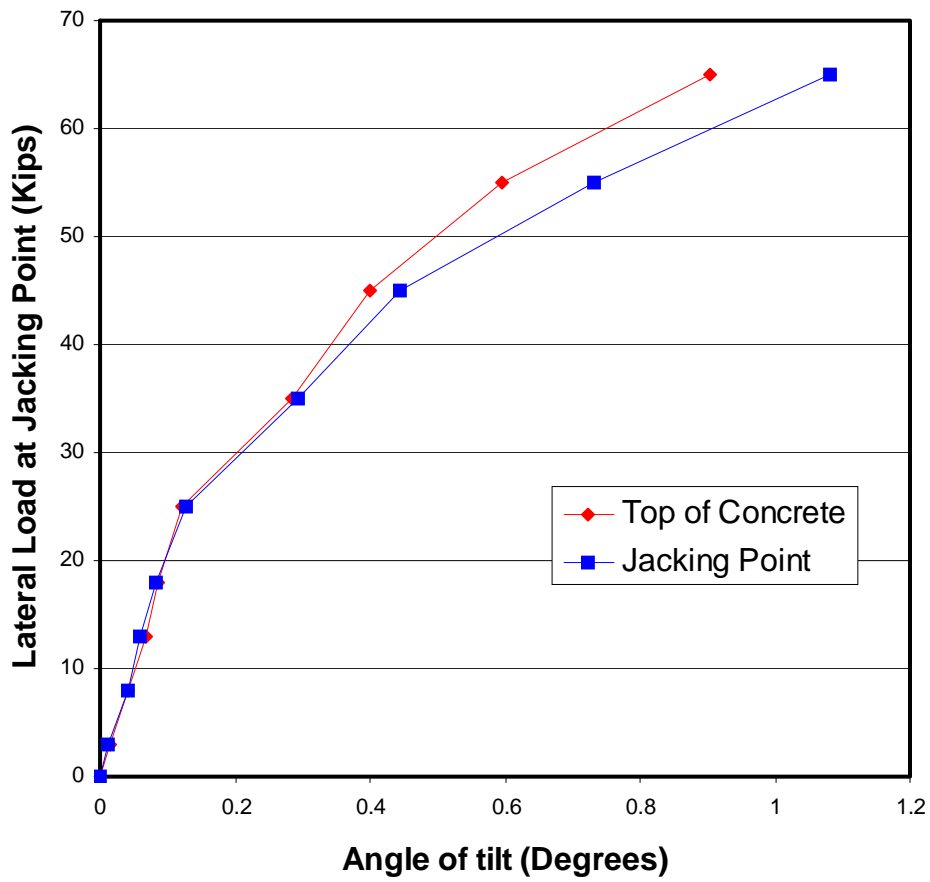
Figure 5.63. Test shaft North, measured angle of tilt

Sandy Site: Southern Shaft
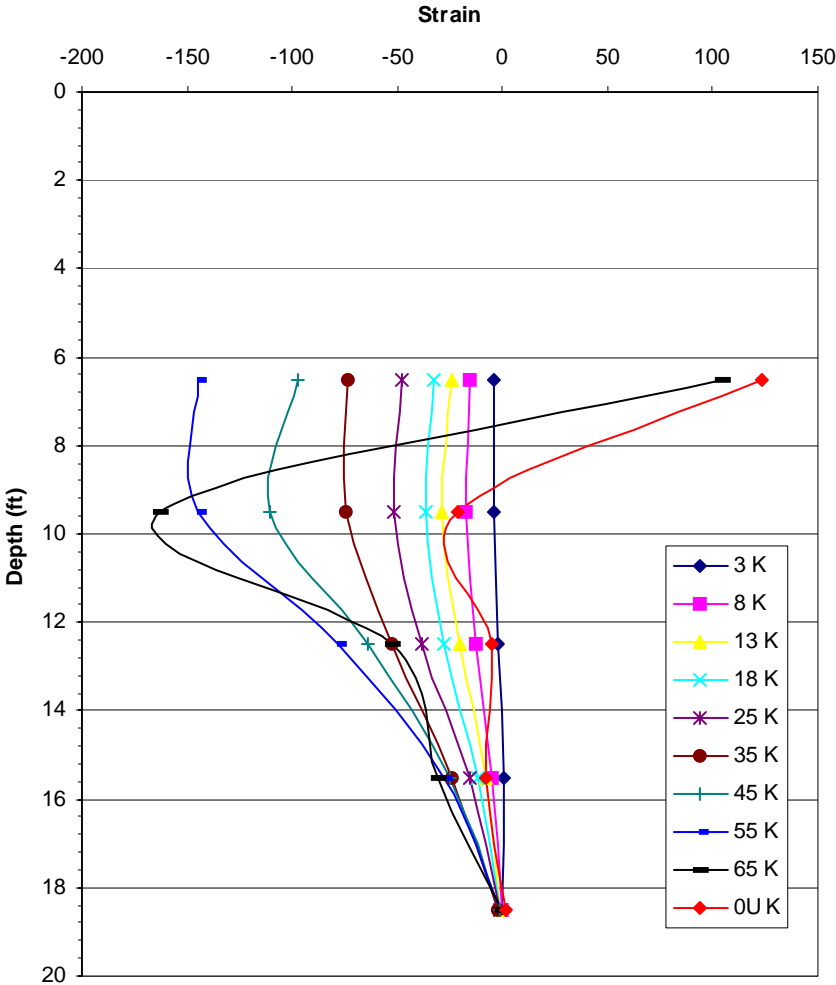
Figure 5.64. Test shaft South, strain vs. depth on compression side

Figure 5.65. Test shaft South, strain vs. depth on tension side

Sandy Site - Southern Shaft
Distance from jacking point to top of concrete is 47"
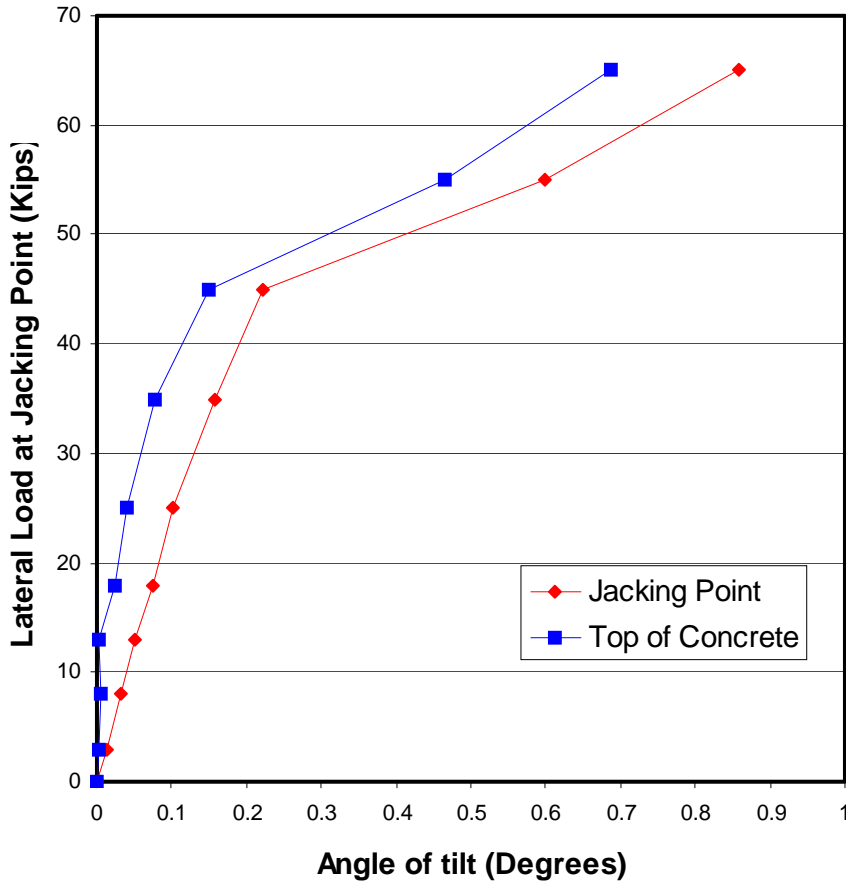
Figure 5.66. Test shaft South, measured angle of tilt

P

4 ft

1 ft

SPT N=13

4 ft

SPT N= 8

6 ft

16 ft

SPT N=10

Sample 4A

9 ft

Silt sand for
all the layers.

SPT N=7

Sample 4B

15 ft

SPT N=7

16 ft

2.5 ft
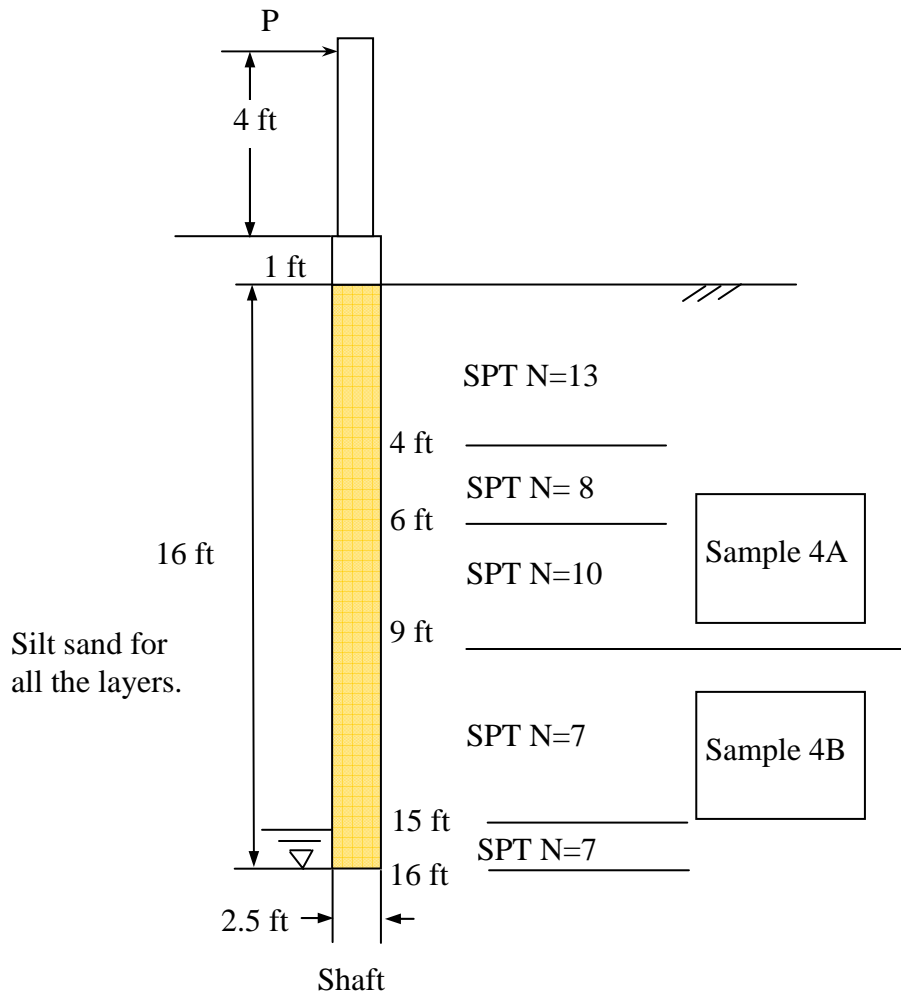
Shaft

Figure 5.67 The shaft setup and soil profile interpreted for CDOT sand site
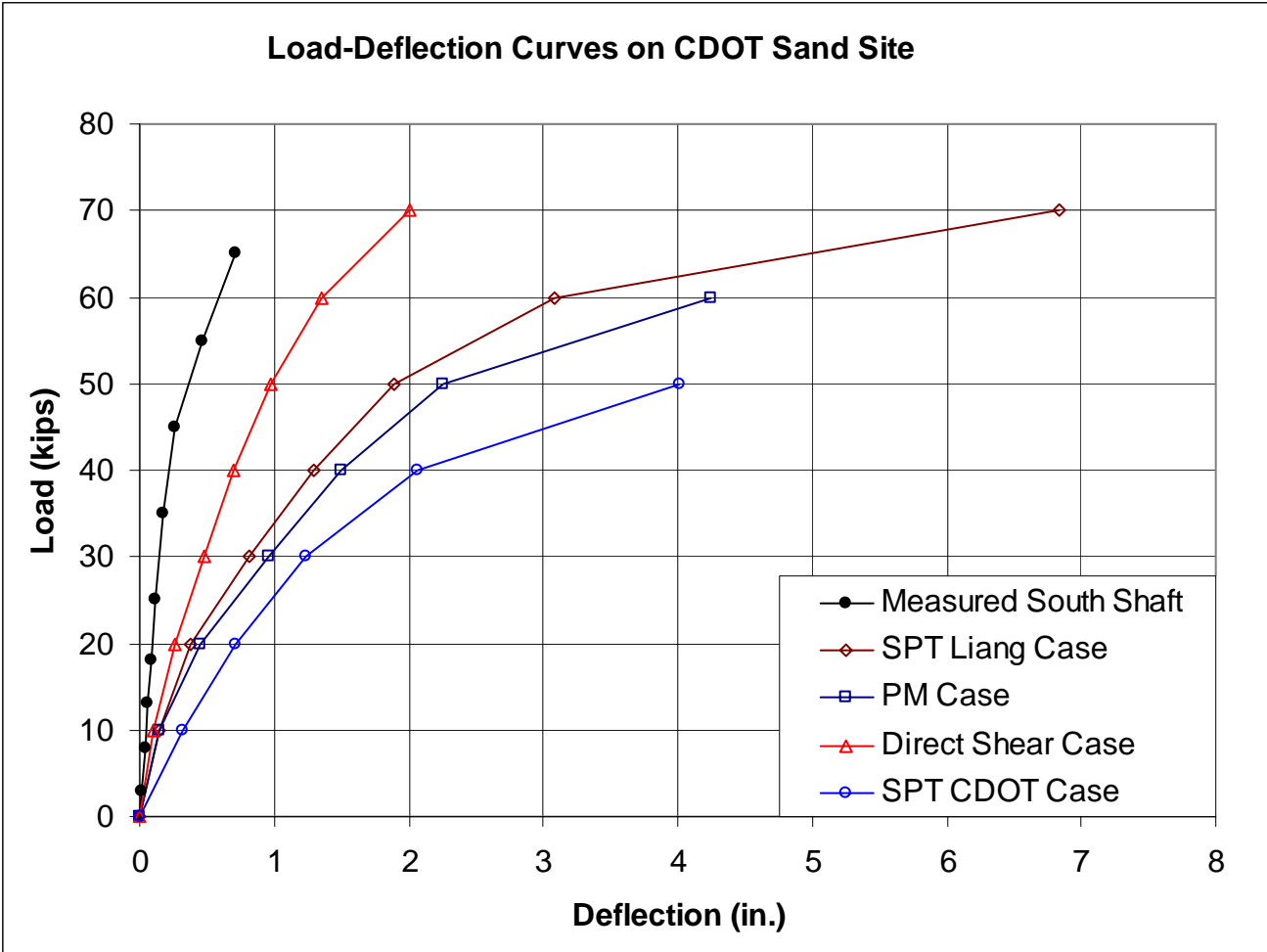
Figure 5.68. Load-deflection curves for CDOT test in sand, South shaft
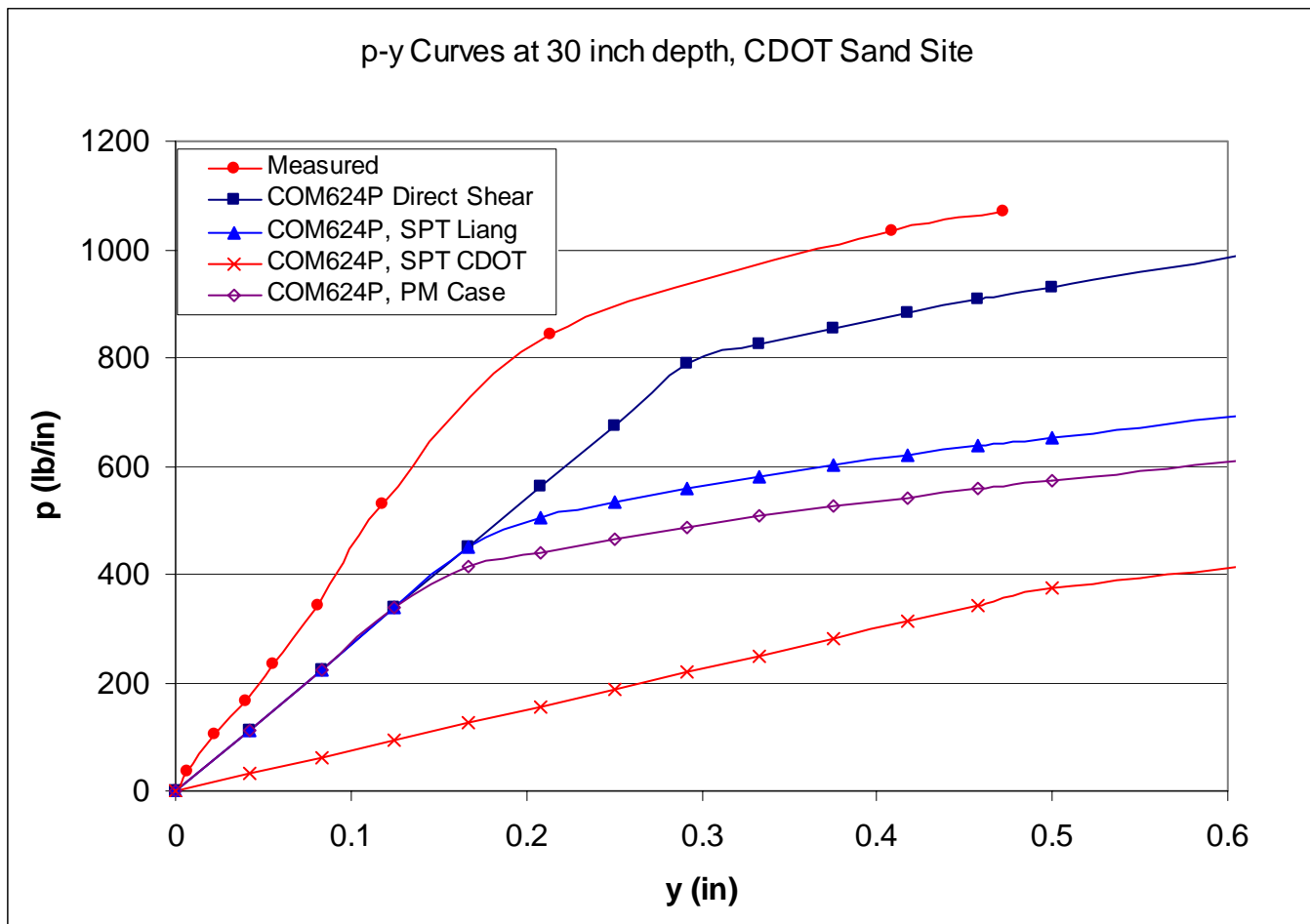
Figure 5.69 Measured and predicted p-y curves based on current stiff clay p-y criteria used in COM624P
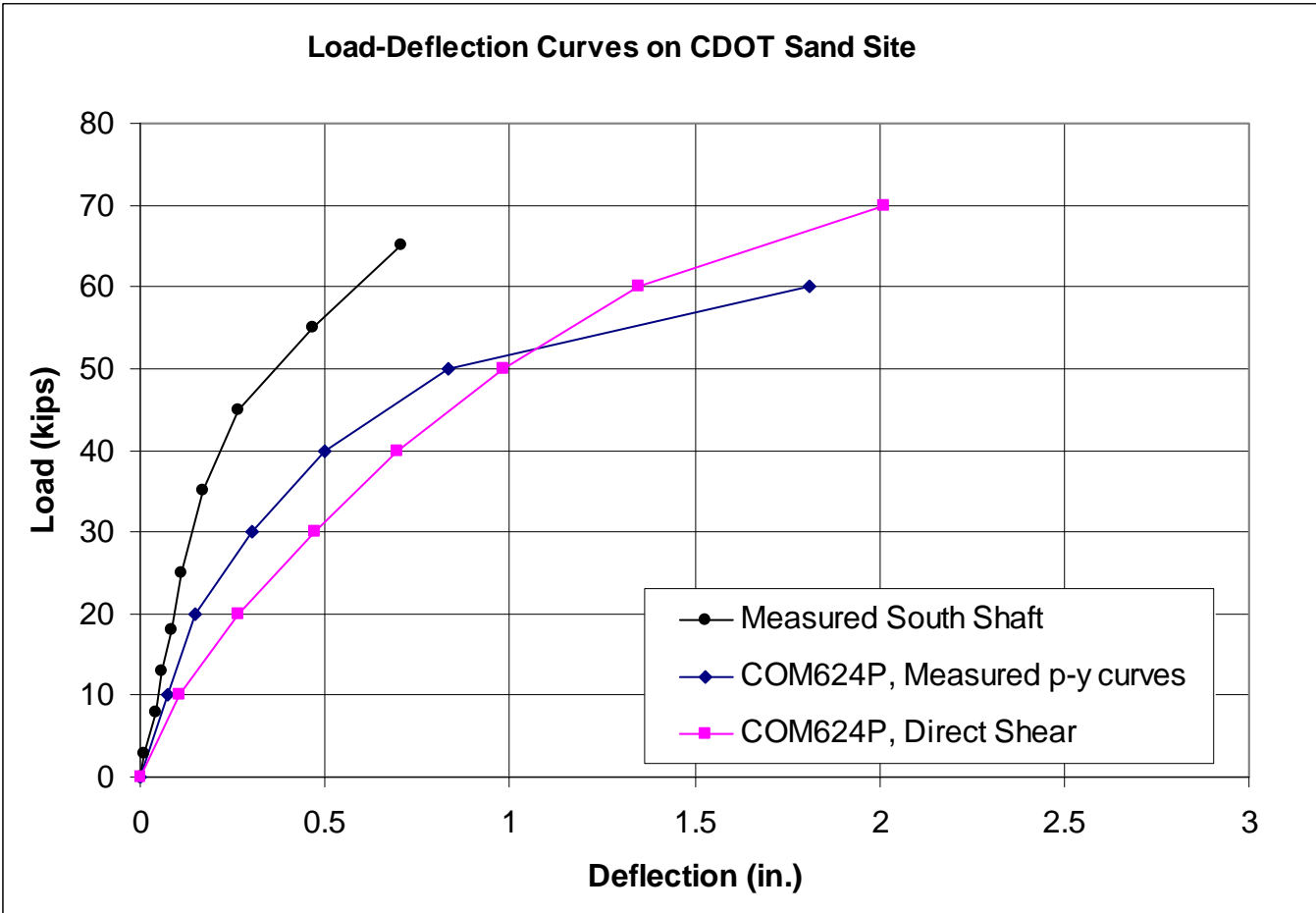
Figure 5.70 Load-deflection curves predicted by using measured p-y curves for sand testing site
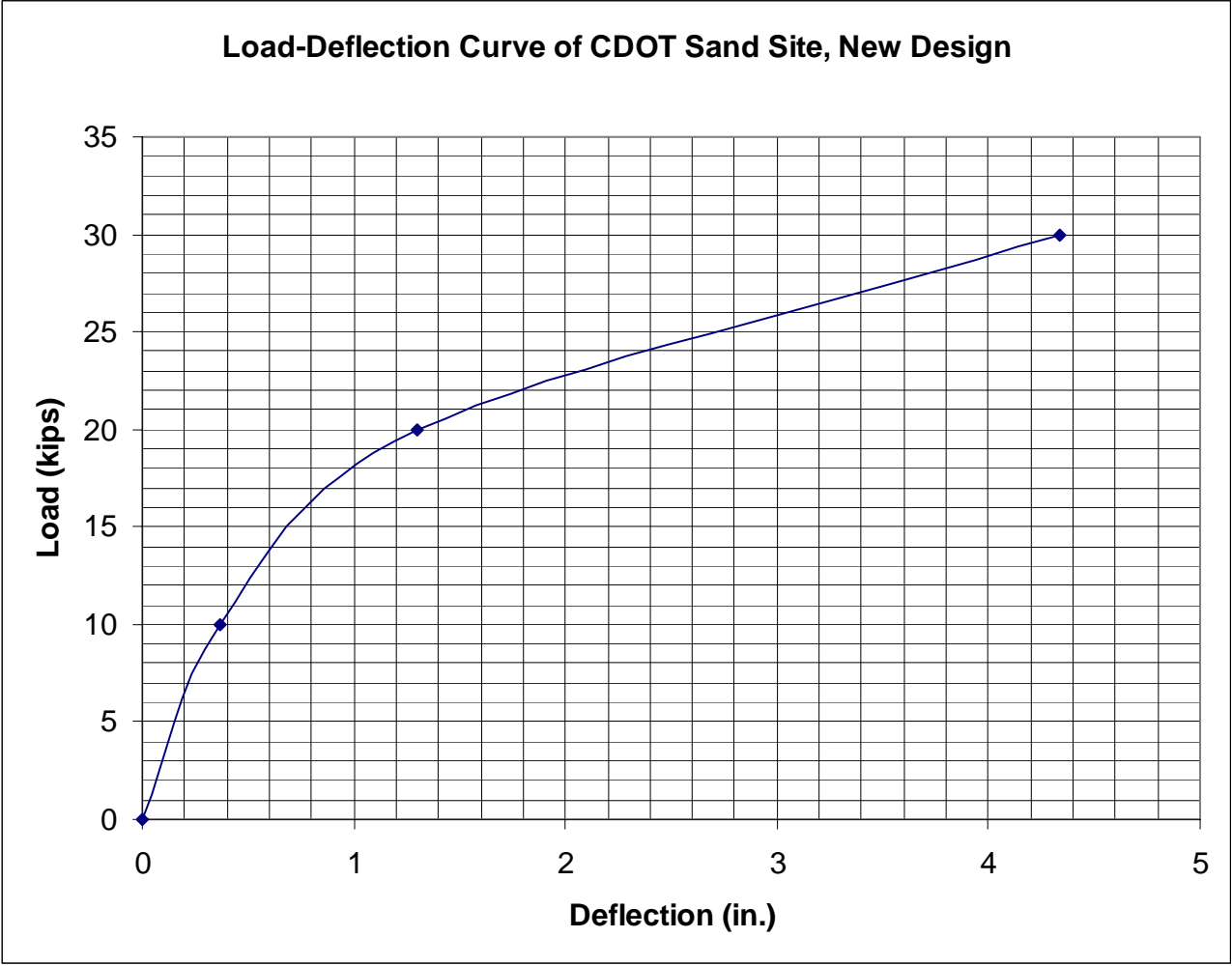
Figure 5.71 Load-deflection curve of new design for CDOT test at sand site

6   FINITE ELEMENT MODELING TECHNIQUES

A true finite element modeling in the continuum framework can be accomplished by the powerful commercial finite element code ABAQUS. The modeling techniques are discussed herein, including the constitutive models for the soil and the interface, and the mesh representation. The modeling technique is validated against one load test result selected from the lateral load test database in Section 4.2 and the two CDOT tests. The intent of this chapter was to demonstrate the developed finite element modeling techniques for specialized drilled shafts projects. It was not the objective of this research to present a design methodology based on FEM approach.

6.1   FEM Modeling Details

6.1.1 The Finite Elements and the Mesh

The finite element chosen for representing the drilled shaft is a 15-node triangular prism element, C3D15, shown in Fig. 6.1. In the earlier stage of the study, the finite element chosen for representing the soil surrounding the shaft was a 21-node brick, reduced integration element, C3D21R. However, it is found that the first order 3-D element C3D8 can also represent the soil mass very well by comparing with the simulation with C3D21R elements; meanwhile the simulation will become more efficiently. Therefore, in the simulation study on CDOT's, C3D8 element is chosen for representing soils; and CIN3D8, a 3-D infinite boundary element, is selected for the outside boundary of soil mass. Fig. 6.1 (a) to (c) depicts the three types of elements adopted for representation of drilled shaft, soils, and out side boundary, respectively.

Fig. 6.2 shows both the side view and 3-D view of the final mesh of CDOT test shaft and surrounding soils. The total depth of the soil mass is 1.5 times the embedment depth of shaft. For CDOT test cases, the shaft embedment depth is 15.7 ft; and then the total soil mass has the depth of 23.7 ft. The outer diameter of soil mass is chosen as 10 times the shaft diameter. For CDOT test cases, the shaft diameter is 3 ft; and then the corresponding soil mass has 30 ft of out diameter. The dimension of final mesh is depicted in Fig. 6.3. The selection of the mesh size is based on minimizing the effect of boundary and also using small size to improve the processing

speed. A coarse mesh is used to simulate the drilled shaft structure to save running time. Initially, in order to save working space and to speed up the analysis, the symmetric model of the drilled shaft under lateral loads is used for validation case, which will be introduced in the following section. However, due to the difficulty of convergence, the full size modeling is used for CDOT test sites.

6.1.2 Constitutive Models for Soils

There are four plasticity models available for modeling soil behavior in the ABAQUS program: Extended Drucker-Prager model, Modified Drucker-Prager/Cap model, Mohr-Coulomb Plasticity model, and Critical State (Clay) Plasticity Model. In the present investigation, Mohr-Coulomb Plasticity model is used since the input parameters are relatively easy to obtain.

6.1.2.1 Overview

The Mohr-Coulomb plasticity model possesses the following capabilities and features.

- It is used to model materials with the classical Mohr-Coulomb yield criterion;
- It allows the material to harden and/or soften isotropically.
- It uses a smooth flow potential that has a hyperbolic shape in the meridional stress plane and a piecewise elliptic shape in the deviatoric stress plane.
- It is used with the linear elastic material model.
- It can be used for design applications in the geotechnical engineering area to simulate material response under essentially monotonic loading.

6.1.2.2 Yield Criterion

The Mohr-Coulomb criterion assumes that failure occurs when the shear stress on any point in a material reaches a value that depends linearly on the normal stress in the same plane. The Mohr-Coulomb model, depicted in Fig. 6.4, is based on plotting Mohr's circle for states of stress at failure in the plane of the maximum and minimum principal stresses. The failure line is the best straight line that touches these Mohr's circles.

Therefore, the Mohr-Coulomb model is defined by

$$\tau = c - \sigma \tan \phi \qquad\qquad\qquad (6.1)$$

where σ is negative in compression. For general states of stress the model is more conveniently written in terms of three stress invariants as

$$F = R_{mc}q - p \tan \phi - c = 0 \qquad (6.2)$$

where

$$R_{mc}(\Theta, \phi) = \frac{1}{\sqrt{3} \cos \phi} \sin(\Theta + \frac{\pi}{3}) + \frac{1}{3} \cos(\Theta + \frac{\pi}{3}) \tan \phi \qquad (6.3)$$

Φ is the slope of the Mohr-Coulomb yield surface in the p-R_{mc}q stress plane, shown in Fig. 6.5, which is commonly referred to as the friction angle of the material and can be dependent on the temperature and the predefined field variables;

c is the cohesion of the material; and

Θ is the deviatoric polar angle defined as

$$\cos(3\Theta) = \left(\frac{r}{q}\right)^3 \qquad (6.4)$$

and

$p = -\frac{1}{3} \text{trace}(\sigma)$ is the equivalent pressure stress,

$q = \sqrt{\frac{3}{2}(S:S)}$ is the Mises equivalent pressure stress,

$r = (9/2S \cdot S \cdot S)^{1/3}$ is the third invariant of deviatoric stress,

$S = \sigma + pI$ is the deviatoric stress.

6.1.2.3 Flow Potential

The flow potential G is chosen as a hyperbolic function in the meridional stress plane and the smooth elliptic function proposed by Menétrey and Willam (1995) in the deviatoric stress plane. A family of hyperbolic potentials in the meridional stress plane is shown in Fig. 6.6, and the flow potential in the deviatoric stress plane is shown in Fig. 6.7.

6.1.3 Simulation of Interaction between Shaft and Soil

The simulation of a contact problem is challenging in the context of finite element analysis. The Florida Pier finite element program uses the spring element to simulate the interaction between

the shaft and the soil, thus avoiding the need for contact simulation. The nonlinear stiffness of the spring element is determined based on semi-empirical p-y relationship commonly used in the COM624P computer program. Therefore, there is really no difference between Florida Pier and COM624P analysis. For a truly continuum based FEM approach, the use of contact for simulating the shaft and soil interaction is necessary. Two kinds of contact simulations are available in ABAQUS, one is contact element, and the other one is surface-based contact interface. The surface-based interface is highly recommended in ABAQUS manual for most type of contact simulations; therefore, the surface-based contact option is chosen in present study.

For the surface-based contact, two surfaces, one is master surface, and the other one is slave surface, are required for defining a contact. The master surface should be a surface which is more rigid than slave surface. In present study, the outside of drilled shaft surface is defined as the master surface; while the inner side of soil surface which is directly surrounding shaft is defined as slave surface. The nodes of master surface could penetrate into slave surface, but it is not allowed for nodes of slave surface to penetrate into master surface.

ABAQUS simulates two kinds of contact behavior for surface-based contact, one is the tangential friction between the two surfaces, and the other one is the load transfer between the two surfaces in normal direction. The basic coulomb friction model, presented in Fig. 6.8, is used to simulate the frictional interaction. The constant friction coefficient is required for input. The effect of contact friction between the shaft and the soil on the lateral behavior of shaft is relatively small, as illustrated by comparison shown in Fig. 6.9.

For the behavior of the interface in normal direction, the default "hard" contact pressure-clearance relation option is adopted in the current FEM modeling of the shaft-soil contact. The "hard" option will provide reasonable contact behavior in normal direction. In this contact option, any pressure can be transmitted between the surfaces if the two surfaces are under contact. The contact pressure reduces to zero, if the interface is separated. Conversely, the separation condition will return back to contact condition, when the clearance between them reduces to zero.

6.1.4 Simulation of Initial Condition

In order to simulate the in-situ initial condition, two steps of loading will be applied as shown in Fig. 6.10. The self weight of the soil and shaft is applied in the first step to simulate the initial effective stress condition. Then, the external lateral load is applied incrementally to allow for calculation of load vs. deflection response of the drilled shaft.

6.2 Validation of FEM Model

As part of this study, extensive trial of various modeling details has been conducted. Furthermore, several load test cases were used to validate the proposed modeling details. Since the main objective of this study is to use the proposed FEM modeling technique to predict the Colorado load test data, a representation plot of one validation exercise is given in Fig. 6.11. The soil profile and the associated soil properties used in the FEM simulation are documented in Table 6.1. The match between the FEM predicted and actual measured load-deflection curves is presented in Fig. 6.11. The comparisons for the deflection vs. depth are shown in Fig. 6.12. It can be seen that as long as the soil parameters and the interface friction properties are properly selected, FEM simulation results can have a good agreement with the actual test results.

Table 6.1 Parameters for Soils

Soil Layers	Depth (ft.-in.)	Cohesion Yield Stress (psi)	Volumetric Plastic Strain	Young's Modulus (ksi)	Materials Cohesion (psi)
Soil1	0 – 24''	6	0	9.9	22
		11	0.008		
		14	0.016		
		15	0.024		
Soil2	24'' – 103''	3	0	4.95	11
		5	0.008		
		7	0.016		
		8	0.024		
Soil3	103'' – 120''	14	0	22.5	50
		25	0.008		
		32	0.016		
		35	0.024		
Soil4	120'' – 144''	15	0	24.75	55
		27	0.008		
		35	0.016		
		39	0.024		

6.3   Simulation of CDOT Test at Clay Site

Two simulation cases have been conducted to simulate the lateral load test results of Shaft 1 at CDOT clay site. The input in the first case is mainly based on the triaxial test results. The equivalent elastic modulus of shaft could range from 3600 ksi to 6000 ksi, depending on the reinforcement ratio as well as load level. In order to identify the effect of shaft modulus on lateral response, three try run of FEM analyses by using elastic modulus of shaft of 4000 ksi, 5000 ksi, and 6000 ksi are conducted and the results of the lateral response are plotted in Fig. 6.13. It can be seen that the effect of initial elastic shaft modulus on lateral response is negligible. Therefore, the initial modulus of drilled shafts is selected as 5000 ksi. The elastic modulus of soils E_s was directly obtained from the triaxial tests results. The cohesion yield stress and corresponding plastic strains depicted in Fig. 6.14 are obtained from deviatoric stress-strain curves of triaxial tests. The input parameters for soil materials are given in Table 6.2. The friction coefficient for clay-shaft interface is assumed as a default value of 0.5 since the effect of friction on lateral response is minimal.

Table 6.2 Input of Soil Parameters from Triaxial Test Results

Layers (ft)	E_s(psi)	C_1(psi)	ε_1	C_2(psi)	ε_2	C_3(psi)	ε_3	C_4(psi)	ε_4
0-2.5	4140	10.35	0	15.5	0.008	17	0.0155	18.3	0.04
2.5-4.5	3320	7.8	0	12	0.029	17.2	0.07	18.3	0.11
4.5-6.5	3320	7.8	0	12	0.029	17.2	0.07	18.3	0.11
6.5-10	1614	6.9	0	10.41	0.016	13.2	0.09	14.8	0.19
10-12.5	789	3.5	0	6.94	0.029	8.5	0.09	9.2	0.19
12.5-16	3474	3.5	0	9	0.023	11.3	0.098	11.7	0.198

The comparison between the FEM predicted and actual measured load-deflection curves is presented in Fig. 6.15. An adjustment of input soil parameters in FEM simulation, including using 30% increased unload modulus from pressuremeter test results to represent soil modulus, was made as shown in Table 6.3 for achieving better match between the FEM predictions and actual test data. The deflection vs. shaft depth for FEM simulations at two lateral load levels (20 kips and 90 kips) is shown in Fig. 6.16 and Fig. 6.17, using triaxial test soil parameters and best match soil parameters, respectively. It is apparent that achieving the matches between the FEM simulation and actual measurement are much more difficult for the deflection vs. depth plot than for the load-deflection curve at shaft top.

The FEM simulation results could be used to infer the p-y curves. The comparisons shown in Fig. 18(a) are for p-y curves at 15 inch depth, using actual load test data (only 24 inch depth is available), ABAQUS FEM simulation with triaxial soil parameters, and ABAQUS FEM simulation with best match. Similar p-y curve comparison plot is shown in Fig. 6.18 (b) for p-y curves at 42 inch depth. Based on observations from these two plots, one may conclude that the ABAQUS derived p-y curves are close to those from measured.

Table 6.3 Adjusted Soil Parameters for Match Case at Clay Site

Layers (ft)	E_s(psi)	C_1(psi)	ε_1	C_2(psi)	ε_2	C_3(psi)	ε_3	C_4(psi)	ε_4
0-2.5	21684	9	0	13	0.008	16	0.016	18.3	0.024
2.5-4.5	21684	7	0	10.5	0.008	13	0.016	15	0.024
4.5-6.5	21684	7	0	10	0.008	12.8	0.016	14.4	0.024
6.5-10	6867	7	0	10	0.008	12	0.016	13.7	0.024
10-12.5	6867	5	0	7	0.008	8.5	0.016	9.4	0.024
12.5-16	6867	6	0	8.5	0.008	10.5	0.016	11.7	0.024

6.4   Simulation of CDOT Test at Sand Site

Two simulation cases have been conducted to simulate the lateral load test at CDOT sand site. The competent south shaft at sand site is used for simulation. The input parameters of the first case is mainly based on the friction angles and cohesions from direct shear tests and the modulus from pressuremeter tests. The initial shaft elastic modulus is chosen as 5000 ksi. The reload modulus E+ from pressuremeter test is utilized to represent the modulus of sands. The cohesion yield stress and plastic strains are selected to be close to measured cohesions by direct shear tests and also make the convergence of the simulation available. The input parameters for soil materials are presented in Table 6.4. The friction coefficient between shaft and sand is assumed to be 0.5, e.g. tan27°.

Table 6.4 Input of Soil Parameters from Direct Shear Tests and PM Tests

Depth (ft)	E_s(psi)	Φ	C_1(psi)	ε_1	C_2(psi)	ε_2	C_3(psi)	ε_3	C_4(psi)	ε_4
0 - 4	5421	41.1	1.84	0	3.2	0.01	4	0.03	4.6	0.05
4 - 6	5421	41.1	1.84	0	3.2	0.01	4	0.03	4.6	0.05
6 - 9	4309	41.1	1.84	0	3.2	0.01	4	0.03	4.6	0.05
9 - 15	7645	39.5	1.12	0	2.0	0.01	2.5	0.03	2.8	0.05
15 - 15.7	7645	39.5	1.12	0	2.0	0.01	2.5	0.03	2.8	0.05

The comparison between the FEM predicted and actual measured load-deflection curves is presented in Fig. 6.19. An adjustment of input soil parameters in FEM simulation, increasing

modulus by 60%, was made as shown in Table 6.5 for achieving better match between the FEM predictions and actual test data. The deflection vs. shaft depth for FEM simulations at two lateral load levels (25 kips and 45 kips) is shown in Fig. 6.20 and Fig. 6.21, using direct shear test and pressuremeter test soil parameters and best match soil parameters, respectively. It is apparent that achieving the matches between the FEM simulation and actual measurement are much more difficult for the deflection vs. depth plot than for the load-deflection curve at shaft top.

The FEM simulation results could be used to infer the p-y curves. The comparisons shown in Fig. 6.22(a) are for p-y curves at 24 inch depth, using actual load test data (only 30 inch depth is available), ABAQUS FEM simulation with lab and pressuremeter test soil parameters, and ABAQUS FEM simulation with best match. Similar p-y curve comparison plot is shown in Fig. 6.22 (b) for p-y curves at 60 inch depth. Based on observations from these two plots, one may conclude that the ABAQUS derived p-y curves are close to those from measured.

Table 6.5 Adjusted Soil Parameters for Match Case at Sand Site

Depth (ft)	E_s(psi)	Φ	C_1(psi)	ε_1	C_2(psi)	ε_2	C_3(psi)	ε_3	C_4(psi)	ε_4
0 - 4	8674	41.1	1.84	0	3.2	0.01	4	0.02	4.6	0.03
4 – 6	8674	41.1	1.84	0	3.2	0.01	4	0.02	4.6	0.03
6 – 9	6894	41.1	1.84	0	3.2	0.01	4	0.02	4.6	0.03
9 – 15	12232	39.5	1.12	0	2.0	0.01	2.5	0.02	2.8	0.03
15 – 15.7	12232	39.5	1.12	0	2.0	0.01	2.5	0.02	2.8	0.03

6.5   Recommended Soil Parameters Determination for FEM Simulation

Based on above analyses, the tests required for determination of soil parameters are tabulated in table 6.6. The friction coefficient between shaft and soils could be chosen as 0.5.

Soils	Soil modulus E_s	C_1-C_4, ε_1- ε_4 [*]	Friction Angle Φ
Clay	Unload modulus of pressuremeter test	CU triaxial test	CU triaxial test
Sand	Reload or unload modulus of pressuremeter test	CU triaxial test or direct shear test	CU triaxial test or direct shear test

Note: * C_1 to C_4 are the cohesion yield stresses; and ε_1 to ε_4 are corresponding plastic strains.

6.6   Summary of FEM Simulation

The 3-D finite element simulations by using ABAQUS techniques on CDOT test sites, tells that the FEM model provides relative conservative prediction on load-deflection curves if the input parameters are obtained from lab or in-situ tests. Based on the two simulations, it can be seen that soil modulus obtained from pressuremeter test provides better prediction than those from triaxial tests. If the shaft modulus is varied with moment and the elastic soil modulus is increased from measured values by certain amount, such as 30%, then the simulation could provide good match with measured results.

During the FEM simulation, the p-y curves are also derived and used for COM624P program to predict the lateral response. Both for clay and sand, the derived p-y curves are very close that derived from measured strains and deflections. This implies that the p-y curves could be derived from FEM simulation.

The ability and versatility of the developed FEM simulation technique for laterally loaded drilled shafts have been demonstrated by means of comparisons with actual load test data. Although the FEM simulation is a very powerful tool, the complexities and time involvement for performing such work are quite demanding. Therefore, the FEM simulation is best reserved for the projects with unusual situations such as extremely large size drilled shafts, exceptional loading conditions, and highly complex soil types and behavior.
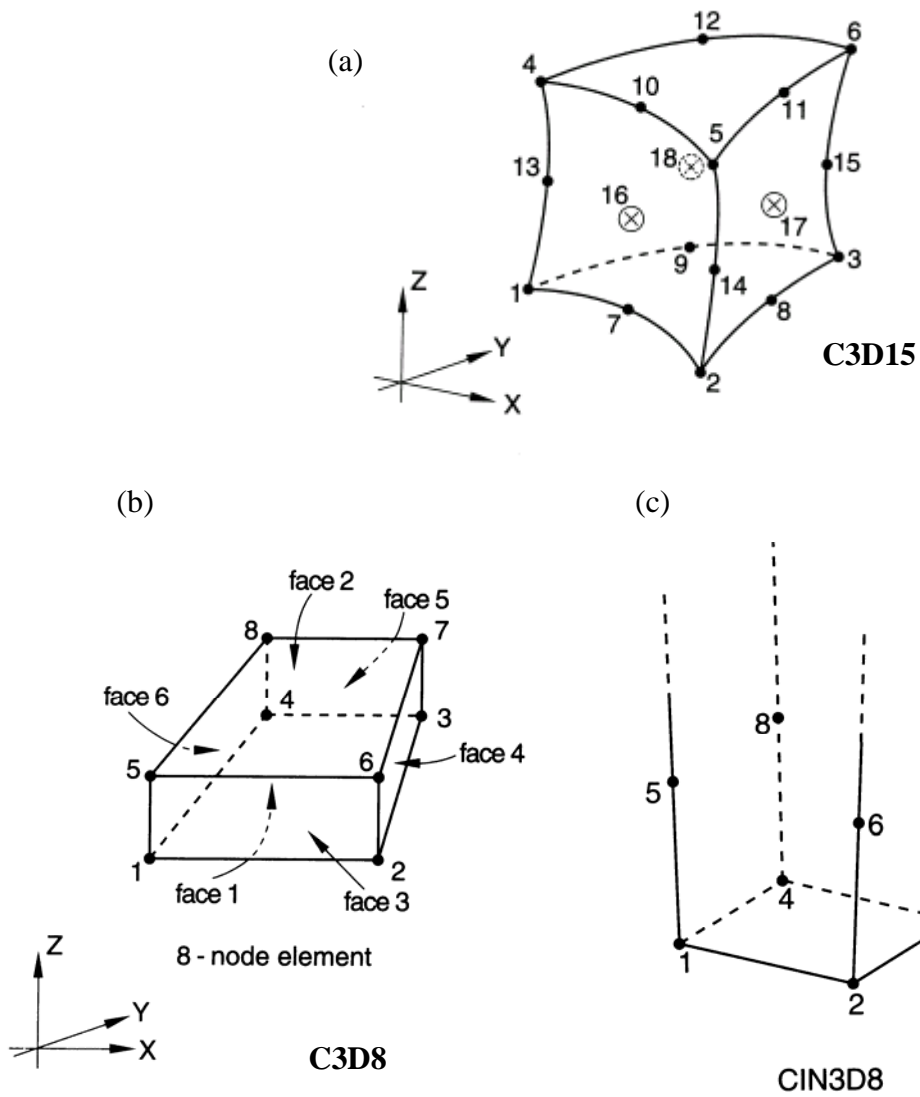
Figure 6.1. Finite elements selected for representation of (a) drilled shaft, (b) surrounding soils, and (c) outside boundary of soils.
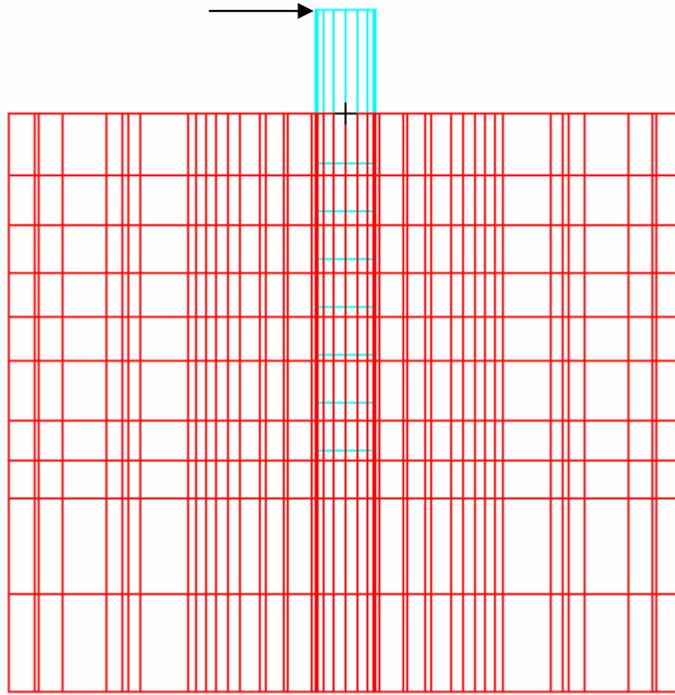
(a) Side View
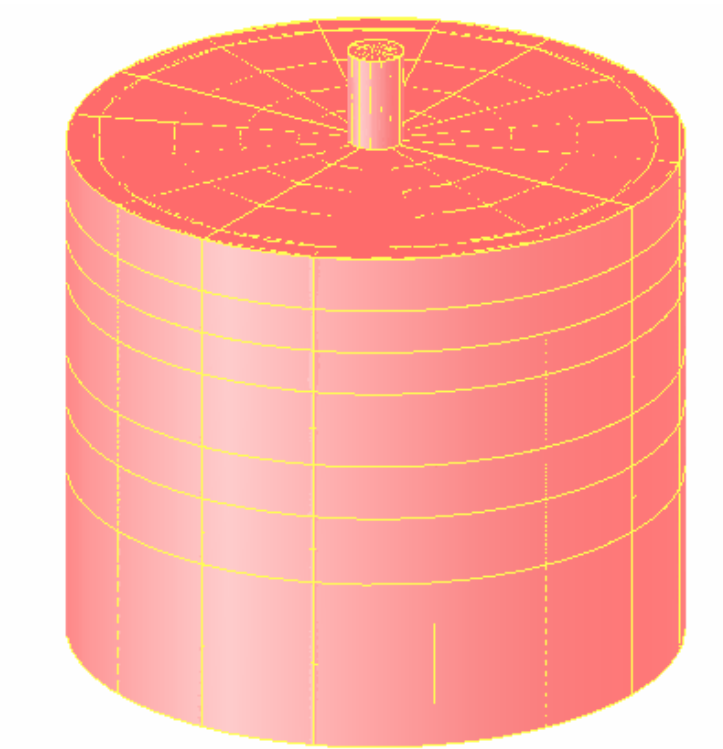
(b) 3-D View

Figure 6.2 FEM mesh representing test shafts and soils at CDOT test sites
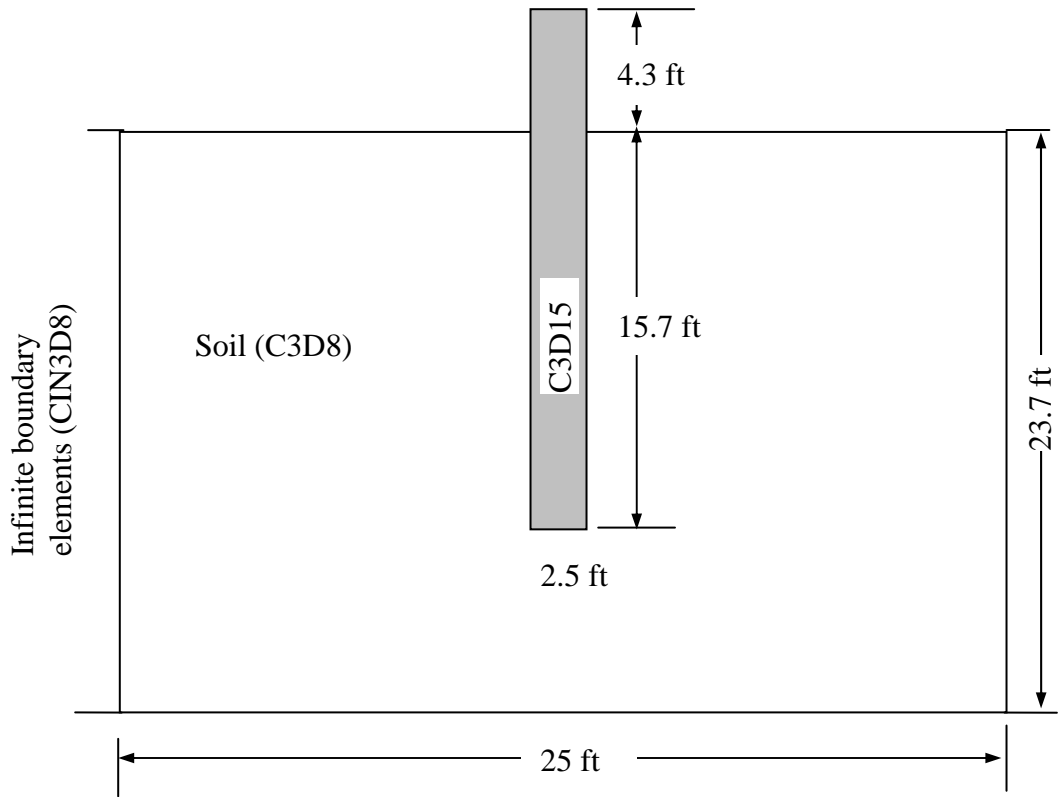
Figure 6.3 Dimensions of the final mesh for CDOT shaft simulations
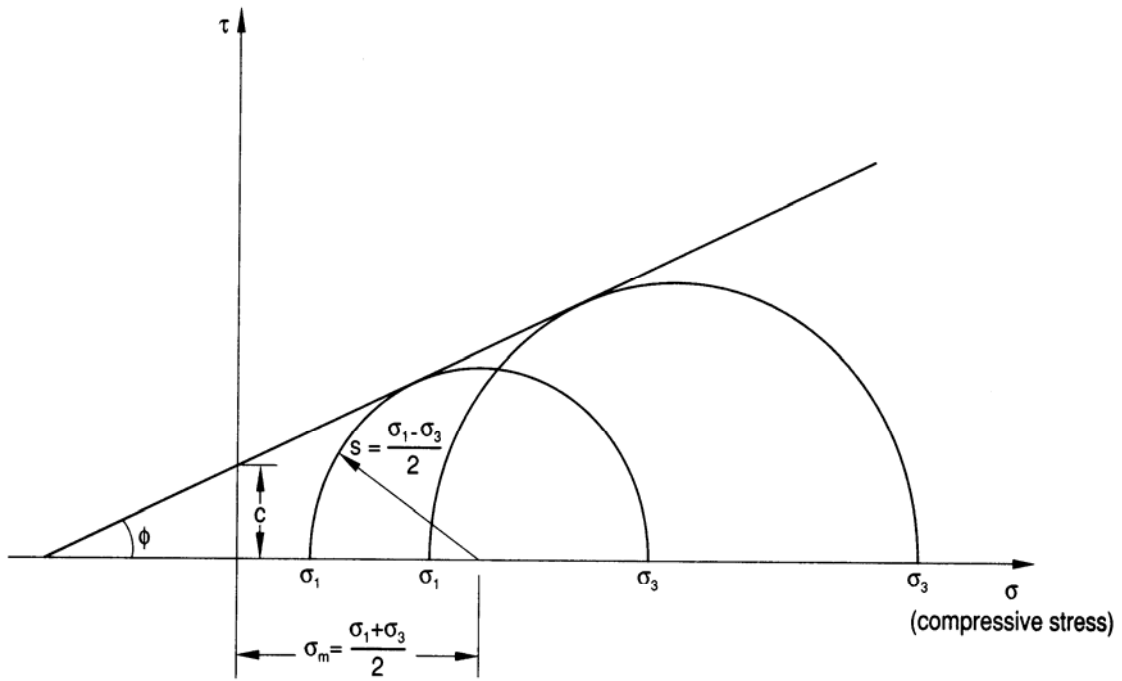
Figure 6.4 Mohr-Coulomb failure model
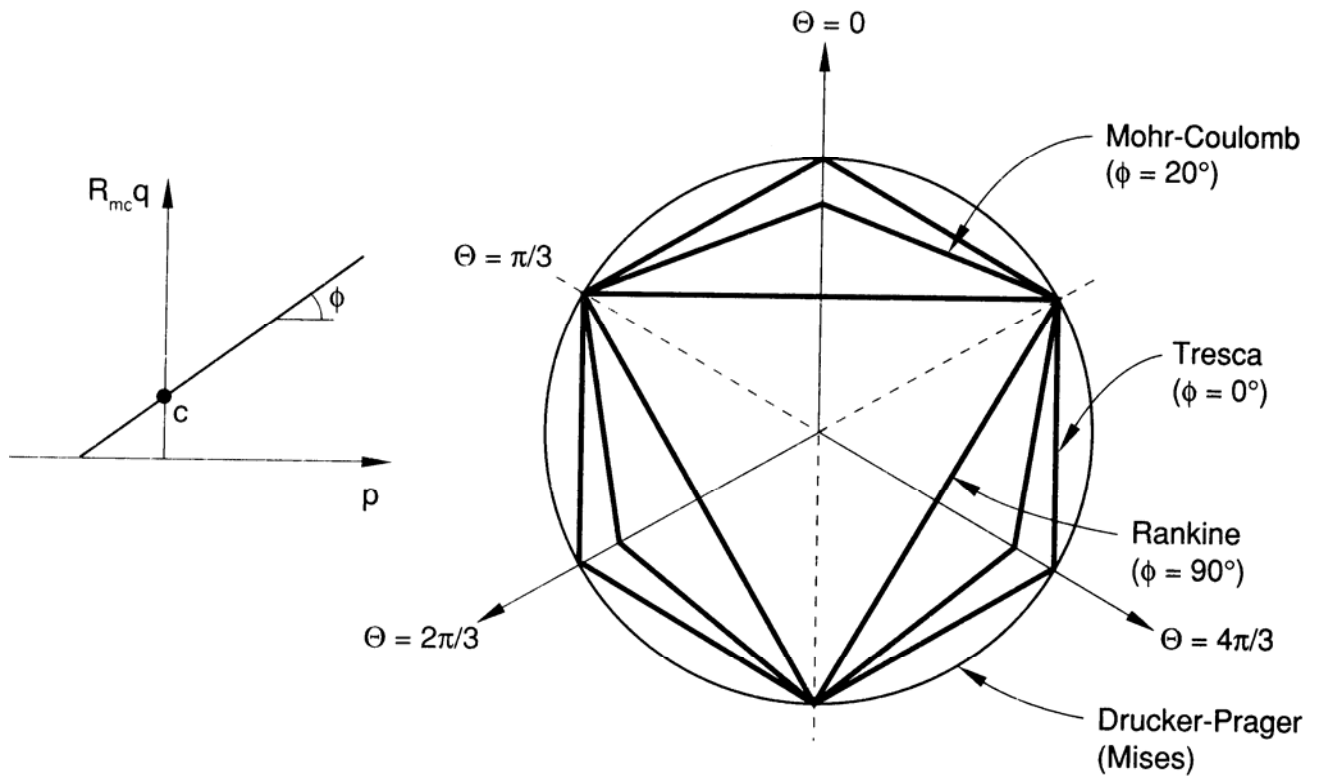
Figure 6.5 Mohr-Coulomb yield surface in meridional and deviatoric planes
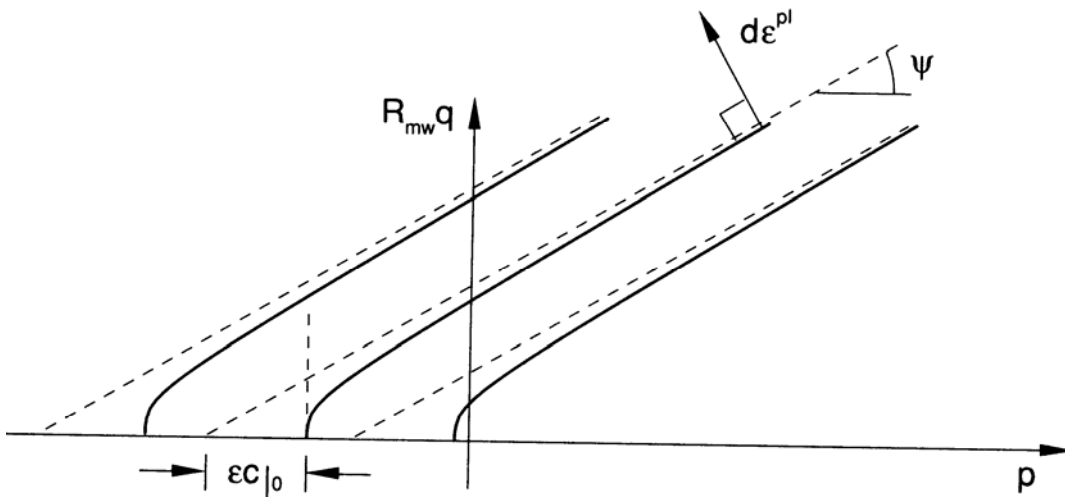
Figure 6.6 Family of hyperbolic flow potentials in the meridional stress plane
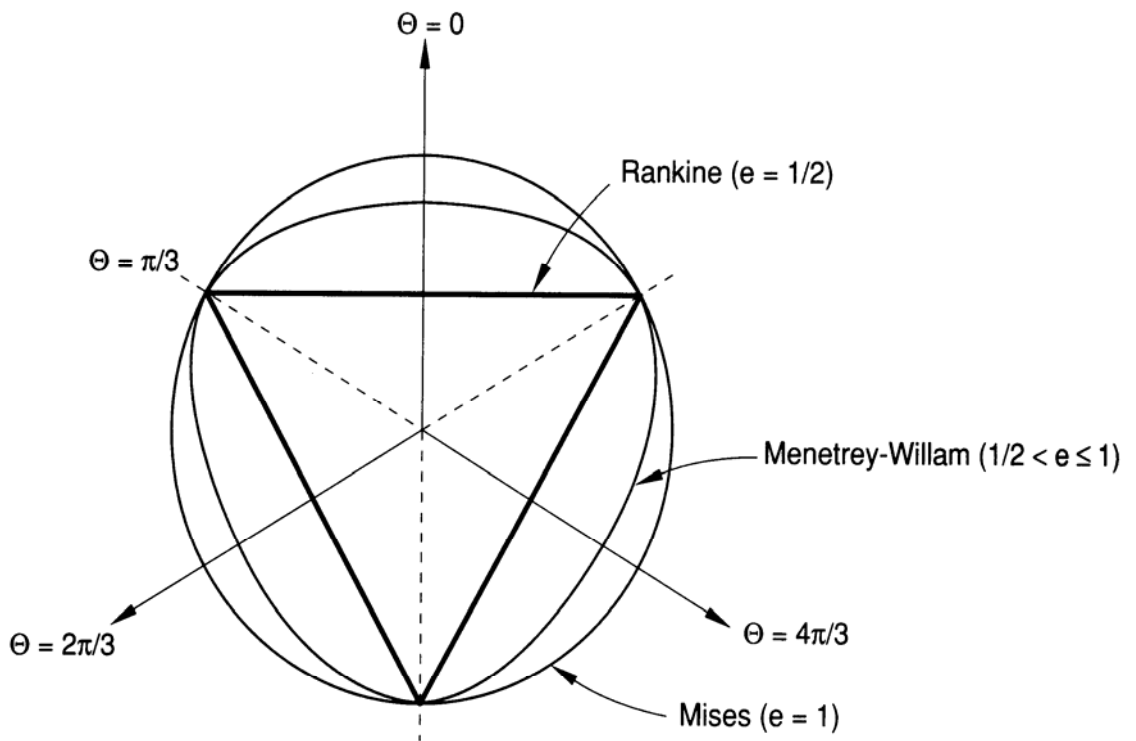
Figure 6.7 Menétrey-Willam flow potential in the deviatoric stress plane
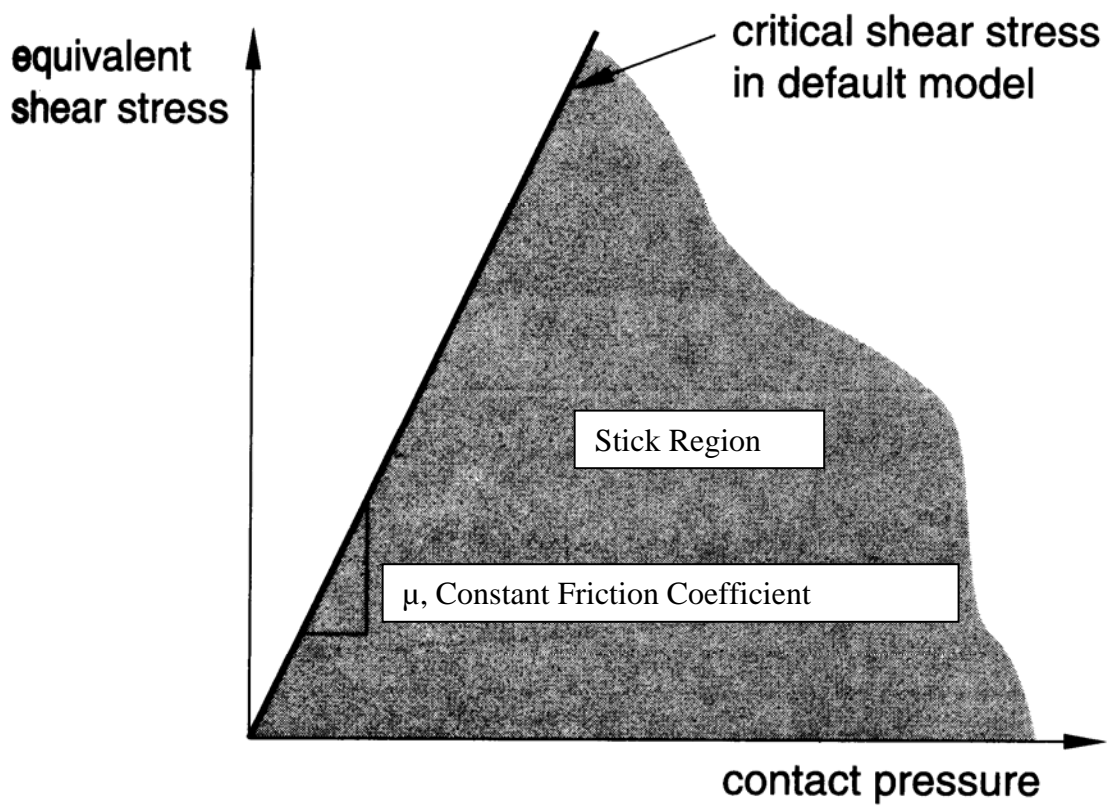
Figure 6.8 Slip regions for the default Coulomb friction model
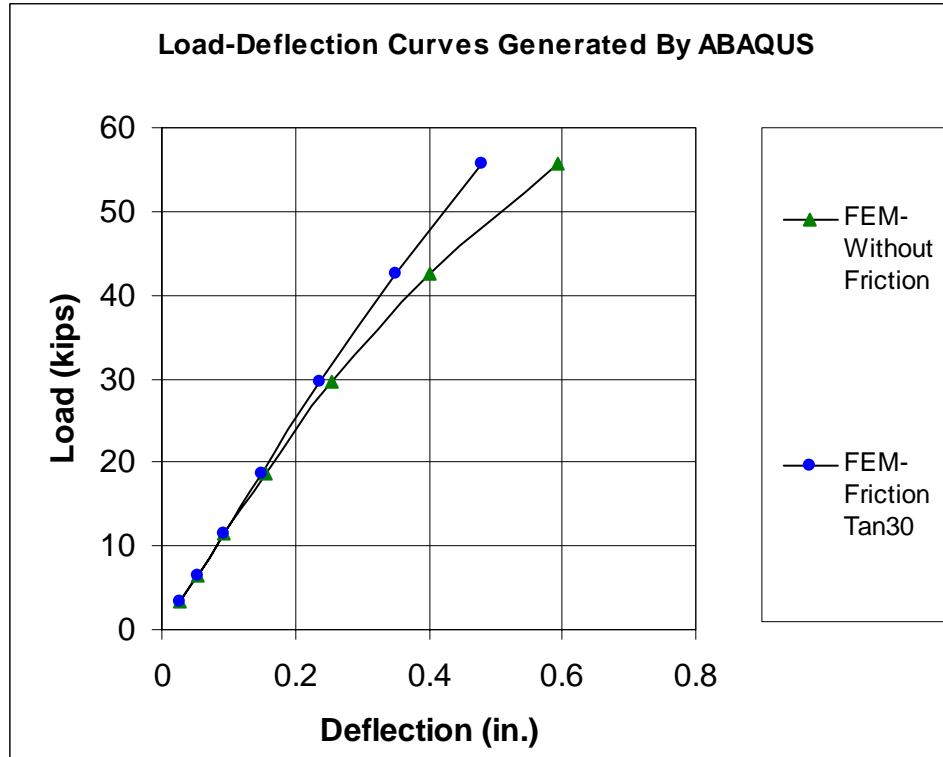
Figure 6.9 The comparison of FEM model with friction and without friction
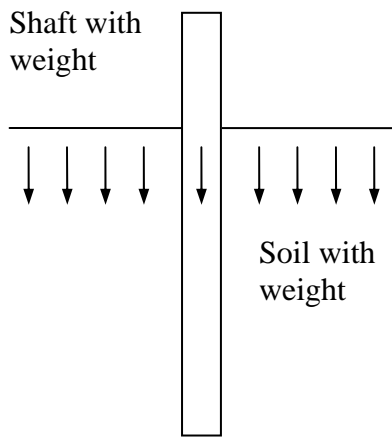
Step 1: Gravity Applied   Step 2: Apply Lateral Load
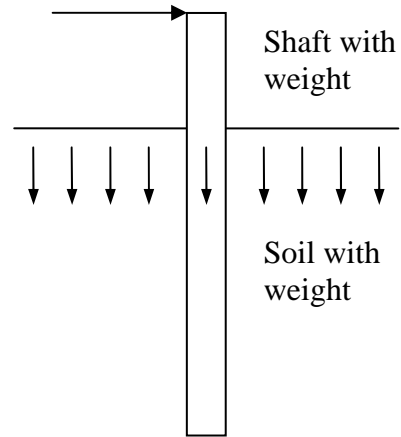
Figure 6.10 Simulation of initial soil effective stress condition
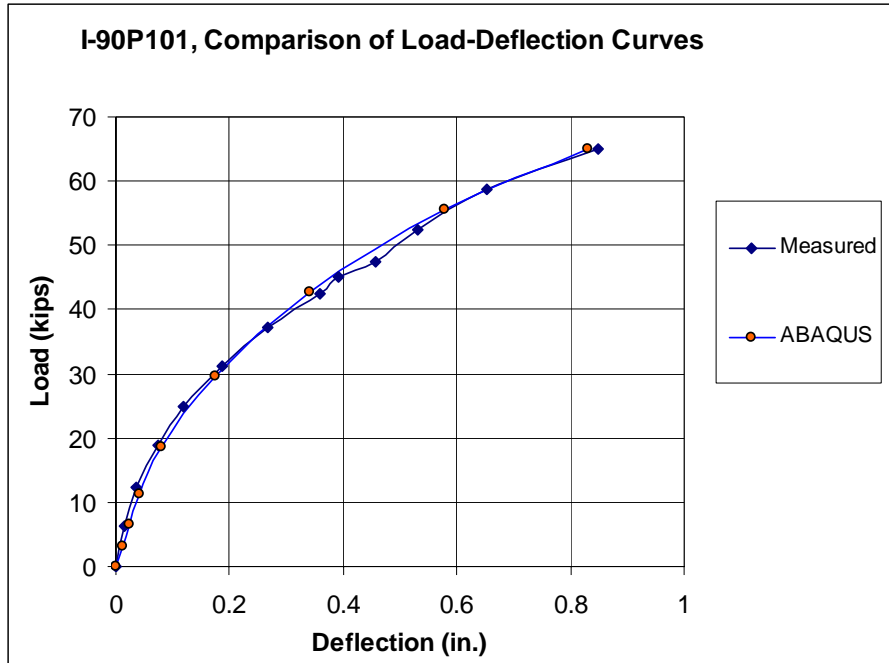
Figure 6.11 The comparison of load vs. deflection curves between measured results and FEM analysis
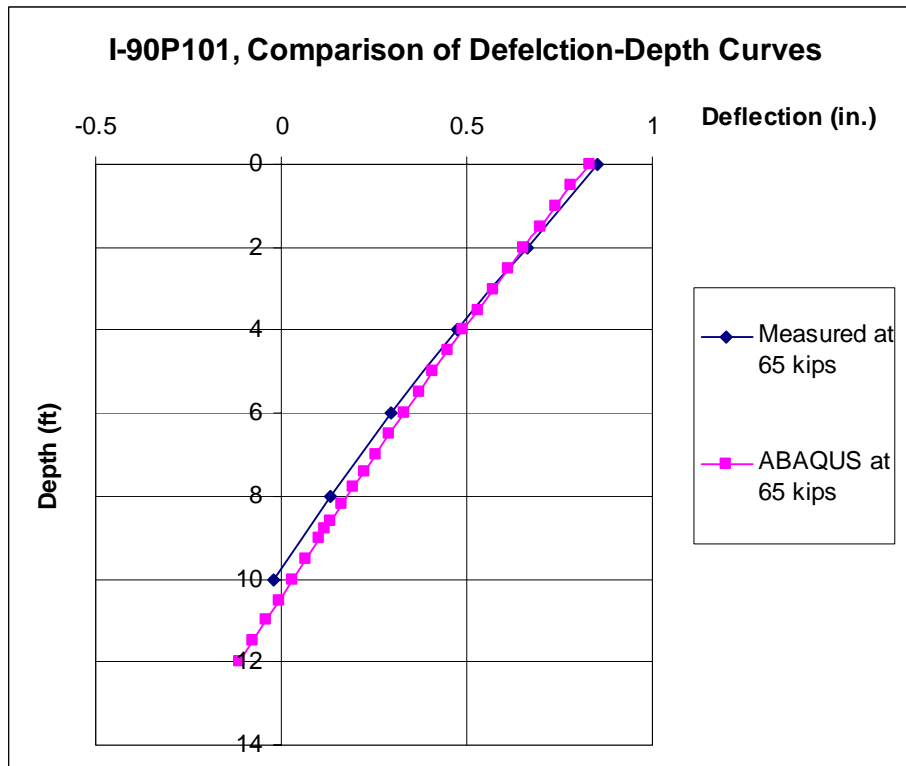
Figure 6.12 The comparison of deflection vs. depth curves between measured results and FEM analysis

6-19
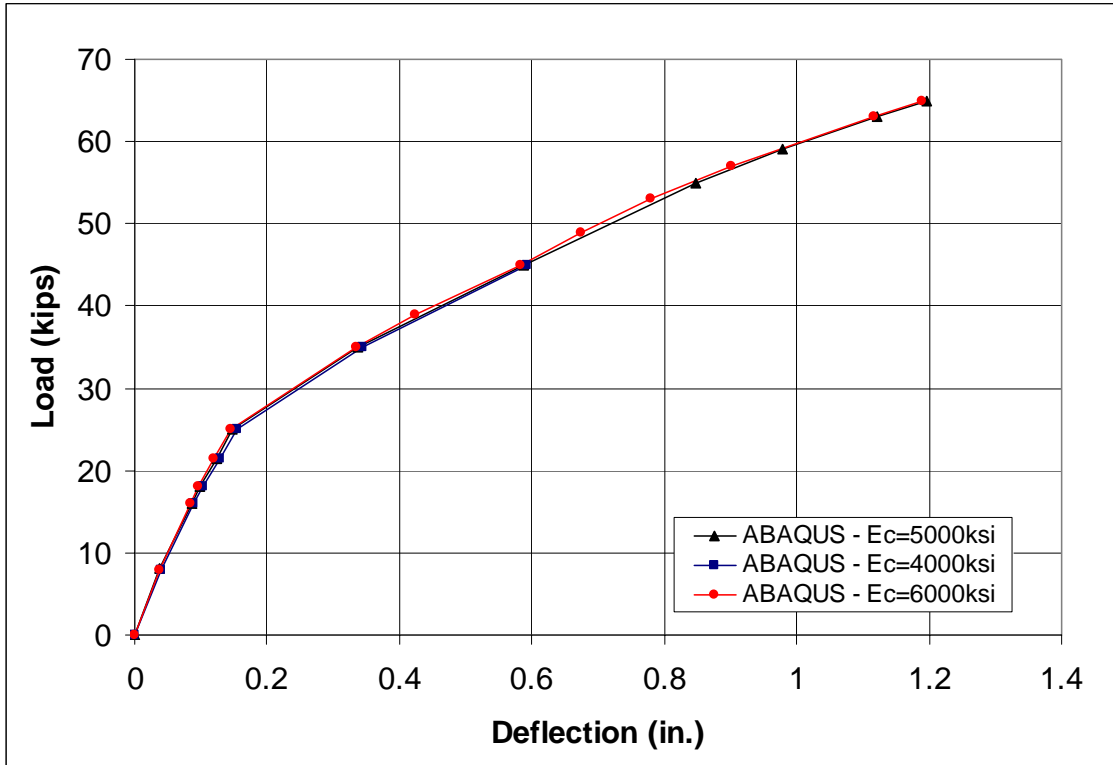
Figure 6.13 The effect of initial elastic modulus of shaft on lateral response
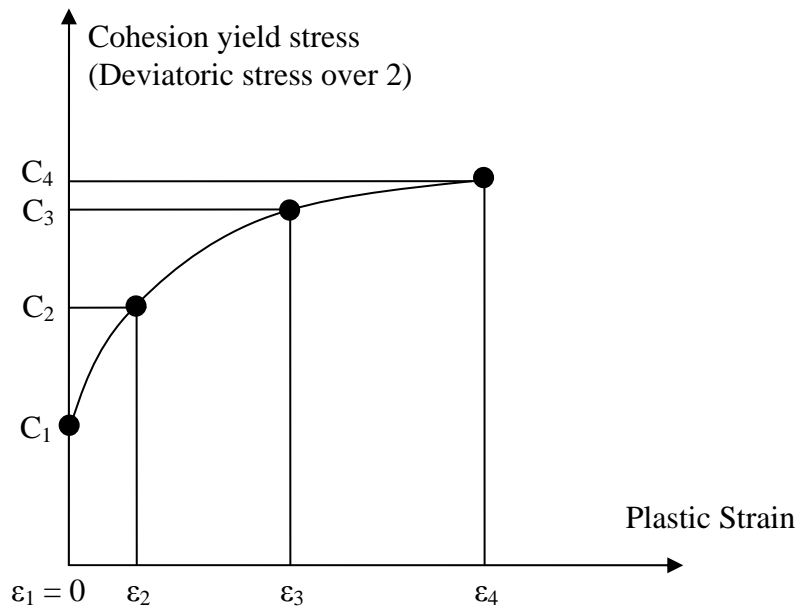
Figure 6.14 Cohesion yield stresses and corresponding plastic strains
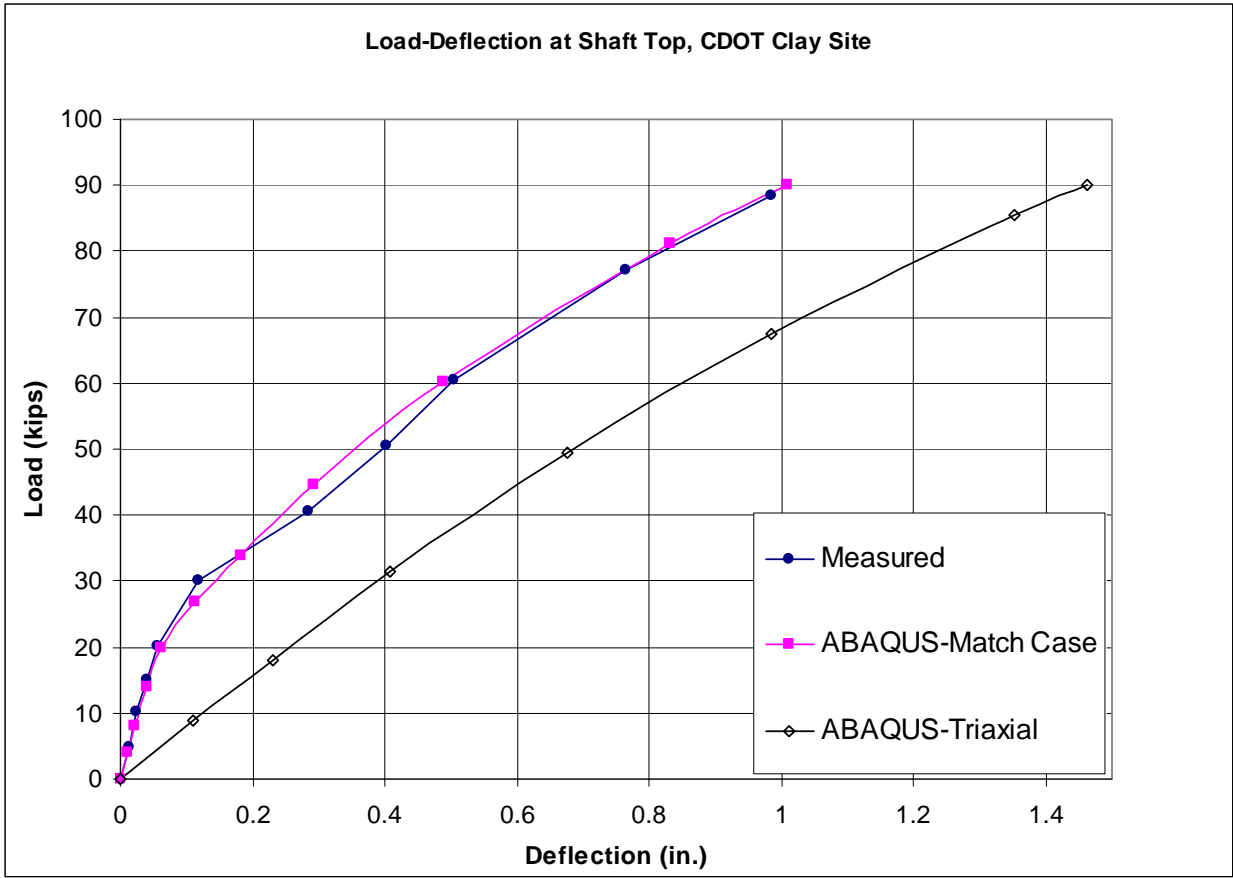
Figure 6.15 Simulated and measured load-deflection curves of CDOT test at clay site
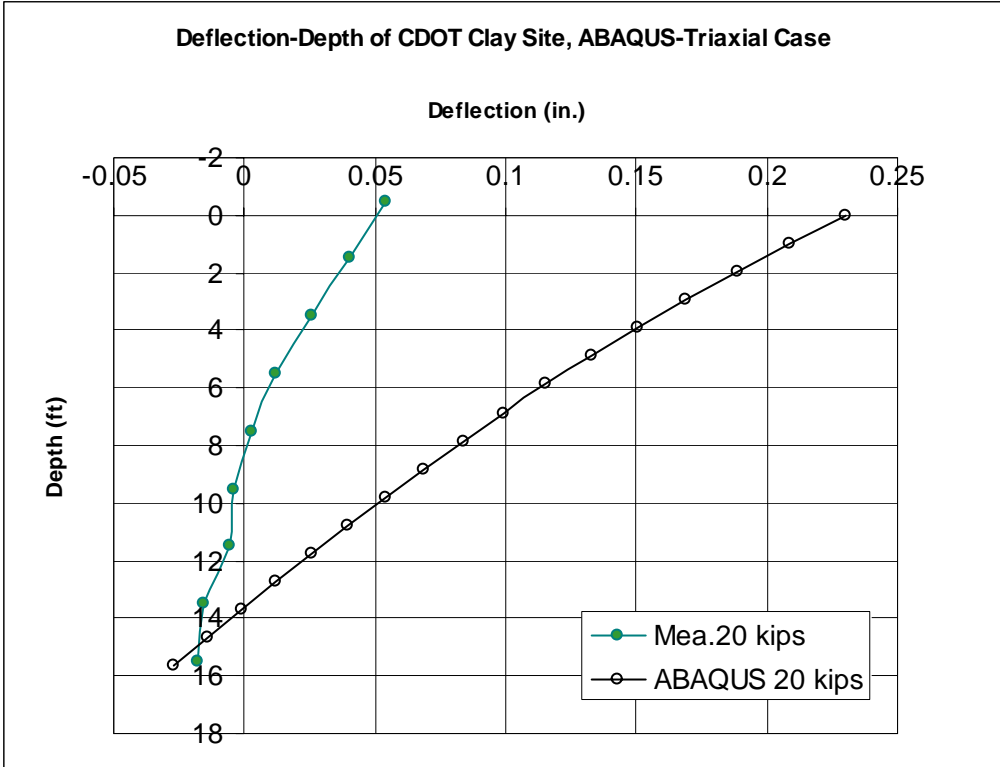
(a) Triaxial case with 20 kips of load
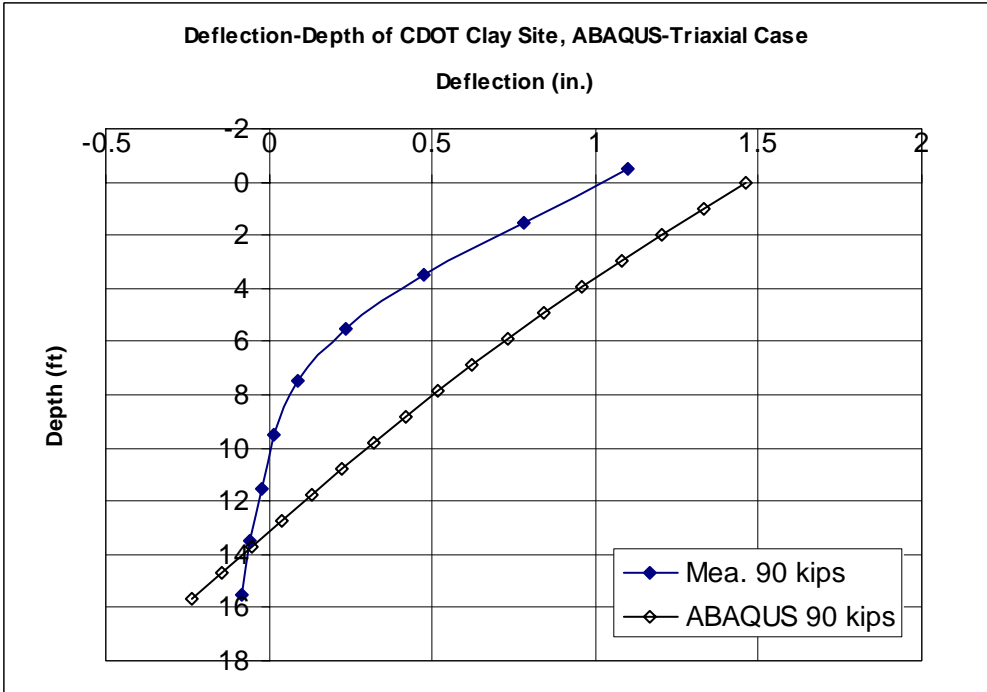
(b) Triaxial case with 90 kips of load

Figure 6.16 Comparisons of measured deflection-depth curves and those from FEM

simulation with soil input from triaxial tests for CDOT test at clay site
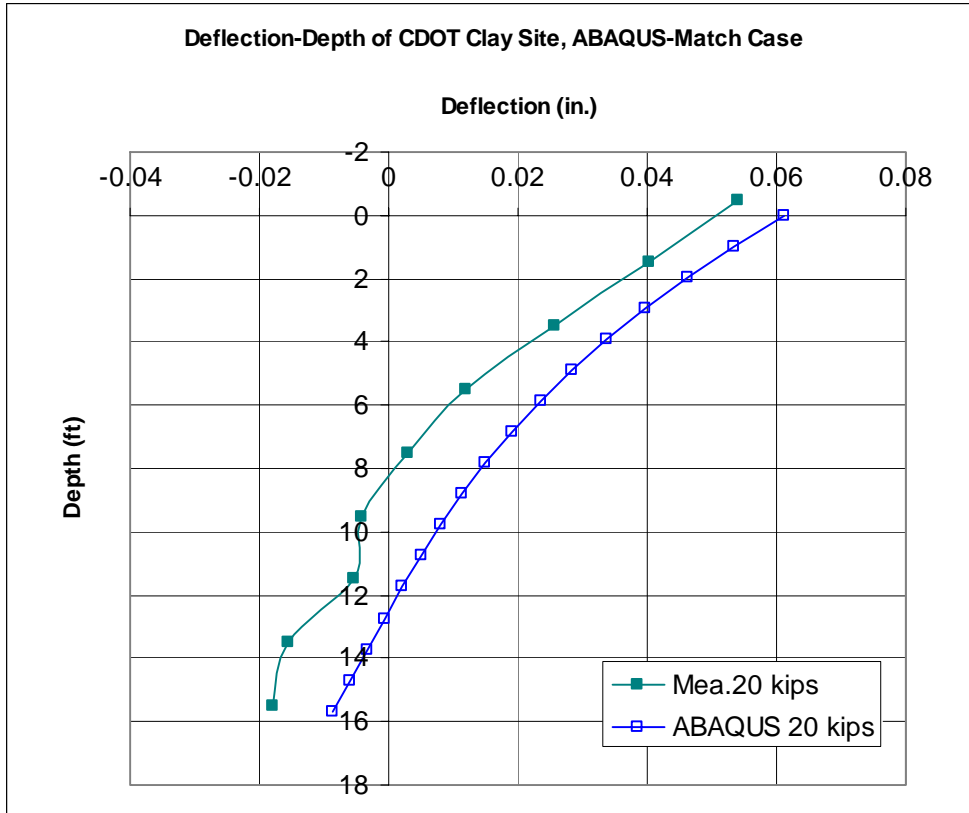
(a) Match case with 20 kips of load
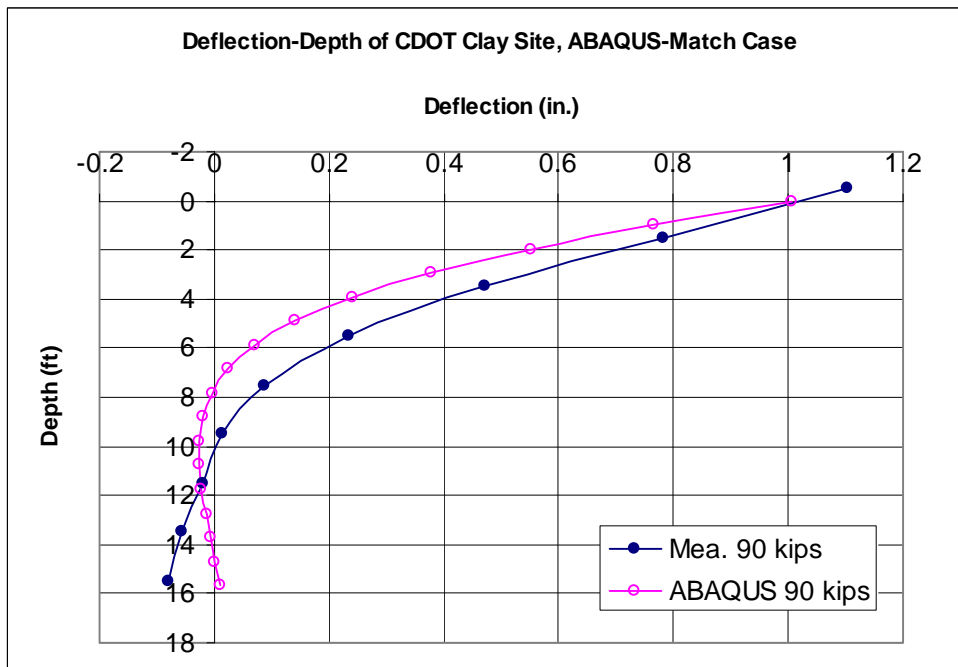
(b) Match case with 90 kips of load

Figure 6.17 Comparisons of measured deflection-depth curves and those from FEM simulation with best match soil input for CDOT test at clay site
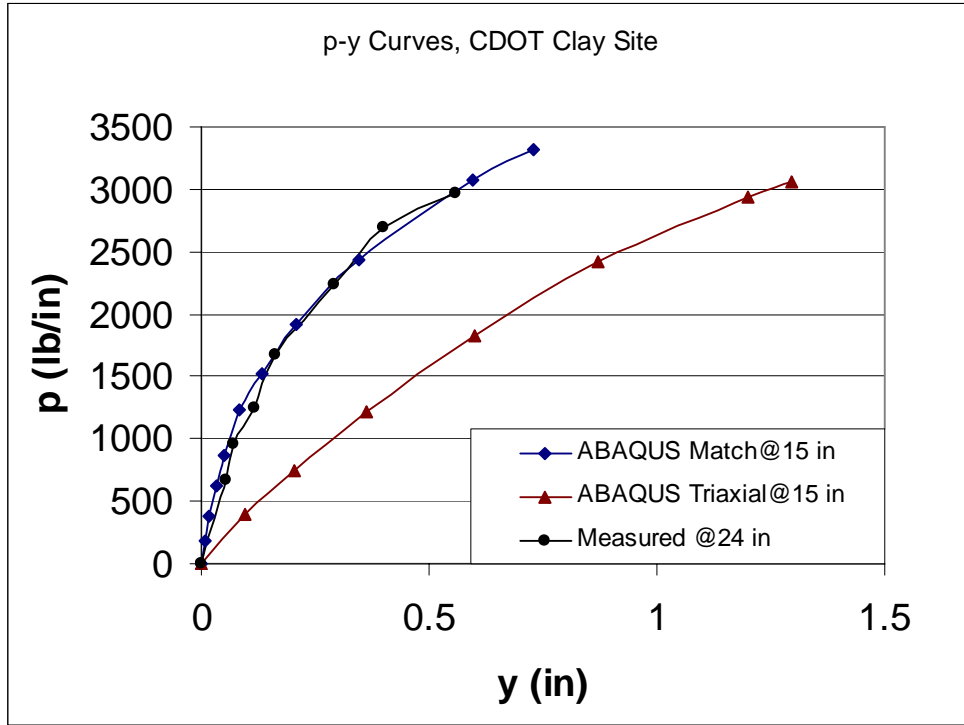
(a) p-y curves at 15 inch depth
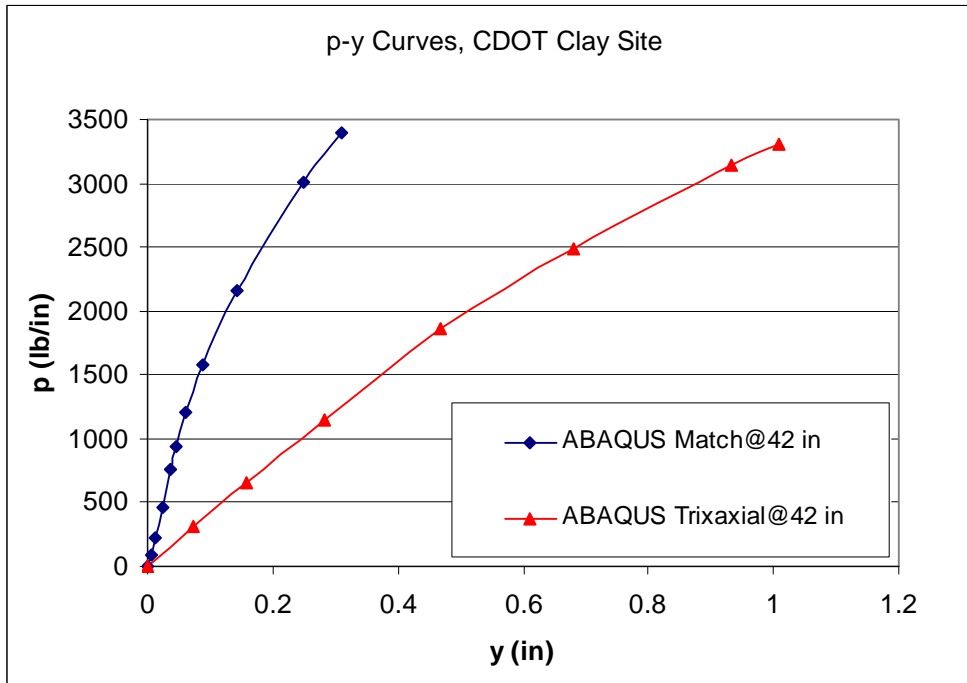
(b) p-y curves at 42 inch depth

Figure 6.18 p-y curves from ABAQUS and COM624P at clay site
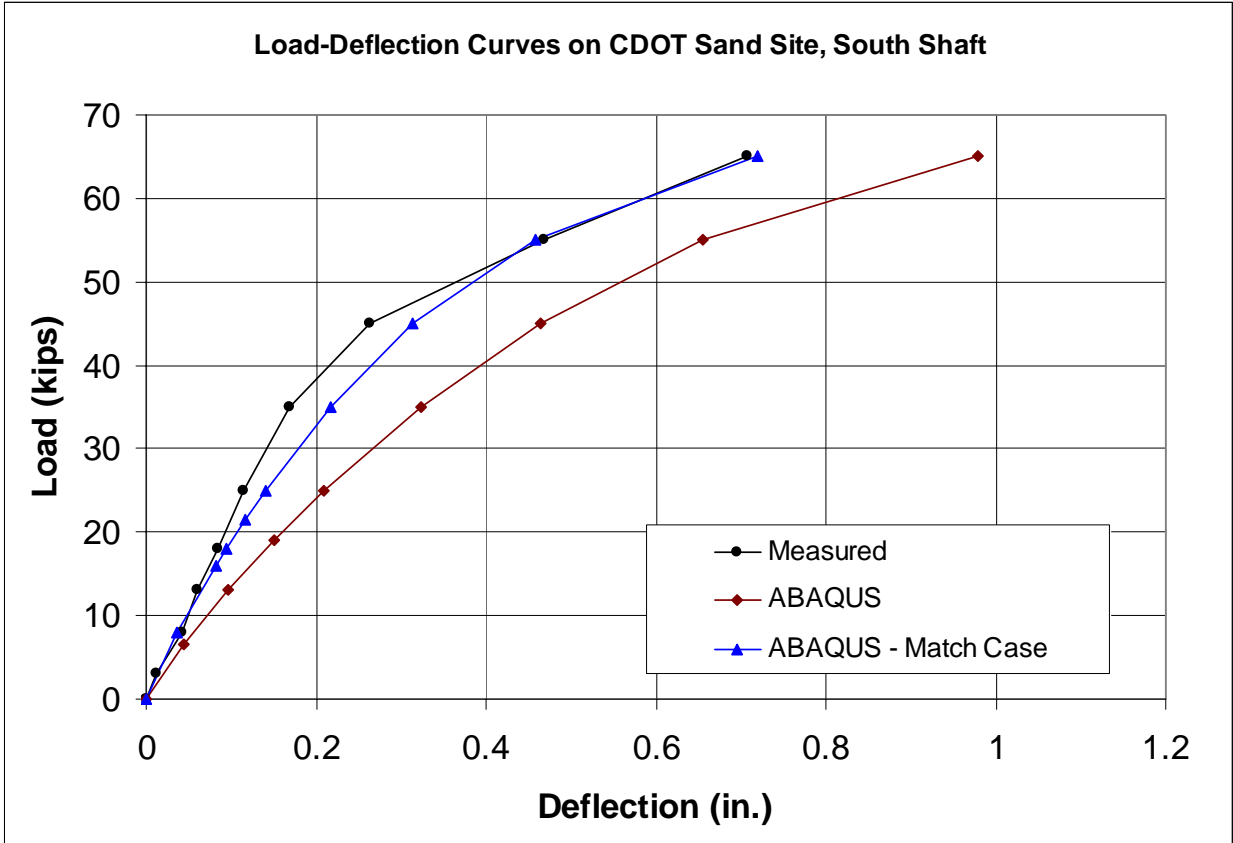
Figure 6.19 Simulated and measured load-deflection curves of CDOT test at sand site
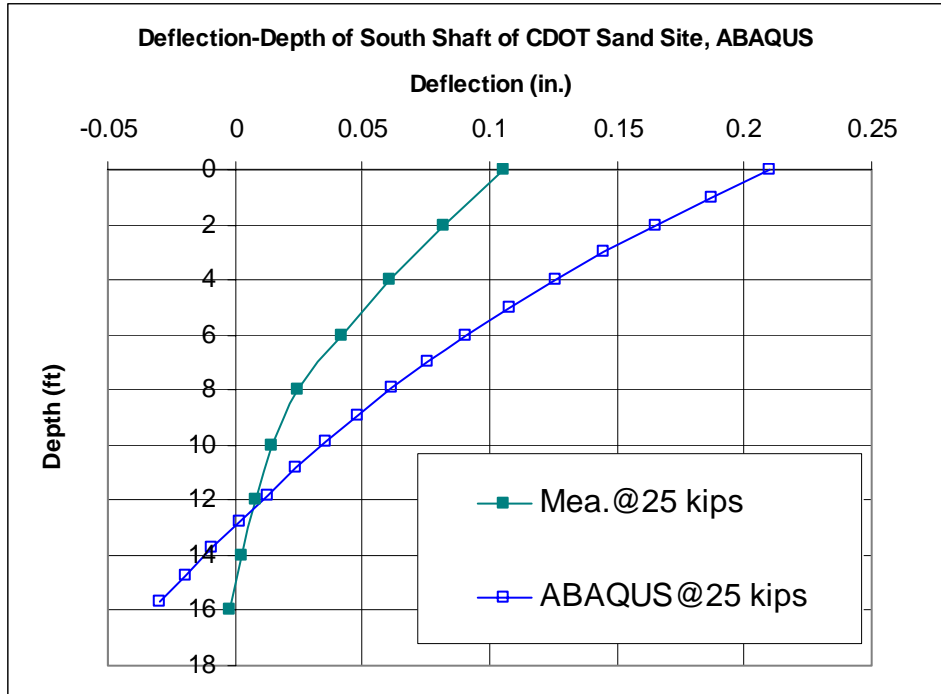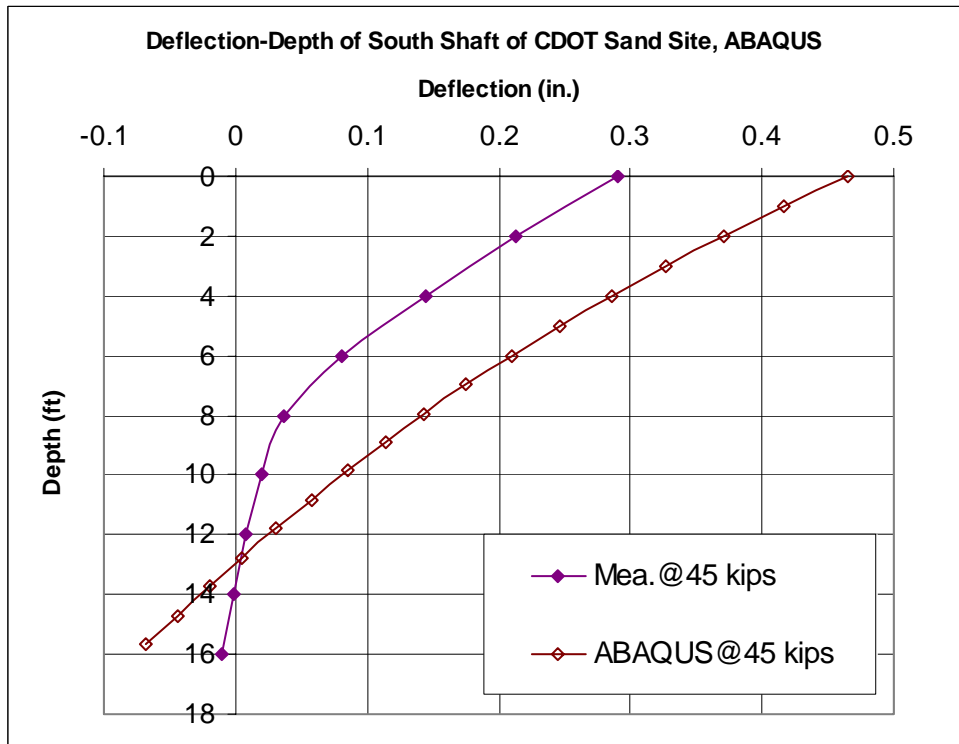
(a) 25 kips of load

(b) 45 kips of load

Figure 6.20 Comparisons of measured deflection-depth curves and those from FEM simulation with soil parameters from lab and PM tests for CDOT test at sand site
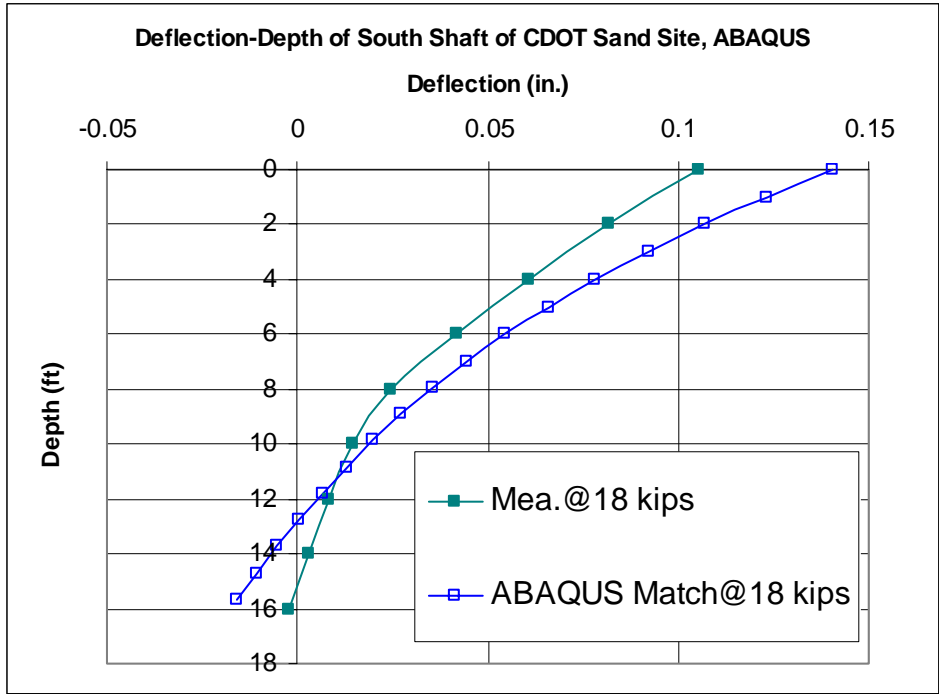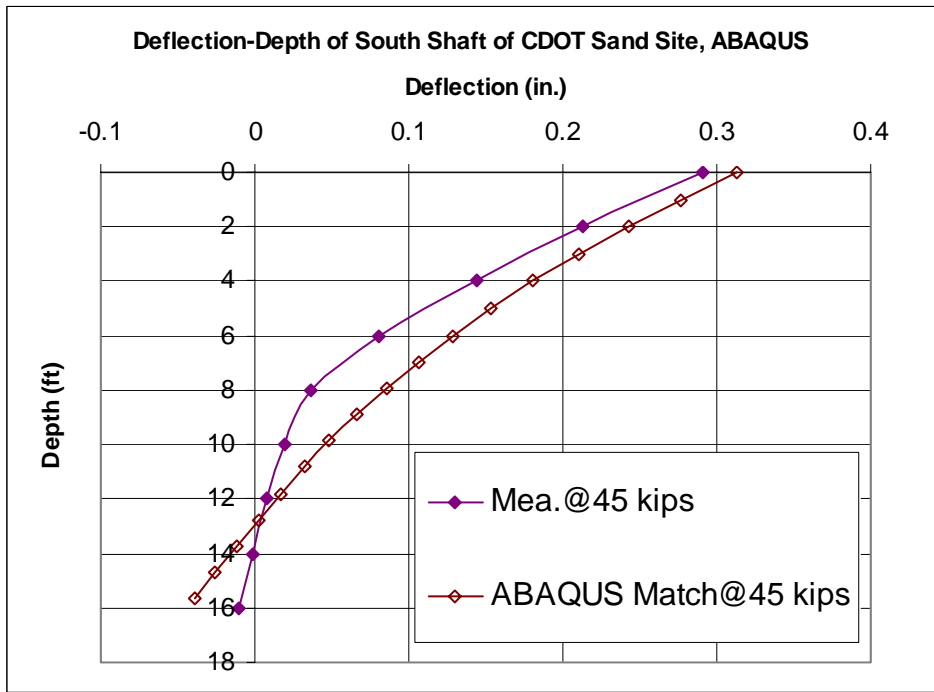
(a) 25 kips of load

(b) 45 kips of load

Figure 6.21 Comparisons of measured deflection-depth curves and those from FEM simulation with best match soil parameters for CDOT test at sand site
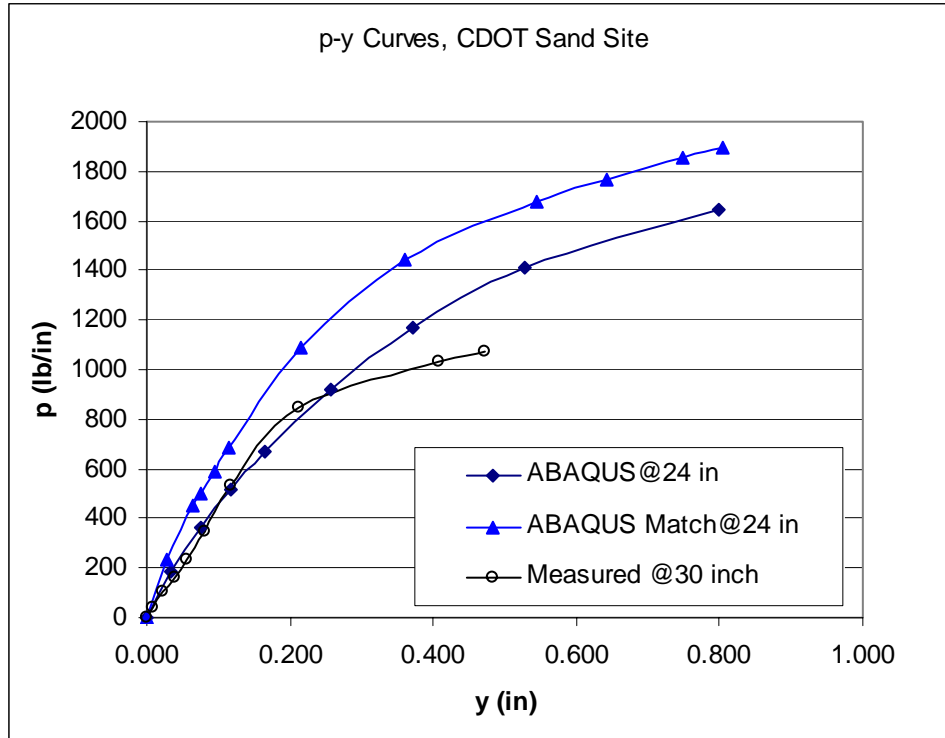
(a) p-y curves at 24 inch depth
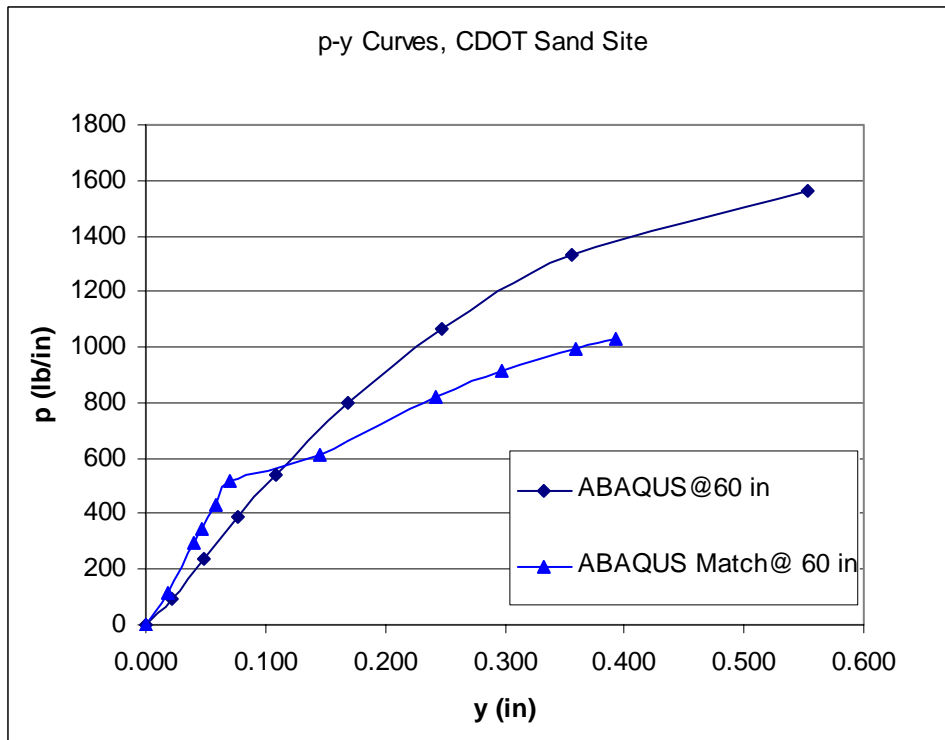
(a) p-y curves at 60 inch depth

Figure 6.22 P-y curves from ABAQUS and COM624P at sand site

7   DRILLED SHAFT INSTRUMENTATION AND LATERAL LOAD TESTING

7.1   Objectives of Lateral Load Tests

The most accurate design method for drilled shafts is to conduct a lateral load test on shafts constructed as planned in the construction project.   Lateral load tests are performed for two general purposes:

❑ To prove that the test shaft is capable of sustaining a given magnitude of lateral load ("proof test"). The test shaft must sustain a load that is twice the working load without excessive lateral movement.

❑ To obtain the ultimate lateral resistance of the shaft, the lateral load-deflection curve, and p-y curves of the soil layer around the test shaft. The structural engineer is to estimate the moments/shears of the production shafts under service and ultimate loading conditions. They can then use this information, especially p-y curves. The structural engineer should decide if the structural design of the shaft will control the design and adjust the steel area and length of the drilled shafts. It is desirable that such test should be conducted during the design phase, under a special contract, or in Phase 1 of a project that involves several phases. The load test data can then be used: 1) to design the production shafts in that project with more confidence (smaller FS and higher resistance factors) that would result in some savings to the project, 2) as research data to improve the design methodology in all future applications.

Load tests are desirable where a large number of shafts are required. It is recommended that an economic study be performed for these large projects to determine the potential savings resulting from performing load tests.

7.2 Description

This item consists of furnishing all materials, equipment, and labor as necessary to instrument and run a lateral load test on two of the plan production drilled shafts. The plan identification numbers for the two selected Item Special drilled shafts are numbered **X** and **Y**. Conduct the tests by utilizing the companion load test drilled shaft in each test as the mutual reaction element.

7.3 General

Conduct the lateral load tests in accordance with the requirements specified in ASTM-D3966. Cylinder strengths for the drilled shaft concrete shall indicate a minimum of **4000** psi (f'_c), prior to applying the moment and lateral load force to the shafts to be tested.

7.4 Materials

Low strength mortar   (need some specs for these items)
Reinforcing steel
Concrete
Structural steel

7.5 Location of Load Tests

Test locations should be selected after the subsurface geotechnical investigation is performed following one or more of these criteria:

- At or close to the project site, in a location that represents all of the production shafts on the project.
- At or close to the weakest soil layer if the design was based on the weakest soil layer (not relevant if uniform soil layer is encountered at the site)
- In flat areas accessible to heavy equipment (important with sacrificial shafts constructed before construction is started).

- At or close to shafts with the highest loads.

7.6   Type of Test Shafts (Production or Sacrificial)

The purpose and type of the load test determine the type of the test shaft. Production test shafts are often selected for proof load testing. Sacrificial test shafts are used for testing to a higher deflection or load than in the acceptable criteria. When the exact locations of the production shafts are not finalized, it is recommended to consider a sacrificial test shaft. Testing of a production shaft can be risky in some areas (e.g., under water).

7.7   Acquisition of New Geotechnical Data at Sites of New Lateral Load Tests

At the locations of new lateral load tests on drilled shafts, comprehensive subsurface geotechnical investigation should be performed as described in the previous section. This is required for the proper design of the load test and to acquire accurate research strength data for the soil layers that could be correlated with the resistance values measured in the load tests. Therefore, it is necessary to perform the geotechnical subsurface investigation before performing the new load test. Three test holes should be drilled at the lateral load test site. Subsurface geotechnical investigation methods at each test hole should be performed as described in this study. It will include auger drilling with standard penetration testing, sampling, subsequent laboratory testing on recovered core specimens, and in-situ pressuremeter testing.

7.8   Drilled Shaft Construction

The two drilled shafts to be tested shall be constructed with structural steel members extending a minimum of half the wall height plus two feet above the top of each drilled shaft, and embedded a minimum of four feet into the shaft. The lateral load shall be applied at a point located at half the wall height above the top of each drilled shaft.

A 12 inch diameter hole shall be drilled for a depth of six feet below the bottom of the **16** feet long production drilled shaft. The 12 inch diameter hole will serve to anchor the bottom six feet

of the slope inclinometer casing. The hole shall be located appropriately and shall be backfilled with sand or low strength mortar.

The constructed Item Special pay length of the two drilled shafts to be tested is 16 feet. A one quarter inch thick (minimum) wall steel drilled shaft casing shall extend from elevation 3 feet below the top of the shaft up to the top of the drilled shafts that are to be laterally load tested for the purpose of strengthening the drilled shaft during the application of the lateral test load.

7.9   Testing Engineer

The installation of the drilled shaft instrumentation and the performance of the lateral load tests shall be performed under the direction of the Testing Engineer. The Testing Engineer shall be a Professional Engineer who has had experience in conducting at least two similar instrumented lateral load tests in the past.

7.10 Instrumentation

Instrumentation sensors (strain gages, inclinometer casing, and couplers) are to be purchased by the contractor. The total quantity of sensors that shall be purchased is summarized in Table 7.1.

The Inclinometer casing and all other sensors, gages, and measuring devices shall be installed under the direction of CDOT Research team. The locations of the strain gages to be installed on the drilled shaft reinforcing steel cages shall be as directed by CDOT Research Team. Inclinometer casings shall be installed in the sand/low strength mortar to a depth at least 6 ft. below the tip of the plan drilled shafts.

Table 7.1 Summary of Required Instrumentation and Devices*

Drilled Shaft # and depth (ft)	Sister Bar (Each)	Inclinometers**		V.W. Tiltmeter	Data Acquisition System	Multi-plexer	W14x109
		Tubes (feet)	Couplers #				
#** – 16 ft.	20 with 50' cable	25	4				2 pieces @10'
#** – 16 ft.	24 with 30' cable	25	4				3 pieces @10'
Total Quantity	44	115	18	None	None	None	50'

* Two dial gages and an LVDT shall be used to measure the lateral movement at the jacking point in each test shaft. A stable reference beam as explained in the testing section shall support the dial gages and LVDT.

** Inclinometer tubes shall be in 5 feet pieces and shall use 12" long couplers.

7.11 Instrumentation Specifications

1. Inclinometer Tubes: Geokon Model 6501 (or an approved equal) pultruded fiberglass inclinometer casing with a nominal 2.5 inch inside diameter, bottom plug and top cap. Inclinometer tubing shall be tied in place prior to placing concrete in the drilled shafts. The inclinometer casing shall be supported by the reinforcing steel.

2. Sister Bar Strain Gages: Geokon Model 4911 VW#4 rebar strain meter with cable (or an approved equal).

3. Vibrating Wire Uniaxial Tiltmeter: Geokon Model 6350 vibrating wire Tiltmeter (or an approved equal).

4. CR10X Data Acquisition System (Geokon Model 8020 MICRO-10 Data logger, or an approved equal).

5. Muliplexers (Geokon Model 8032, or an approved equal).

6. Enclosure Box (Traffic enclosure manufactured by Southern Manufacturing, 501 Herndon Ave Orlando, Fl 32803, Telephone: 800-866-5699 Fax: 407-894-5373, or an

approved equal). The size of the box should be a minimum of 4 feet wide by 5 feet high by 2 feet deep.

All of the instruments and accessories shall be installed according to the manufacturer's recommendations and as directed by the Testing Engineer

7.12 Testing

Conduct the lateral load test according to the requirements specified in ASTM-D3966: Standard Test Method for Piles under Lateral Loads. The standard loading procedure outlined in the ASTM-D3966 standards should be followed.

The structural design of the load frame system shall be performed by the Testing Engineer and submitted to CDOT for approval at least 10 working days prior to beginning construction of the drilled shafts to be tested. The design load for each drilled shaft is based on a 27 psf wind pressure applied at the mid height of the wall. Based on an assumed 10 feet high wall and a center-to-center spacing of 23 feet, the resultant force at mid height of the wall is 6.21 Kips applied at a height of 11 feet above the top of the drilled shaft. The maximum test load, which includes a factor of safety of three, is 20 kips applied at 11 feet above the top of the drilled shaft. The maximum design load for the testing device shall be a minimum of 75 Kips to be applied 11 feet above top of shaft. The test will be stopped prior to applying the maximum design load if CDOT determines that excessive deflection is occurring.

A stable reference beam system for mounting the dial gages and LVTDs to monitor the movement of the drilled shafts at the points of load application shall be provided. The reference beam shall be rigid and firmly supported at a minimum distance of at least three shaft diameters from the center of the test shafts.

The work shall include, but not be limited to:

1. Furnishing the instrumentation, the load application, and testing equipment.
2. Installing the instrumentation, operating load application, and monitoring equipment.
3. Performing structural analysis using the collected data from the lateral load tests.

4. Furnishing a final report.

7.13 Equipment

The contractor shall furnish all equipment necessary to perform and dismantle the lateral load tests in compliance with the ASTM-D3966 Standard Test Method for Piles Under Lateral Loads, and to assist the CDOT Research Team in installing the instruments and data collection devices. The load shall be applied utilizing an arrangement of components that will provide the required maximum test load (i.e. load equivalent to 3 times the design load specified in the plans). The jack and the load cell shall each have a capacity that is 15% greater than the specified maximum test load. The load cell and the jack shall be accompanied with documentation verifying that they have been calibrated within the past year.

The contractor shall provide a protective work area, including provisions such as a tent or shed for protection of the load test equipment and personnel from inclement weather.

7.14 Report

A detailed report containing the lateral load test results shall be prepared and submitted to the Project Engineer for approval. The report shall include:
 (a) Drawings of the instrumentation plans.
 (b) Graphs and tables of load vs. lateral deformation.
 (c) Horizontal movement along the depth of the shaft determined from inclinometer data.
 (d) Angle of tilt of the drilled shaft at the tiltmeter locations.
 (e) Strain readings from the strain gages embedded in the drilled shafts and the computed bending moment and axial forces at each load level.
 (f) Back-calculations using the load test results to determine the pertinent parameters for the soil and bedrock p-y curves.
 (g) Recommended design parameters for future drilled shaft projects.
 (h) All calibration sheets for the instruments used in the tests.

(i) All data gathered from the instruments in an electronic format with enough explanation to make it understandable by the Project Engineer.

7.15 Method of Measurement and Payment

Payment for the instrumentation and lateral load testing of the drilled shafts includes:

1. Furnishing instrumentation and the load application equipment.
2. Drilling and backfilling the 6 feet long, 12 inch diameter hole below the actual production drilled shafts.
3. Installing and operating the instrumentation and load application equipment.
4. Dismantling of the load test equipment and structural members.
5. Performing analysis by using the collected data from the lateral load tests.
6. Furnishing a final report.

After receiving and approved final report, payment will be made at the contract lump sum price bid for Item Special Drilled Shafts Instrumentation and Load Testing. Table 7.2 provides the summary of required materials.

Table 7.2 Summary of Required Material

Drilled Shaft # and depth (ft)	C10x30	Dywidag Rods 1.5" Dia.	1.5"x0.5"x0.25" Angles to weld the gages on	2"x2"x0.25" Angle for Reference beams	W14x109
#** – 16 ft.	2 pieces 5' long		65'	30'	2 pieces @10'
#** – 16 ft.	2 pieces 5' long		65'	30'	3 pieces @10'
Total Quantity	4 pieces 5' long	80' plus 4 couplers	130'	60'	50'

The research team will provide the following measuring devices:

1. Data Acquisition.
2. Multiplexers

3. Dial Gages.

CDOT or the contractor needs to provide an inclinometer device to measure the deflection in the inclinometers during testing.

The contractor shall provide the required steel to setup the load test as per the drawings prepared by E.L. Robinson Engineering of Ohio Company. This includes, the W14x109, The C10x30, the bearing plates, the Dywidag 1.5" diameter rods, the reference beam to support the dial gages, the L4x4x 3/8, the 1"x.5"x.25" angles, and welding machine to weld the strain gages end blocks.

Prices of Devices and gages:
1. Vibrating wire VSM-4000 Strain gages are $110 each and the cable is $0.41 per foot. ($110x44 + 1960 ft. x $0.41 per foot = $6079)
2. Inclinometer tubes are around $8.00 per foot. ($8x115 + 18 Couplers x $5 = $1010)
3. Steel plates to weld strain gages on (Angle 1x0.5"x0.25") 130' costs
4. 50' of W14x109 (50x109x$1.2 per pound = $6540)
5. Steel angels 2"x2"x0.25 for reference beams 60 feet total
6. C10x30 four pieces 6' long
7. Steel Plates 12"x12"x1" total of 3.
8. Steel Plates 48"x12"x1" total of 2.
9. Nuts and washers for the Dywidag 1.5" rods. 10 of each.

7.16 Recommendations for Improving the Load Test

1. Use of circular reinforcing cage with stirrups all the way to the bottom of the shaft should be emphasized in the future load tests.
2. The size of the steel H-Beam should be smaller than the size of the reinforcing cage to provide for some clearance. More important, there should be a precise method to measure the lateral load exerted on each test shaft. In addition, the ground elevation and the moment arm for the two test shafts of the load test should be the same.
3. To extend the H- beam all the way to the bottom of the shaft as in Ohio's load tests.

4. To design the layout of the load test based on the results of simple geotechnical tests. First, the diameter should be selected based on the recommended values in the construction project. However, the length of the shafts should be based on our expectation of the results of the load test tests, not what will be used in production shafts based on very conservative design. For example, the Broms method can be used to estimate the length with a factor of safety of 2 and without neglecting 1.5 d. This is to ensure the full mobilization of the plastic resistance of the soil around the test shaft.

Additionally, after the geotechnical investigation performed at the load test site, numerical simulation of the load test, as illustrated in Chapter 6, can be performed for a better design of the load test.
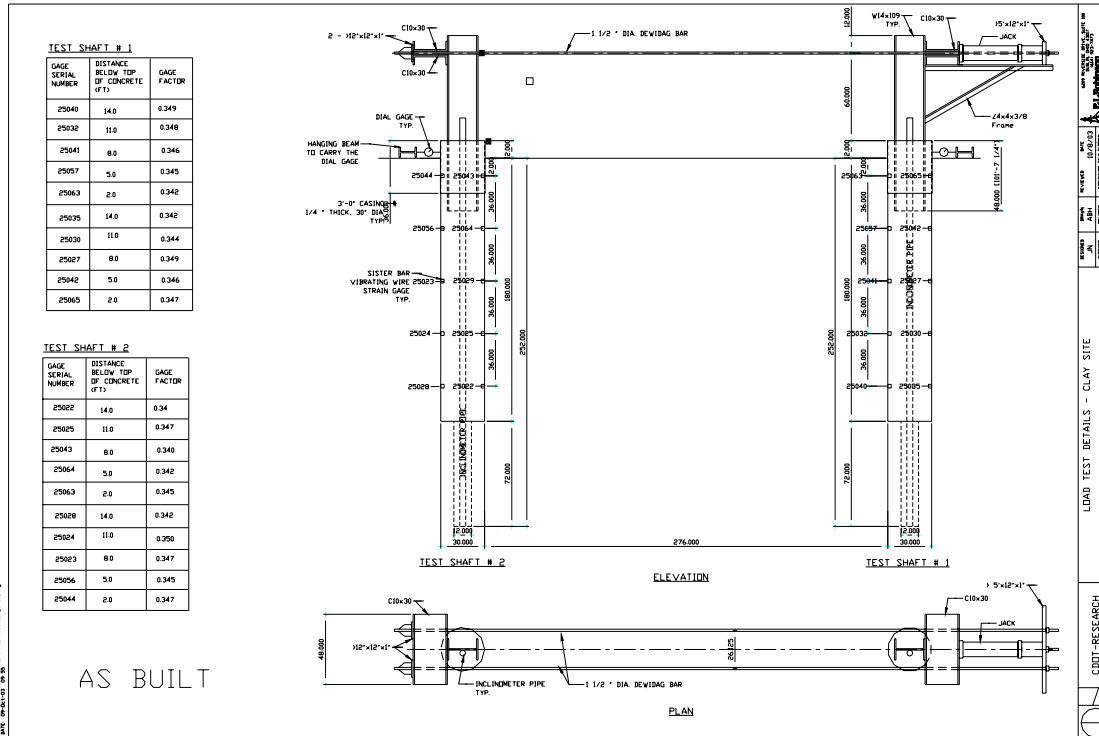
Figure 7.1 Setup and calibration values for strain gages at test site I clay site

SOUTH SHAFT

GAGE SERIAL NUMBER	DISTANCE BELOW TOP OF CONCRETE (FT)	GAGE FACTOR
25036	14.5	0.347
25038	11.5	0.345
25061	8.5	0.35
25062	5.5	0.345
25050	2.5	0.349
25039	14.5	0.343
25037	11.5	0.346
25059	8.5	0.349
25060	5.5	0.352
25058	2.5	0.349

NORTH SHAFT

GAGE SERIAL NUMBER	DISTANCE BELOW TOP OF CONCRETE (FT)	GAGE FACTOR
25031	14.5	0.436
25026	11.5	0.348
25052	8.5	0.345
25051	5.5	0.345
25045	2.5	0.342
25034	14.5	0.342
25033	11.5	0.339
25054	8.5	0.349
25053	5.5	0.346
25055	2.5	0.346

AS BUILT

LOAD TEST DETAILS – SAND SITE

CDOT-RESEARCH

Figure 7.2 Setup and calibration values for strain gages at test site II sand site

8   CONCLUSIONS

Objective 1: Determine the Needs, Benefits, Potential Cost-Effectiveness, and Justification

The research team has reviewed current practice by CDOT engineers and consultants pertaining to the design and analysis of drilled shafts for supporting sound barrier walls, signs, and signals. These reviews, together with relevant AASHTO Guidelines and Ohio DOT practice, were presented in Chapter 3 of this report.

Sound Barrier Walls

It was found that a fundamental discrepancy in the design and analysis philosophy exists between the CDOT engineers and consultants. CDOT engineers tend to rely mainly on the strength limit based approach; whereas, consultants prefer the use of the LPILE program for serviceability based approach. Several methods were used by CDOT engineers to estimate lateral capacity, while conservative F.S. of 2.5 to 3 was used. Often, CDOT engineers eliminated the top 5 ft of soils to accommodate concerns with possible soil degradation, moisture infiltration, or desiccation. The comparison study documented in Chapter 4, based on hypothetical cases and load test data, has resulted in a recommendation of using the Broms method with a lowered F.S. of two. Based on the study of two Colorado load test results, performed as part of this research, a cost saving of 25% could be realized with the proposed design approach.

The accuracy of the Broms method in predicting the ultimate capacities of drilled shafts relies on the ability to input appropriate soil strength parameters. For clay, as discussed in Chapter 5 of the report, the most appropriate soil testing method is the triaxial CU test or direct shear test. For clay, the Broms method using the soil strength parameters interpreted from the pressuremeter test with FHWA (1989) soil strength interpretation equation or SPT method with Liang (2002) correlation charts also provides a reasonable capacity estimate. For sand, SPT with Liang (2002) correlation provides the best soil strength interpretation. The Pressuremeter test would provide reasonable soil strength interpretation as well.

The success of the serviceability based design approach requires the establishment of acceptable performance (deflection) limit and accurate analysis tools such as LPILE or COM624P. This research has established the acceptable deflection corresponding to the soil's elastic limit for repetitive loading at the head of the drilled shaft on the basis of geotechnical consideration of drilled shaft-soil interaction in order to provide consistency between strength limit and service limit approaches. One should note that the structural details of the sound barrier walls would ultimately govern the allowable deflection.

The accuracy of LPILE or COM624P analysis in capturing the load-deflection behavior of drilled shafts hinges on the ability to input representative p-y curves. For clay, as discussed in Chapter 5, the most accurate soil parameters determination is the triaxial test or direct shear test. The pressuremeter test and SPT test with correct interpretation could yield reasonable soil parameters as well. For sand, direct shear, SPT, and pressuremeter tests yield reasonable and conservative interpretation on soil parameters required for generating p-y curves.

From the FEM simulations of two Colorado load tests, it was concluded that initial elastic parameters (Young's modulus and Poisson's ratio) of the soil exert the greatest influence on the predicted initial portion of the load-deflection curve of the drilled shaft subjected to lateral load. The strength parameters and the yielding/hardening parameters govern the later portion of the load-deflection curve. Pressuremeter tests in sand and clay have been shown to provide more accurate soil modulus parameters than the techniques using laboratory tests for FEM analysis.

Overhead Signs and Signals

CDOT engineers have developed standard drawings for foundation design of overhead sign structures and traffic signals. The foundation design is based on fairly conservative assumed soil properties. The lateral capacity of the foundation is calculated using the Broms method, while torsional capacity is estimated by the CDOT in-house method. A factor of safety of 2.5 to 3 is adopted for lateral load, while 1.25 to 1.5 is adopted for torsional load. CDOT engineers limit the deformation to be within elastic response (0.1 to 0.2 inch) to avoid accumulation of irrecoverable

deformation with cyclic wind loads. CDOT engineers have observed no failures or excessive deformations of the drilled shafts designed according to this approach.

The research has shown that the torsional capacity estimated from the CDOT method gives the highest capacity among the methods studied in chapter 4. The CDOT method was never verified by field torsional load testing. The combination of mixed granular and cohesive soil properties, in conjunction with relatively high F.S. for lateral loads and very low F.S. for torsional load, perhaps makes the CDOT approach predict the torsional capacity.

Objective 2: Identify Most Accurate Methods to Predict Nominal Response (Ultimate Capacity and Deformation) of Drilled Shafts

Various existing methods for predicting ultimate lateral and torsional capacity of drilled shafts have been evaluated using compiled load test data and two Colorado load test results. Both advantages and limitations of each method were reviewed and summarized in Chapter 2. Among the methods evaluated, including Broms, Brinch-Hansen, sheet piling, and caisson methods, the Broms method provided consistent and safe predictions of ultimate capacity, while others provided either inconsistent or unreliable estimates. CDOT geotechnical engineers seem to neglect the upper 5 feet of clay soils for lateral load resistance. Design performed by consultants may or may not eliminate the capacity in the upper several feet of the shaft. The Broms method eliminates the capacity of 1.5 times the shaft diameter of the clay soil layer for lateral load resistance.

The torsional capacity of drilled shafts in clay can be estimated more accurately by the Florida District 7 method. On the other hand, the Florida Structure Design Office method seemed to provide a more accurate estimate of torsional capacity of drilled shafts in sand.

Structural engineers often establish deflections limits and they are based on individual's engineering judgment. It appears that ¼ inch of deflection at the ground line is considered non-issue and a deflection of ½ inch has been considered acceptable. In Colorado, it appears that ¼ inch of deflection at the ground line is considered insignificant and a deflection of ½ inch is

considered acceptable. Most engineers cited 1" at the ground under service loading conditions as a maximum, and some stated that deflections greater than 1" may be acceptable in some situations. A tilting to the sound barrier walls of 0.833% was established for the T-REX project. This was selected based on aesthetic, not structural concerns. This resulted in deflections at the ground level typically less than 1" but occasionally slightly greater than one inch. Liang (1997) developed design charts for both 1% and 1.5% wall height as allowable deflections at wall top. In the AASHTO LRFD Bridge Design specifications, the allowable horizontal movement at drilled shafts head is specified as 1.5" for bridge foundations. Ohio DOT allows either 1" or 1.5" for design of sound walls. From the drilled shaft performance viewpoint and to be consistent with the strength limit with F.S of two, the authors of this report recommends a permissible lateral deflection of 1 inch at the head of the drilled shaft. Mr. Dick Osmun from Staff Bridge recommends limiting the deformation for signs and signals to the soil's elastic limit under repetitive loading estimated with LPILE to avoid accumulation of irrecoverable deformation with cyclic wind loads.

Deformations of laterally loaded drilled shafts can be accurately predicted by COM624P (or the equivalent LPILE program) with p-y curves characterized by appropriate soil parameters. This research indicated that laboratory triaxial CU tests or direct shear test would be desirable tests for determining accurate soil parameters to generate p-y curves. As an alternative, SPT correlations could be used for cohesionless soils. The pressuremeter test may be used for determining strength parameters of cohesive soils. The prediction made by the NAVFAC DM7 method is very sensitive to the input of the subgrade soil reaction coefficient. NAVFAC DM7 provides a linear deflection prediction along the initial modulus but does not define the limits for the initial modulus as does COM624P or the LPILE program. Thus, its use for predicting drilled shaft deflection is not recommended.

Finite element modeling details have been developed and used to simulate two lateral load tests performed in Denver, Colorado. The commercial finite element code, ABAQUS, was used for this purpose. The FEM analysis requires knowledge and training on the part of engineers in order to successfully model the complex three-dimensional interaction nature of the drilled shaft. Moreover, since the elasto-plastic constitutive model is used for representing nonlinear, stress

path dependent, irrecoverable stress-strain behavior, and the computation resource requirement (in terms of runtime and memory storage) is quite demanding. The FEM simulation technique could be a useful tool, however, for development of new sets of p-y curves for unique soil types, unusual size (dimension) of the drilled shaft, or complex loading conditions.

Objective 3: Develop Practical Procedures to Perform Instrumented Load Tests

The research team has developed a standard special note for performing instrumented lateral load tests, which can be adopted by CDOT engineers or consultants in developing their design plans. Instrumented lateral load tests should be considered for CDOT projects that involve construction of a large number of drilled shafts or that have unique soil conditions at the construction site. For sound barrier wall projects, if the number of the drilled shafts to be constructed is large, then it would be beneficial to arrange for lateral load tests in an effort to derive site–specific p-y curves in the COM624P analysis.

9   RECOMMENDATIONS AND BENEFITS

9.1   Recommendations for CDOT Structural Engineers and Consultants

9.1.1 Sound Barrier Walls: Recommendations

The following two simple uniform strength limit state and serviceability limit state design methods are recommended to determine the required drilled shaft length of sound walls (use the larger length of the two methods):

1. For the strength limit, use the Broms method and a F.S. of two to determine the required drilled shaft length. Lateral soil resistance in the upper 1.5 D (D is shaft diameter) of the shaft is neglected in the Broms method for cohesive soils, so no additional depth should be neglected as may be recommended in the geotechnical report.

2. For the serviceability limit, use COM624P (LPILE) to estimate the lateral deflection of the drilled shaft. From the drilled shaft performance viewpoint and to be consistent with the strength limit with F.S of two, the authors of this report recommends a permissible lateral deflection of 1 inch at the head of the drilled shaft. Mr. Dick Osmun from Staff Bridge recommends limiting the deformation for signs and signals to the soil's elastic limit under repetitive loading estimated with LPILE to avoid accumulation of irrecoverable deformation with cyclic wind loads. Other suggestions for the permissible lateral deflection are presented in Chapter 8.

Note 1: In order to ensure accurate solutions from these design methods, appropriate geotechnical test methods must be used for obtaining soil parameters as described below.

Note 2: Consideration of possible loading rate effect, cyclic loading effect, ground water table fluctuations, and effect of lateral load induced moment on the soil resistance are addressed (Section 4.5).

The most accurate design method for drilled shafts is to conduct a load test on test shafts constructed as planned in the construction project. Chapter 7 provides a standard special note for

performing instrumented lateral load tests, which can be adopted by CDOT engineers or consultants in developing their design plans. Instrumented lateral load tests should be considered for CDOT projects that involve construction of a large number of drilled shafts or that have unique soil conditions at the construction site. Lateral load tests are performed for two general purposes: 1) to design production shafts with more confidence, resulting in large cost savings to the project, and 2) as research data to improve the accuracy of simple design methods for drilled shafts supporting sound walls and extract the resistance factor required in the LRFD method.

Finite element modeling should be considered in large or very critical projects with uncommon field and loading conditions. See Sections 2.1.3 and Chapter 6 for more on these methods (Florida Pier program and ABAQUS software). Chapter 6 demonstrated the modeling capabilities and versatility of ABAQUS software for specialized drilled shaft projects. For FEM based methods, the unload-reload soil moduli (or their average) of the pressuremeter tests should be used for interpretation of soil modulus.

9.1.2 Sound Barrier Walls: Justifications

Various existing methods for predicting ultimate capacity and deflection of drilled shafts supporting sound walls were evaluated in this study using data of hypothetical cases, a load test database carefully selected from literature and Ohio's test results, and two new lateral load tests performed in Colorado on sand and clayey soil sites as a part of this study. The methods include the Broms method, COM624P method, sheet piling method, caissons program, Brinch Hansen method, and NAVFAC DM-7 method. Conclusions and findings were:

1. For the compiled load tests, the Broms method and COM624P method provide safer and more accurate predictions than other methods, while others provided either inconsistent or unreliable estimates.
2. For the compiled load tests, the actual FS will be about 4 for test shafts in clays and from 2.6 to 6.2 for sands.
3. LRFD calibration of the compiled load tests suggested that FS of 2 for the Broms method is appropriate.
4. The Broms method yielded reasonable FS for the two load tests performed in this study.

5. For the compiled and new load tests, a permissible deflection of 1 inch was also found appropriate for both sand and clay sites from drilled shaft performance viewpoints, not from structural consideration of the shaft, which need to be checked to remain within acceptable design limits. The two new load tests suggest that the equivalent F.S. based on 1.0 inch permissible deflections would range between 2.4 and 4.8 for clayey site and 2.3 to 3.7 for the sand soil site.

6. For the compiled and new load tests, the COM 624P computer program is capable of predicting shaft deflection at the working load of 20 kips.

Other justification factors are:

- The Broms and p-y method are the methods preferred by the FHWA. The Broms method for cohesive and cohesionless soils is capable of considering several boundary conditions at the pile head (free and fixed) and can handle short and long piles.

- The prediction made by the NAVFAC DM7 method is very sensitive to the input of the subgrade soil reaction coefficient. At best, NAVFAC DM7 can only provide linear or elastic deflection predictions for lateral loads up to 1/3 of the ultimate lateral load. Thus, its use for predicting drilled shaft deflection is not recommended.

- Sheet piling method: the hand calculations are cumbersome. Applicable for short piles embedded in homogeneous cohesionless soils. Developed for sheet piles, which may exhibit different behavior from drilled shafts.

- Caisson program: The program cannot be run correctly for cohesive soil conditions.

9.1.3 Design Methods for Overhead Signs and Signals

Current CDOT practice for overhead signs and signals could continue. CDOT engineers have developed standard drawings for foundation design of overhead sign structures and traffic signals. The foundation design is based on fairly conservative assumed soil properties. The lateral capacity of the foundation is calculated using the Broms method, while torsional capacity is estimated by the CDOT in-house method. A factor of safety of 2.5 to 3 is adopted for the lateral load, while 1.25 to 1.5 is adopted for the torsional load to prevent torsion from controlling drilled shaft depths. CDOT engineers limit the deformation to be within elastic response (0.1 to 0.2 inch) to avoid accumulation of irrecoverable deformation with cyclic wind loads. CDOT engineers

have observed no failures or excessive deformations of the drilled shafts designed according to this approach.

Ideally, design of the drilled shaft for overhead signs and signals for lateral load should follow the same recommendation as the sound barrier walls, provided that CDOT engineers can accept more accurate method for torsional capacity analysis. This was not possible because of lack of sufficient quantity of credible torsional load test data. The limited number of torsional load tests suggests the torsional capacity may be over-estimated by the CDOT method. However, with overly conservative assumption of soil properties, in conjunction with relatively high F.S. for lateral loads and very low F.S. for torsional load, the CDOT approach may have a self-compensating mechanism that minimizes the effect of the overestimate of torsional capacity mentioned in the above. This could explain the fact that CDOT engineers have not observed any foundation failure in the past.

However, it is strongly recommended that additional research work be conducted to obtain reliable torsional load test data in Colorado so that a more accurate analysis method could be identified.

9.2 Recommendations for CDOT Geotechnical Engineers and Consultants

Ground water table elevation should be carefully identified in field geotechnical exploration work and the highest possible elevation of GWL should be estimated and used in the design. For clays, use saturated strength parameters under the water table and in-situ strength parameters for water above GWL. Appropriate p-y criteria for above and below the ground water table should be used in COM624P or LPILE analysis. The unit weight required by the Broms method could be obtained from laboratory test or SPT correlations. Tables 3.9 and 3.10 are recommended to estimate the k and ε_{50} for the COM624P (or LPILE) program.

9.2.1 Cohesive Soils

The most appropriate soil testing methods to determine the cohesive soil parameters required for the Broms and COM624P methods are:

- The triaxial CU test or direct shear test as described in Chapter 5 of this report. It is convenient to use the simpler direct shear test that could easily be performed in CDOT on a routine basis.

- The pressuremeter test with FHWA (1989) soil strength interpretation equation.

- The SPT method with Liang (2002) correlation charts, currently adopted by the Ohio DOT. These are presented in Tables 3.9 and 3.10, which also provide recommendations for all the other parameters required in the LPILE program.

- The CDOT procedure for estimation of strength and LPILE parameters based on SPT could be used but the results of this study indicates that it is very conservative (i.e., underestimates strength by 50%).

9.2.2 Cohesionless Soils

The most appropriate soil testing methods to determine the cohesionless soil parameters required for the Broms and COM624P methods are:

- The SPT with Liang (2002) correlation provides best soil strength interpretation.

- The Pressuremeter test would provide reasonable soil strength interpretation as well.

- The SPT with CDOT correlations methods just for strength parameters (Table 3.2) not for the parameters required in the LPILE program.

The lateral load test on the sandy soil deposit seems to suggest that direct shear test over-predicts the strength of the soil. In future load tests, a laboratory test using direct shear test apparatus needs to be conducted on the reconstituted sand specimens to the same density as the in-situ density.

9.3   Benefits

The research has resulted in the following benefits.

Based on the evaluation of the two Colorado lateral load test results for sound walls, the proposed design/analysis approach has shown to yield roughly 25% cost saving in both cohesive

and cohesionless soil deposits. This can be attributed to the recommended Broms method of analysis together with the reduced factor of safety requirement from 3 to 2.

A more uniform design method was put forward in this research report for designing drilled shaft foundations for sound barrier walls. This uniformity ensures that less man-hours are needed in deciding on analysis methods. The approach incorporates both strength limit based design and the serviceability based analysis, thus ensuring a more consistent design outcome with a comparable margin of safety from both the ultimate capacity and allowable deflection viewpoint.

The research has provided recommendations for proper geotechnical test methods to characterize pertinent soil parameters needed for both ultimate capacity prediction and p-y curve generation in COM624P or LPILE analyses. The recommended geotechnical test methods would allow CDOT engineers to economize resources in planning out soil testing programs, thus potentially saving costs as well.

The research has provided a standard instrumented lateral load test note in Chapter 7, which can be used by CDOT engineers to specify a lateral load test in the design/construction plans. For a project that involves construction of a large quantity of drilled shafts, or when unique soil conditions and complex loading combinations exist, the lateral load test prior to final design decision could potentially offer cost savings to the project.

10 REFERENCES

AASHTO, (1989, 1992) *"Guide Specifications for Structural Design of Sound Barriers"*, Washington, D.C.

AASHTO, (1994), *LRFD Bridge Design Specifications*, "Section-10: Drilled Shafts", Published by the American Association of State Highway and Transportation Officials (AASHTO), First Edition.

AASHTO (1998) LRFD *Bridge Design Specifications*, Second Edition.

AASHTO (2001), *"Standard Specifications for Structural Supports for Highway Signs, Luminaries and Traffic Signals,"* 4th Edition.

AASHTO, (2002) Interim - *"Guide Specifications for Structural Design of Sound Barriers"*, Washington, D.C.

AASHTO (2003) Interim - LRFD *Bridge Design Specifications*, Second Edition.

ABAQUS Standard User's Manual, Version 5.8, Hibbitt, Karlsson & Sorensen, Inc. 1998.

Barker, R.M., Duncan, J.M., Rojiani, K.B., Ooi, P.S.K., Tan, C.K., and Kim, S.G. (1991) "Manuals for the Design of Bridge Foundations," NCHRP Report 343, *Transportation Research Board*, National Research Council, Washington, DC.

Bhushan, K., Lee, L.J., and Grime, D.B. (1981) "Lateral Load Tests on Drilled Piers in Sand." *Drilled Piers and Caissons: Proceedings of a Session at the ASCE National Convention*, St Louis, MO, USA. Conference Code: 00225. P. 114-131.

Bhushan, K., and Askari, S. (1984) "Lateral-Load Tests on Drilled Pier Foundations for Solar Plant Heliostats." *Laterally Loaded Deep Foundations: Analysis and Performance*, ASTM STP 835, J.A. Langer, E.T. Mosley, and C. D. Thompson, Eds., ASTM, pp. 140-156.

Brinch Hansen, J. (1961). "The ultimate resistance of rigid piles against transversal forces." *Geoteknisk Institut.Bull.*, No.12, Copenhagen.

Broms, B.B.(1964a) "Lateral resistance of piles in cohesive soils" *Journal of the Soil Mechanics and Foundation Division*, Vol. 90, No. SM2, pp27-63.

Broms, B.B.(1964b) "Lateral resistance of piles in cohesionless soils" *Journal of the Soil Mechanics and Foundation Division*, Vol. 90, No. SM3, pp 123-157.

Carter, J.P., and Kulhawy, F.H., (1988) *Analysis and Design of Drilled Shaft Foundations Socketed into Rock*, Cornell University, Ithaca, New York.

Casagrande, A., and Shannon, W.L., (1948) "Strength of soils under dynamic loads," *Proceedings of the American Society of Civil Engineers*, ASCE, pp. 591-608.

Chow, Y. K., (1985) "Torsional Response of Piles in Non-Homogeneous Soil," *Journal of Geotechnical Engineering*, ASCE, Vol. 111, pp. 942-947.

Davidson, J.L., Hays, C.O., Jr., and Hagan, E.M., Jr., (1976) "Design of drilled shafts supporting highway signs", *Transportation Research Record*, issue 616, pp 62-66.

Dutt, R. N., (1976) *Torsional response of piles in sand*, Ph.D. thesis, Univ. of Houston, Texas.

FHWA (1989). "The Pressuremeter Test for Highway Applications" FHWA Publication No. FHWA-IP-89-008, Department of Transportation, Federal Highway Administration, McLean, VA 22101-2296, USA.

Guo, W.D., and Randolph, M.F., (1996) "Torsional Piles in Non-Homogeneous Media," *Computers and Geotechnics*, No. 19, pp. 265-287.

Hache, R.A.G., and Valsangker, A. J., (1988) "Torsional Resistance of Single Pile in Layered Soil," *Journal of Geotechnical Engineering*, ASCE, V. 114, pp. 216-220.

Hepworth and Jubenville, "Drilled Pier Foundations in Shale, Denver Colorado Area", *Drilled Piers and Caissons,* American Society of Civil Engineers, October 28, 1981, p. 68.

Kulhawy, F.H., and Chen. Y.-J., (1995) "A Thirty Year Perspective of Broms' Lateral Loading Models, as Applied to Drilled Shafts," *Bengt B. Broms Symposium on Geotechnical Engineering*, Singapore, pp. 225-240.

Lee, K. L., Seed, H. B., and Dunlop, P., (1969) "Effect of Transient Loading on the Strength of Sand," *Proceedings of the 7th International Conference on Soil Mechanics and Foundation Engineering*, Vol. 1, Mexico City, Mexico, pp. 239-247.

Lefebvre, Guy, and LeBoeuf, Denis, (1987) "Rate effects and cyclic loading of sensitive clays," *Journal of Geotechnical Engineering*, ASCE, Vol. 113, No. 5, pp 476-489.

Liang, R.Y. (1997) "Pressuremeter to Predict Lateral Load Capacity of Drilled Shafts on Slope," Final Report, FHWA/OH-97/005, ODOT.

Liang, R.Y., (2002) "Drilled Shaft Foundations for Noise Barrier Walls and Slope Stabilization," Final Report, FHWA/OH-2002/038, ODOT.

Lin, S.S., and AlKhaleefi, A.L. (1996) "Torsional Behavior of Cracked Reinforced Concrete Piles in Sand," *Journal of The Chinese Institute of Engineers*, Vol.19: (6), pp. 689-696.

Matasovic, N., and Vucetic, M. (1995) "Generalized cyclic-degradation-pore-pressure generation model for clays" *ASCE Journal of Geotechnical Engineering*, Vol. 121(1), pp: 33-42.

Menétrey, Ph. And Willam, K.J. (1995) "Triaxial failure criterion for concrete and its generalization." *ACI Structural Journal*, 92:311-18, May/June.

NAVFAC DM-7 (1971), Department of the Navy, Naval Facilities Engineering Command, "Design Manual – Soil Mechanics, Foundations and Earth Structures" .

Nowak, A.S., (1992) "Calibration of LRFD Bridge Design Code", NCHRP 12-33, Report prepared for National Cooperative Highway Research Program by Department of Civil Engineering, University of Michigan, Ann Arbor, MI.

O'Neill, Michael Wayne, (1964) "Determination of the Pile-Head, Torque-Twist Relationship for a Circular Pile Embedded in a Clay Soil," Master Thesis, The University of Texas at Austin.

Orchant, C. J., Kulhawy, F.H., and Trautmann, C.H. (1988) "Reliability-Based Foundation Design for Transmission Line Structures Volume 2: Critical Evaluation of In-Situ Test Methods, EL-5507 Final Report, Report prepared by Cornell University for the Electric Power Research Institute, Palo Alto, CA.

Poulos, Harry G. (1975) "Torsional Response of Piles," *Journal of the Geotechnical Engineering Division*, V. 101, GT10, pp. 1019-1035.

Poulos, H.G. (1982) "Single pile response to cyclic lateral load" *ASCE Journal of Geotechnical Engineering Div*, Vol. 108(GT3), pp: 355-375.

Randolph, M. F. (1981) "Piles Subjected to Torsion," *Journal of the Geotechnical Engineering Division*, American Society of Civil Engineers, Vol.107, issue 8, pp. 1095-1111.

Reese, L.C., and Matlock, H. (1956). "Non-dimensional solutions for laterally loaded piles with soil modulus proportional to depth." Proc., 8th Texas Conf. on soil Mech. and Found. Engrg., Austin, Tex.

Seed, H.B., and Lundgren, R., (1954) "Investigation of the Effect of Transient Loadings on the Strength and Deformation Characteristics of Saturated Sands." *Proceedings of the American Society of Civil Engineers*, Vol. 54, pp. 1288-1306.

Sheahan, T.C., Ladd, C.C., and Germaine, J.T., (1996) "Rate-dependent undrained shear behavior of saturated clay," *Journal of Geotechnical Engineering*, ASCE, Vol. 122, No. 2, pp 99-108.

Stoll, U. W. (1972) "Torque Shear Test of Cylindrical Friction Piles," *Civil Engineering*, ASCE, Vol. 42, pp.63-65.

Tawfiq, K. (2000) "Drilled shaft under torsional loading conditions", *Final report Federal Highway Administration*, Florida Department of Transportation.

Whitman, R.V., and Healy, K.A., "Shear Strength of Sands During Rapid Loading," *Journal of the Soil mechanics and Foundations Division*, ASCE, Vol. 88, No. SM2, PP. 99-132.

Yamamuro, J. A. and Lade, P. V., (1993) "Effects of strain rate on instability of granular soils," *Geotechnical Testing Journal*, GTJODJ, Vol. 16, No. 3, pp. 304-313..

Yasuhara, K. (1994) "Post cyclic undrained strength for cohesive soils" *ASCE Journal of Geotechnical Engineering*, Vol. 120(11), pp:1969-79.

APPENDICES

The appendices are only available in electronic format:

http://www.dot.state.co.us/Publications/PDFFiles/drilledshaft2.pdf

DRILLED SHAFT DESIGN FOR SOUND

BARRIER WALLS, SIGNS, AND SIGNALS

APPENDICES A - F

APPENDIX A

SURFICIAL SOILS AND BEDROCK OF COLORADO

AND GEOLOGIC OVERVIEW, WITH EMPHASIS

ON THE URBAN FRONT RANGE CORRIDOR

TABLE OF CONTENTS

1.0   INTRODUCTION

Over much of the state, Colorado surficial and shallow soils and bedrock are highly variable due to repeated episodes of mountain building, subsidence, igneous intrusion and extrusion, and glaciation. Within many provinces or trends, however, soil and bedrock character vary within definable limits due to similar geologic history, thus allowing for generalizations of their geotechnical properties. Emphasis in this report is on soil and bedrock conditions likely to affect structures rather than total geologic aspects.

This study concentrates on shallow subsurface conditions of soil and bedrock usually encountered for sound barrier walls, overhead signs, and similar structures along the Urban Front Range Corridor (the Corridor). For our purposes, the Corridor is defined by a combination of geologic/geomorphic and population/transportation factors. From west to east, it covers the far eastern portion of the Rocky Mountains Front Range, the Frontal Hogback, and the valleys and uplands divisions of the Great Plains Western Piedmont Sub-Province. It extends from approximately Fort Collins on the north, including the Greeley area, to Pueblo on the south, thus capturing the State's dominant population centers along Interstate 25. An outline of the statewide geological environment is also presented including a brief overview of soil and bedrock conditions along other (non-Front Range) important highway corridors.

2.0   SUMMARY OF SOIL AND BEDROCK CONDITIONS IN THE URBAN FRONT RANGE CORRIDOR

Soils and bedrock that exist along the Urban Front Range Corridor vary considerably as a result of the geologic processes that formed them. This section provides a brief overview of the soil and bedrock types often found in the Corridor and discusses engineering properties that may affect laterally loaded drilled shafts. More detailed geologic descriptions are presented in later sections of this report.

2.1   Soil Deposits

2.1.1   General Soil Types

Soils in the Corridor vary from clean sands and gravels to clays and silts. Sands and gravels are commonly encountered near existing and historic river channels including the South Platte River, Cherry Creek, Plum Creek, St. Vrain River, Cache la Poudre River, Arkansas River, and many others. Remains of previous valley floors or alluvial fans can be seen in gravel capped terraces in many areas. Alluvial clays and silts are also occasionally present within the river deposits, although the clay soils are much more common than silt soils. Silt is very often present as a minor constituent in alluvial sands and gravels. Eolian sands and clays are often located east of the major historic rivers, coinciding with the prevailing westerly winds. Sometimes these soils compress upon wetting and may require special design considerations. Significant thicknesses of residual surficial soils also exist in some areas, although to a lesser extent than alluvial and eolian deposits. Even less common are soils of colluvial (slope wash) origin which often contain the full range of soil types frequently mixed with bedrock fragments. Most sands and gravels typically encountered are rounded to subangular, and clays possess low to high plasticity. Due to the many geologic processes that created the soil deposits in the Corridor, significant variations in material types are common, often times over relatively short distances both horizontally and vertically.

Man-placed fill soils comprised of the full range of natural soil types, and sometimes bedrock fragments, are common along the Corridor. Cuts and fills are an inherent part of highway development and often have significant thicknesses at overpasses and in areas with moderate or greater topographic relief. Fill soils may also be found in old sanitary landfills, old aggregate pits, and in low lying areas that were raised for development to reduce the risk of flooding. In the case of sound barrier walls, berms are sometimes constructed to reduce the height of the wall so a nominal thickness of fill is typical to most sound barrier projects. Typically, fill soils have been placed under relatively controlled circumstances in recent decades, but there are exceptions. It remains CDOT practice to allow contractors to place construction debris within the right of way outside

of the roadway prism defined by a 1:1 outward slope from the edge of shoulder. These fills are typically uncontrolled.

2.1.2 Plasticity

Plasticity of fine grained soils in the Front Range Urban Corridor ranges from non-plastic to low plastic silts to very high plastic clays. Silt soils are not encountered very frequently. Most of the clays possess medium plasticity with plasticity indexes in the range of 15 to 30. Liquid limits are most often below 50, but higher liquid limits and plasticity indexes are occasionally observed. Liquid limits greater than about 70 are rare. Medium to high plasticity clays have the potential to be expansive when wetted. The swell potential depends on many factors including moisture content, dry unit weight, mineral composition, particle size gradation, and Atterberg Limits. Where swelling soils exist, it is likely that required caisson depths to resist uplift forces will control the design instead of lateral loading conditions. Of course, both conditions would need to be checked.

2.1.3 Moisture Content and Ground Water

Moisture contents of soils in the Corridor usually range from slightly moist to wet below the ground water table. Dry soils, defined for our purposes as not having visible moisture, are occasionally encountered. Saturated soils exist in areas of poor surface drainage, below the ground water elevation, and sometimes several feet above the ground water table due to capillary action in fine grained soils. Depths to ground water are highly variable, and localized perched water conditions frequently exist. Generally, however, the ground water table near permanent flowing water channels is likely to be at approximately the same level as the water surface. Ground water elevations rise further away from the river or creek and often correlate with the ground surface topography, but sometimes the ground water surface is highly variable.

2.1.4 Consistency or Density

The consistency and density of cohesive and cohesionless soils, respectively, also vary considerably. Cohesive soil consistency runs the gamut of the generally accepted

classifications from very soft to hard, and cohesionless soils also vary over the entire density range from very loose to very dense. Most cohesive soils encountered in the Corridor typically are medium (UC strength of 0.5 to 1.0 tsf or SPT of 4 to 8) to very stiff (UC of 2.0 to 4.0 tsf or SPT of 15 to 30). Consistency tends to vary inversely with moisture content; relatively dry cohesive soils are stiffer than soils with greater moisture. Most cohesionless soils range from medium dense (SPT of 10 to 30) to dense (SPT of 30 to 50).

2.1.5 General Distribution of Near Surface Geomaterials

The foregoing discussion categorizes soil types based on whether they are cohesive or cohesionless. In reality, many soils in Colorado do not fit neatly into one category or the other; they have cohesive and frictional components. It is assumed that most soils with greater than 70% passing the #200 sieve in Colorado will behave largely in a cohesive manner, and those with fewer than 30% fines will behave largely in a frictional manner. Estimated proportions of geomaterials likely to be encountered near the ground surface in the more populated areas of the Front Range Urban Corridor at sound barrier wall, overhead sign, or signal projects are presented in the Table A-1 to provide a general idea of the typical soil distribution. Silts are fine grained, but have little cohesion and are not commonly encountered in the Urban Corridor.

Table A-1

Material Type	USCS Symbols Included	Fines Content (%<#200)	Estimated Distribution (%)
Clay, silt	CL, CH, ML, MH	>65	20a
Sand, gravel	SW, SP, GW, GP, SC, SM, SW-SC, etc.	<35	20b
Intermediate soils	SC, SM, CL, CH, MH	35-65	60c

a. Silt soils are a minor percentage.

b. Gravel soils are a small percentage.

c. A majority (est. 75%) of these soils are clay.

d. Estimated total distribution of soils based on USCS criteria is 65% clay (and silt) and 35% sand (and gravel).

The research team was hesitant to provide estimated distributions in the above table because of the great difficulty in selecting and evaluating an appropriate data set. Consequently, these estimates are primarily based on representative values deemed reasonable by several local consulting and CDOT geotechnical engineers that provided their opinions. USGS maps (see references) were also reviewed. The values presented in the table should not be considered absolute, but are presented to provide a relative indication of the frequency of occurrence along the Corridor and to help identify which soil conditions should be targeted for future lateral load tests. A review of exploratory boring logs and laboratory data conducted for several CDOT and Geocal, Inc. projects indicated that the above estimated distributions are reasonable. It is important to bear in mind that any particular project could have several soil types, or it could have only one general type of soil. Therefore, it is critical that site specific subsurface investigations be conducted.

2.2   Bedrock

2.2.1   Generalized Distribution

Except for transitional zones where bedrock is very highly weathered, the interface between soil and bedrock is usually fairly well defined along the Corridor. A major unconformity (period of non-deposition and/or erosion) due to uplift along the mountain front has separated younger soil from older bedrock. Bedrock units in the Corridor are distributed into four major settings (arranged as younger to older for the age of their generally included units):

1. Early Tertiary (Paleocene) coarse sandstone and conglomerate units, the youngest bedrock, are primarily limited to the central part of the Corridor forming major exposures in the Monument Highlands.

2. For valleys and uplands of the Western Plains Piedmont (the dominant portion of the Corridor), upper Late Cretaceous sedimentary rocks are intermittently exposed through soil cover throughout the northern and

southern parts and comprise most of the bedrock likely to be encountered in foundations.

3. The mountain front belt includes a wide age range (Triassic to Pennsylvanian) of diverse sedimentary rocks that are exposed in a variably wide and locally intermittent band immediately east of the mountains. Jurassic to lower Late Cretaceous age shale and sandstone-dominant, tilted strata are intermittently well exposed along the narrow Frontal Hogback and as flatter lying outcrops in the Arkansas River valley near Pueblo.

4. Pre-Cambrian igneous and metamorphic rocks are exposed pervasively in mountainous areas along the west margin of the Corridor.

2.2.2   Common Bedrock Types within the Corridor

Most drilled shafts are likely to be constructed where upper Late Cretaceous sedimentary rocks exist (item 2 above) which includes most of the Denver metro area, Fort Collins, Greeley, Boulder, Colorado Springs, and Pueblo areas. Major bedrock units include the Denver, Arapahoe, & Lower Dawson Formations and the Laramie Formation, Fox Hills Sandstone, and Pierre Shale. Other bedrock types (items 1, 3, and 4 above) are discussed in Section 4 of this report.

2.2.2.1 Denver, Arapahoe, and Lower Dawson Formations

The Denver, Arapahoe, & Lower Dawson Formations encompass a broad, arc-shaped band sweeping from northern Denver around the Monument Highlands with the general arrangement being Denver Formation dominant to the north (under most of the Denver metropolitan area), Arapahoe Formation in the center, and Lower Dawson Arkose to the south (around Colorado Springs). These units, although sometimes separately mapped, are largely age equivalent and interfinger with each other over long distances.

The Denver Formation mostly consists of claystone/shale, over most of the Denver area, with thinner interbeds of siltstone, weakly to well cemented sandstone, and infrequent conglomerate. Claystone/shale, as well as tuffaceous sandstone, are well noted for having major vertical and horizontal zones with high to very high swell potential; non-

sandy claystone is frequently highly plastic when saturated. Claystone clays and ash-derived sandstone clays are montmorillonite rich (frequently termed "bentonitic") often including seams of nearly pure bentonite. Where unweathered, the formation includes a blue-green-gray claystone (and sandstone in some areas) locally known as the "Denver Blue". The "Denver Blue's" upper surface is not a stratigraphic horizon, but rather an irregular weathering/alteration zone that is often transitional. The bluish color has been observed to change to a predominantly grayish color after exposure to air.

The Arapahoe Formation is generally coarser than the Denver Formation. The two are frequently mapped as Denver-Arapahoe Undifferentiated in the Denver area. The formation is generally described as well stratified, interbedded claystone/shale, siltstone, sandstone, and conglomerate. A well-developed lower Arapahoe conglomerate is frequently only weakly cemented and is a significant aquifer. Conglomerate and sandstone units have variable low to moderate swell potential; siltstone and claystone/shale have moderate to high swell potential.

Lower Dawson Arkose also tends to be well interbedded with layers of conglomerate, coarse sandstone, shale, and silty fine sandy shale (termed "mudstone"). The coarser units usually have moderately well graded quartz and feldspar sands with granitic pebbles ("arkose"); local coal beds are noted. Clay rich and clay-dominant zones have moderate to very high swell potential and moderate to high plasticity, particularly in the Austin Bluffs area north of Colorado Springs.

2.2.2.2 Laramie Formation, Fox Hills Sandstone, and Pierre Shale

Laramie Formation, Fox Hills Sandstone, and Pierre Shale formations occur in two broad situations: (1) intermittently exposed in moderately dipping beds east of the mountain front (immediately east of the Frontal Hogback) from Ft. Collins to Denver and (2) with thin soil mantles in gently dipping and near flat lying units in the Louisville area and along Interstate 25 between Colorado Springs and Pueblo.

The Laramie Formation is dominated by thinly bedded shale and siltstone with common hard to friable sandstone interbeds, lesser thin hard conglomerate, and lignitic to sub-bituminous coal beds. The formation is sandier in the lower portion. Most Laramie clays are dominantly kaolinitic with usually low to moderate swell potential; the middle third tends to be montmorillonitic with resulting high swell potential. Sandstones vary from weakly to well cemented.

Foxhills Sandstone units are cross-bedded and quartz sand-dominant. Relatively thin interbeds of claystone/shale, mudstone, and coal occur throughout. The sands are generally weakly cemented and friable; they are important aquifers with medium to high permeability, particularly north of Denver.

The Pierre Shale is a very thick, claystone/shale-dominant formation with numerous thin bentonite beds throughout. The bedrock units are almost always suspect for moderate to very high swell potential, medium to high plasticity, and low slope stability nearly everywhere they are encountered along the Corridor. Thin sandstone interbeds occur throughout the formation. Significantly thick sandstone members are present in several areas at different stratigraphic positions. Hard limestone masses (butte formers in outcrop) occur in the middle portion to the south. To the south, the middle portion also contains appreciable gypsum content that may affect sulfate-susceptible cement.

2.2.3 Depth to Bedrock

Depths to the most common bedrock units are highly variable and depend on geologic processes that have occurred in an area and sometimes man's activities in the form of cut/fill operations. There is a large area of near surface bedrock in the Monument Highlands between southern Denver and northern Colorado Springs. Bedrock predominates the near surface geomaterials closer to the Rocky Mountain Front Range at the western edge of the Urban Front Range Corridor. In other areas of the Corridor, bedrock may exist near the surface or could be much deeper beneath alluvial deposits,

sometimes in the range of 80 to 100 feet. Generally, however, bedrock is likely to be encountered within the upper 50 feet of geomaterials at most sites. Bedrock is intermittently located within the upper few feet in many areas of the overall Corridor.

An estimated percentage of surficial geomaterials likely to be comprised of bedrock at a sound barrier, sign, or signal project in populated areas along the Corridor is on the order of 10 to 15 percent. Even within the population centers of the Corridor, bedrock occurs much more frequently than 15 percent of the projects when the total length of typical sound barrier, overhead sign, and traffic signal caisson depths is considered. It is important to note that the upper portion of geomaterials along a caisson provides the greatest resistance to lateral loads, although this is a function of pier diameter. Overhead sign foundations have the greatest depths because of the loading conditions on this type of structure, with typical depths in the range of 17 to 24 feet according to CDOT standard plans. Bedrock is very often encountered within the upper 25 feet; however, depths to bedrock are highly variable as discussed above.

2.2.4 Bedrock Hardness

The most common bedrock types in the Corridor, discussed in Section 2.2.2, are sedimentary deposits that have been heavily overconsolidated by as much as 1,000 feet of overburden that was subsequently eroded to the present day terrain. The previous overburden pressure, degree of weathering, and amount of cementation of sandstone or conglomerate, are the key factors that largely determine the hardness of the bedrock. Unconsolidated, undrained shear strengths in the Denver Formation range from 3 ksf to 30 ksf, and shear strengths in the Denver Blue range from 8 ksf to more than 30 ksf (Hepworth & Jubenville, 1981). Standard penetration test results generally range from about 30 to 80 for the non-Denver Blue bedrock, although some highly weathered areas may have SPT values in the teens. Denver Blue bedrock normally has SPT blow counts of at least 80. Denver Blue claystone/sandstone bedrock typically has blow count values in the range of 50/8" to 50/2", and sometimes this is the first 6 inches of a drive that would normally not be recorded for a SPT. SPT refusal also occurs. Bedrock hardness varies from very low strength to moderate strength according to International Society of

Rock Mechanics classification criteria. The weaker bedrock is better described in terms of soil consistency terminology in the range of very stiff to hard and tends to behave similar to heavily overconsolidated clay.

Another CDOT study currently underway dealing with axial drilled shaft capacity has yielded some useful data on the bedrock strength of the metro Denver area. As part of this study, Osterberg load cell tests (O-cell), pressure meter testing, and coring with subsequent unconfined compression testing was performed on the weaker brown claystones and the harder, gray "Denver Blue" claystone/sandstone. O-cell tests at two sites with relatively weak bedrock (SPT ranging from about 30 to 60) indicated ultimate caisson end bearing values on the order of 50 ksf, and three O-cell tests in the much harder bedrock indicate ultimate end bearing values of greater than about 250 ksf. Pressure meter tests conducted indicated unconfined strengths in the general range of 10 ksf to 20 ksf for the weaker bedrock and 50 ksf to greater than 150 ksf for the harder bedrock. Unconfined compression (UC) tests on the weaker bedrock generally ranged from 5 ksf to 20 ksf. UC tests on the relatively hard bedrock indicated strengths ranging from 50 ksf to 300 ksf; the higher values are from well cemented, clayey sandstone bedrock.

3.0   STATE-WIDE GEOLOGY SUMMARY

Colorado is situated across three continental-scale geologic and geomorphic provinces, each with remarkably different history and conditions and all with important subdivisions. They roughly divide the state into north-south trending thirds. From east to west they include: (1) The gently structured western margin of the Great Plains including the broad Colorado Piedmont gently sloping east from the Front Range, (2) complexly structured multiple major mountain ranges of the Central Rocky Mountains including significant intermountain valleys, and (3) intermediately structured uplifts and downwarps of the Western Plateaus. For brevity, the following paragraphs in this summary concentrate on present day conditions, especially as related to soil and bedrock distribution, rather than details of geologic history and structure. A simplified guide comparing relative geologic ages to absolute time and common formations is shown on the Colorado Geological

Survey publication "Colorado Geologic Highway Map" included in the envelope at the end of this report.

3.1   Western Great Plains

Colorado's geologic share of the Great Plains is basically a broad, stable shelf floored by an unexposed metamorphic "basement" and a relatively uniform layer of Paleozoic through Early Mesozoic clastic (transported particles, *e.g.,* sandstone, siltstone, & claystone/shale) and carbonate (limy precipitates and particles, *e.g.,* limestone & dolomite) sedimentary rocks. The later have only limited exposure in the southeast corner of the state and along a narrow mountain front band immediately east of the Front Range. The shelf is gently deformed as a relatively wide, deep trough paralleling the Front Range (the Denver and Raton Basins) that has preserved a thick accumulation of Cretaceous age claystone/shale-dominant sedimentary rocks with significant sandstone, and much lesser limestone, members. Older portions of these Cretaceous units extend more thinly eastward into Kansas. Cretaceous rocks have major surface exposures or form relatively shallow bedrock along the Front Range Urban Corridor (as detailed in Section 4.2) and along all of Interstate 25, along the broad valleys of the Platte River (Interstate 76 & U.S. 36) and Arkansas River (U.S. 50), high plains drainage basins such as Big Sandy Creek (portions of Interstate 70, U.S. 40 & 287), and the Chaquaqua Plateau (greater Las Animas County area). The Paleozoic through Cretaceous strata are flat lying to very gently dipping throughout the province except for being steeply upturned along the mountain front of the Front Range and moderately folded and faulted in structures of the Canon City embayment west of Pueblo (U.S. 50).

Cretaceous rocks are mantled by a wide range of variably thin to thick Quaternary age alluvial (water transported) soils in the flood plains and terraces of river valleys and major tributaries. They are also commonly overlaid by broad, relatively thin sheets of unconsolidated eolian (wind born) deposits on many upland surfaces between the Platte and Arkansas Rivers. These uplands (or "high plains", particularly in the northeast, far east, and southeast parts of the state) also include significant mantles of Middle to Late

Tertiary clay, sand, and gravel that are variable loose (soil) to well cemented (bedrock) as typified by the Pawnee Buttes and high terraces along the Platte River near Sterling.

3.2 Central Rocky Mountains

This rugged belt includes numerous major ranges (*e.g.,* the Front Range, Sangre de Cristo Mountains, Mosquito Range, Sawatch Range, and Elk Mountains) of tremendous geologic complexity due to a history of repeated regional mountain building oscillations from the Early Pre-Cambrian to today. They nonetheless have some broad commonalties. The cores of the ranges consist of deeply rooted older Pre-Cambrian age metamorphic material derived from intermediately to highly altered, preexisting sedimentary and igneous rocks (now quartzite, schist, gneiss, and mixed-type migmatites). Except for the less altered quartzite, most have moderately to well developed foliation (preferred alignment of mineral constituents with resulting planes of relative weakness). The metamorphic complexes are widely intruded by younger Pre-Cambrian plutonic igneous rocks of mostly granitic composition. Some of the intrusions (*i.e.,* the Pikes Peak Batholith west of Colorado Springs) are so large as to dominate much of a range leaving only smaller metamorphic remnants exposed. The granitic rocks tend to be massive (non-foliated). Both the metamorphics and granitics tend to be pervasively fractured with multiple intersecting joint sets. Both small and major faults are common; a few, particularly in Summit-Lake Counties and along the west side of the Sangre de Cristo Mountains have been active in the Quaternary Period. The granitic masses are noted for weathering deeply on gentle to intermediate slopes and where well fractured, forming granular and porous residuum and colluvium. Transportation corridors crossing Pre-Cambrian-dominated bedrock include Interstate 70 from just west of Golden to near Dillon, U.S. 50 from west of Canon City to near Coaldale, and U.S. 50 over Monarch Pass.

During periods of uplift of the Rocky Mountain ranges, large amounts of sediments, particularly coarse clastics, were shed onto adjacent lowlands. When erosion or tectonic sagging lowered the mountains, marine incursion resulted in thick finer clastic and carbonate deposits. Substantial remnants of these Paleozoic through lower Early

Cretaceous sedimentary rocks are preserved in fault blocks within the mountains and on their flanks. These are frequently steeply dipping, highly faulted, and occasionally highly folded. These remnants tend to be to be aligned in narrow, north-south trending bands. Example areas include: (1) The S.H 9 corridor from the Blue River Valley and Kremmling on the north, through Dillon and Breckenridge, to Fairplay on the south, (2) S.H. 160 over La Vita Pass, (3) S.H. 50 from Coaldale to near Salida, and (4) along Interstate 70 in the greater Vail area. Depressions in the foundering surface of the ancestral Rockies created some enclosed basins that promoted relatively thick evaporite deposits (calcium sulfate/gypsum in particular). These evaporite-rich sediments are unstable, tend to flow under pressure, and create highly contorted zones where overlaid by, or interbedded with, clastic and carbonate rocks (as exemplified by Pennsylvanian age interbedded units along Interstate 70- in the Eagle Valley between Eagle and Dotsero). They are also soluble and may cause sinkholes to develop.

Superimposed on the Pre-Cambrian ranges and Paleozoic-Cretaceous remnants are several relatively flat lying Tertiary age volcanic fields with thick, layered deposits of tuff (hardened ash) and andesitic lava. The lava is often very resistant to erosion resulting in, for example, the Rabbit Ears Range (U.S. 40 southeast of Steamboat Springs). Less resistant tuff exist in the floors of some valley areas such as much of South Park (S.H. 9 south of Hartsel). Well-faulted and folded Early Tertiary conglomerate, sandstone, and coaly shale units mantle older rocks in a large area of North Park and the Rabbit Ears Range (U.S. 40 and S.H. 9).

3.3   Western Plateaus

West of the Central Rocky Mountains, a series of gently to moderately structured geologic basins and uplifts are broadly termed the Plateau Province due to the frequently high, similar elevation of much of the surface. This surface is occasionally punctuated with relatively more complex mountains that are more localized than the Rocky Mountain ranges. Features of this province (generally from north to south) include the following the following major subdivisions:

Sand Wash Basin in the northwest corner of the state (including the U.S. 40 corridor west of Craig) is dominated in the surface and shallow subsurface by thick sequences of mixed clastic sedimentary rocks ranging from conglomerate to claystone/shale including oil shale and some coal. The basin tends to be rimmed with Cretaceous shale-dominant units that include significant sandstone members, major coal beds, and swell-prone claystone/shale portions (U.S. 40 between Steamboat Springs and Craig). The large Piceance Basin to the south is situated between S.H. 64 west of Meeker and S.H. 92 north of Delta and including the Interstate 70 corridor from Glenwood Springs to Grand Junction. It has a very similar sequence of Tertiary sedimentary rocks ringed by Jurassic-Cretaceous sedimentary units. The narrow Grand Hogback on the east side includes major ridge-forming sandstone units as well as thick coal deposits (*e.g.,* the Newcastle area along Interstate 70 between Glenwood Springs and Rifle). The west and southwest sides of the Piceance Basin are defined respectively by the uplifts of Douglas Creek Arch (along S.H. 139, Grand Junction to Rangely) and Uncompahgre Plateau (Southwest of Interstate 70 at Grand Junction). These uplifted flanks have created some of the most extensive Cretaceous sedimentary rock exposures in the state.

The Uncompahgre Plateau, centered in Montrose County, was created by gentle arching of Pre-Cambrian granitic rocks that have limited exposure along the crest (*e.g.,* along S.H. 114 between Whitewater and Gateway). Deep incisions of the uplift have created striking cliff exposures of the thick mantling and very resistant red-brown Triassic age sandstone, siltstone, and shale. Less resistant Jurassic to Cretaceous mixed clastic rocks cover most of the flanks of uplift.

The southwestern portion of the state includes portions of two major and remarkably different basins (Paradox and San Juan Basins) separated by the Colorado Plateau (that sometimes gives its name to the entire Western Plateaus Province). The Paradox Basin contains a series of large, well-defined folds trending northwest-southeast with unique "reversed topography": the anticlinal (upwards) folds tend to be valleys due to evaporite dissolution while the synclinal (downward) folds are higher. The basin is composed of thick sections of Permian to Pennsylvanian age arkosic sandstone-conglomerate, shale,

limestone, and evaporities (salt, gypsum, potash, etc.). The evaporities have tended to flow towards the basin center to form large unstable masses less dense than the surrounding rock. Paradox Valley along S.H. 90 (centering at Redrocks) is an example of a trend with salt at and near the surface. Portions of the folds and basin flanks have Triassic-Permian cliffs of very hard siltstone and sandstone (same as the Uncompahgre Uplift) as well as thick Cretaceous shale (including bentonitic layers) and sandstone units (as along U.S. 141 from Placerville to Uravan).

Rocks of the Colorado Plateau are very gently structured and deeply incised by the west-flowing Dolores River and major tributaries. Triassic age cliff-forming conglomerate (limestone pebble), sandstone, siltstone, and shale are exposed in deeper canyons. They are thickly mantled by Cretaceous shale, calcic shale, and resistant sandstone units (including the cliffhouse ledges at Mesa Verde National Park). The area along U.S. 160 from Mancos to Cortez typifies much of the Plateau. Thick eolian (wind born) sandy soil has developed in large patchy areas along U.S. 160 from Northdale to Cortez.

The San Juan Basin extends south from Durango (*e.g.,* along U.S. 550 and S.H. 511) into New Mexico. The northern upturned rim (Pagosa Springs to Durango, U.S. 160) exposes the same Cretaceous clastic units as the Colorado Plateau in alternating sandstone hogbacks and shale valleys. The main, very gently south sloping basin has thick Tertiary arkosic sandstone/conglomerate, volcaniclastic (volcanic particles) sandstone/conglomerate, and shale exposed at the surface.

There are two major sub-provinces in the southwest quarter of the state that are geologically separate from the Central Rockies and Western Plateaus that surround them: The Needle Mountains/San Juan Mountains and the San Luis Valley. The Needle Mountains are cored by an uplifted, intensely faulted complex of metamorphosed volcanic-sedimentary rocks intruded by large gabbroic (ferro-magnesium rich) intrusive masses. This complex is surrounded by thick, well-structured layers of Permian-Pennsylvanian age arkosic sandstone/conglomerate, siltstone, shale and lesser limestone, and Mississippian limestone-dolomite. U.S. 550 from Hermosa to Silverton cuts through

the center of the area. The adjacent San Juan Mountains are deeply underlain by Cretaceous sedimentary rocks, but owe their existence to widespread Tertiary volcanic flows of varying rhyolite-andesite-basalt composition. These hard, resistant units tend to be well-fractured (often well-jointed in columnar patterns) and vuggy. They are interbedded with frequently thick, less resistant ash, tuff (granular volcanics), and inter-flow conglomerates (frequently water bearing). The entire San Juan Volcanic Field is well-faulted and flows are frequently cut by intrusive dikes of rhyolitic-andesitic composition. The flows vary from flat lying to moderately dipping except for large, circular areas of volcanic collapse/explosion that are highly structured (called caldara, as with the Silverton, Lake City, and Creede mining districts). Slopes at higher elevations contain thick soil deposits of glacial drift and down-slope colluvium; both tend to be relatively well-graded and commonly contain unweathered boulders. Transportation corridors crossing the volcanics include U.S. 160 (Pagosa Springs to Del Norte, including Wolf Creek Pass), S.H. 149 (South Fork to Lake City), and U.S. 550 (Silverton to Ouray).

The San Luis Valley is a major geologic basin with thick unconsolidated sediments covering most of the valley floor (as U.S. 285 and S.H. 17 south of Villa Grove to Antinito and U.S. 160 from Ft. Garland to Monte Vista). These include some of the oldest soils in the state ranging in age from Tertiary through Holocene and are composed of mixed alluvial gravel, sand, and silt as well as eolian sand (the most noteworthy deposits being Holocene age dunes at Great Sand Dunes National Monument). The valley is frequently rimmed with coarser Pleistocene gravel-dominated alluvial deposits including sand, silt, and clay interbeds; west and south side gravels contain abundant volcanic clasts and ashy clays. The southeast side of the valley (U.S. 16 east of Ft. Garland) has Tertiary age conglomerate, sandstone, and siltstone exposed on faulted terraces. These sediments were derived from the east-adjacent Sangre de Cristo Mountains and include small boulders.

4.0   FRONT RANGE URBAN CORRIDOR SUBSURFACE CONDITIONS

Soils and bedrock of the Front Range Urban Corridor (defined in Section 1.0) are the focus of this section. Emphasis on the Corridor is made because a large percentage of sound barrier, overhead sign, and signal projects occur in this region of the state. Whereas Sections 2.0 and 3.0 presented a general overview of the distribution of soils and bedrock, basic engineering characteristics of the typical deposits, and a statewide geology synopsis, this section provides more descriptive geology characteristics and geographic distribution of the various geomaterials in the Corridor.

4.1 SOILS OF THE CORRIDOR

4.1.1   Stratigraphic Relationships

Unconsolidated materials were deposited and later modified under a relatively limited group of conditions along the Corridor during Pleistocene to Holocene time. Except for the greater output of coarse sediment and water flow during intermittent periods of Pleistocene glacial melting, the depositional settings were very similar to those of today. These conditions were related to each area's distance from the mountain front, position along or between streams that cut into the pediment (sloping bedrock surface), and the steepness of the slope. Bedrock exposure in the uplifted mountain front of Front Range igneous and metamorphic rocks and Frontal Hogback sedimentary rocks has been a feature of the Corridor since early Pleistocene time. They have supplied clastic debris in a variety of environments that resulted in today's soil cover. These depositional and non-depositional (weathering) environments and their related processes have been active throughout this period with some being more dominant than others depending on whether the process occurred during a glacial or an inter-glacial period.

Along the Corridor, these soils have been generically grouped and mapped according to relative age, constituents, and interpreted depositional environment of the material. The larger portion are generally named "alluvium" (dominantly water-borne mixed sediments) and identified with a name whose area typifies the group as a whole. Flood plain (river

and stream channels, overbanks, and areas within stream meanders including very low terraces) alluvium was deposited along rivers and larger tributary stream valleys (<u>Post-Piney Creek</u> and <u>Piney Creek Alluvium</u>). Terrace alluvium resulted from slightly older mixed deposits having been cut through by the streams with progressively older benches occupying progressively higher positions above the streams (<u>Piney Creek, Broadway, and Louviers Alluvium</u>).

Between areas of the active stream influence, the pediment uplands are mantled by still older mixed environment deposits (streams, alluvial fans, soil creep, etc.) that have been subject to longer periods of limited deposition or non-deposition, less focused erosion, and more diagenetic (post-depositional) chemical change (<u>Slocum, Verdos, Rocky Flats, and Nussbaum Alluvium</u>).

It is also recognized that, since depositional environments extend through geologic time, some non-alluvial groups are time transitional resulting in one group extending through the time range of other groups. This is common in dominantly wind born deposits (<u>Eolian Sand and Loess</u>) and soils resulting from a combination of gravity and slower water flow (particularly, slope wash <u>Colluvium</u>). Gravity dominant processes have resulted in geologically instantaneous and areally restricted soil bodies (<u>Landslide and Talus Deposits</u>) along some very steep slopes.

4.1.2   Generalized Distribution
Except for the complex rolling uplands of the Monument Highlands (where Tertiary bedrock outcrops are dominant over a large area), the overall north-south distribution of soil along the Corridor is similar. Relatively unweathered flood plain, terrace, and pediment alluvium deposits are common east of the Frontal Hogback although thicknesses of the groups vary considerably depending on distance from the original stream valleys (many of which closely parallel modern stream flood plains). Variably unweathered to slightly weathered wind born deposits are spotty over wide areas and are commonly pervasive and thick east of major streams and rivers. Gently sloping upland surfaces between stream valleys are commonly mantled by pediment alluvium that is

weathered proportional to its age and that frequently has characteristics strongly influenced by bedrock source material. Steeper slopes, including the east face of the Frontal Hogback and narrow valleys west of the Hogback, are commonly covered with unweathered to moderately weathered slope wash colluvium with material derived from, and strongly influenced by, near upslope bedrock and soil. Colluvial, alluvial, and mass wasting/gravity deposits in the mountainous areas are generally scattered and thin over metamorphic bedrock; colluvium/residuum is common and occasionally thick over granitic-type bedrock.

A common situation along the corridor is, within the distance of a mile or two, to have very young flood plain alluvium near valley center, progressively older alluvial terraces on the valley slopes, further older pediment alluvium capped by eolian material on the adjacent uplands, and colluvial slope wash grading from one to another. In some areas, terrace deposits underlie flood plain soils where the present day stream has not cut into the older deposits. Age ranges for the groups vary along the Corridor; for simplification, the following sections use the most commonly reported ages in the greater Denver area (north central portion of the Corridor).

4.1.3 Major Soil Groups, Largely Age Sequential

4.1.3.1 Lower Level, Flood Plain Alluvium

Post-Piney Creek Alluvium (Late Holocene): These deposits are generally centered along major drainages and larger tributaries, including very low terraces, and are characterized by moderately to well stratified (layered and interbedded) sand, silt, and clay with minor small gravel. The accumulations are noted as commonly having zones of humic bog clay, partiqularly in the upper portions. Thicknesses of 3 to 10 feet are most common. Permeability is usually poor to moderate. Water tables are frequently high, especially in the spring and early summer. Stability of shallow foundations has been reported in the literature as generally fair to good except for being very poor to poor in organic-rich clay zones.

Piney Creek Alluvium (Early to Middle Holocene): This unit is found in the bottoms of most valleys and tributaries and as low level terraces; with well stratified sand, silt, and clay having interbedded sandy (and sometimes clayey) small to medium gravel, particularly in the basal portions. The upper part is frequently finer and more humic than the lower; lower level gravels occasionally contain cobbles and small boulders, particularly when closer to the mountain front or along rivers and larger streams. The coarser fractions tend to be unweathered. These sediments commonly extend under younger Post-Piney Creek material. Thicknesses commonly range from 5 to 20 feet. Permeabilities are usually moderate in sand and gravel-rich sections and poor elsewhere. Water tables tend to be high in the lower valleys and deeper in upper tributaries and terraces. Clay swell potential is usually considered as low, but may grade to moderate in non-sandy clay zones. Foundation stability is generally poor in areas with significant clay and humic content and good in coarser deposits.

4.1.3.2 Upper Level, Terrace Alluvium

Broadway Alluvium (Late Pleistocene): This material was deposited in multiple stream, terrace, and slope environments and is usually found today on frequently well defined, intermediate-level terraces above rivers and major tributaries. These are generally well stratified, lightly weathered sand and coarser gravel accumulations with silty interbeds. The entire group tends to be more clayey and silty (and humic north of Denver) in its upper portion. Clayey gravel zones are developed at the base in some areas, which occasionally include sound (unweathered) cobble-size material. Very bouldery and cobbly gravels are noteworthy along Monument and Fountain Creeks in the Colorado Springs area. Thickness is commonly in the 8 to 25 foot range with moderate to high permeability except in more silty and clay-rich zones. Water tables are usually intermediate to lower with frequently high yields in wells. Foundation stability is generally considered good.

In areas of lower rainfall and low water table, dry and silt-rich areas of Broadway and Piney Creek Alluvium have been found to exhibit variably slight to marked tendencies

for subsurface piping and the formation of shallow cavities. These areas tend to collapse and create small to moderate sized depressions and sinkholes up to 15 feet deep. Settlement is greatest and most common in areas of very intermittent storm water runoff and is accelerated by man-caused interruptions to the natural drainage process (creating standing water). Areas particularly prone to such collapse include portions of the I-25 corridor between Colorado Springs and Pueblo and along U.S. 50 near Pueblo. This condition may have potential for post-construction instability in otherwise stable soils.

Louviers Alluvium (Middle to Late Pleistocene): Louviers Alluvium is found mostly on higher level terrace remnants and often extends onto upland surfaces as pediment remnants frequently having a strong colluvium aspect. The group is typified by being coarse sand-dominant with common cobble gravels. Soils of the group tend to be more cobbley and contain a few boulders in deposits closer to the mountain front. Similar to the younger Broadway Alluvium, bouldery cobbley gravels are common along Monument and Fountain Creeks. Weathering tends to be light to moderate with some oxide cementation locally common; cobbles and boulders tend to be sound. Thicknesses most commonly range up to 10 to 15 feet, although they locally may be as much as 35 feet. Permeablities are usually high to very high if cementation is absent. Water tables are usually intermediate to lower; flows may be high. Soils of the group are generally considered to have high foundation stability.

4.1.3.3 Upland Surfaces, Pediment Alluvium

Slocum Alluvium (Middle Pleistocene): These predominantly stream and alluvial fan-deposited soils are positioned on dissected pediments and often contain material derived from underlying and nearby bedrock. They are commonly eroded on their upper surface substantially from original maximum thickness. This erosion has resulted in the most common thickness ranging up to 6 to 15 feet with local, un-eroded areas having as much as 40 feet of accumulation. Deposits are frequently laterally extensive. The group is usually composed of well-stratified pebble clay, silt, sand, and gravel with a few cobbles and boulders. Locally, the group includes significant zones of coarse sand and gravel

with common large cobbles and small boulders; such units may be silty in the upper portion. Soils in this group are frequently moderately to well weathered with some of the gravel through boulder component no longer sound. These coarser fractions are commonly calcium carbonate coated. Zones with a thick calcareous silt component are noted in the southern end of the Corridor. Permeabilities are usually high in uncemented sand and gravel intervals and low elsewhere. Foundation stability is usually considered good except for the moderate swell potential of some very clayey or silty intervals or where the expansive bedrock claystone fragments make up a significant portion of the gravels. Water tables tend to be highly variable.

In many areas, the Slocum Alluvium, particularly in the upper portion, contains 1 to 3 feet thick, wide-spread, calcium carbonate-enriched layers interpreted to represent paleosols (relict or "fossil" soil surface weathering horizons). The constituents are cemented to bedrock-like hardness. This hardness is particularly noteworthy where the cementation occurs in cobble-boulder interbeds. This has created conditions where the vertical soil profile goes from soft, through hard to very hard ("false bedrock"), then back into relatively soft to intermediate material. This same condition of well-developed paleosols is also common in the Verdos and Rocky Flats Alluvium.

Verdos Alluvium (Lower to Middle Pleistocene): These more diverse alluvial deposits are typically found on dissected pediment surfaces above the Slocum Alluvium and have frequent wide areal extent. They are typified by (1) poorly stratified gravel with clay to sand lenses locally common, (2) interbedded gravel to cobbley gravel and silty pebbly sand, or (3) sandy coarse gravel with cobbles and small boulders. The entire formation tends to be more silty and/or clayey in the upper portion. Calcareous silt is common throughout these soils in the southern portion of the Corridor. Local thin volcanic ash beds are noted, particularly in the north central portion of the Corridor. Like the Slocum Alluvium, the upper Verdos surface has commonly been eroded. Thickness ranges up to 20 feet except for some un-eroded areas with up to 40 feet present. Hard, calcareous-cemented paleosol layers are noted in the upper portion, very similar to those in the

<u>Slocum Alluvium</u>. Permeabilities are usually high in cleaner, uncemented sand and gravel and low elsewhere. Foundation stability is usually fair to good except for being poor to fair in the more clayey zones where weathered clays exhibit moderate swell potential. The more ashy layers may be suspected of having relatively high plasticity. Water tables tend to be highly variable.

<u>Rocky Flats Alluvium</u> (Later Early Pleistocene): These coarsely granular, near mountain front deposits attain significant thickness (averaging approximately 15 feet) and areal extent only in the Highway 93 area of the north central Corridor between Boulder and Golden. They are composed of poorly graded bouldery, cobbley, sandy gravel (likely of alluvial fan origin) and commonly calcium carbonate-enriched and sometimes moderately cemented. Many of the included stones are moderately to well weathered and unsound.

<u>Nussbaum Alluvium</u> (Early Pleistocene): These uppermost pediment soils are likely alluvial fan remnants that occupy only small scattered sites along the mountain front and around isolated topographic highs from Denver to just south of Colorado Springs. They have a similar composition and character to <u>Rocky Flats Alluvium</u> and are in the 8 to 15 feet thick range.

Up to 100 feet thick deposits of age-equivalent pebble gravel have been mapped over an extensive area on Baculite Mesa northeast of Pueblo, however the area is well way from immediate highways or significant population. Geotechnical characteristics for this unusually thick soil have not been found to be described in the literature.

4.1.4 Major Soil Groups, Largely Transitional

Because of the nature of their deposition, several types of soil accumulations (other than the previously described alluvial deposits) were often laid down in multiple environments and over a range of older soils.

4.1.4.1 Eolian Sand (Holocene to Late Pleistocene)

These sand soils were transported by wind and tend to be thickest east of rivers and major stream tributaries. They are most common on lower upland surfaces. The sands, and their downwind <u>Loess</u> equivalents, are particularly common in the Greater Denver and Longmont-Loveland-Greeley areas and east of the I-25 corridor between Colorado Springs and Pueblo. The soils are dominated by very fine to medium grained quartz sand and zones of sandy silt or sandy clay (particularly near the eastern margins). Although locally cross-bedded, they are generally massive (non-stratified) overall. These dune and sheet sand deposits are usually less than 10 feet thick, but in numerous areas extend to 30 feet thick. Permeability is high to very high in the cleaner sands with resulting frequently low water tables. Foundation stability tends to be good under moderate static loads and moderate to poor under heavy or vibratory loads. Low to moderate compression upon wetting is sometimes observed.

4.1.4.2 Loess (Early Holocene through Late Pleistocene)

These soils are also derived from wind born particles, but are the finer equivalents of the <u>Eolian Sands</u>. They are silt and clay-dominate, frequently with a very fine sandy component, and often are found to grade laterally into Eolian Sand. The deposits tend to be massive. They are usually less than 10 feet thick, but occur locally as thick as 25 feet. Vertical permeability is usually moderate with the horizontal component being low. Water tables tend to be low. Foundation stability is usually moderated when loesses are dry, but poor when wet. Uneven wetting of these silty soils frequently results in marked differential settling. Swell potentials are low to moderate except when very clayey where they may grade to high. Significant deposits are usually found on upland surfaces in the same general areas as Eolian Sands. Loess soils are often porous and consequently may exhibit low to high compression upon wetting.

4.1.4.3 Colluvium (Early Holocene through Middle Pleistocene)

These deposits form on moderate slopes throughout the Corridor as a result of the weathering of underlying and upslope soil and bedrock. A combination of gravity (soil creep) and water runoff (sheet wash) moved the weathered material down slope and contributed to further weathering. Colluvial soils are the clay-enriched equivalent of the material from which they were derived and are therefore highly variable from area to area. Common characteristics are a wide size range of components, non-stratification, and the tendency to have very gradational lateral contacts with other soil types. A frequently found accumulation is sandy silty clay that is slightly to commonly gravelly. A common field occurrence is where older upslope terrace deposits grade down slope into colluvial soil that in turn grades down into younger flood plain alluvium. The down slope creep aspect of the depositional process often results in substantial cobbles and small boulders being included in a dominantly clay matrix.

Thicknesses are highly variable. All except the hardest, steepest bedrock exposures usually have at least a thin layer of colluvial soil. As slopes decrease, colluvial components tend to further accumulate and weather, thereby becoming more clayey and thicker (up to 20 feet, but more commonly 10-foot maximum). Vertical and horizontal heterogeneity is common. Permeability is generally low to very low, although permeability largely depends on the clay content. Stability characteristics are greatly dependent on the original source material and degree of clay alteration from the weathering process. Deposits closely derived from expansive bedrock claystone/shale, ashy/bentonitic sandstone, or montmorillonite-rich soils may have low strength and moderate to very high swell potential.

4.1.4.4 Residual Soils

The term <u>Residuum</u> is frequently applied to soils resulting from bedrock or older soil weathering, usually on very gentle slopes that have not undergone significant "colluvium-like" movement. These soils are usually very thin and are often considered the normal

topsoil and not separately mapped. A locally important exception along the far western margin of the Corridor is the occurrence of <u>Grus or Decomposed Granite</u> (Late Pleistocene to Holocene) over granitic bedrock in mountainous areas of the Front Range. This soil is highly porous and consists of coarsely granular, angular (frequently near cubic) fragments of quartz and feldspar. Transition from underlying deeply weathered bedrock is gradual, frequently over a considerable distance. Deposits may be as thick as 5 to 8 feet and commonly thicken further into downslope colluvium.

4.1.4.5 Steeper Slope Deposits (Late Holocene to Middle Pleistocene)

<u>Landslide Deposits</u> are rock and soil debris mixes, usually bouldery to sandy silt and clay, some of which may still be active. These accumulations are spotty, but numerous along the Frontal Hogback, mountain front, and flanks of isolated mesas throughout the Corridor. Like <u>Colluvium</u> deposits, these soils are non-stratified, heterogeneous throughout, and with a wide range of component sizes. Unlike colluvium, they usually have sharp upslope and side margins; down slope toes frequently grade into colluvial materials. Thicknesses are most commonly less than 15 feet. Engineering stability depends on the degree of current slope, water saturation, percent clay, and swell-prone component content; higher values of any equate to lower stability.

<u>Talus Deposits</u> are direct rock fall accumulations at the base of cliffs and very steep slopes. They are typified by a high portion of large, angular to subangular rock fragments with few fines. They tend to be relatively homogeneous and are non-stratified with sharp upslope and lateral margins. The downslope toes often grade into colluvium. These bodies may be laterally numerous and cover a substantial cumulative area. Permeability is almost always high to very high. Stability is usually considered low, even in older deposits.

4.1.5 Special Soil Conditions

4.1.5.1 Artificial Fill (Recent)

Areas with substantial thicknesses and areal extent of man-placed materials are moderately common along nearly the entire Corridor and are very common in some

locales. Except for modern engineered fills, composition and physical character are as varied as the reasons they were placed and each must be separately evaluated. Most fills are likely to be in the 5 to 20 foot maximum thickness range, however highway embankments to 90 feet are known. Some areas or situations of known or suspect significant fills along the Corridor include:

- Old aggregates pits along the flood plains of rivers and major tributaries near metropolitan areas that have been backfilled for development (*i.e.,* numerous sites along the South Platte River immediately north of Denver and eolian sand quarries in Colorado Springs).

- Metropolitan area major highway interchanges.

- Near modern riverbanks in population centers where mixed debris were placed for waste disposal and soil for leveling off for development (e.g., Cache la Poudre River in Ft. Collins, South Platte River and Cherry Creek in Denver, Fountain Creek in Colorado Springs, and the Arkansas River in Pueblo.).

- Mine dumps, particularly Laramie Formation coal mine sites, most of which are thought to have been non-engineered (*i.e.,* extensive dump fields from sub-bituminous coal mines in the Greater Broomfield area including Highway 36 and Interstate 25).

- Smelter dump areas (*i.e.,* Globeville neighborhood/I-25 in Denver and the major CF&I slag pile in southeastern Pueblo).

- Old sanitary landfills in low-lying areas formerly on the margins of population centers (*i.e.,* Commerce City near Sand Creek and Interstate-270).

4.1.5.2 Bedrock Definition, Potential Problems

Two geologic conditions exist in multiple soil groups that may make the definition of the soil-bedrock interface difficult in auger borings. One is the occurrence of sound crystalline boulders or beds of large cobbles within soil deposits (especially 1- Piney Creek Alluvium near the mountain front and near larger streams, 2- Louviers, Slocum, and Verdos Alluvium, and 3- some Colluvium deposits). The other situation is the presence of frequently widespread, thoroughly cemented paleosol (relict weathering

horizons) gravels within otherwise normal soil intervals (especially <u>Slocum, Verdos, and Rocky Flats Alluvium</u>).

4.2   BEDROCK OF THE CORRIDOR

4.2.1   Generalized Distribution

Except for transitional zones where bedrock is very highly weathered, the interface between soil and bedrock is usually well defined along the Corridor.   A major unconformity (period of non-deposition and/or erosion) due to uplift along the mountain front has separated younger soil from older bedrock and represents most of the entire Tertiary Period of geologic time in most areas.   Bedrock units having likely potential impact on drilled shafts in the Corridor are distributed in four major settings (arranged as younger to older for the age of their generally included units):

5.   Early Tertiary (Paleocene) coarse sandstone and conglomerate units, the youngest bedrock, is primarily limited to the central part of the Corridor forming major exposures in the Monument Highlands.

6.   For valleys and uplands of the Western Plains Piedmont (the dominant portion of the Corridor), upper Late Cretaceous sedimentary rocks are intermittently exposed through soil cover throughout the northern and southern parts and comprise most of the bedrock likely to be encountered in foundations.

7.   The mountain front belt includes a wide age range (Triassic to Pennsylvanian) of diverse sedimentary rocks that are exposed in a variably wide and locally intermittent band immediately east of the mountains.   Jurassic to lower Late Cretaceous age shale and sandstone-dominant, tilted strata are intermittently well exposed along the narrow Frontal Hogback and as flatter lying outcrops in the Arkansas River valley near Pueblo.

8.   Pre-Cambrian igneous and metamorphic rocks are exposed pervasively in mountainous areas along the west margin of the Corridor.

4.2.2   Major Bedrock Groups

4.2.2.1 Early Tertiary Bedrock of the Monument Highlands

<u>Upper Dawson Arkose</u> (Paleocene): Outcrops of this formation dominate the area along I-25 from the southern suburbs of Denver to northern Colorado Springs. Soil cover is generally limited to thin colluvium/residuum on gentle slopes and thin to moderate alluvium restricted to a few valleys. Younger (Oligocene) <u>Castle Rock Conglomerate</u> is common and highly visible in the area, but is limited to mesas/highlands above most major transportation routes. The Upper Dawson consists of an intricately interfingering, lensing series of members including quartz-feldspar sandstone, sandy and bouldery well cemented conglomerate, friable (weakly cemented) clay-rich sandstone, and claystone-siltstone. Well-cemented zones are very hard. Clayey horizons (including clay matrix sandstones) have high swell potential; less silty or sandy claystone layers may be very plastic when saturated. Other layers are considered stable to very stable.

4.2.2.2 Bedrock of the Piedmont (Western Plains Valleys and Uplands)

<u>Denver, Arapahoe, & Lower Dawson Formations</u> (Paleocene to Latest Cretaceous): These non-marine units, although sometimes separately mapped, are largely age equivalent and interfinger with each other over long distances. All are limited to a broad, arc-shaped band sweeping around the Monument Highlands with the general arrangement being: Denver Formation dominant to the north (under most of the Denver metropolitan area), Arapahoe Formation in the center, and Lower Dawson Arkose to the south (around Colorado Springs). Except for harder sandstone outcrops near Colorado Springs, most of the material is mantled by variably thin to very thick soil.

The <u>Denver Formation</u> is claystone/shale-dominant over most of the Denver area, with thinner interbeds of siltstone, tuffaceous (volcanic ashy) sandstone weakly to well cemented, and lesser conglomerate commonly with volcanic rock clasts. Cemented sandstones may be very hard. Claystone/shale, as well as tuffaceous sandstone, are well noted for having major vertical and horizontal zones with high to very high swell potential; non-sandy claystone is frequently highly plastic when saturated. Claystone

clays and ash-derived sandstone clays are montmorillonite rich (frequently termed "bentonitic") often including seams of nearly pure bentonite. The formation is a major contributor to unstable conditions in overlying soils where Denver Formation claystone fragments may be common. In the western portion of the Denver area (Morrison Quadrangle), the formation contains thick intervals interpreted as paleo-mudflow deposits containing a jumble of boulder-size claystone fragments in claystone/shale matrix; these units are noted for high swell potential and high plasticity. Where unweathered, the formation includes a waxy, blue-green-gray claystone locally known as "The Denver Blue". The "Denver Blue's" upper surface is not a stratigraphic horizon, but rather an irregular weathering/alteration zone that is often transitional.

The Arapahoe Formation is generally coarser, less prone to have volcanic components, and has some slightly older portions than the Denver Formation. The two are frequently mapped as Denver-Arapahoe Undifferentiated in the Denver area. The formation is generally described as well stratified, interbedded claystone/shale, siltstone, sandstone, and conglomerate. A well-developed lower Arapahoe conglomerate is frequently only weakly cemented and is a significant aquifer. Conglomerate and sandstone units have variable low to moderate swell potential; siltstone and claystone/shale have moderate to high swell potential.

Lower Dawson Arkose also tends to be well interbedded with layers of conglomerate, coarse sandstone, shale, and silty fine sandy shale (termed "mudstone"). The coarser units usually have moderately well graded quartz and feldspar sands with granitic pebbles ("arkose"); local coal beds are noted. Clay rich and clay-dominant zones have moderate to very high swell potential and moderate to high plasticity, particularly in the Austin Bluffs area north of Colorado Springs.

Laramie Formation, Fox Hills Sandstone, and Pierre Shale (Late Cretaceous): These formations, listed from younger to older, occur in two broad situations: (1) As

intermittently exposed in moderately dipping beds east of the mountain front (immediately east of the Frontal Hogback) from Ft. Collins to Denver and (2) with thin soil mantles in gently dipping and near flat lying units in the Louisville area and along Interstate 25 between Colorado Springs and Pueblo. In these areas, the upper (Laramie) units are non-marine, the Fox Hills has transitional marine interfingerings, while the lower (Pierre) rocks are generally of marine origin. Unlike younger bedrock, these units are much more widespread and are more consistent within each member over wide areas.

The <u>Laramie Formation</u> is dominated by thinly bedded shale and siltstone with common hard to friable sandstone interbeds, lesser thin hard conglomerate, and lignitic to sub-bituminous coal beds. Coal beds are as thick as 14 feet (although usually much less) and were mined extensively over wide areas and at numerous locations. The formation is sandier in the lower portion; basal sandstone beds may be equivalent to some of the <u>Fox Hills Sandstone</u>. Most Laramie clays are dominantly kaolinitic with usually low to moderate swell potential; the middle third tends to be montmorillonitic with resulting high swell potential. Sandstones vary from weakly to well cemented.

<u>Foxhills Sandstone</u> units are cross-bedded and quartz sand-dominant. Relatively thin interbeds of claystone/shale, mudstone, and coal occur throughout. The sands are generally weakly cemented and friable; they are important aquifers with medium to high permeability, particularly north of Denver. They are considered to have good to very good foundation stability.

The <u>Pierre Shale</u> is a very thick, clay/shale-dominant formation with numerous thin bentonite beds throughout. These rocks are almost always suspect for moderate to very high swell potential, medium to high plasticity, and low slope stability almost everywhere they are encountered along the Corridor. Thin, subordinate, frequently friable sandstone interbeds occur throughout the formation. Significantly thick sandstone members are present in several areas at different stratigraphic positions (the middle level Hygiene Member to the north and the lower Apache Member to the south are noteworthy). Hard limestone masses (butte formers in outcrop) occur in the middle portion to the south. To

the south, the middle portion also contains appreciable gypsum content (Sharon Springs Member) that may affect sulfate-susceptible cement.

4.2.2.3 Bedrock of the Mountain Front, Frontal Hogback, and Arkansas River Valley

4.2.2.3.1 Colorado Group

The Colorado Group is exposed along the immediate east side of the Hogback from the northern end of the Corridor to Denver; dips are too steep for it to be encountered in most foundation situations east of this relatively narrow strip. Constituent formations are also present to the south where they appear as low scattered outcrops or are thinly soil mantled over wide areas (in the Arkansas River valley, west of Interstate 25 and around Pueblo). The formations in this Group are of marine origin and include (from younger to older):

Niobrara Formation (Lower Early Cretaceous): Includes upper chalky shale members (Sharon Springs Shale and Smoky Hill Shale) with thin hard limestone interbeds and thin bentonite and gypsum layers and a lower hard and thick-bedded limestone member (Ft. Hayes Limestone) with limey shale partings and thin bentonite beds.

Benton Shale Equivalents (Lower Late Cretaceous to Upper Early Cretaceous): These include the Carlile Shale, Greenhorn Limestone, and Graneros Shale that contain non-calcareous claystone and siltstone, calcareous shale with hard thin limestone beds, limestone with claystone/shale and siltstone interbeds, and thick clay shale units. The Greenhorn and Graneros formations are noted for common bentonite beds to several inches thick that are vertically numerous in some areas.

Shale units throughout the Group have moderate to very high swell potential and are noteworthy contributors to soil instability in much of the southern portion of the Corridor. Gypsum-rich zones may yield sulfates contributing to breakdown of cement.

4.2.2.3.2   Older Sedimentary Rocks

These diverse units are exposed only along the narrow mountain front and Hogback belt and dip too steeply to be encountered in foundation situations elsewhere in the Corridor. The formations are laterally persistent.   Except for the non-marine and frequently conglomeratic members (Fountain Formation), they also tend to have similar content over long distances. They are typically moderately hard to very hard and, except in areas of intense fracturing, usually stable to very stable. Expansive clays are absent. Steep dip and alternating hardness may combine to deflect auger borings out of the vertical. Limestone and dolomitic limestone units (near Colorado Springs and possible north of Ft. Collins) may be vuggy or cavernous. Thick gypsum deposits (Morrison Formation) may affect sulfate-sensitive cement. Noteworthy formations included in this category include (youngest to oldest):

Dakota Group (Early Cretaceous): Ridge-forming sandstone members with lesser shale interbeds; Dakota Hogback and Perry Park are notable exposures.

Morrison-Ralston Creek Formations (Late Jurassic): Thickly interbedded claystone, siltstone, and sandstone with thin limestone beds and thin to moderately thick gypsum layers. Garden of the Gods at Colorado Springs has notable exposures of some of these units (along with Permian Lyons sandstone), and is sometimes mapped together with the Lykins Formation (Jurassic-Triassic; thickly interbedded limestone, shale, siltstone, and sandstone).

Lyons Sandstone (Permian): Persistent, hard quartz sandstone, finely bedded and frequently cross-bedded. Noted for easily parting in 1 to 6 inch layers ("flagstone"); quarried near Lyons for dimension and decorative stone.

Fountain Formation (Permian-Pennsylvanian): Arkosic conglomerate and sandstone with sandy shale interbeds and lenses ("fanglomerate"); great vertically and lateral variability. Notable resistant outcrops are at Redrocks Park and Roxborough Park.

<u>Leadville Limestone, Manitou Limestone, & Peereless Dolomite</u> (Mississippian- Late Cambrian): These hard, carbonate-dominated sedimentary rocks are limited to the area west of Colorado Springs.

4.2.2.3.3 Bedrock of the Mountainous Areas

Older Pre-Cambrian age metamorphic rocks of mixed origins are intruded by younger Pre-Cambrian granitic rocks along the far western margin of the Corridor.

<u>Granitic Plutons</u>:   These generally massive, crystalline rocks have a range of compositions generally described as "granitic" (granite, grano-diorite, quartz monzonite, and similar); they are commonly intruded by irregular, coarsely crystalline pegmatite dikes. They are hard where unweathered, but commonly weather deeply (to 50 feet has been reported in the Air Force Academy area) forming thick residuum soil termed "grus". Multiple systems of well-defined fractures are the rule. Except for highly fractured and deeply weathered areas, foundation stability is good to very good.

<u>Metamorphic Rocks of the Ancestral Rocky Mountains</u>: These generally hard to very hard rocks were derived from a variety of pre-existing sedimentary and igneous units that were subject to heat and pressure of deep burial. They have undergone moderate to moderately severe mineral alteration and consist dominantly of quartzite and meta-conglomerate, schist, granitic gneiss, and intensely mixed types (migmatites). Except for the quartzites, they usually have significant foliation (strong preferred alignment of minerals) with resulting planes of relative weakness. In some areas, the original sedimentary bedding planes remain as interfaces of relative weakness. As a whole, these rocks tend to be pervasively fractured with multiple joint sets. In addition to the larger granitic intrusive masses, the metamorphic rocks also commonly contain irregular pegmatite dikes. Foundation stability is generally good except in areas of intense fracturing and where foliation dips as steep (or more steeply) than the slope and in the same direction.

References

Hepworth and Jubenville, "Drilled Pier Foundations in Shale, Denver Colorado Area",
Drilled Piers and Caissons, American Society of Civil Engineers, October 28,
1981, p. 68.

Publications listed below were reviewed by Geocal to provide a framework for state-wide geology and added detail along the Front Range Urban Corridor. The standard quadrangle scale maps (1:24,000) provided selected engineering characteristics for representative areas along the corridor. This list is not a comprehensive bibliography for the area or state. Abbreviations for common publication agencies are included at the end of the list.

CGS Environmental Geology Series 7: Potentially Swelling Soil and Rock in the Front Range Urban Corridor, 1974.

CGS Map MI-8: Colorado Geologic Highway Map (with GTR Mapping, 1:100,000), 1991 Rev.

CGS Rocktalk V.4-N.4: Ground Subsidence and Settlement Hazards in Colorado, 10/2001.

USGS Map MF-631: Geologic Map & Engineering Data for the Highlands Ranch Quadrangle, CO (1:24,000), 1974.

USGS Map MF-761: Geology, Montrose 1º x 2º Quadrangle, CO (1:250,000), 1976.

USGS Map MF-2347: Generalized Surficial Geologic Map of the Denver 1º x 2º Quadrangle, CO (1:250,000), 2001.

USGS Map MF-2388: Generalized Surficial Geologic Map of the Pueblo 1º x 2º Quadrangle, CO (1:250,000), 2002.

USGS Map OF-78-532: Preliminary Geologic Map of the Greeley 1º x 2º Quadrangle, CO & WY, (1:250,000), 1978.

USGS Map OF-78-878: Map Showing Artificial Fill in the Greater Denver Area, CO, (1:100,000), 1978.

USGS Map OF-80-321: Bedrocked Surficial Engineering Geologic Maps, Littleton Quadrangle, CO, (1:24,000), 1980.

USGS Map OF-80-654: Preliminary Engineering Geologic Map of the Morrison Quadrangle, CO, (1:24,000), 1980.

USGS Map GQ-1229: Geologic Map of the Niwot Quadrangle, CO, (1:24,000), 1975.

USGS Map GQ-1392: Geologic Map of the Lafayette Quadrangle, CO, (1:24,000), 1977.

USGS Map GQ-1413: Geologic Map of the Highlands Ranch Quadrangle, CO, (1:24,000), 1977.

USGS Map GQ-1427: Geologic Map of the Fort Logan Quadrangle, CO, (1:24,000), 1978.

USGS Map GQ-1453: Geologic Map of the Arvada Quadrangle, CO, (1:24,000), 1979.

USGS Map GQ-1524: Geologic Map and Physical Properties of the Surficial and Bedrock Units of the Englewood Quadrangle, CO, (1:24,000), 1980.

USGS Map GQ-1541: Geologic Map of the Commerce City Quadrangle, CO, (1:24,000), 1980.

USGS Map GQ-1567: Geologic Map of the Sable Quadrangle, CO, (1:24,000), 1983.

USGS Map GQ-1625: Geologic Map of the Horsetooth Reservoir Quadrangle, Larimer, CO, (1:24,000), 1989.

USGS Map I-360: Geology, Structure, and Uranium Deposits of the Moab Quadrangle, CO & UT, (1:250,000), 1983.

USGS Map I-408: Geology of the Northwest and Northeast Pueblo Quadrangles, (1:24,000), 1964.

USGS Map I-558: Geologic Map of the Trinidad Quadrangle, South-central CO, (1:250,000), 1969.

USGS Map I-560: Geologic & Structure Contour Map of the LaJunta Quadrangle, CO & KS, (1:250,000), 1968.

USGS Map I-629: Geology, Structure, and Uranium Deposits of the Cortez Quadrangle, CO & UT, (1:250,000), 1972.

USGS Map I-687: Geologic Map of the Lower Cache La Poudre River Basin, North-central CO, (1:62,500), 1972.

USGS Map I-731: Generalized Surficial Geologic Map of the Denver Area, CO, (1:62,500), 1972.

USGS Map I-790-A: Geologic Map of the Morrison Quadrangle, CO, (1:24,000), 1972.

USGS Map I-736: Geologic & Structure Map of the Grand Jumction Quadrangle, CO & UT, (1:250,000), 1973.

USGS Map I-764: Geologic Map of the Durango Quadrangle, Southwestern Colorado, (1:250,000), 1983.

USGS Map I-856-H: Geologic Map of the Greater Denver Area, Front Range Urban Corridor, CO, (1:100,000), 1979.

USGS Map I-857-F: Geologic Map of the Colorado Springs – Castle Rock Area, Front Range Urban Corridor, CO, (1:250,000), 1979.

USGS Map I-885-G: Geologic Map of the Boulder – Greeley Area, CO, (1:100,000), 1978.

USGS Map I-944: Geologic Map of the Lamar Quadrangle, CO & KS, (1:250,000), 1976.

USGS Map I-972: Geologic Map of the Craig 1º x 2º Quadrangle, North-western Colorado, (1:250,000), 1981.

USGS Map I-999: Geologic Map of the Leadville 1º x 2º Quadrangle, Northwestern Colorado, (1:250,000), 1988.

USGS Map I-1022: Geologic Maps of the Pueblo 1º x 2º Quadrangle, South-central Colorado, (1:250,000), 1984.

USGS Map I-1092: Maps Showing Geology, Structure, Oil & Gas Fields in the Sterling 1º x 2º Quadrangle, CO, NE, & KS, (1:250,000), 1978.

USGS Map J-1289: Surficial Geologic Map of the Grand Junction 1º x 2º Quadrangle, CO & UT, (1:250,000), 1981.

USGS Map I-1346: Surficial Geologic Map of the Craig 1/2º x 1º Quadrangle, Moffat & Routte Counties, CO, (1:100,000), 1982.

USGS Map I-1526: Geologic Map of the Vernal 1º x 2º Quadrangle, CO, UT, & WY (1:250,000), 1985.

USGS Map MF-631: Geologic Map ang Engineering Data for the Highlands Ranch Quadrangle, Arapahoe and Douglas Counties, Colorado, 1974.

USGS Professional Paper 551: General Engineering Geology of the US Air Force Academy Site, CO, 1967.

USGS Professional Paper 1230: Environmental Geology of the Front Range Urban Corridor and Vicinity, CO, 1982.

USGS & CGS Indidental Map: Geologic Map of Colorado, (Tweto, 1:500,000), 1979, (with companion: Geologic Cross Sections across Colorado, Tweto, 1983).

Abbreviations for common publication agencies:
> CGS- Colorado Geological Survey
> USGS- United States Geological Survey

Appendix B

Analysis Methods for Lateral Response of Drilled Shafts

Several analytical approaches have been proposed to carry out analysis of laterally loaded piles/drilled shafts. This appendix basically serves as a detailed reference attachment for all the methods that we have discussed in the report.

1. Brinch Hansen Method:

This approach developed by Brinch Hansen in 1961 is recommended for short rigid piles. It is based on earth pressure theory for c-ϕ soils. Basically, it consists of determining the center of rotation by taking moment of all forces about the point of load application and equating it to zero.
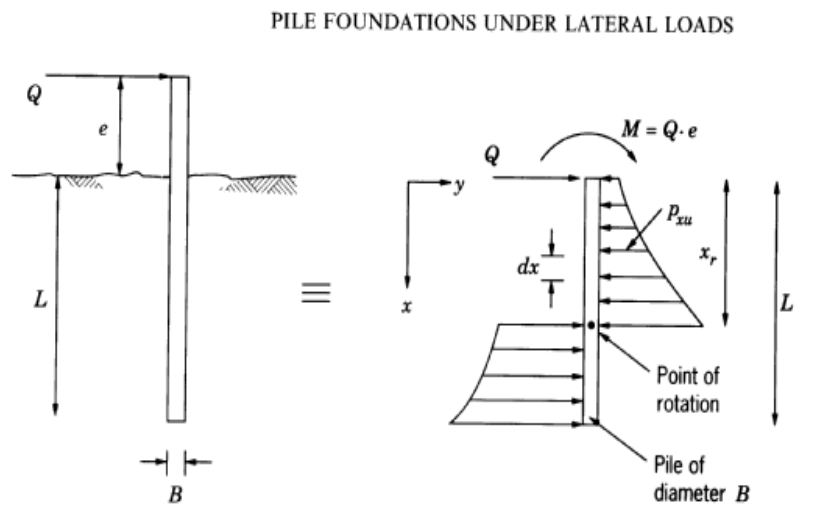
Figure B-1. Mobilization of lateral resistance for a free-head laterally loaded rigid pile

To calculate the ultimate resistance as depicted in Fig. B-1, sum of the horizontal forces are equated to zero. Therefore, the equation for ultimate soil resistance at any depth is given by

$$p_{xu} = \sigma_{vx}k_q + ck_c \qquad (B-1)$$

where, $\quad \sigma_{vx}$ = vertical effective overburden pressure

$\quad$ c = cohesion of soil

$\quad k_c$ & k_q = factors that are function of ϕ and x/B and can be obtained from Fig. B-2.
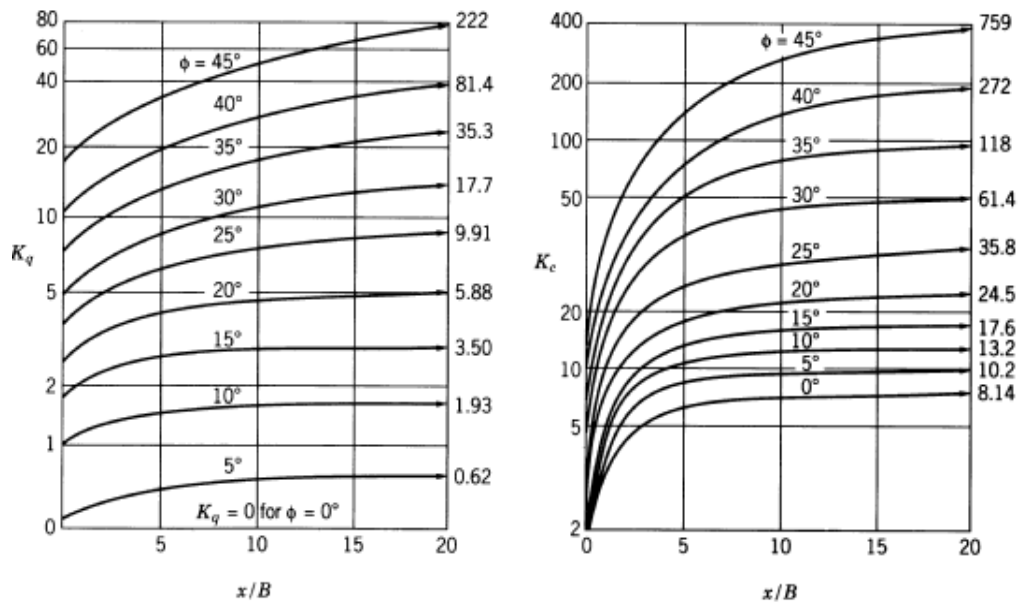
Figure B-2. Coefficients kq and kc

As shown in Fig. B-1, the lateral resistance diagram along the length of the pile and the assumed center of rotation are determined. Moment is taken about the point of application of lateral load Q_u, once the assumption is made for the point of rotation at some depth x_r below ground. If the moment calculated is a small value or near zero, the assumed center of rotation is considered correct. Thus, calculating moment at x_r, we can get the value of lateral load Q_u.

This approach is applicable to c-ϕ soils and valid both for layered and uniform soils. The disadvantages are that the method applies only to short piles and requires a trial-and-error procedure to locate point of rotation in the calculation.

2. Broms Method:

Broms proposed this method in 1964 for lateral resistance of vertical piles. The approach is separately described for piles in cohesive soils and cohesionless soil.

First considering the case in cohesive soil, the assumption is made to consider pile to be equivalent to a beam on an elastic foundation. It suggests a simplified distribution of soil resistance as being zero from the ground surface to a depth of 1.5d and constant value of 9Cu below this depth, where Cu is un-drained shear strength. The probable failure mechanisms for unrestrained or free head piles are shown for short and long pile along with soil reaction distribution in Fig. B-3 (a). Length of pile is L = 1.5d+f+g.
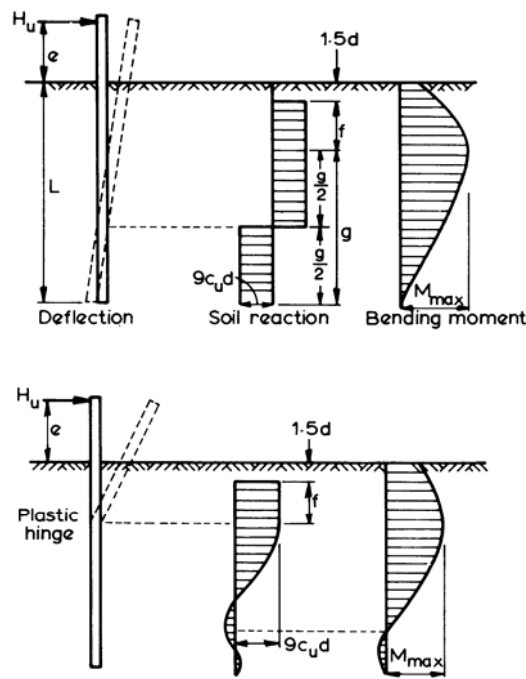
Figure B-3. Failure mechanisms for a) short and b) long free headed piles in cohesive soil

(after Polous and Davis)

For the short free-headed pile, failure takes place when the soil yields along the total length of the pile and the pile rotates as a unit around a point located at some depth below the ground surface.

The location of maximum moment and where shear is zero is defined as $f = \dfrac{H_u}{9C_u d}$, where $H_u =$ ultimate lateral load. The maximum moment at this location is $M_{max} = H_u(e + 1.5d + 0.5f)$, and the part of the pile with length g resists the bending moment $M_{max} = 2.25dg^2C_u$. Thus, we can calculate the ultimate lateral resistance from the equations given for maximum moment location and maximum moment. The dimensionless ultimate lateral resistance plotted as a function of dimensionless embedment length, as shown in Fig. B-4 (a), can be used directly to determine the ultimate lateral resistance. This dimensionless solution is based on the assumption that $M_y > M_{max}$.
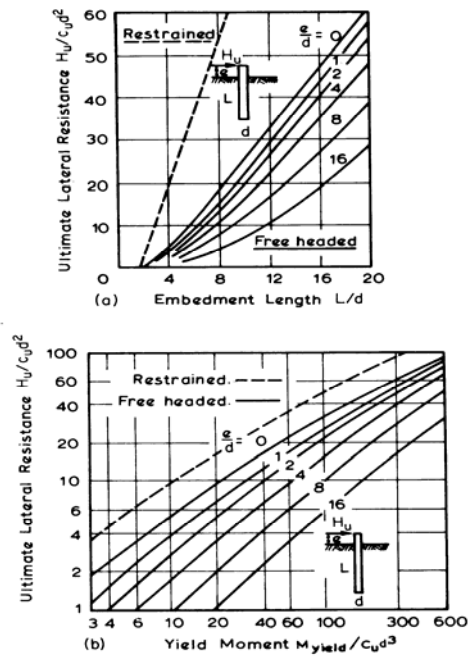
Figure B-4. Ultimate lateral resistance in cohesive soils a) short piles and b) long piles (after Poulos and Davis)

For free headed long piles, the mechanism of failure when a plastic hinge forms at the maximum bending moment is shown in Fig. B-3 (b) and is assumed that failure occurs when $M_y = M_{max}$. The corresponding dimensionless solution for the ultimate lateral resistance is shown in Fig. B-4 (b).

For restrained or fixed head short piles, failure occurs when the applied lateral load is equal to the ultimate lateral resistance of the soil, and the pile moves as a unit through the soil. The ultimate lateral resistance can be calculated by $H_u = 9C_u d[L - 1.5d]$ and the maximum negative moment. $M_{max(neg)} = H_u(0.5L + 0.75d)$ has to be less than or equal to M_y in order for pile to fail. Fig. B-5(a), (b) and (c) shows the deflection, soil reaction and moment distribution for a short, intermediate and long restrained pile.
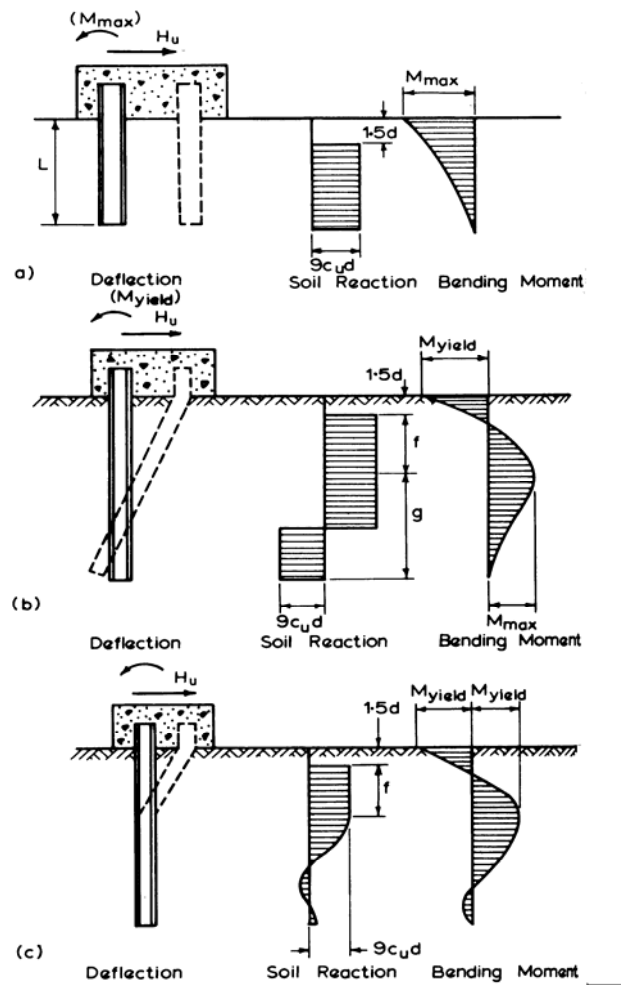
Figure B-5. Ultimate lateral resistance in cohesive soils a) short piles and b) long piles (after Poulos & Davis)

For restrained intermediate length piles, failure occurs when the restraining moment equals to the ultimate moment resistance of the pile section M_y and the pile rotates around a point located at some depth below the ground surface, while the maximum positive bending moment occurs at a section located at a depth $(1.5d + f)$. For the failure to occur $M_{max(pos)}$ necessarily has to be less than the yield or ultimate moment of resistance of the pile section M_y. Also, the ultimate lateral resistance can be obtained directly by the dimensionless solutions given in the Fig. B-4 (a).

For restrained long piles, failure occurs when two plastic hinges form along the pile, where the first one occurs at the section of the maximum negative and the second one at the section of maximum positive moment. The resulting ultimate lateral resistance can be calculated when the maximum positive bending moment is equal to the ultimate moment resistance of the pile section M_y as

$$H_u = \frac{2M_y}{(1.5d + 0.5f)}.$$ Also, the ultimate resistance can be determined from Fig. B-4 (b).

Now, for the second case in the cohesionless soil, the assumptions made are: 1) on the back of the pile, action of active earth pressure is neglected, 2) along the front of the pile, distribution of active earth pressure is equal to three times the Rankine's passive pressure, 3) no influence of the shape of the pile section on the distribution of ultimate soil pressure or the ultimate lateral resistance, and 4) the full lateral resistance is mobilized at the movement considered.

The first step is to decide whether the pile is short or long. For this, rotation is assumed to be about a point close to the tip, and high pressure acting near this point are replaced by a single concentrated force at the tip. $H_u = \dfrac{0.5\gamma dL^3 K_p}{e + L}$ is obtained by taking moment about the toe. Deflection of the pile and soil reaction and moment distribution for free headed short and long piles

is shown in Fig. B-6 (a) and (b), respectively. Location of the maximum moment is obtained by

$$f = 0.82 \sqrt{\frac{H_u}{dk_p\gamma}}$$ and the maximum moment by $M_{max} = H_u\left(e + \frac{2}{3}f\right)$. If the calculated value of H_u

results in $M_{max} <= M_y$, then the pile is considered as short and the assumption is correct. If the calculated value of H_u results in $M_{max} > M_y$, then the pile is considered as long and H_u can be calculated taking $M_{max} = M_y$. Also, the ultimate lateral resistance can be obtained directly from dimensionless solution given in Fig. B-7 (a) and (b).
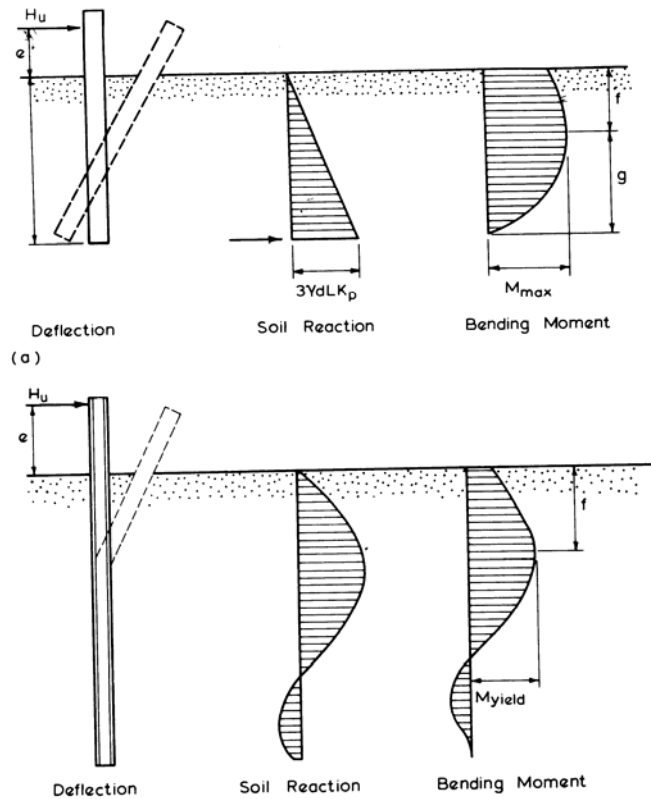
Figure B-6. Free head piles in cohesionless soil   (a) short (b) long (after Poulos and Davis)
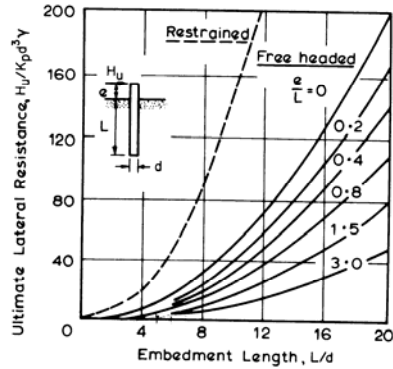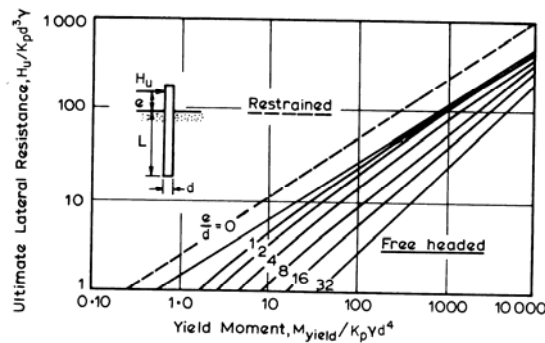
Figure B-7.Ultimate lateral resistance of piles in cohesionless soil

(a) short (b) long (after Poulos and Davis)

For short restrained piles, failure occurs when the load applied to the pile is equal to the ultimate lateral resistance of the soil and is expressed as $H_u = 1.5\gamma L^2 dk_p$. But this is only applicable when the maximum negative moment is less than the M_y of the pile. The ultimate lateral resistance is also plotted in the dimensionless form as shown in Fig. B-7 (a) and the failure mechanism is shown in Fig. B-8 (a).

Failure for the intermediate pile takes place when the $M_{max(neg)}$ at the head of the pile reaches the yield resistance and is shown in the Fig. B-8 (b). The high negative lateral earth pressure acting

close to the toe of the pile is approximated as the concentrated force as shown in the Fig. B-8 (b). Thus, the equation to calculate H_u is expressed as $H_u = 0.5\gamma dL^2 k_p - M_y$. This is applicable only when the $M_{(pos)}$ developed at the depth f is less than M_y. The dimesionless ultimate resistance based on the calculated value is plotted in Fig. B-7 (a).

For long restrained pile, failure takes place when two plastic hinges form and the pile turns into a mechanism as shown in Fig. B-8(c). The two plastic hinges forms when both, $M_{max(pos)}$ at depth f and $M_{max(neg)}$ at the bottom of the pile reach M_y. Considering that the total shear force at the f is equal to zero, we can calculate by the equation $f = 0.82\sqrt{\dfrac{Hu}{\gamma dk_p}}$. Therefore, the ultimate lateral resistance can be obtained from $Hu = \dfrac{M_{max(pos)} + M_{max(neg)}}{e + 0.54\sqrt{\dfrac{Hu}{\gamma dk_p}}} = \dfrac{2M_y}{e + 0.54\sqrt{\dfrac{Hu}{\gamma dk_p}}}$.

The ultimate lateral resistance as determined form the equation is plotted in Fig. B-7(b) as a function of the dimensionless yield or plastic moment resistance.
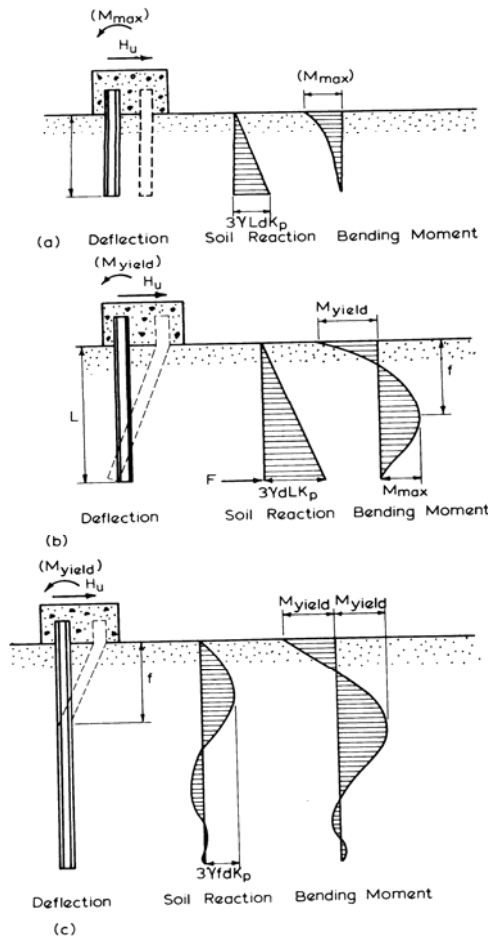
Figure B-8. Restrained piles in cohesionless soil (a) short (b) intermediate and (c) long (after Poulos and Davis)

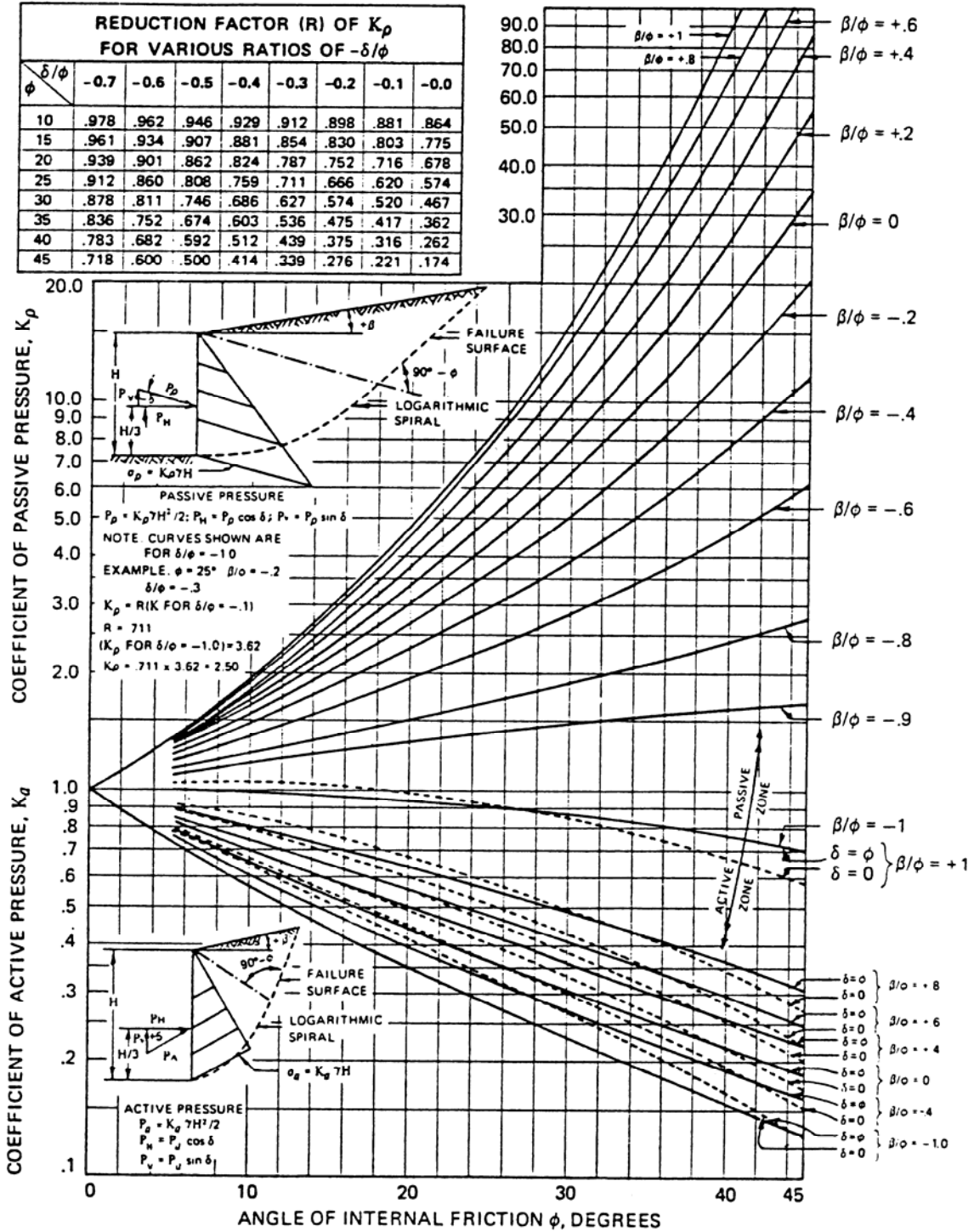## 3. Sheet Piling Method (AASHTO Specifications)

This method was initially developed for sheet piles embedded in cohesionless soils and is based on the earth pressure theory. For cohesionless fills, $\phi > \beta$ (slope angle) and generally fills are designed for a FS of 1.25, where $FS = \dfrac{\tan\phi}{\tan\beta}$. Also for cohesive fills, $\tan\phi$ is assumed to be equal to $1.25\tan\beta$ and the unit cohesive soil strength of the soil as c=0. The wall friction angle δ for concrete piles is considered as $\delta = (2/3)\phi$.

Given the ϕ and γ, the active and passive pressures of slope and/or level ground can be determined using the chart shown in Fig. B-9. It gives the reduction factors for active and passive pressures. Fig. B-10 shows the distribution of active and passive pressures acting on pile.
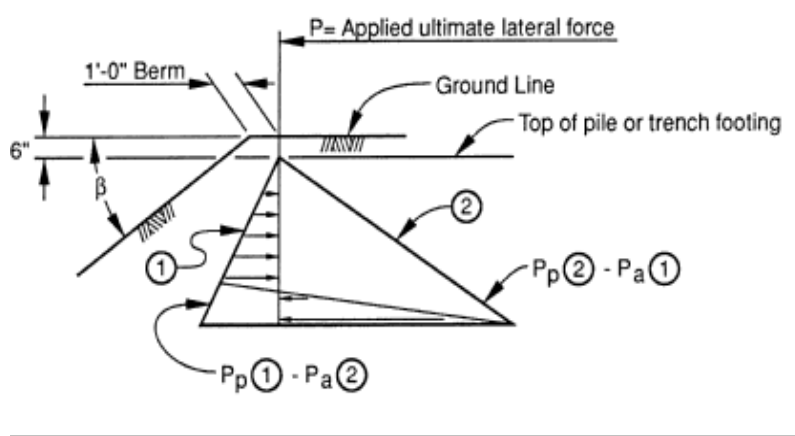
(Printed with permission from United States Steel)

Active and passive coefficients with wall friction (sloping backfill) (after Caquot and Kerisel[21])

Figure B-9

Figure B-10. Pile pressure diagram

Fig. B-11 shows the embedment determination for pile embedded in level ground. Pile diameter and the appropriate isolation factor considered to get the effective passive pressure are used in the calculations.
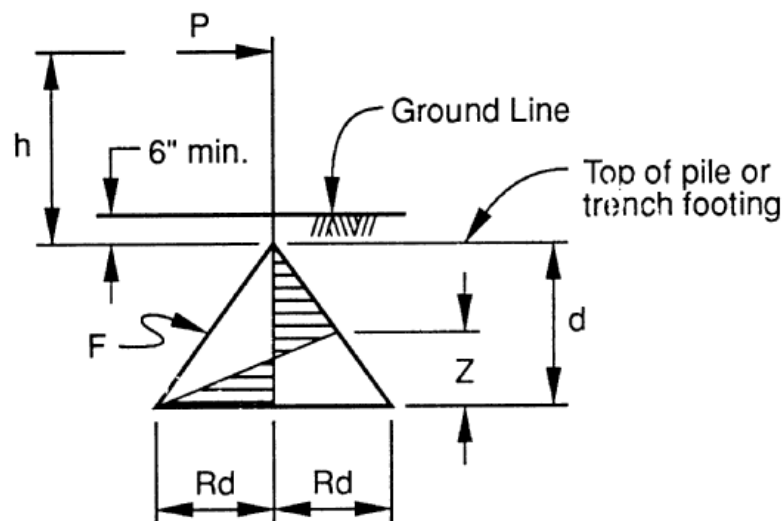
Figure B-11. The calculation schematic diagram for pile embedment depth

The following equations are given in reference to Fig. B-11 to determine the embedment depth;

$$\Sigma F_{H} = 0 = (2Rd)(1/2)(Z) - (1/2)(Rd^{2}) + P, \tag{B-2}$$

$$Z = d/2 - P/Rd \tag{B-3}$$

$$\Sigma M = 0 = \frac{Rd^{3}}{12} - \frac{2Pd}{3} - \frac{P^{2}}{3Rd} - Ph \tag{B-4}$$

where, h = distance form top of the pile to the point of application of load,

d = depth of embedment of pile

R = Allowable net horizontal ultimate lateral soil pressure.

This method is cumbersome to use as it requires hand calculations and is applicable only to short piles. The earth pressure distribution in the sheet piling approach is quite different from that in the drilled shaft.

4. Caisson Program:

The Caisson Program is developed by a CDOT engineer, Michael McMullen. The program is based on the theory developed by Davidson, et al (1976), assuming that full plastic strength of the soil is developed for calculating the ultimate capacity. Davidson's method assumes rigid-body motion of the pile and the lateral soil resistance varies linearly with the depth at ultimate load but reverses direction at the point of rotation of the shaft.
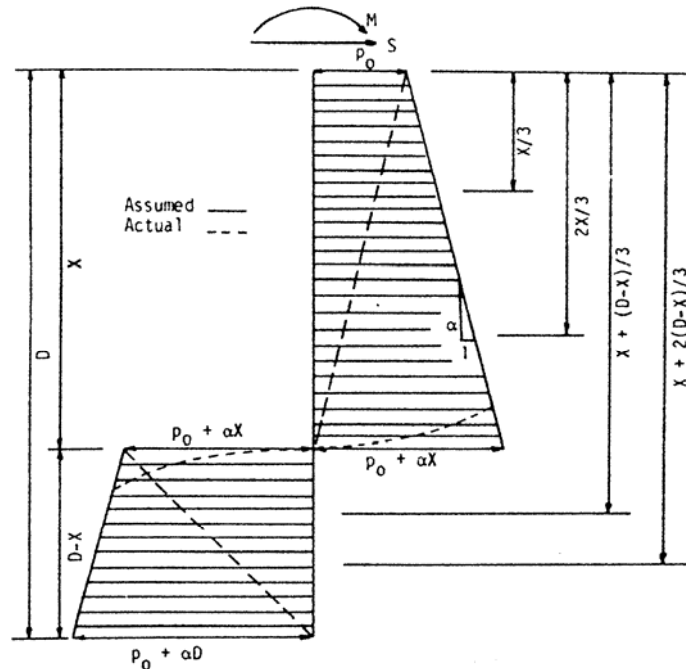

Figure B-12. Ultimate soil resistance for cohesive soil.

For cohesive soil, Fig. B-12 shows the actual and assumed soil-resistance distributions at failure. The values of the applied lateral load (S) and the bending moment (M) can be found with the following equilibrium equations.

$$S = p_0(2X - D) + (\alpha/2)(2X^2 - D^2) \qquad \text{(B-5)}$$

$$M = -p_0(X^2 - D^2/2) - (\alpha/3)(2X^3 - D^3) \qquad \text{(B-6)}$$

where α = slope of the soil resistance diagram,

p_0 = ultimate soil resistance at the ground surface,

D = the pile embedment depth, and

X = the unknown distance to the point of rotation.
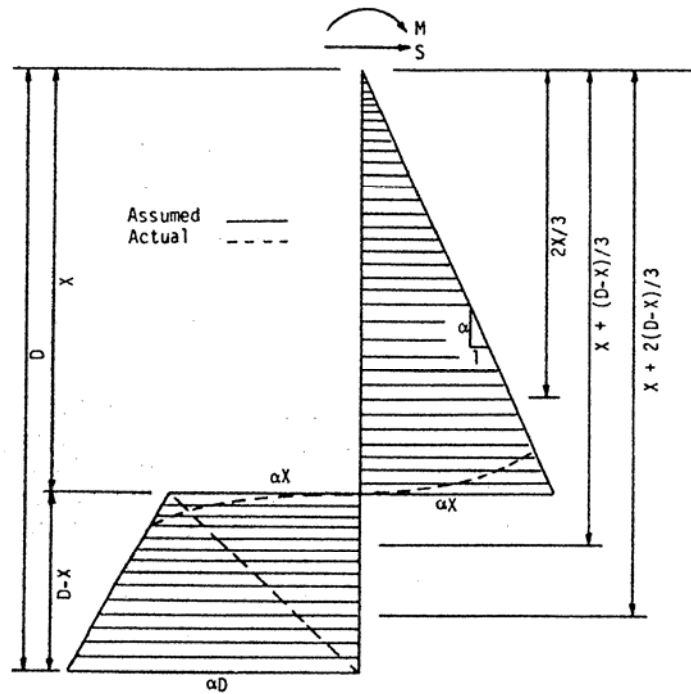
Figure B -13. Ultimate soil resistance for cohesionless soil.

For cohesionless soils, Fig. B-13 shows the actual and assumed soil-resistance distributions at failure. By applying equilibrium conditions to the assumed soil distribution, the equations for S and M can be found as follows.

$$S = (\alpha / 2)(2X^2 - D^2)$$ (B-7)

$$M = (-\alpha / 3)(2X^3 - D^3)$$ (B-8)

The soil strength is based on the following equation (Equation 9-7 in "Basic Soils Engineering" by B.K. Hough), which was generated for footing foundation.

$$p_{ult} = K_1 N_c c + K_2 \gamma_1 N_\gamma B + N_q \gamma_2 D_f$$ (B-9)

where K_1, K_2 = coefficients dependent on the type of footing,

N_c, N_γ, N_q = bearing capacity factors,

C = unit cohesion,

γ_1 = effective unit weight of soil below footing grade,

γ_2 = effective unit weight of soil above footing grade in depth D_f,

B = breadth of footing,

D_f = depth of the footing below exterior ground.

The above coefficients of the soil strength equation were calibrated from many testing results with an optimization program developed by Mr. Michael McMullen.

The program can only apply to homogeneous cohesive or cohesionless soil. The program, however, has shown problems when run for cohesive soil conditions. The method cannot provide deflection information.

## 5. P-Y Method

P-Y method is based on a numerical solution of a physical model based on a beam on Winker foundation shown in Fig. B-14. A number of empirical p-y curves for typical soil conditions based on the field test results have been developed. Reese (1984, 1986) has developed procedures for describing the soil response surrounding a laterally loaded pile for various soil conditions by using

a family of p-y curves. Analytical expression used for p-y curves are complex and can be found in numerous references, such as Wang, Shih-Tower and Reese, L.C.'s report in 1993.
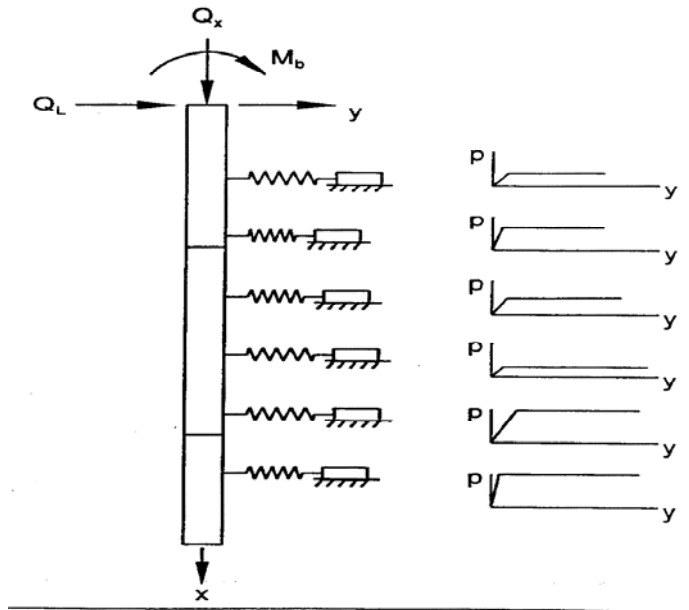
Figure B-14. COM624P Pile-Soil Model

By solving the beam bending equation using finite difference or finite element numerical techniques, solution of pile behaviors can be obtained.
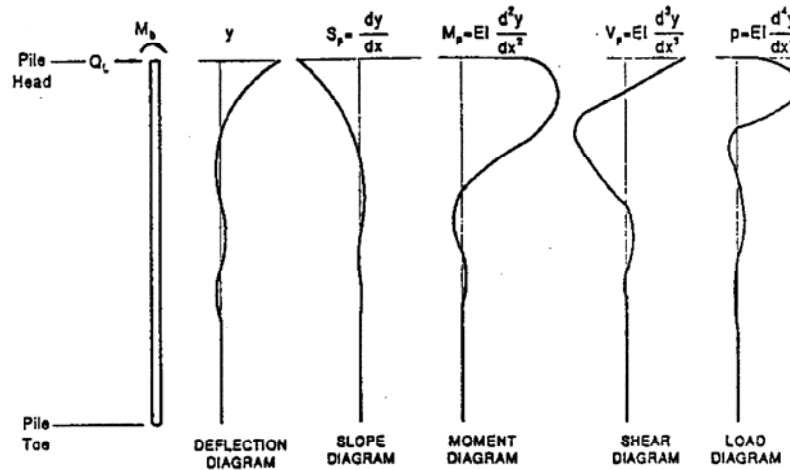
Figure B-15. Graphical presentation of COMP624 results.

Typical output from the computer program COM624P (LPILE) is depicted in Fig. B-15. The advantages of this method are that it accounts for the nonlinear behavior of the soils.

6. NAVFAC DM-7

This approach is based on Reese and Matlock's non-dimensional solutions for laterally loaded piles. Different simplified approaches are used for computing lateral pile-load versus deformation relationship based on complex soil conditions and/or non-linear soil stress-strain relationships. For coarse grained soil, pile deformations can be estimated assuming that the modulus of elasticity (E_s) increases linearly with depth and that the linear increase in coefficient of subgrade reaction k_h is in accordance with $k_h = \dfrac{fz}{D}$,

> where, k_h = coefficient of lateral subgrade reaction (tons/feet^3)
>
> f = coefficient of variation of lateral subgrade reaction (tons/ft^3). Chart given in the Fig. 16 is used to select the value of f.
>
> z = depth (feet)
>
> D = width / diameter of loaded area (feet)

For stiff to hard clays, modulus E_s is assumed constant with depth, and the procedure for the conversion of constant modulus E_s to an equivalent modulus E_s that varies linearly with depth is given stepwise as follows:

- Given a value of constant E_s, assume a value of f.
- Compute depth Z to point of zero deflection of pile from the figures shown below
- Recompute f so that value of $f_z = 2E_s$.
- Recompute depth z with revised f and alter f again so that $f_z = 2E_s$
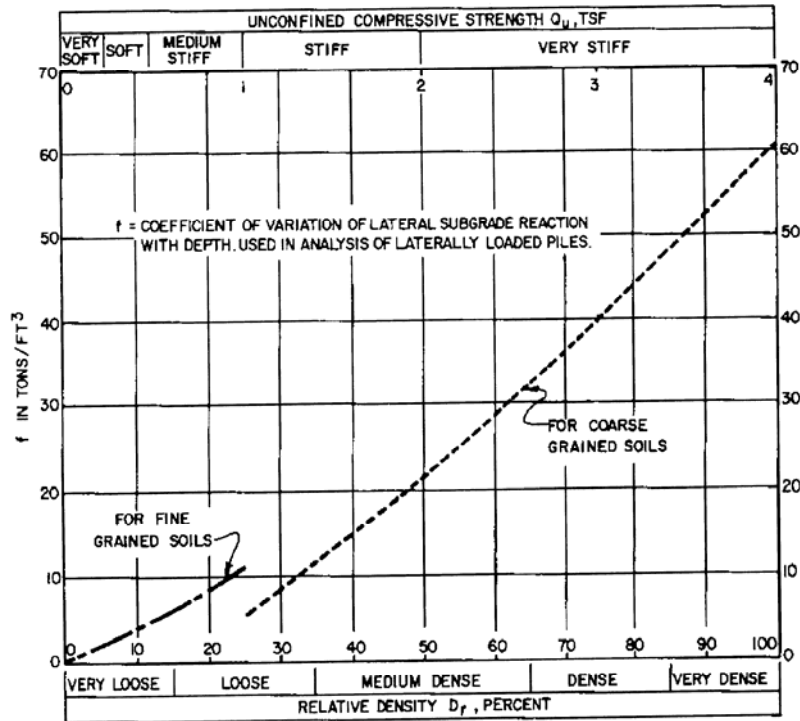
Figure B-16. Coefficient of variation of subgrade reaction

Three principal boundary conditions: flexible cap, rigid cap at ground surface and rigid cap at elevated position, are considered for the method and are explained with the design procedures in Fig. B-17. Fig. B-18 through Fig. B-20 provide the calculation charts for these three boundary conditions. This method provides only elastic solutions. The lateral load cannot exceed about 1/3 of the ultimate lateral load capacity.
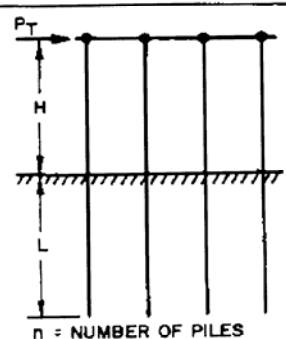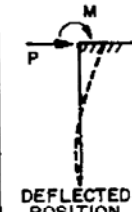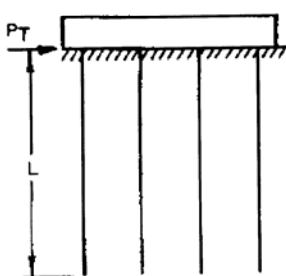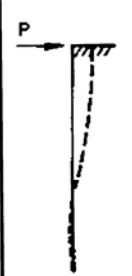
CASE I. FLEXIBLE CAP, ELEVATED POSITION		
CONDITION	LOAD AT GROUND LINE	DESIGN PROCEDURE
P_T ... H ... L ... n = NUMBER OF PILES	FOR EACH PILE: $P = \dfrac{P_T}{n}$ $M = PH$ M P DEFLECTED POSITION	FOR DEFINITION OF PARAMETERS SEE FIGURE 12 1. COMPUTE RELATIVE STIFFNESS FACTOR. $T = \left(\dfrac{EI}{f}\right)^{1/5}$ 2. SELECT CURVE FOR PROPER $\dfrac{L}{T}$ IN FIGURE 11. 3. OBTAIN COEFFICIENTS F_δ, F_M, F_V AT DEPTHS DESIRED. 4. COMPUTE DEFLECTION, MOMENT AND SHEAR AT DESIRED DEPTHS USING FORMULAS OF FIGURE 11. NOTE: "f" VALUES FROM FIGURE 9 AND CONVERT TO LB/IN^3.

CASE II. PILES WITH RIGID CAP AT GROUND SURFACE		
P_T ... L	P	1. PROCEED AS IN STEP 1, CASE I. 2. COMPUTE DEFLECTION AND MOMENT AT DESIRED DEPTHS USING COEFFICIENTS F_δ, F_M AND FORMULAS OF FIGURE 12. 3. MAXIMUM SHEAR OCCURS AT TOP OF PILE AND EQUALS $P = \dfrac{P_T}{n}$ IN EACH PILE.

CASE III. RIGID CAP, ELEVATED POSITION		
P_T ... H ... H_0 ... L	DEFLECTED POSITION θ_2 M P P M θ_1	1. ASSUME A HINGE AT POINT A WITH A BALANCING MOMENT M APPLIED AT POINT A. 2. COMPUTE SLOPE θ_2 ABOVE GROUND AS A FUNCTION OF M FROM CHARACTERISTICS OF SUPERSTRUCTURE. 3. COMPUTE SLOPE θ_1 FROM SLOPE COEFFICIENTS OF FIGURE 13 AS FOLLOWS: $\theta_1 = F_\theta \left(\dfrac{PT^2}{EI}\right) + F_\theta \left(\dfrac{MT}{EI}\right)$ 4. EQUATE $\theta_1 = \theta_2$ AND SOLVE FOR VALUE OF M. 5. KNOWING VALUES OF P AND M, SOLVE FOR DEFLECTION, SHEAR, AND MOMENT AS IN CASE I. NOTE: IF GROUND SURFACE AT PILE LOCATION IS INCLINED, LOAD P TAKEN BY EACH PILE IS PROPORTIONAL TO I/H_0^3.

Figure B-17. Design procedure for laterally loaded piles

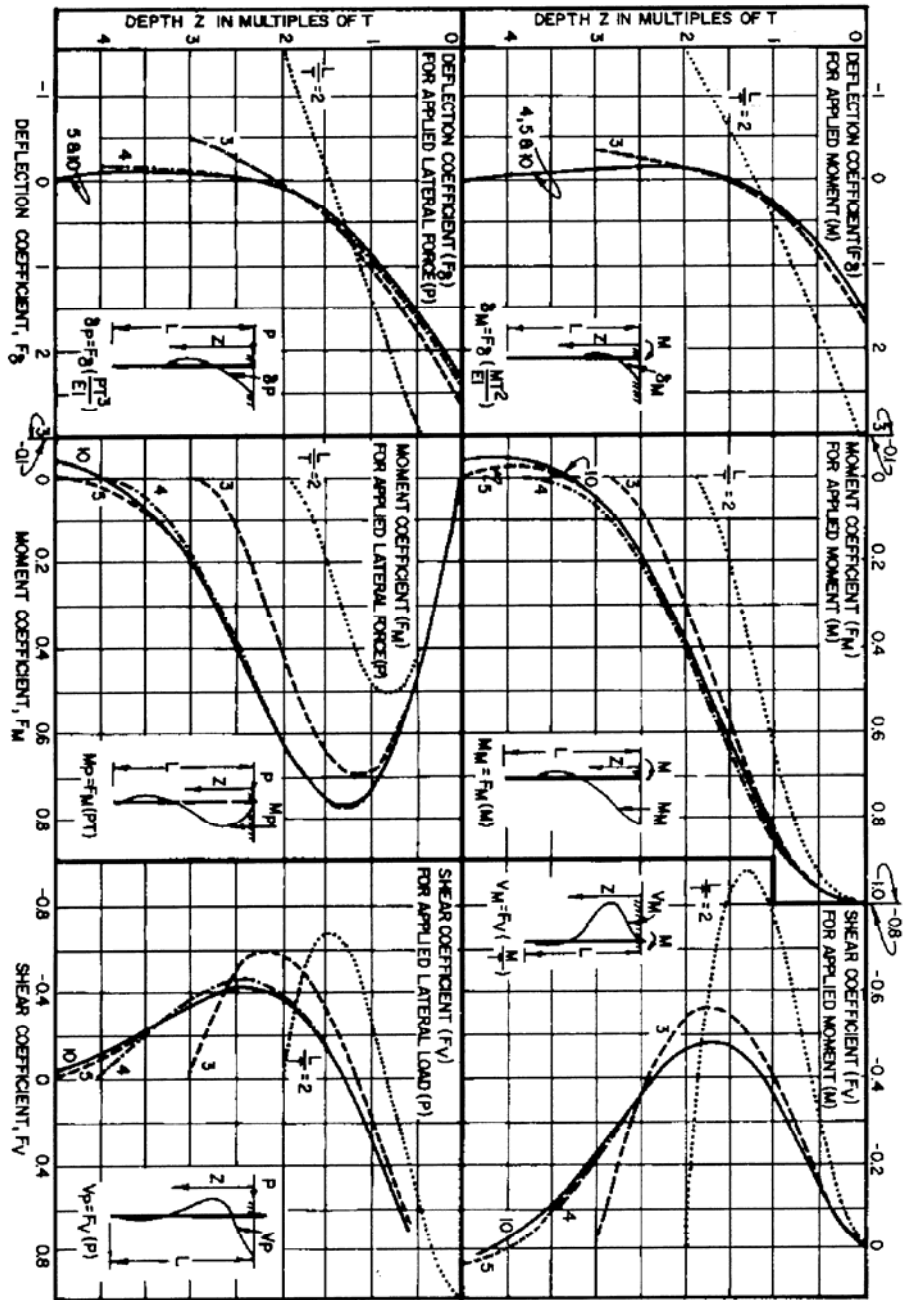**Figure B-18. Influence values for pile with applied lateral load and moment**

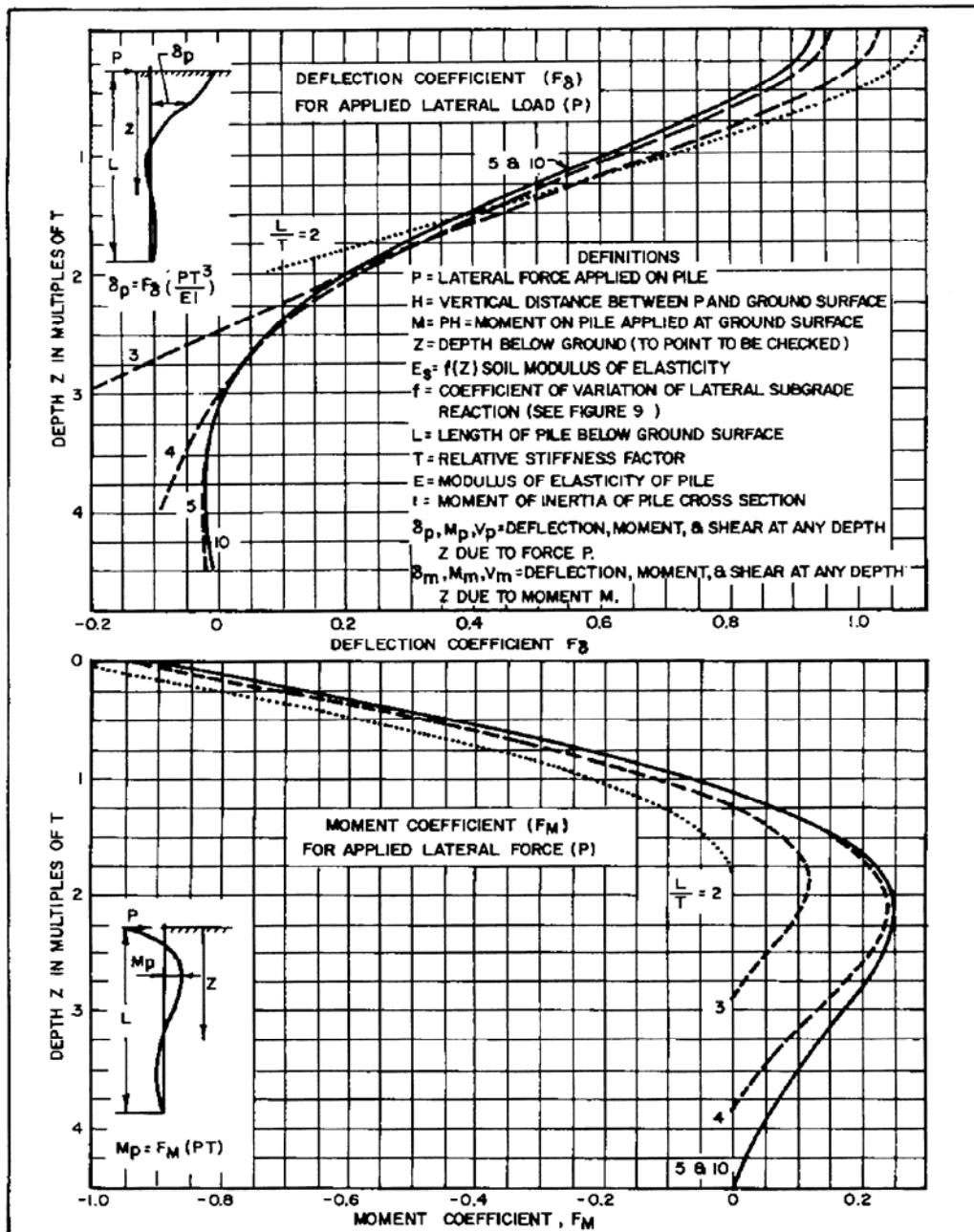(Case I. Flexible Cap or Hinged End Condition)

B-22

Figure B-19. Influence values for laterally loaded pile

(Case II. Fixed Against Rotation at Ground Surface)

B-23
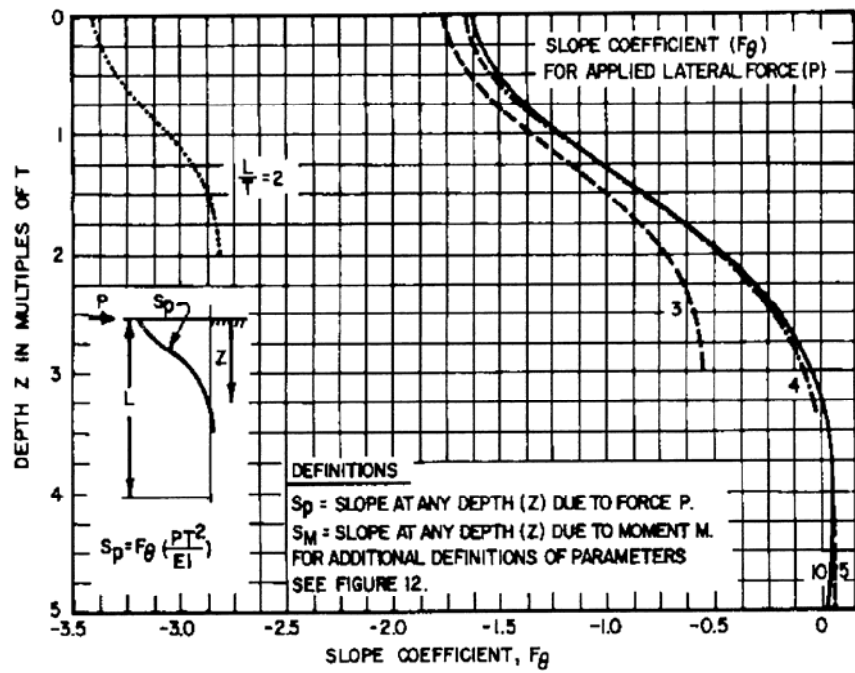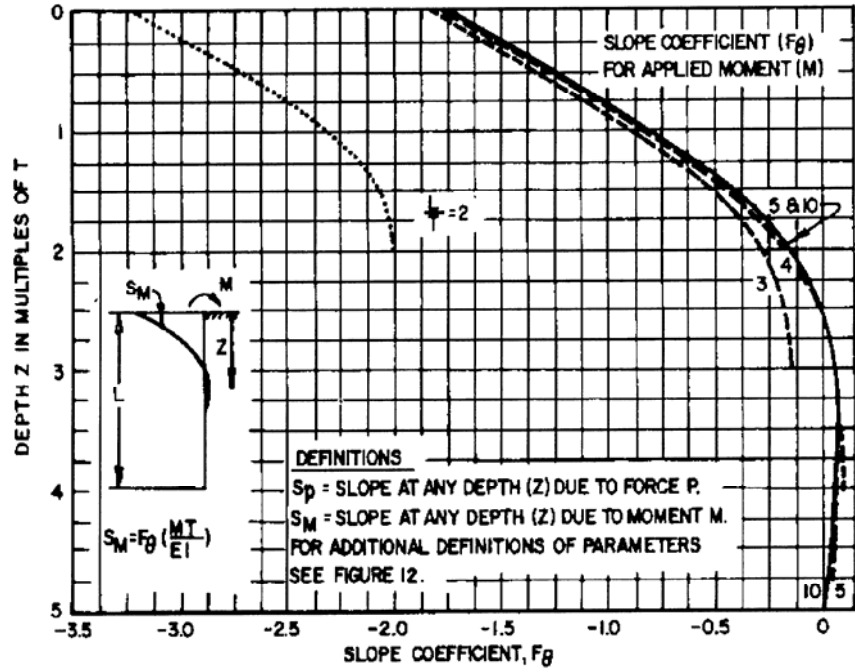
Figure B-20. Slope coefficient for pile with lateral load or moment

Appendix C

Analysis Methods for Torsional Response of Drilled Shafts

Introduction

Structures may be subjected to significant laterally loads due to wind, wave or earthquake actions. These loads my induce torque on piles due to the eccentricity of the lateral loads. During the past few decades, increasing attention is being focused on the torsional response of piles. The researches can be grouped into two schools of thought. The first one pertains to the theory analysis of torsion-twist behavior based on the assumptions that the foundation soil behaves as a linear or non-linear elastic material. The second category focuses on the limit equilibrium analysis where the ultimate capacity of the shaft is governed by the shear strength of the foundation soil.

1. Existing analytical and numerical methods for torsional response of piles

1.1 Methods for all kind of soils

O'Neill (1964) established a closed form differential equation solution for the pile-head torque and twist relationship for the case in which both the pile and the soil are assumed to have linear torque-twist properties.

The linear relationships are expressed as:

$$T(z) = T_0 e^{-z\sqrt{\beta\lambda}} \tag{C-1}$$

$$\left(\frac{T}{\theta}\right)_{pilehead} = \sqrt{\frac{\lambda}{\beta}} \tag{C-2}$$

in which,

> T_0 = The torque applied at the top of the pile
>
> β = The reciprocal of the product of the pile material shear modulus, G_p, and its polar moment of inertia, J
>
> λ = A function of the tosional restraint of the soil = $4\pi r^2 G_s$
>
> r = Radius
>
> G_s = Shear modulus of the soil

The above linear interaction problem is based on the assumption that the torsional restraint of the soil can be represented for all rotations and for all depths by a single

parameter, λ. However, the boundary effects near the top of the pile and non-linear soil response could preclude the use of a value for λ which is constant with depth.

In order to include the non-linearity, O'Neill (1964) suggested a discrete element model that simulates torsional behavior of a circular, prismatic pile. A three-element portion of that model is shown in Figure C-1.
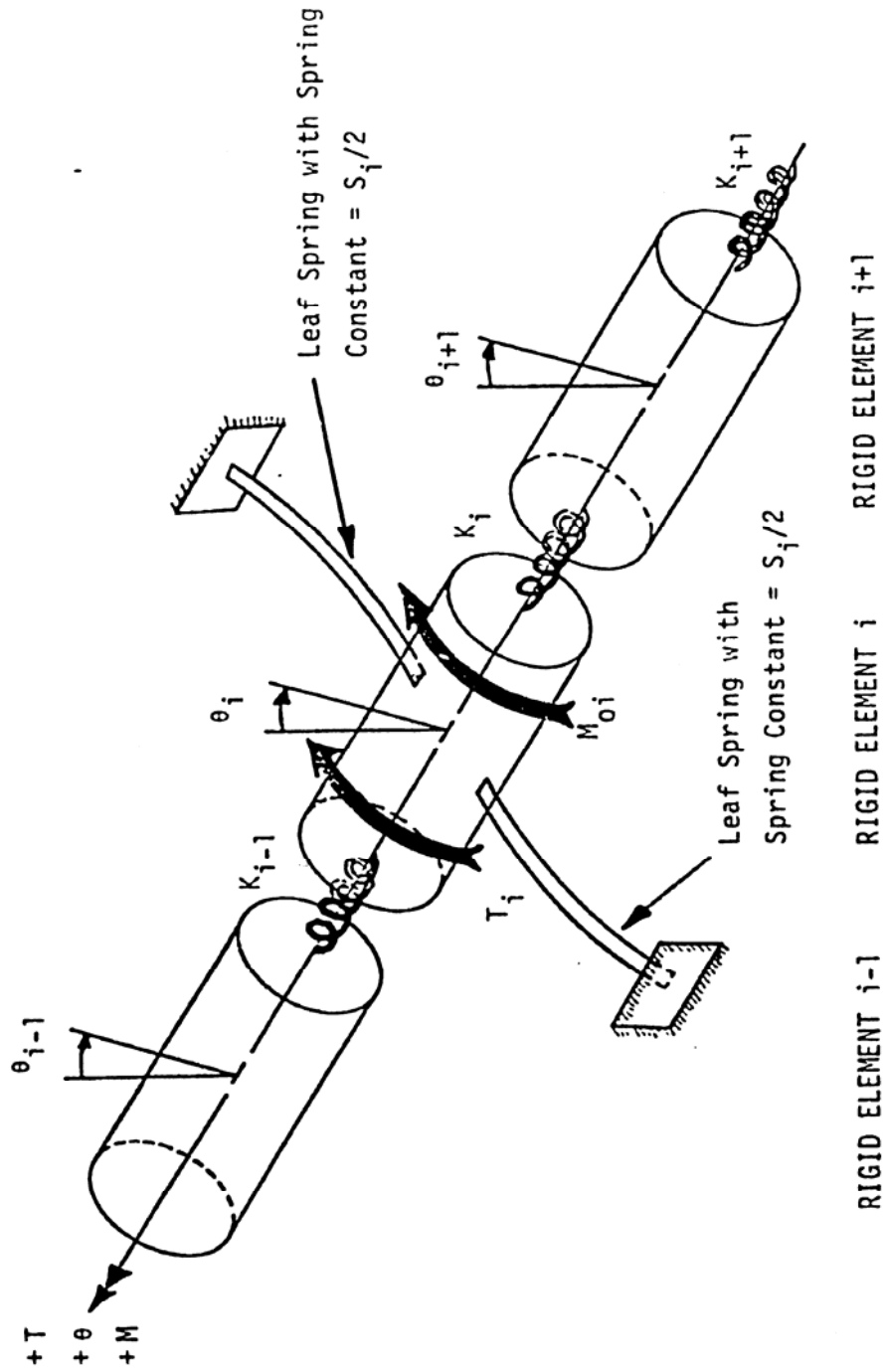
Figure C-1. Mechanical Finite Element Model of Torsionally Loaded Pile for Simulating Torque-Twist Behavior (After O'Neill, 1964)

The mechanical model is composed of rigid elements connected by torsional springs with spring constants k_i. The non-linear torsional resistance of the soil can be represented partially by a spring constant S_i and partially by a fixed moment M_{0i}.

The relationship of twist angle and torque is given by:

$$\theta_i = \frac{(T_i + M_{0i}) + k_{i-1}A_{i-1}}{C_i} + \frac{K_i}{C_i}\theta_{i+1} \tag{C-3}$$

where $C_i = k_{i-1}(1 - B_{i-1}) + k_i - S_i$

$$A_i = \frac{(T_i + M_{0i}) + k_{i-1}A_{i-1}}{C_i}$$

$$B_i = \frac{k_i}{C_i}$$

In order to solving non-linear torque-twist problems, an iterative procedure may be used by successively adjusting the S values and M_0 values to insure compatibility between S and θ everywhere along the pile until closure within a specified tolerance, usually expressed in terms of rotation at the pile head, is achieved.

Poulos(1975) presented a numerical elastic analysis of the response of a single cylindrical pile subjected to torsion by using integral equation techniques. The parametric solutions for the rotation of the pile head are presented, for both a uniform soil and a soil in which shear modulus and pile-soil adhesion increase linearly with depth.

Fig.C-2(a) shows the problem. The pile shaft is divided into n equal cylindrical elements and the base is composed of m annular elements, each element being acted upon by an unknown uniform interaction stress [Fig. C-2(b)].
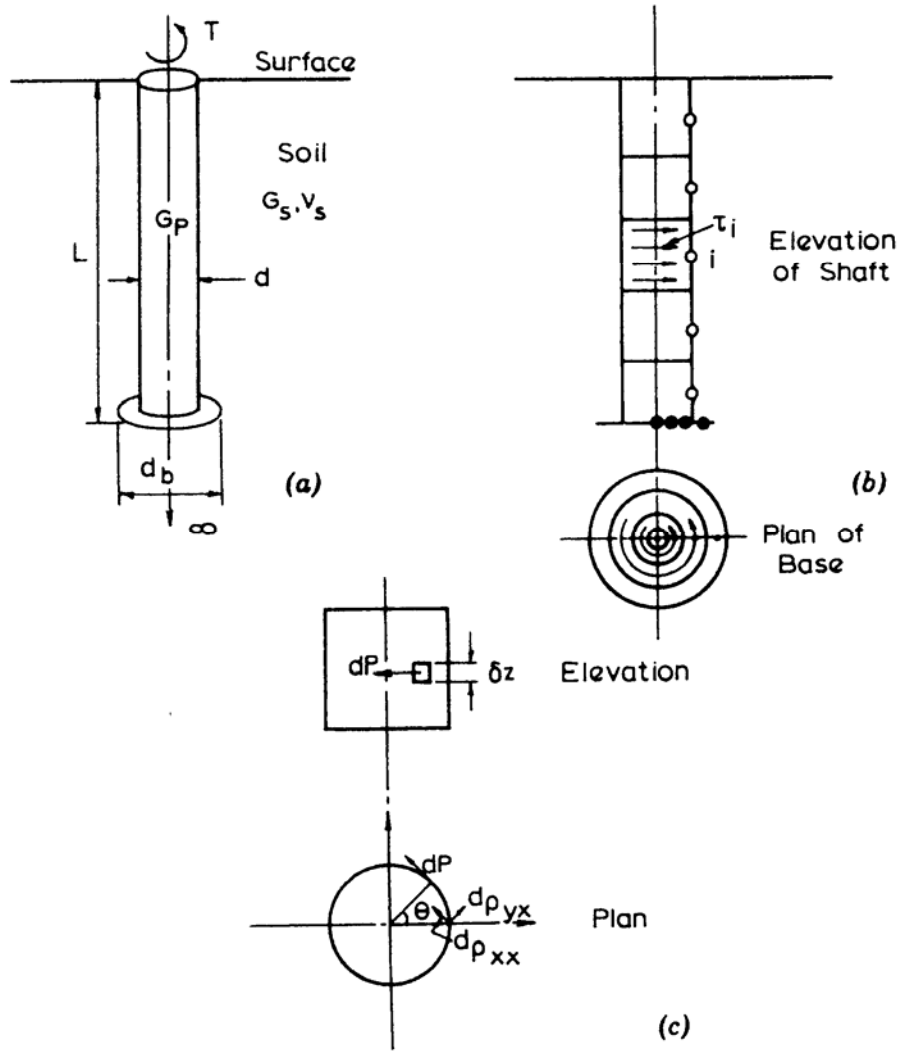
Figure C-2 Definition of Problem:(a) Geometry; (b) Division of Pile into Elements; (c) Detail of Area of Element (After Poulos 1975).

For a uniform-diameter pile in a soil with constant shear modulus and pile- soil adhesion, the top rotation can be expressed as

$$\phi = \frac{T}{G_s d^3} \frac{I_\phi}{F_\phi} \qquad \text{(C-4)}$$

For a soil having shear modulus and pile-soil adhesion that increase linearly with depth, the top rotation can be given by

$$\phi = \frac{T}{N_G d^4} \frac{I'_\phi}{F'_\phi} \qquad \text{(C-5)}$$

in which I_ϕ, I_ϕ' = elastic rotation influence factor; G_s = soil shear modulus, and F_ϕ, F_ϕ' = correction factor for the effects of pile-soil slip, N_G = rate of increase of shear modulus with depth($G_s = N_G z$) .

Randolph (1981) presented closed-form solutions for the torsional stiffness of a pile in homogeneous soil and a soil where the stiffness is proportional to depth, based on a simple assumption that the shear stress $\tau_{z\theta}$ is negligible compared to $\tau_{r\theta}$. The analysis also assumes that the soil deforms in an elastic or pseudo-elastic manner.

For homogeneous soil, the shear modulus of soil G is constant.

For rigid circular pile, the torsional stiffness of pile top is given by

$$\frac{T_t}{Gr_0^3\phi_t} = \frac{16}{3} + 4\pi\frac{l}{r_0} \tag{C-6}$$

in which G = the shear modulus of the soil, r_0 = the radius of pile, Φ_t= the rotation of the pile top, T_t = the torque of pile top.

For flexible pile, the torsional stiffness of pile top is given by

$$\frac{T_{top}}{Gr_0^3\phi_{top}} = \frac{\left(\dfrac{16}{3} + 4\pi\dfrac{l}{r_0}\dfrac{\tanh(\mu l)}{\mu l}\right)}{\left(1 + \dfrac{32}{3\pi\lambda}\dfrac{l}{r_0}\dfrac{\tanh(\mu l)}{\mu l}\right)} \tag{C-7}$$

in which $\mu l = \left(\dfrac{8}{\lambda}\right)^{1/2}\left(\dfrac{1}{r_0}\right)$, $\lambda = G_p/G_s$.

When the applied torque approaches ultimate torque, the torsional stiffness of the head of pile can be estimated as:

$$\frac{T_t}{\phi_t} \approx 2\frac{(GJ)_p}{l} \tag{C-8}$$

For Soil Shear Modulus Proportional to Depth

The assumption is also made that the soil deforms in an elastic or pseudo-elastic manner. For rigid pile, the torsional stiffness of the pile head is written as

$$\frac{T_t}{mr_0^4 \phi_t} = \frac{1}{r_0} \left(\frac{16}{3} + 2\pi \frac{1}{r_0} \right) \tag{C-9}$$

For flexible pile, the governing differential equation is

$$\frac{d^2\phi}{dz^2} = \frac{8}{\lambda' r_0^2} \frac{z}{r_0} \phi \tag{C-10}$$

in which $\lambda' = G_p /(mr_0)$.

Solution of this equation is possible in terms of Airy functions. By applying the pile base boundary condition, torsinal stiffness can be calculated.

When the applied torque approaches ultimate torque, the torsional stiffness of the head of pile can be estimated as:

$$\frac{T_t}{\phi_t} \approx 1.5 \frac{(GJ)_p}{1} \tag{C-11}$$

Chow (1985) presented a discrete element approach for the analysis of torsional response of piles in nonhomogeneous soil. This approach can deal with complex soil stratification, and arbitrarily varying pile sections. However, the modulus of subgrade reaction is linear, so this method only gives out the solution for linear soil response.

The governing equilibrium equation using the modulus of subgrade reaction approach is given by

$$-G_p J \frac{\partial^2 \psi}{\partial z^2} + k_\psi \psi = 0 \tag{C-12}$$

in which G_p = shear modulus of pile material; J = polar second moment of area of pile section; ψ = angle of twist of pile; k_ψ = modulus of subgrade reaction of soil undergoing torsion; and z = depth coordinate.
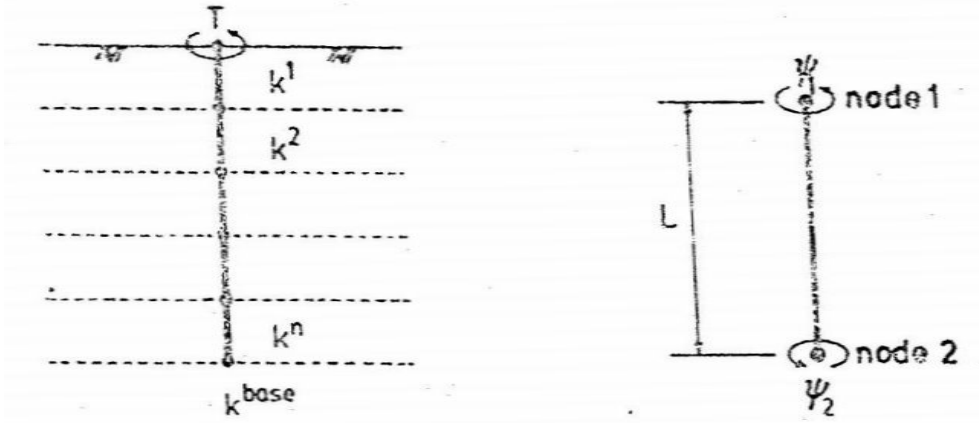
Figure C-3 (a) Discrete Element Model For Torsional Response of Pile (after chow 1985)

(b) Typical Torsional Discrete Element (after chow 1985)

The soil is discretized into a series of elements connected at the nodes. The soil is also divided as horizontal layers, each layer with a modulus of subgrade reaction, k as shown in Fig. C-3(a). Fig.C-3(b) shows the typical element. The continuous variable, ψ, is approximated in terms of its nodal values ψ_1 and ψ_2 through

$$\psi = \{n\}^T \{ \psi \} \tag{C-13}$$

in which $\{n\} = \left\{ \begin{array}{c} 1 - \dfrac{Z}{L} \\ \dfrac{Z}{L} \end{array} \right\}$, and $\{\psi\} = \left\{ \begin{array}{c} \psi_1 \\ \psi_2 \end{array} \right\}$

Applying Galerkin method to the governing equation results in the following element matrix equation:

$$[K_p]\{\psi\} + [K_s]\{\psi\} = \{0\} \tag{C-14}$$

in which the pile element matrix is

$$K_p = \int_0^L G_p J \left\{ \frac{\partial n}{\partial z} \right\} \left\{ \frac{\partial n}{\partial z} \right\}^T dz$$

and the soil element matrix is

$$[K_s] = \int_0^L k_\psi \{n\} \{n\}^T dz$$

Assembly of the stiffness matrix for the pile-soil system is done element by element. In this way, soils with complex stratification and piles with arbitrarily varying sections can be dealt with.

The modulus of subgrade reaction of soil at the pile shaft is given by

$$k_\psi^{side} = 4\pi Gr_0^2 \qquad\qquad (C\text{-}15)$$

in which G = shear modulus of soil; and r_0 = pile radius.

For soil the shear modulus is proportional to depth, G = mz, in which m = rate of increase of shear modulus with depth. The modulus of subgrade reaction per unit increase in depth is given by

$$k_\psi^* = 4\pi mr_0^2 \qquad\qquad (C\text{-}16)$$

The subgrade reaction modulus of pile tip is given by

$$k_\psi^{base} = \frac{16}{3} Gr_0^3 \qquad\qquad (C\text{-}17)$$

Hache & Valsangkar (1988) developed simple mathematical solutions for torsionally loaded pile in a layered soil and nondimensional charts for design purpose. Actually, the nondimensional solutions and charts for two layer soils are similar with Poulos(1975) suggested parametric solution for one layer homogeneous soil. The advantage is this solution can deal with piles in layered soils. The analysis assumes elastic soil response.

The solutions are based on Randolph's (1981) simplified elastic solution. Fig.C-4 depicts the pile-soil analysis model.
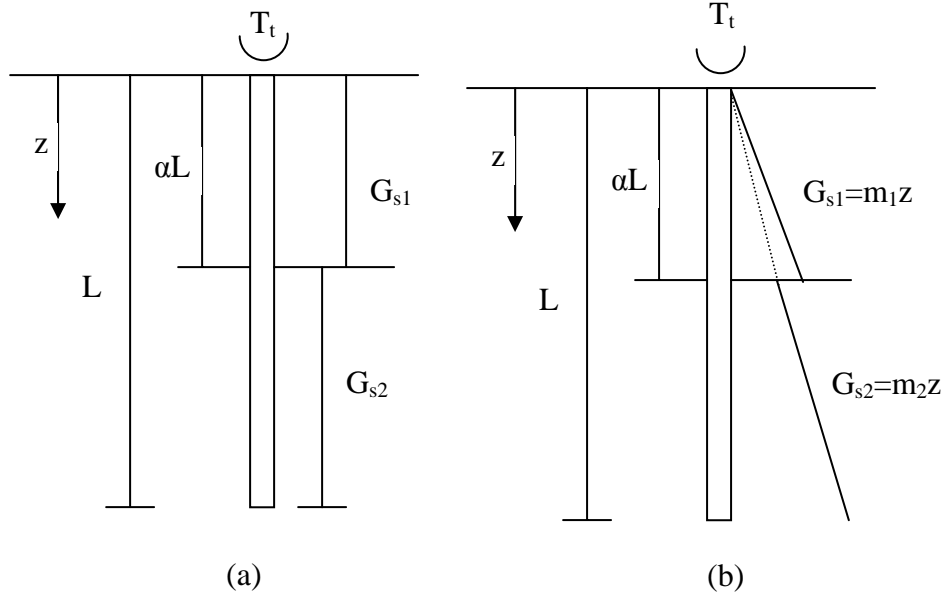
Figure C-4. Pile in Two-Layered Soil: (a) Homegeneous Layers; (b) Nonhmeogeneous Layers

For homogeneous layered soil, the governing differential equations are (Randolph 1981; Scott 1981)

$$\frac{\partial^2 \phi}{\partial z^2} - \eta \lambda_2'^2 \phi = 0, 0 \le z \le \alpha L \tag{C-18}$$

$$\frac{\partial^2 \phi}{\partial z^2} - \lambda_2'^2 \phi = 0, \alpha L \le z \le L \tag{C-19}$$

in which $\lambda_2' = \sqrt{\left(4\pi r_0^2 G_{s2}\right) / (GJ)_p}$; $\eta = G_{s1}/G_{s2}$; $(GJ)_p$ = pile torsional stiffness; r_0 = radius of the pile; z = depth from the soil surface; L = length of the pile; and αL = thickness of the upper layer.

The solutions are

$$\phi = C_1 e^{-\sqrt{\eta}\lambda_2' z} + C_2 e^{-\sqrt{\eta}\lambda_2' z}, 0 \le z \le \alpha L; \tag{C-20}$$

$$\phi = C_3 e^{-\lambda_2' z} + C_4 e^{\lambda_2' z}, \alpha L \le z \le L; \tag{C-21}$$

For a two-layered soil where the shear modulus is linearly varying with depth:

C-11

$$\frac{\partial^2 \phi}{\partial z^2} - \eta_1 \lambda_2^3 z\phi = 0, 0 \le z \le \alpha L \qquad (C-22)$$

$$\frac{\partial^2 \phi}{\partial z^2} - \lambda_2^3 z\phi = 0, \alpha L \le z \le L \qquad (C-23)$$

in which $\lambda_2 = 3\sqrt{\left(4\pi r_0^2 m_2\right)/(GJ)_p}$; $\eta_1 = m_1/m_2$; and m_1 and m_2 are slopes of the soil stiffness variation with depth. The solutions are:

$$\phi = C_1\beta(\eta_1^{1/3}\lambda_2 z) + C_2 z\xi(\eta_1^{1/3}\lambda_2 z), 0 \le z \le \alpha L; \qquad (C-24)$$

$$\phi = C_3\beta(\lambda_2 z) + C_4 z\xi(\lambda_2 z), \alpha L \le z \le L; \qquad (C-25)$$

Using the pile top and tip boundary conditions and the result equations, nondimensional solutions and charts are developed. The relationship between twist angle of pile top and applied torque is given by

$$\phi_t = \frac{T_t L}{(GJ)_p}(I_\phi) \qquad (C-26)$$

Guo & Randolph (1996) presented analytical and numerical solutions for the torsional response of piles embedded in non-homogeneous soil by assuming that the stiffness profile of the soil follows a simple power law with depth.

The soil modulus is assumed as a power law variation of depth, given by

$$G_i = A_g z^n \qquad (C-27)$$

in which G_i is the initial shear modulus at depth z; A_g is a modulus constant; and n is the depth exponent, referred to here as the non-homogeneity factor.

The limiting shaft friction τ_f is also assumed as a power law variation with depth, as

$$\tau_f = A_t z^t \qquad (C-28)$$

in which A_t is a constant that determines the magnitude of shaft friction, and t is the corresponding non-homogeneity factor, and t = n is assumed.

Elastic solution

The ratio of torque and rotation can be expressed as

$$\frac{T(z)}{\phi(z)} = \pi_t^{1/2m} C_t(z) \frac{(GJ)_p}{L} \tag{C-29}$$

in which

$$\pi_t = \left(\frac{\pi d^2 A_g L^{n+2}}{(GJ)_p} \right)^m$$

$$C_t(z) = \frac{C_1(z) + \chi C_2(z)}{C_3(z) + \chi C_4(z)} \left(\frac{z}{L} \right)^{n/2} ;$$

$$C_1(z) = -K_{m-1} I_{m-1}(y) + K_{m-1}(y) I_{m-1} ; \quad C_2(z) = K_m I_{m-1}(y) + K_{m-1}(y) I_m ;$$

$$C_3(z) = K_{m-1} I_m(y) + K_m(y) I_{m-1} ; \quad C_4(z) = -K_m I_m(y) + K_m(y) I_m ;$$

I_{m-1}, I_m, K_m, and K_{m-1} are the values of the Bessel functions for $z = L$;

$$\chi = \frac{16 G_b r_0^3 L}{3(GJ)_p} \frac{1}{\pi_t^{1/2m}}$$

Elastic-plastic solution

The soil response is modeled as elastic-perfectly plastic. The torque at the pile head, T_t, can be given by

$$T_t = T_e + 0.5\pi d^2 \frac{A_t L_1^{n+1}}{n+1} \tag{C-30}$$

in which,

$$T_e = 0.5\pi_t^{1/2m} C_t(\mu L) \frac{A_t}{A_g} \frac{(GJ)_p}{L} ;$$

$$\mu = L_1/L;$$

L_1 = the length of pile where slip has occurred.

And the twist angle of the pile head can be expressed as:

$$\phi_t = \phi_e + \frac{L_1}{(GJ)_p} \left(T_e + 0.5\pi d^2 \frac{A_t L_1^{n+1}}{n+2} \right) \tag{C-31}$$

where $\phi_e = \dfrac{A_t}{2A_g}$.

Pile response with hyperbolic soil model

Non-linear response of the soil is assumed as a hyperbolic stress-strain law, where the secant shear modulus G is written as

$$G = G_i (1 - R_f \frac{\tau}{\tau_f})$$ (C-32)

in which R_f is the hyperbolic parameter that controls the ratio of the secant modulus at failure, to the initial tangent modulus G_i.

And the angle of twist of the pile will be given by

$$\phi = \left(\frac{v}{r} \right)_0 = \frac{\tau_f}{G_i} \frac{1}{2R_f} [-\ln(1 - \psi)]$$ (C-33)

in which $\psi = R_f \tau_0 / \tau_f$, τ_0 the shear stress at the side of pile.

For rigid piles, the angle of twist will be uniform down the pile, so the overall torsional stiffness can be written in the form adopted by Randolph (1981) as

$$\frac{T_t}{A_g L^n r_0^3 \phi_t} = \frac{16}{3} + \frac{4\pi}{n+1} \frac{L}{r_0} \frac{-\psi}{\ln(1-\psi)}$$ (C-34)

For flexible piles, it is necessary to use a numerical approach so that the non-linear torque transfer curve can be implemented. A spreadsheet program, GASPILE has been developed for torsional loading.

Lin (1996) proposed a finite element numerical procedure for the analysis of torsional behavior of cracked reinforced concrete pile. A trilinear torque-twist model is employed to represent the torsional response of the reinforced concrete pile element with maximum torsional stresses. The remaining part of the pile is modeled as a linear elastic torsional behavior. Hyperbolic nonlinear model is employed to model the torsional resistance of the soil along the pile shaft. Both linear and nonlinear analyses were performed and showed the importance of taking into account the changing of pile stiffness once concrete has cracked.

1.2. Methods for rock

Carter & Kulhawy (1988) presented an approximate linear elastic solution for torsionally loaded shafts in rock. The solution followed Randolph's (1981) approximate solution for torsional response of piles in soils.

For homogeneous rock, the solutions will be developed for two cases, one for shaft in a "complete" rock socket and one for shaft in a "side shear only" socket.

For complete socket, the torsional stiffness of pile head is given by:

$$\frac{T}{G_r B^3 \phi} = \frac{(\frac{2}{3})(\frac{1}{\xi}) + \pi(\frac{D}{B}) \frac{\tanh(\mu D)}{\mu D}}{1 + (\frac{64}{3\pi\lambda\xi})(\frac{D}{B}) \frac{\tanh(\mu D)}{\mu D}} \qquad (C\text{-}35)$$

in which $\xi = G_r / G_b$, D = the length of shaft, $\mu^2 = 32/(\lambda B^2)$ and $\lambda = G_e / G_r$, $G_e = (GJ)_c /(\pi B^4 / 32)$, B = shaft diameter, $(GJ)_c$ = shaft torsional rigidity, G_r = elastic shear modulus of rock, G_b = the shear modulus of rock below shaft.

For side shear socket, the stiffness can be given by

$$\frac{T}{G_r B^3 \phi} = \pi(\frac{\tanh[\mu D]}{\mu D})(\frac{D}{B}) \qquad (C\text{-}36)$$
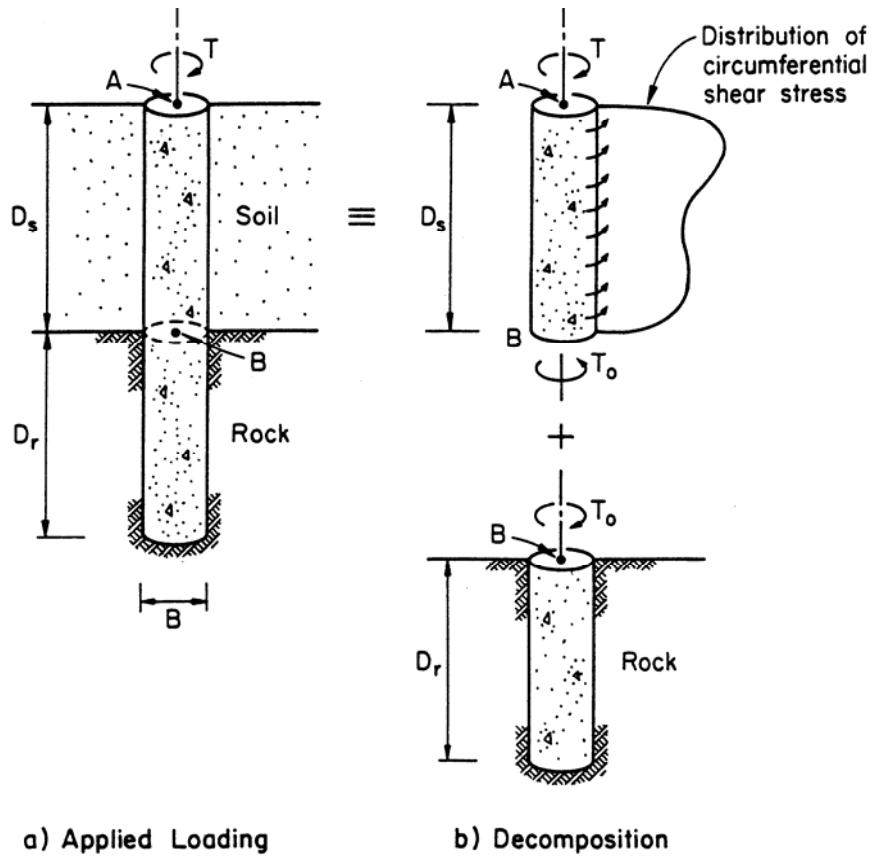
Figure C-5. Rock Socketed Shaft under Torsional Loading with Overlying Soil

For soil overlying rock conditions (Fig. C-5), an assumption is made that the presence of the soil layer could be ignored completely, in which case zero shear stress would be considered at the face of the shaft. Then the twist angle between point A and point B is:

$$\phi_{AB} = \frac{TD_s}{(GJ)_c} \tag{C-37}$$

This quantity combined with the twist of the lower portion of the shaft embedded in the rock would give the overall twist at the groundline, ϕ.

For cohesive soil, the twist of point A relative to B is given by

$$\Phi_{AB} = \frac{1}{(GJ)_c}(TD_s - \pi B^2 D_s^2 \tau_f / 4) \tag{C-38}$$

For cohesionless, Φ_{AB} can be given by

$$\Phi_{AB} = \frac{1}{(GJ)_c}(TD_s - \frac{\pi}{12}B^2 D_s^3 \rho) \tag{C-39}$$

Florida Pier Analysis Program suggested a hyperbolic curve to model the non-linear T-θ behavior (Fig. C-6). The curve is defined as

$$T = \frac{\theta}{a + b\theta} \tag{C-40}$$

where the coefficients a and b are given by

$$\frac{1}{a} = \text{initial slope} = \left(\frac{dT}{d\theta}\right)_i = 4\pi r_0^2 G_i \Delta L$$

$$\frac{1}{b} = T_{ult} = 2\pi r_0^2 \tau_{ult} \Delta L$$

This hyperbolic model does not consider the pile tip stiffness.
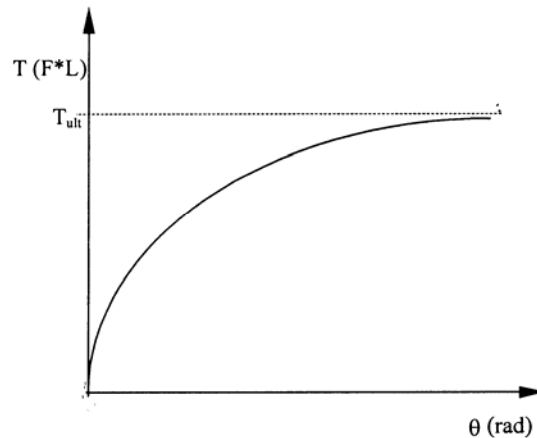
Figure C-6 Hyperbolic representation of T-θ curve

2.Existing methods for ultimate torsional resistance of piles

2.1 Methods For all kind of Soils

FDOT Structural Design Office Method

FDOT Structural Design Office Method only deals with the torsional problem of drilled shaft under simple torsional load, and the method assumes that the soil behaves as a rigid

plastic material, but the soil can be cohesive or cohesionless. By discretizing the drilled shaft, the method can also be applied to stratified soil. For cohesionless soil the method can be applied as follows:

$$T_s = (K_0 \cdot \gamma \cdot 0.5L^2) \cdot \pi \cdot D \cdot \tan\delta \cdot 0.5D \qquad \text{(C-41)}$$

in which T_s = side torsional resistance, ft-kips,

$\quad$ K_0 = at rest lateral earth pressure coefficient,

$\quad$ γ = effective soil unit weight, lb/ft^3,

$\quad$ L = length of drilled shaft foundation, ft,

$\quad$ D = diameter of drilled shaft foundation, ft,

$\quad$ δ = friction angle at the soil-concrete interface, in the case of drilled foundations, it is equal to the internal friction angle of the soil, φ of embedded soil.

Additionally, the base torsional resistance can be calculated as:

$$T_b = W \cdot \tan\delta \cdot 0.33D \qquad \text{(C-42)}$$

in which T_b = base torsional resistance, ft-kips,

$\quad$ W = weight of the drilled shaft foundation, kips,

$\quad$ D = diameter of the drilled shaft foundation,

$\quad$ δ = same definition as above

After determining the side and base frictional resistance, the total torsional capacity of the drilled shaft

$$T_{total} = T_s + T_b. \qquad \text{(C-43)}$$

Colorado Department of Transportation design methods for torsion.

The torsional design methods for CDOT practice was developed by Richard Osmun. For torsion in cohesive soils, the torsional resistance comes from side resistance and base resistance. The side resistance for the top 1.5D of shaft length is neglected. Then, the total torsional capacity of drilled shaft in clay is given by:

$$T_{clay} = \pi D(L - 1.5D)c(D/2) + \pi(D^2/4)c(D/3) \qquad \text{(C-44)}$$

in which, D = shaft diameter, L = the embedment length of drilled shaft, c = cohesion of soil. A 1.25 safety factor for the torsional design of drilled shafts in cohesive soils was used to keep torsion from controlling the shaft depth.

For torsion in cohesionless soils, both the side resistance and base resistance contribute to the total torsional capacity of drilled shaft. For the calculation of the side resistance, the side friction, f, is calculated by

$$f = K\sigma'_v\mu \tag{C-45}$$

in which K = earth pressure coefficient, σ'_v = effective overburden pressure, μ = friction coefficient. For the determination of the value of K, the following procedure is carried out.

The weight of the soil mass in the sliding wedge is larger for a circular configuration than for a planer configuration, therefore, K = $\eta(1-\sin\varphi)$ where η = volume of a slice (circular segment) divided by the volume of a wedge (planer segment), and φ = friction angle of soil.

L

L

45°

(a) At rest failure plane

θ

R

S

S

L

Slice
(circular
segment)

Wedge
(planer
segment)

(b) Plan view of slice and wedge

L

θ

L

R

(c) Sliding slice

L-R

θ

L

(d) Planer wedge
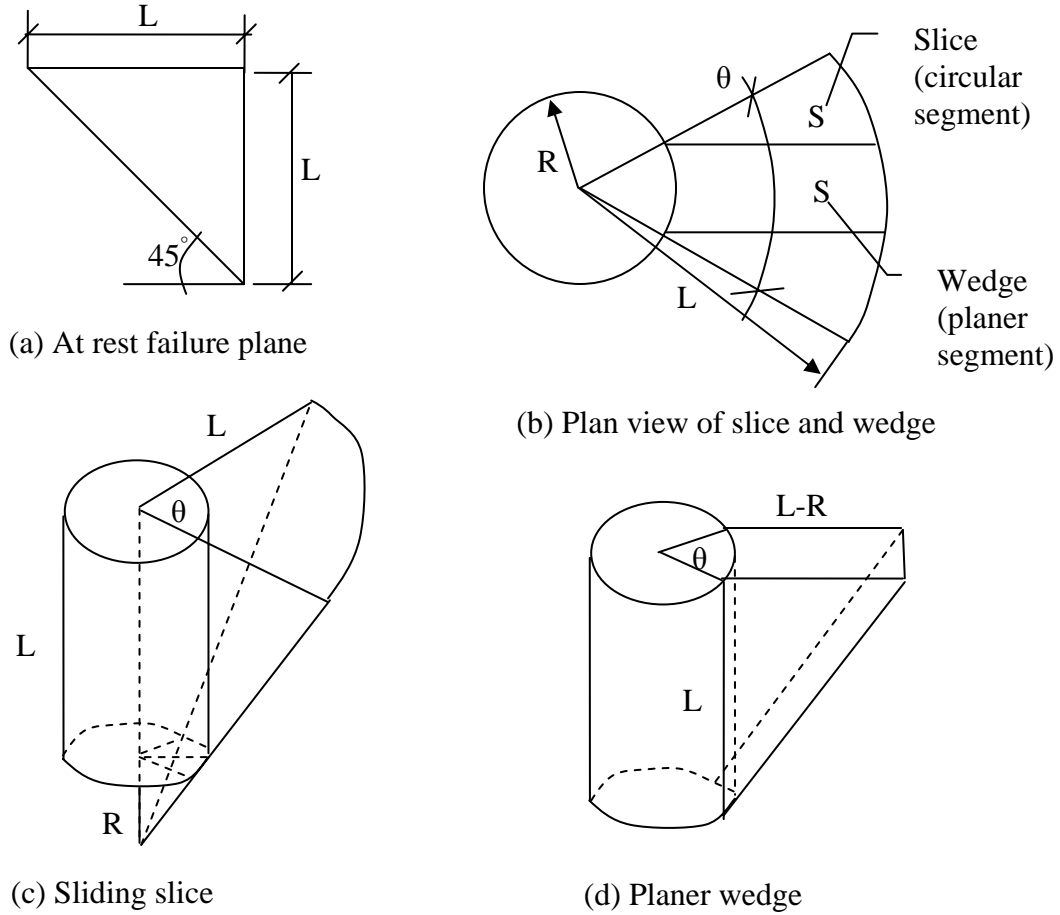
Figure C-7 Sliding Wedge

The volume of slice excluding the shaft volume involved in the slice is:

$$V_L = \frac{1}{3}\pi L^2(L+R)\frac{\theta}{2\pi} - \frac{\theta}{2\pi}\pi R^2 L - \frac{1}{3}\pi R^2 R\frac{\theta}{2\pi} \approx \frac{1}{6}(L^3 - R^3)\theta - \frac{\theta}{2}R^2 L \approx \frac{1}{6}L^3\theta \quad \text{(C-46)}$$

(If R is small compared to L)

in which L = shaft embedment length, R = the radius of drilled shaft, θ = the slice angle shown in Fig. C-7.

The volume of wedge is:

$$V_R = \frac{R\theta(L-R)L}{2} \approx \frac{R\theta L^2}{2} \quad \text{(If R is small compared to L)} \quad \text{(C-47)}$$

Then, the value of η can be calculated as:

$$\eta = \frac{V_L}{V_R} \approx \frac{L}{3R} \qquad\qquad (C\text{-}48)$$

Correspondingly, K can be rewritten as:

$$K = \eta K_0 = \frac{L}{3R}(1 - \sin \phi) \qquad\qquad (C\text{-}49)$$

Therefore, the total torsion capacity of drilled shaft in sand contributed from side resistance and base resistance, can be given by:

$$T_{sand} = (K\gamma \frac{L}{2})(L)(\pi D)\mu(\frac{D}{2}) + w\mu(\frac{D}{3}) \qquad\qquad (C\text{-}50)$$

in which, $K = \eta(1-\sin\varphi)$, $\eta = 2L/(3D)$ for circular drilled shaft, $\mu = \tan\delta$, δ = soil friction angle φ if the side contact between shaft and soil is very rough, w = the weight of shaft. A 1.25 safety factor for the torsional design of drilled shafts in cohesionless soils was used to keep torsion from controlling the shaft depth.

2.2 Methods For Sands

Florida District 5 Method

Florida District 5 Method uses the ultimate skin friction from the SHAFTUF program to determine the side friction of the drilled shaft. And the side torsional resistance is

$$T_s = Q_s (D/2) \qquad\qquad (C\text{-}51)$$

Also the base torsional resistance is

$$T_b = 0.67 \cdot (W + A_y) \cdot \tan(0.67\varphi) \cdot (D/2) \qquad\qquad (C\text{-}52)$$

in which W = the weight of drilled shaft, lbs,

A_y = vertical loading upon the drilled shaft, lbs,

By summing the side and base resistance, the total resistance can be obtained.

Additionally, District 5 proposed to use O'Neill and Hassan approach for shaft subjected to axial loads. And the following equation for cohesionless soil is suggested

$$f_s = \sigma_{vz} \cdot \beta \qquad\qquad (C\text{-}53)$$

in which σ_{vz} = effective vertical stress, β = load transfer ratio and it can be estimated as:

For $N_{spt} < 15$, $\beta = (N/15) \, \beta_{nominal}$; for $N_{spt} > 15$, $\beta_{nominal} = 1.5\text{-}0.135 \sqrt{z}$, $1.2 \geq \beta_{nominal} \geq 0.25$, in which z = depth below ground surface, ft.

The total side friction can be described as

$$Q_s = \pi \cdot D \cdot L \cdot f_s \qquad \text{(C-54)}$$

And the base resistance to torsional loading is

$$Q_b = 0.67 \cdot (W + A_y) \cdot \tan(\delta) \qquad \text{(C-55)}$$

Thus the total torsional resistance is

$$T = Q_s \cdot (D/2) + Q_b \cdot (D/2). \qquad \text{(C-56)}$$

Tawfiq (2000) proposed a method for ultimate torsional capacity of drilled shaft in sands under torsional and lateral loading conditions. The method obtains the net lateral soil pressure along the shaft by combining the soil pressure from subgrade reaction method and the threshold lateral pressure from Rankin's theory. Then, the maximum torsional resistance is determined by using limiting shear stress from net lateral soil pressure along the shaft.

Subgrade reaction approach is adopted for determining the lateral soil pressure of drilled shaft under lateral loads. The lateral pressure distribution at each depth was considered as a combination of active pressure and pressure due to the lateral load. The resultant pressure around the shaft perimeter at specified depths was calculated by using Smith's suggestion (Fig. C-8) for the pressure distribution.
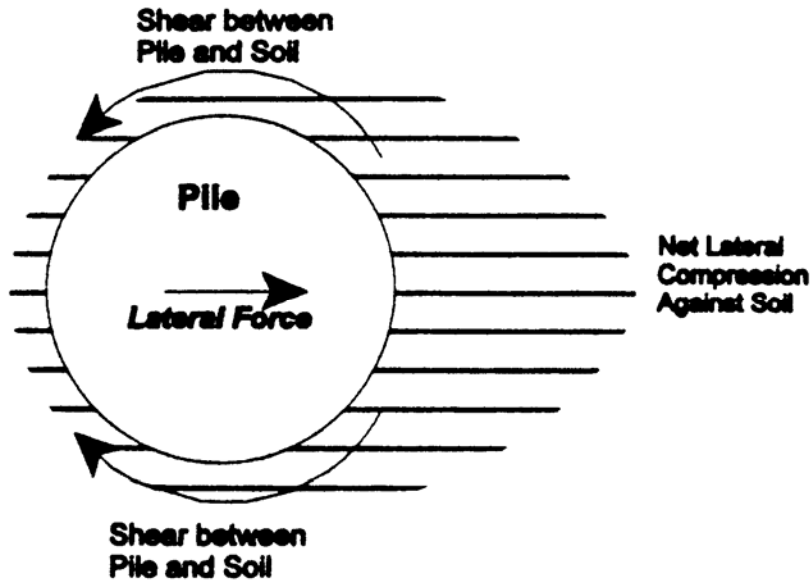
Figure C-8 The soil resistance to lateral pile movement has both compression and shear components. The sum of them is the p in p-y curves (After Smith, 1989)

The Rankin's method is used to set the threshold lateral pressure along the shaft (Fig C-9). Then, the net soil pressure is integrated along the shaft (Fig. C-10).

The limiting side shear stress is determined by

$$\tau = p_h \tan \delta \qquad \text{(C-57)}$$

in which p_h = integrated net soil pressure along the shaft

δ = soil-shaft angle of friction $\approx \varphi$ = soil angle of friction. It is recommended that a factor of 0.5 to 0.6 is used when attapulgite or bentonite slurries are used.

Finally, the ultimate torsional capacity of resistance can be obtained with

$$T = \sum_{0}^{n} \sum_{0}^{nang} R^2 \frac{2\pi}{nang} \frac{L}{n} \tan(\delta)\tau \qquad \text{(C-58)}$$

in which n = segment number of shaft along shaft depth

$nang$ = angle number of shaft section.
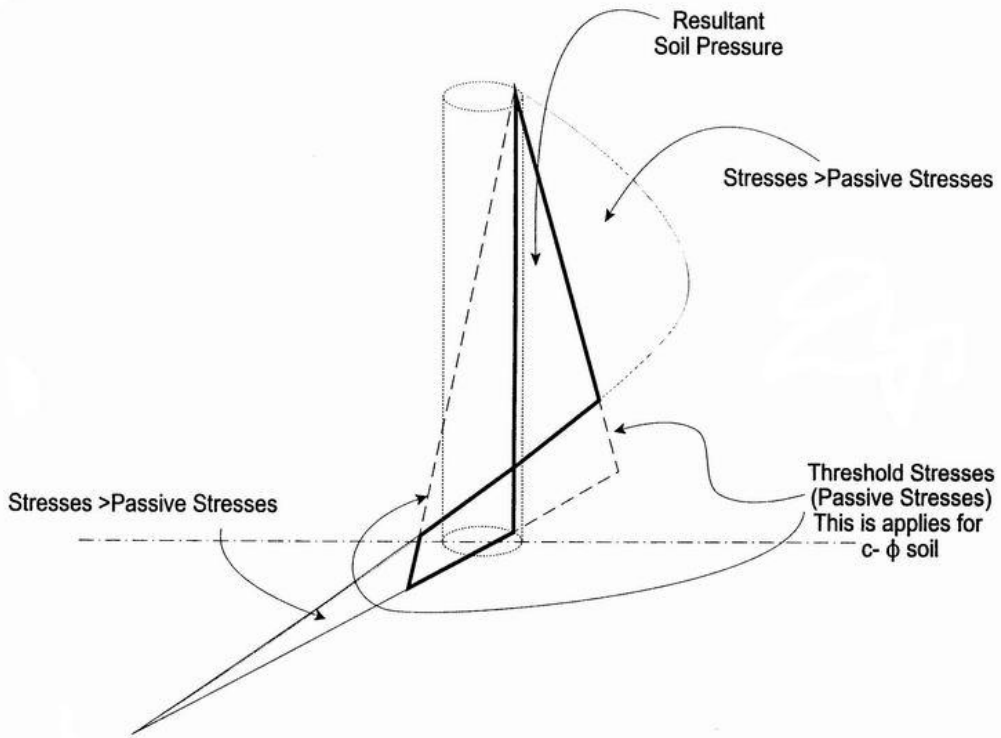
Figure C-9. Setting the threshold pressure (Rankin's Pressure) at each depth along the shaft (after Tawfiq 2000)
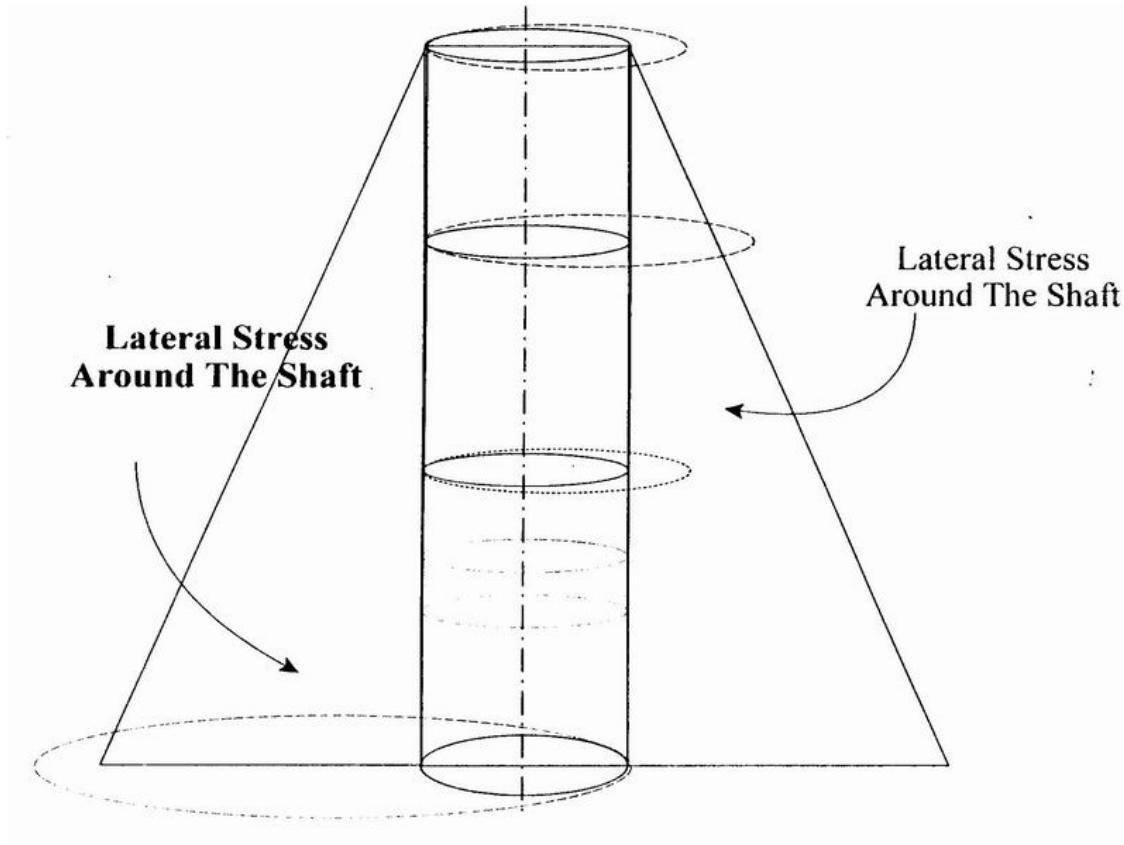
Figure C-10 Final Pressure along the Shaft (After Tawfiq 2000)

2.3 Methods For Clay

Florida District 7 Method

Florida District 7 Method is based on the α method for drilled shaft in clay. According to α method (Tomlinson, 1971), the unit friction is

$$f_s = \alpha \cdot C + \overline{q} \cdot K \cdot \tan \delta \tag{C-59}$$

in which α = the adhesion factor,

C = average cohesion (or S_u) for the soil stratum of interest,

$\overline{q}$ = effective vertical stress on element of the shaft,

δ = effective friction angle between soil and pile material,

K = coefficient of lateral earth pressure ranging from K_0 to about 1.75, values close to K_0 are generally recommended and

$$K_0 = (1 - \sin \varphi)\sqrt{OCR} \tag{C-60}$$

in which OCR = the over consolidation ratio.

The total base resistance is calculated as

$$Q_b = 0.67 \cdot (W + A_y) \cdot \tan(\delta) \qquad\qquad (C\text{-}61)$$

in which W = the weight of the deep drilled shaft, lbs,

A_y = vertical loading upon the drilled shaft, lbs.

Then total base torsion resistance can be calculated as

$$T_b = Q_b(0.67 \cdot D) \qquad\qquad (C\text{-}62)$$

The total torsional side resistance can be obtained by using

$$T_s = p \cdot L \cdot \sum f_s \cdot D / 2 \qquad\qquad (C\text{-}63)$$

in which p = circumferential area of drilled shaft foundation, pD,

L = length of drilled shaft foundation, ft,

D = diameter of drilled shaft, ft.

Thus, the total torsional resistance is the summation of the side and base torsional resistance.

2.4 Methods For Rocks

N/A

3.The Tests of Pile's Torsional Response

3.1 Torsion Tests --- In Clay

Stoll (1972) devised a field torque shear load test to determine the required penetration depth of friction piles in clay. He conducted two field torsion load tests on steel pipe piles of 0.273m external diameter and 6.3mm wall thickness. Fig.C-11 shows the typical test setup. An early setup includes dial gage and reference beam to measure torque displacement at top of the test pile. Fig.C-12 shows the test results.
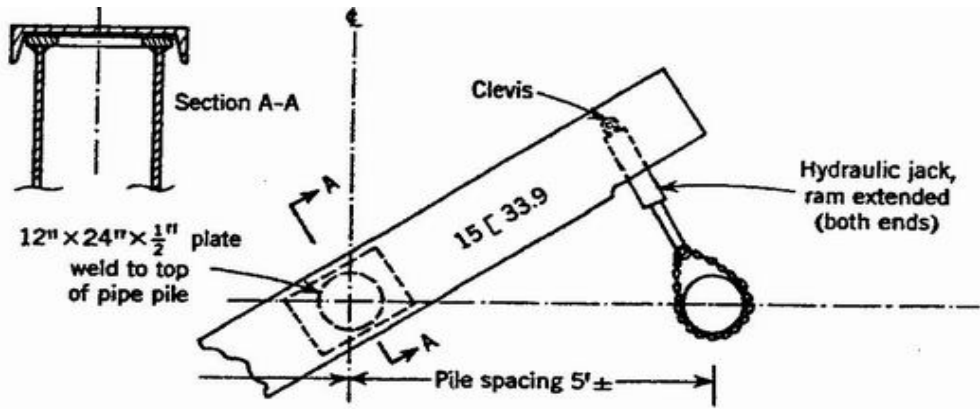
Figure C-11 Pile Torque Shear Test Set Up (After Stoll 1972)
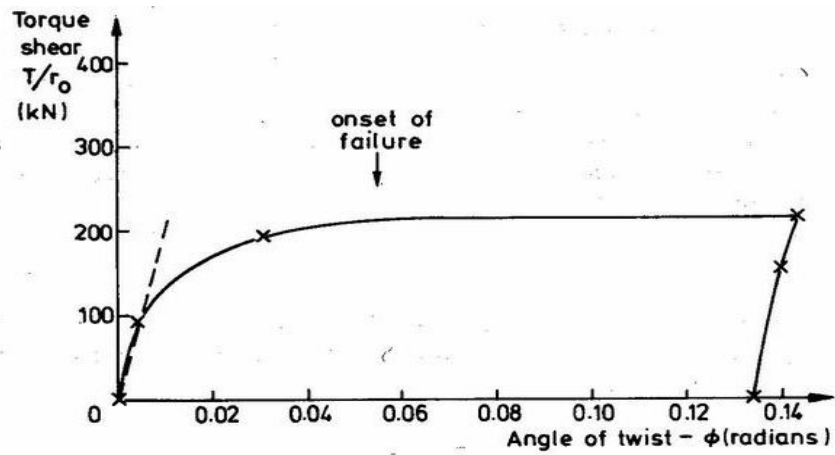
Figure C- 12 Results from Torsional Load Tests

(After Stoll 1972): (a) Pile A-3 (b) Pile V-4

Poulos (1975) conducted Model Pile Tests. The piles were of solid aluminum, ranging in length from about 6 in. (152mm) to 20 in. (508mm) and in diameter from 0.5 in. (13mm) – 1.5 in. (38mm). The soil used was Kaolin clay. After initial soil consolidation, four piles were installed in each test.

The rotation of the pile was measured by a dial gage mounted on an arm that was bolted to the base of the loading spindle. A pile was considered to have failed after it has rotated through 2 degree. The test results pointed out the possibility of using the shear modulus G from axial load test data to predict both working load and ultimate behavior of piles subjected to torsion. Typical comparisons between calculated and observed torque versus rotation curves to failure are shown in Fig.C-13.
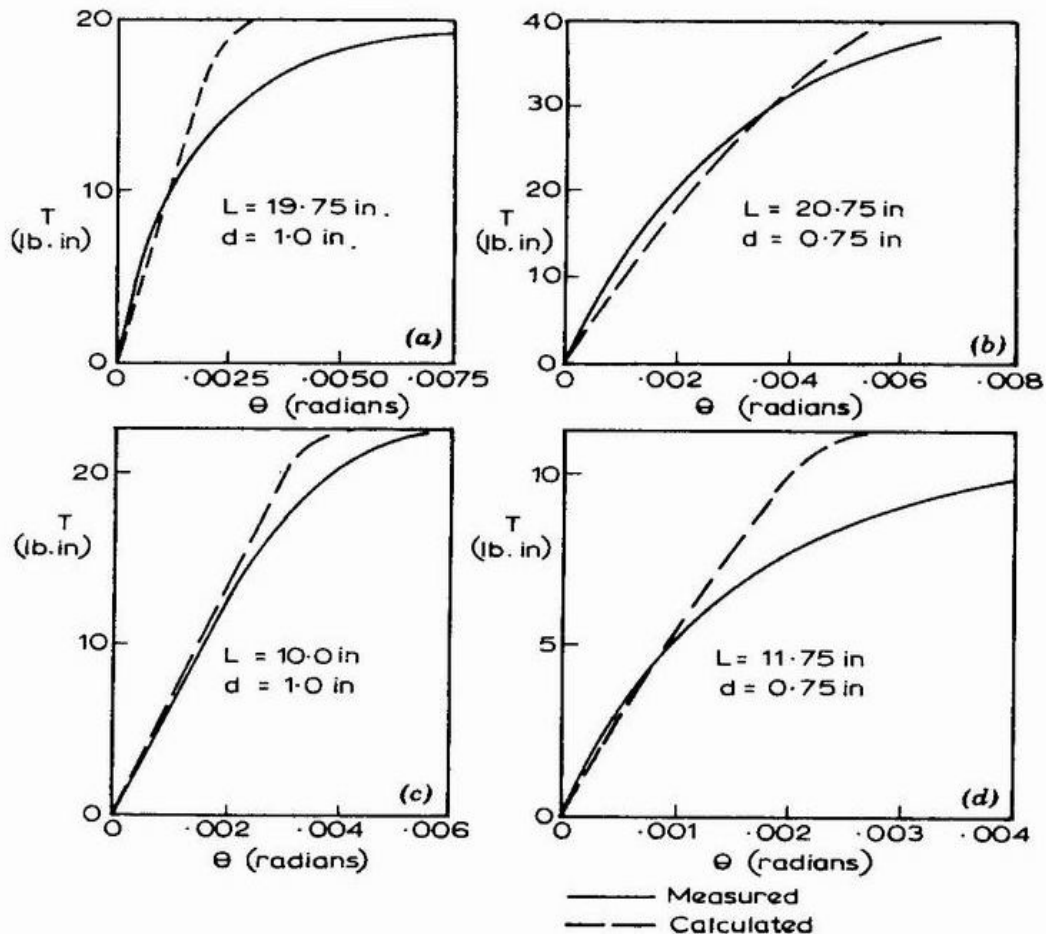
Figure C-13 Typical Comparisons between Measured and Calculated Torque versus Rotational Curves (After Poulos 1975)

3.2 Torsion Tests --- In Sands

Dutt (1976) conducted model tests to investigate the load-deformation characteristics of piles subjected to torsion in relation to the stress-strain behavior of the surrounding soil. And, he tried to establish a method to predict the torque-twist curve by using shear stress-strain behavior of the surrounding soil.

A 1.9 inches (48.3mm) OD circular aluminum pile and a square aluminum pile of 2 inches (50.8mm) outside dimensions were used in this investigation. Strain gages were utilized to measure the distribution of torque along the embedded length of the pile. The twist angle of pile-head was measured through a dial gage. A number of triaxial compression and direct shear tests were performed on samples prepared for torsion tests.

In order to get the torque-twist curves and shear stress-strain curves along the pile length from the measured torque distribution along the length of piles and the pile-head torque-twist curve, Dutt employed a computational procedure depicted in Fig. C-14.
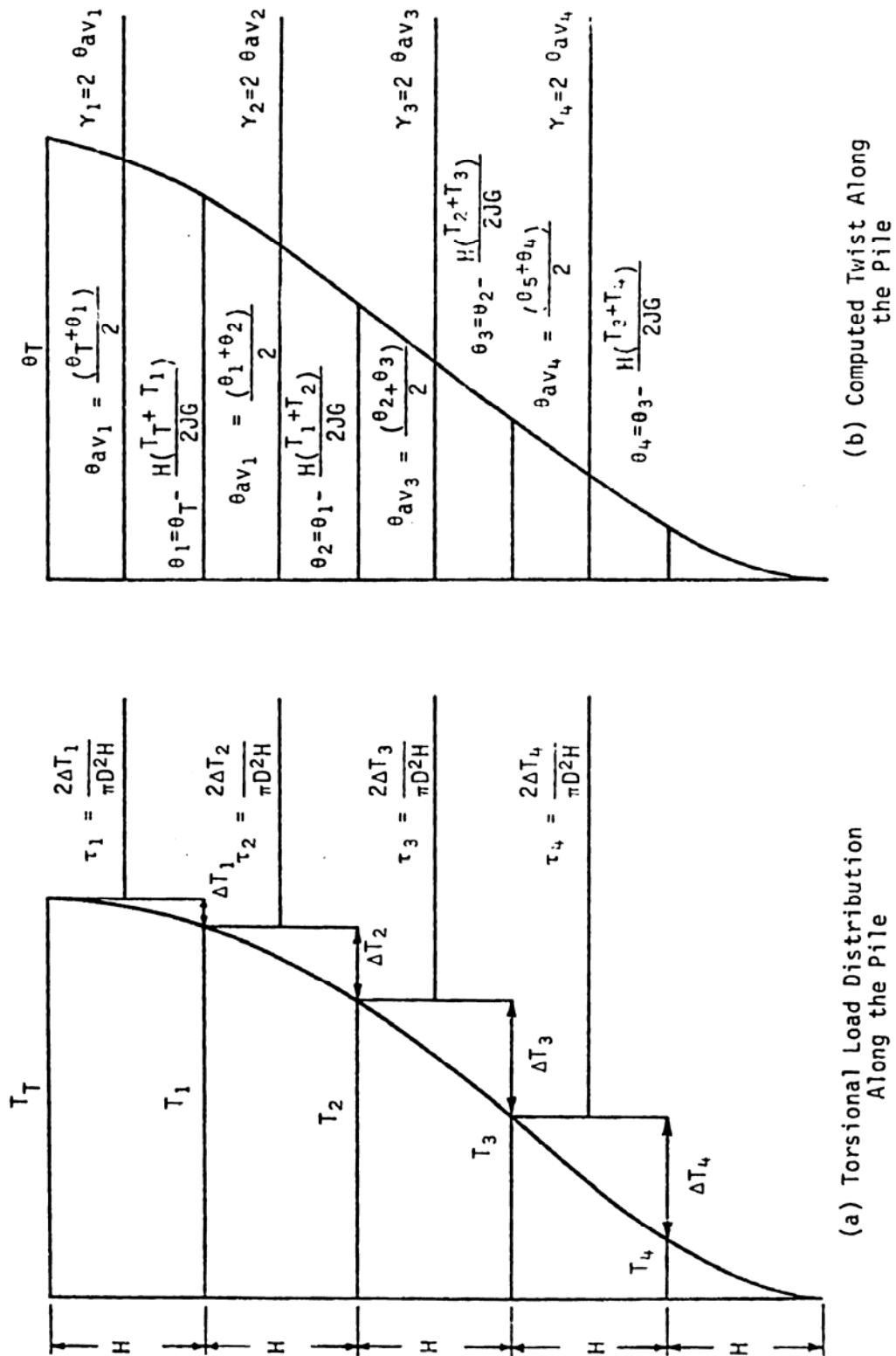
Figure C-14. Example Graphical Illustration for the Development of Mobilized Shear Stress-Strain Curves

In order to establish the correlation between T-φ curves with soil properties. Dutt (1976) employed a shear stress-strain relationship suggested by Tucker (1960) to represent soil properties as

$$\gamma = A\tau^n \tag{C-64}$$

where γ is the unit shearing strain due to a unit shearing stress τ. The parameters n and A are properties of the material.

After correlation the measured T-φ curves with τ-γ curves, Dutt gives out some suggestions on the determination of A and n. Then, with suggested n and A, the τ-γ curves can be determined to predict T-φ curves. The following Equations are employed to compute T-φ curves. Here the notation φ is the same with θ.

$$T = \frac{\pi D^2 H\tau}{2} \tag{C-65}$$

$$\theta = \frac{\gamma}{2} \tag{C-66}$$

Tawfiq (2000) carried out some scaled model shaft tests for torsional response of drilled shaft in sands. The shaft used for tests is 20 inches long and 4 inches in diameter. The testing setup consisted of a 4' diameter and 5' depth steel chamber where a strain controlled loading system was installed (Fig. C-15). Two 20 gallon buckets were used to apply the constant rate of loading. The torsional displacement was recorded with a dial indicator and a scale.

The model test results show that the rotation resistance dropped by about 65 to 50 percent for the bentonite and attapulgite slurries compared with the dry soil condition. In order to determine the residual frictional resistance, the shaft was rotated back to its original position and another torsional load was applied again in dry soil. The test results show that the frictional capacity was reduced by 70 to 77%.

Additional test was conducted to determine the base resistance by eliminating the side friction. And the test results show that the base resistance has a very small contribution to the total torsional resistance.

Under combined loading conditions, the torsional resistance will increase. Test results show that the torsional capacity increased two folds after adding 20 lb lateral load on the shaft.
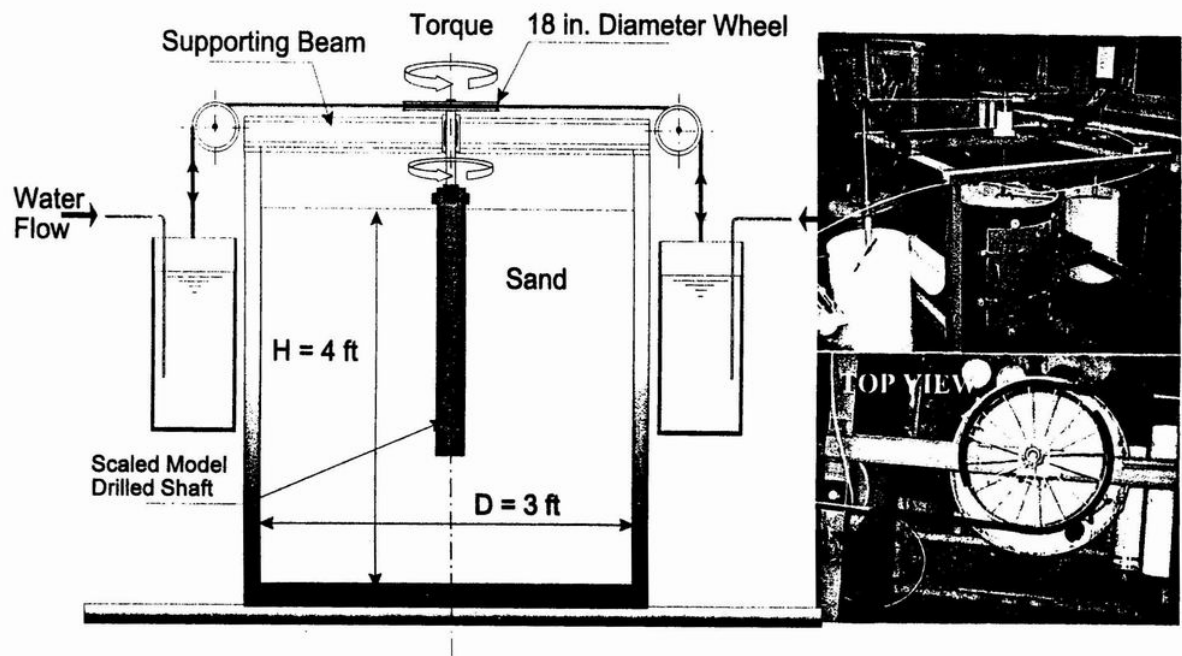
Figure C-15 Scaled Model Torsional Testing Apparatus

Tawfiq (2000) conducted 3 full-scale torsion tests of drilled shafts under combined lateral, overturning and torsional loads in sands. Four drilled shaft with 4' diameter and 20' long were installed, three of them for testing and the other one for supporting. The tested drilled shafts were constructed with polymer slurry, bentonite slurry and dry hole method, respectively. A loading arm consisted of 12" by 12" section and 5/8" thick was constructed to apply lateral loads (Fig. C-16). In order to record the rotation angle, four laser devices were mounted on the shaft and four foam boards were located at 20' from testing setup.

Full-scale field tests show the dry shaft demonstrated the largest capacity, and the shaft was gradually loaded up to structure failure at 490,000 ft-lb torsional loads. The rotation of the shaft was very small.

However for the shaft constructed using bentonite slurry, the rotational displacement was very noticeable at 180,000 ft-lb torsional loads. The load application was stopped at 280,000 ft-lb when no more increase in the loading could be recorded.

For the shaft constructed with polymer slurry, the shaft has similar performance as the dry hole shaft. The maximum load reached to 420,000 ft-lb, and structure failure was occurred.

These tests indicated that the construction method did make the difference in the torsional capacity.
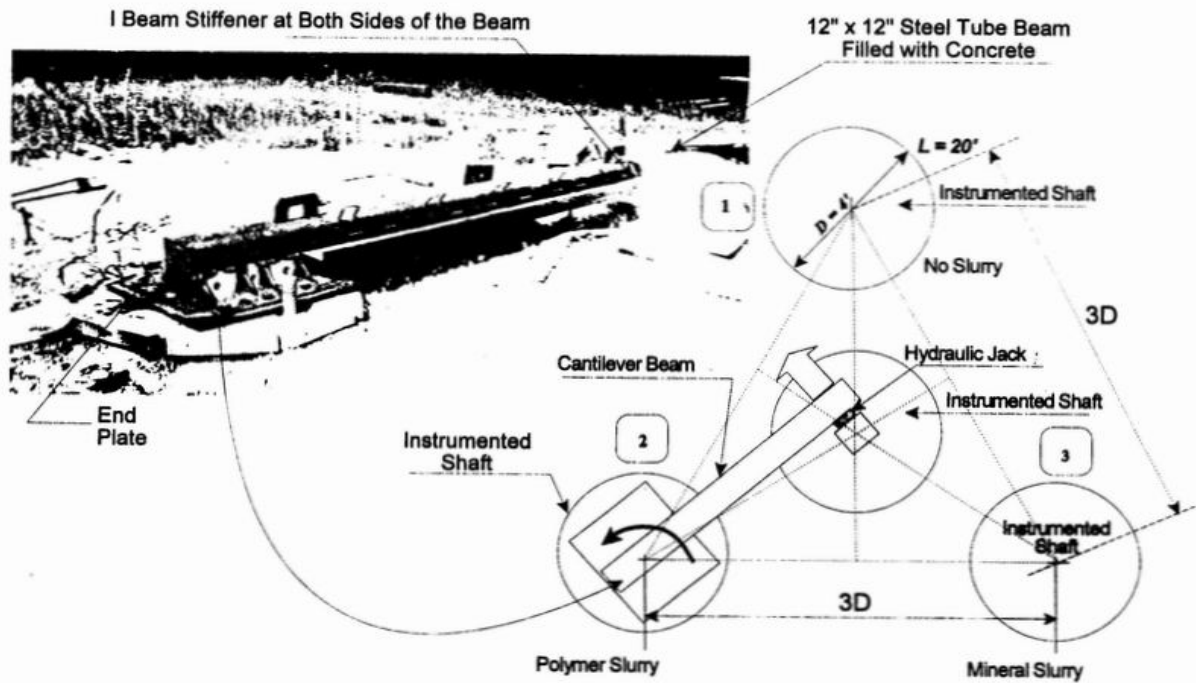
Figure C-16 Field Test Arrangement

Appendix D

The Lateral Load Test Database

Note: Only the drilled shafts embedded in clay are selected and all the tests are conducted in OHIO

Applied Load

h

Drilled Shaft

L

D

d
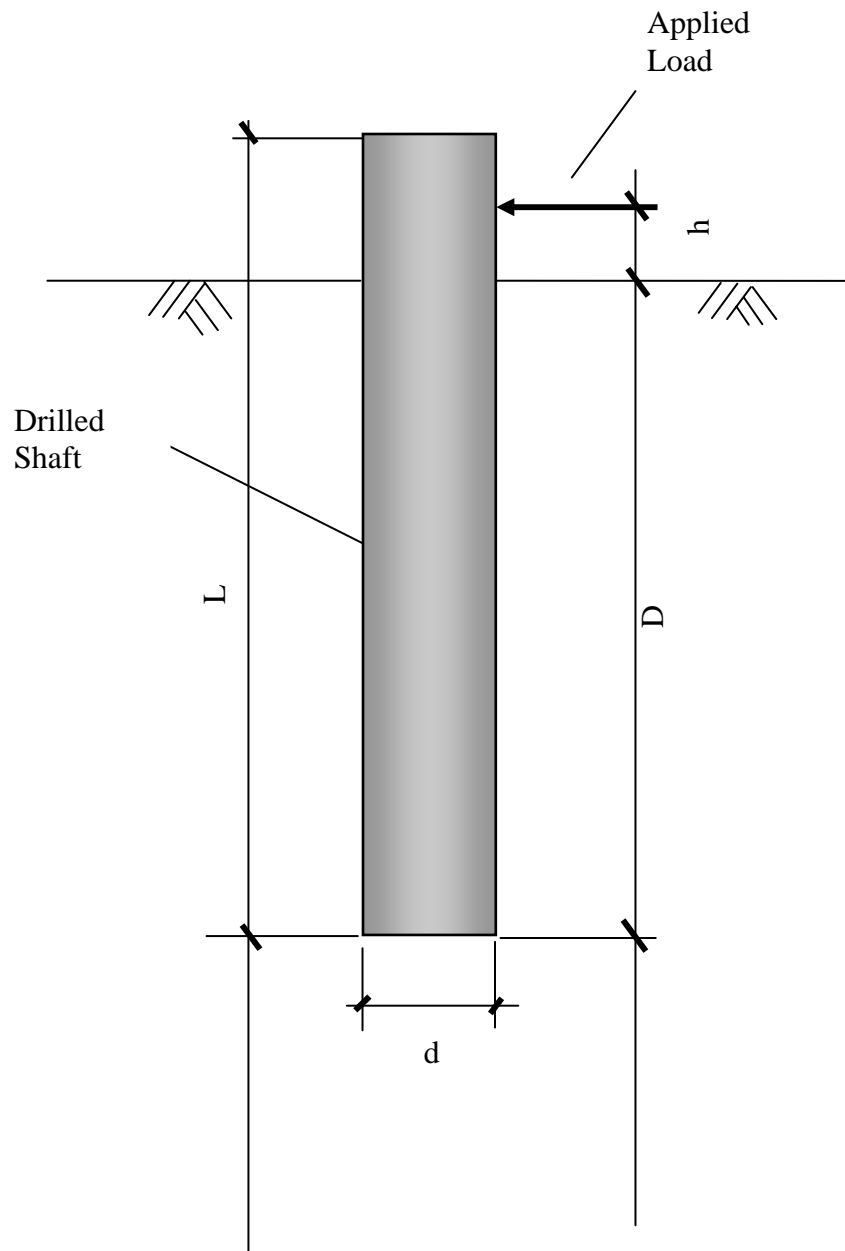
The Notations Definition for Lateral Load Test Database

Project Name: I-70 (Columbus, Ohio), Shaft 1 and Shaft 2, Columbus (L=9.5', D=9.5', h=0', d=30")

Depth (ft)	Description	SPT-N/12" Average	COM624P Soil classification	C_u (psi)	ϕ (deg)	Ks (pci)	ε_{50}	γ (pci)
0 to 1	Fill Material	22	3	21		1000	0.005	0.078
1 to 4	Stiff Clay	18	3	16		1000	0.005	0.075
4 to 18	Stiff Clay	34	3	27 to 35		1000	0.005	0.075

Project Name: I-90 Sound Barriers Projects, Cuyahoga County,OH, 12ft, Shaft 2, (L=25', D=12', h=10', d=30")

Depth (ft)	Description	SPT-N/12" Average	COM624P Soil classification	C_u (psi)	ϕ (deg)	Ks (pci)	ε_{50}	γ (pci)
0 to 3	Brown sand with brick concrete scat fill, MOIST	22	3	19.0		1000	0.005	0.078
3 to 5	Brown very fine sand with some silt, WET	20	3	17.4		1000	0.005	0.077
5 to 7	Brown fine sandy SILT with a trace of CLAY, some possible thin CLAY seams, MOIST	35	3	30.0		2000	0.004	0.078
7 to 9	Brown fine sandy SILT with a trace of CLAY, some possible thin CLAY seams, MOIST	28	3	24.3		1000	0.005	0.082
9 to 12	Brown changing to gray SILTY CLAY with some small ROCK fragment, MOIST	27	3	23.4		1000	0.005	0.081

D-4

Project Name: I-90 Sound Barriers Projects, Cuyahoga County,OH, 8ft Shaft 1, (L=21'-8", D=8'-8", h=10',d=30")

Depth (ft)	Description	SPT-N/12" Average	COM624P Soil classification	C_u (psi)	ϕ (deg)	Ks (pci)	ε_{50}	γ (pci)
0 to 3	Brown sand with brick concrete scat fill, MOIST	22	3	19.0		1000	0.005	0.078
3 to 5	Brown very fine sand with some silt, WET	20	3	17.4		1000	0.005	0.077
5 to 7	Brown fine sandy SILT with a trace of CLAY, some possible thin CLAY seams, MOIST	35	3	30.0		2000	0.004	0.078
7 to 9	Brown fine sandy SILT with a trace of CLAY, some possible thin CLAY seams, MOIST	28	3	24.3		1000	0.005	0.082
9 to 12	Brown changing to gray SILTY CLAY with some small ROCK fragment, MOIST	27	3	23.4		1000	0.005	0.081

Project Name: I-90 Sound Barriers Projects, Cuyahoga County,OH, 8ft Shaft 2 (L=21'-8", D=8'-5", h=10'-3", d=30")

Depth (ft)	Description	SPT-N/12" Average	COM624P Soil classification	C_u (psi)	ϕ (deg)	Ks (pci)	ε_{50}	γ (pci)
0 to 3	Brown sand with brick concrete scat fill, MOIST	22	3	19.0		1000	0.005	0.078
3 to 5	Brown very fine sand with some silt, WET	20	3	17.4		1000	0.005	0.077
5 to 7	Brown fine sandy SILT with a trace of CLAY, some possible thin CLAY seams, MOIST	35	3	30.0		2000	0.004	0.078
7 to 9	Brown fine sandy SILT with a trace of CLAY, some possible thin CLAY seams, MOIST	28	3	24.3		1000	0.005	0.082
9 to 12	Brown changing to gray SILTY CLAY with some small ROCK fragment, MOIST	27	3	23.4		1000	0.005	0.081

I-90 Noise Wall Project, OH, Shaft 1 (P 101) and Shaft 2 (P 100) (L=12'/10', D=12'/10', h=0', dim=30"/36")

Depth (ft)	Description	SPT-N/12" Average	COM624P Soil classification	C_u (psi)	ϕ (deg)	Ks (pci)	ε_{50}	γ (pci)
0 to 2	Very stiff, gray CLAY (A-7-6), trace sand, trace to no asphalt and wood fragment, moist	24	3	22		1000	0.005	0.08
2 to 8.6	Stiff, gray CLAY (A-7-6), trace sand, trace to no asphalt and wood fragment, moist	11	3	11		500	0.007	0.075
8.6 to 10	Very soft to medium hard, decomposed to weathered, gray SILT SHALE Encountered spoon refusal at 11.3 feet, augered to 11.5 feet and began coring bedrock.	50/0.4	3	50		150	0.004	0.084
10 to 13	Soft, highly weathered to weathered, gray SILT SHALE with nearly horizontal laminar bedding (fissile), good quality as RQD. U. C. Strength at 12.8 feet = 442 psi	50/0.3 RDQ=80%	3	55		2000	0.003	0.084
	TERMINATION DEPTH = 13.0 FEET							

Shaft Cross Section and Measured Load-Deflection Data for Lateral Load Test Database
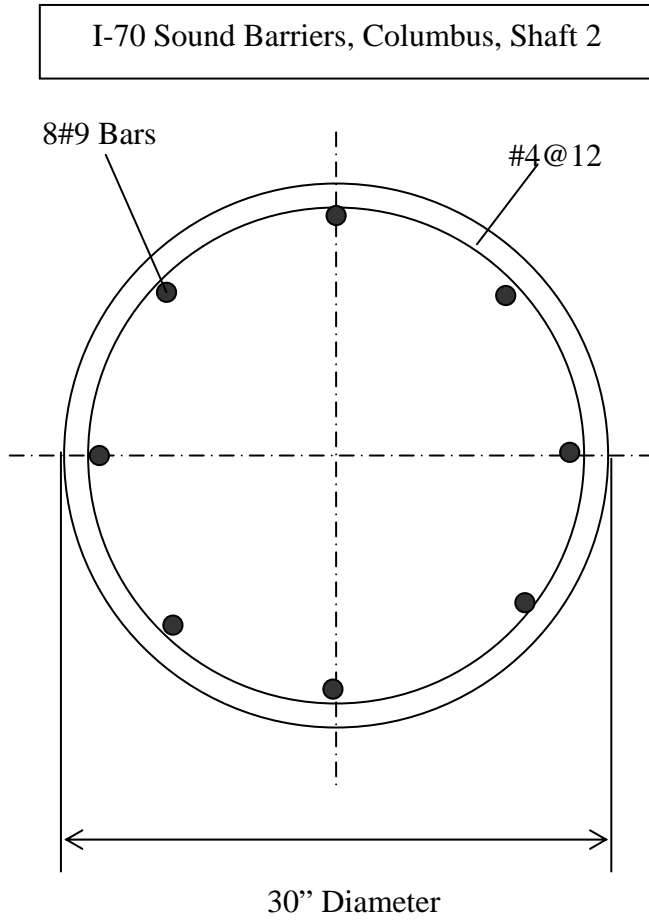
I-70 Sound Barriers, Columbus, Shaft 1

8#9 Bars

#4@12

30" Diameter

$I = 39760 \ in^4$

$A = 707 \ in^2$

$E_{avg} = 4415201 \ lb/in^2$

Load (kips)	Deflection (in.)	
	Dial Gage	Inclinometer
0.00	0.000	0.000
2.50	0.012	0.005
3.75	0.015	0.002
5.00	0.021	0.001
7.50	0.031	0.005
10.00	0.036	0.007
15.00	0.061	0.008
17.50	0.076	0.022
22.50	0.094	0.044
27.50	0.116	0.062
30.00	0.135	0.092
32.50	0.154	0.118
37.50	0.213	0.201
40.00	0.239	0.229

I-70 Sound Barriers, Columbus, Shaft 2

8#9 Bars

#4@12

30" Diameter

$I = 39760 \text{ in}^4$

$A = 707 \text{ in}^2$

$E_{avg} = 4415201 \text{ lb/in}^2$

Load (kips)	Deflection (in.)	
	Dial Gage	Inclinometer
0.00	0.0000	0.0000
2.50	0.0018	0.0033
3.75	0.0031	0.0075
5.00	0.0066	0.0075
7.50	0.0123	0.0090
10.00	0.0180	0.0084
15.00	0.0237	0.0102
17.50	0.0325	0.0162
22.50	0.0412	0.0267
27.50	0.0553	0.0390
30.00	0.0702	0.0426
32.50	0.0938	0.0627
37.50	0.1149	0.0849
40.00	0.1333	0.1155

I-90 Sound Barriers, 12 ft Depth, Shaft 2

W

30" Diameter

$I = 69471/51471$ in^4

$A = 804$ in^2

$E_{avg} = 6472076$ lb/in^2

Load (kips)	Deflection (in.)	
	Dial Gage	Inclinometer
0.000		0.0000
13.250		-0.0084
26.500		0.1122
53.000		0.5220
79.500		1.0870
37.750		1.0350
0.000		0.4902
39.750		0.8730
84.800		1.1388
53.000		1.1328
0.000		0.7140
106.000		1.6506

I-90 Sound Barriers, 8 ft Depth, Shaft 1

W

30" Diameter

$I = 69471/51471$ in^4

$A = 804$ in^2

$E_{avg} = 6472076$ lb/in^2

Load (kips)	Deflection (in.)	
	Dial Gage	Inclinometer
0.000		0.0000
10.60		0.1080
15.90		0.1869
20.00		0.2760
31.80		0.4773
42.40		1.0089
47.70		1.2375
31.80		1.2309
15.90		1.1697
0.00		0.6891
15.90		0.9270
31.80		1.1307
47.70		1.6116
53.00		1.9047

I-90 Sound Barriers, 8 ft Depth, Shaft 2

W

30" Diameter

$I = 69471/51471 \text{ in}^4$

$A = 804 \text{ in}^2$

$E_{avg} = 6472076 \text{ lb/in}^2$

Load (kips)	Deflection (in.)	
	Dial Gage	Inclinometer
0.000		0.0000
10.60		0.1254
15.90		0.2106
20.00		0.3162
31.80		0.5475
42.40		1.1775
47.70		1.4427
31.80		1.4379
15.90		1.3752
0.00		0.8544
15.90		1.1358
31.80		1.3446
47.70		1.8894
53.00		2.2335

I-90 Sound Barriers, Shaft 100

8#9 Bars

#4@12

36" Diameter

$I = 82448\ \text{in}^4$

$A = 1018\ \text{in}^2$

$E_{avg} = 4415201\ \text{lb/in}^2$

Load	Deflection (in.)	
(kips)	Dial Gage	Inclinometer
0.00	0.0000	0.0000
6.25	0.0120	0.0054
12.25	0.0285	0.0270
18.75	0.0550	0.0510
25.00	0.0915	0.0744
31.25	0.1460	0.1218
37.25	0.2200	0.1968
42.50	0.3030	0.2670
45.00	0.3330	0.3108
47.50	0.3945	0.3660
52.50	0.4755	0.4506
58.75	0.5990	0.5382
65.00	0.8200	0.7896
50.00	0.8020	0.7746
37.50	0.8020	0.7668
25.00	0.7750	0.7338
12.50	0.7095	0.6666
0.00	0.4075	0.3720

I-90 Sound Barriers, Shaft 101

8#9 Bars

#4@12

30" Diameter
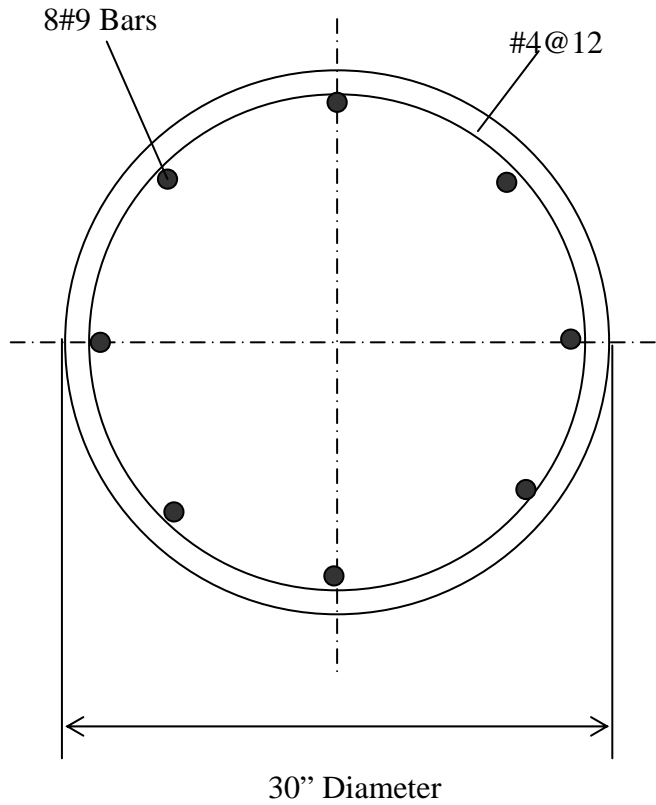
$I = 39760 \text{ in}^4$

$A = 707 \text{ in}^2$

$E_{avg} = 4415201 \text{ lb/in}^2$

Load (kips)	Deflection (in.)	
	Dial Gage	Inclinometer
0.00	0.0000	0.0000
6.25	0.0140	0.0180
12.25	0.0355	0.0504
18.75	0.0730	0.0570
25.00	0.1195	0.1110
31.25	0.1870	0.1794
37.25	0.2665	0.2754
42.50	0.3600	0.3390
45.00	0.3910	0.3624
47.50	0.4575	0.4596
52.50	0.5325	0.5250
58.75	0.6530	0.6612
65.00	0.8500	0.8712
50.00	0.8270	0.8610
37.50	0.8255	0.8484
25.00	0.7940	0.8340
12.50	0.7220	0.7650
0.00	0.3755	0.3798

Appendix E

Design Spreadsheet for Lateral Loaded Drilled Shafts Supporting

Sound Walls

Design Spreadsheet for Lateral Loaded Drilled Shafts Supporting Sound Walls,

- Clay

The numbers with red color or Italic are values of input parameters.

Broms' method, using Unsaturated soil parameters from lab test

1. Parameters

Soil weighted average cohesion C_u =   *14.3*   psi

Embedded length L =   *12*   ft, =   144   in.

Drilled shaft height above ground , e =   *9*   ft, =   108   in.

Drilled shaft diameter D =   *30*   in., =   2.5   ft.

2. Calculate the ultimate capacity P_{ult}

$a = 9C_uD$ =   3861

$b = L-1.5D$ =   99

$c = e+(L+1.5*D)/2)$ =   202.5

$P_{ult} = (sqrt(c^2+b^2/4)-c)*2a$ =   **46**   kips

3. Check maximum moment in the shaft

$f = P_{ult}/(9C_uD)$ =   11.9   in., =   0.994   ft.

$M_{max} = P_{ult}*(e+1.5D+0.5f)$ =   **609.9**   kips-ft   < M_y *777*   kips-ft

So, the ultimate capacity estimated by Broms' method is   **46**   kips.

Note: the yielding moment of drilled shaft M_y can be obtained from COM624P analysis

4. Design load

The Factor Safety of   2   is adopted.

Calculated Design Load =   23   kips   > required design load =   17.3   kips

Design Spreadsheet for Lateral Loaded Drilled Shafts Supporting Sound Walls - Sand

  Suggested New Design for CDOT sound barrier wall's drilled shafts in sand

Broms' method, using soil parameters correlated from SPT N values by using Liang (2002)'s correlation.

1. Parameters

Soil average cohesion $C_u =$ *0*   psi
Shaft length L =   *12*   ft, =   144   in.
Shaft height above ground , e =   *9*   ft, =   108   in.
Shaft diameter D =   *30*   in., =   2.5   ft.
Friction angle =   *33*
Unit weight =   *0.069*   lb/in^3 0.119   kip/ft^3

2. Calculate the ultimate capacity P_{ult}:

$K_p = (1+\sin\Phi)/(1-\sin\Phi) =$ 3.4
$P_{ult} = 0.5\gamma dL^3 K_p/(e+L) =$ 42   kips

3. Check maximum moment in the shaft.

At f = $0.82*(P_{ult}/D* K_p*r)^{0.5} =$ 5.26   ft
$M_{max} = P_{ult}*(e+0.67f) =$ **520.6**   kips-ft $< M_y =$ *555*   kips-ft

$P_{ult}=$ 42   kips
Note: the yielding moment of drilled shaft M_y can be obtained from COM624P analysis.

4. Design load

  The Factor Safety of   2   is adopted.
Calculated Design Load =   21   kips   > required design load =   17.3   kips

Appendix F

Selected Bibliography

References Related to Lateral Response of Drilled Shaft:

O'Neill, Michael W., and Reese, Lymon C. (1999) "Drilled shaft: Construction procedure and design methods" *Publication No. FHWA-IF-99-025*, Vol-I, 1-21

Zhang, L. (1999) " *Analysis and design of drilled shafts in rock*." PhD thesis, Massachusetts Institute of Technology, Cambridge, Mass.

Broms, B.B.(1964a) "Lateral resistance of piles in cohesive soils" *Journal of the Soil Mechanics and Foundation Division*, Vol. 90, No. SM2, pp27-63.

Broms, B.B.(1964b) "Lateral resistance of piles in cohesionless soils" *Journal of the Soil Mechanics and Foundation Division*, Vol. 90, No. SM3, pp 123-157.

Poulos, H.G., and Davis, E.H. (1980). *Pile foundation analysis and design*. John Wiley & Sons, NY.

Indiana department of Transportation (1996) "General Instructions for Bridge Structure Investigation", *Geotechnical section and division of materials and tests* Indiana department of Transportation.

Mokwa, R.L.(1999) "*Investigation of the resistance of pile caps to lateral loading*", PhD thesis, Virginia Tech, VA.

Sun, K. (1994). "Laterally loaded piles in elastic media," *J. Geotech Engrg., ASCE*, 120(8), 1324-1344

Ashour, M. Member, ASCE, Norris, G. Member, ASCE, and Pilling, P., (1998) "Lateral loading of a pile in layered soil using the strain wedge model" *Journal of geotechnical and geoenvironmental engineering*, pp:303-315.

AASHTO *LRFD BRIDGE DESIGN SPECIFICATIONS*, "Section-10: Drilled Shafts", Published by the American Association of State Highway and Transportation Officials (AASHTO), First Edition, 1994.

AASHTO, (1989) "*Guide Specifications for Structural Design of Sound Barriers*", Washington, D.C.

Davidson, J.L., Hays, C.O., Jr., and Hagan, E.M., Jr., (1976) "Design of drilled shafts supporting highway signs", *Transportation Research Record*, issue 616, pp 62-66.

Hough, B.K., (1969) "*Basic Soils Engineering*", Publication: John Wiley and Sons.

Liang, R.Y. (1997) "Pressuremeter to Predict Lateral Load Capacity of Drilled Shafts on Slope," Final Report, FHWA/OH-97/005, ODOT.

Liang, R.Y., (2002) "Drilled Shaft Foundations for Noise Barrier Walls and Slope Stabilization," Final Report, FHWA/OH-2002/038, ODOT.

ABAQUS Standard User's Manual, Version 5.8, Hibbitt, Karlsson & Sorensen, Inc. 1998.

AASHTO (2001), "*Standard Specifications for Structural Supports for Highway Signs, Luminaries and Traffic Signals*," 4th Edition.

NAVFAC DM-7 (1971), Department of the Navy, Naval Facilities Engineering Command, "Design Manual – Soil Mechanics, Foundations and Earth Structures" .

Prakash, Shamsher, and Sharma, Hari (1990) "Pile Foundations In Engineering Practice" pp:322-342, Publication: John Willey & Sons.

AASHTO LRFD Bridge Design Specifications, First Edition, 1994.

Kulhawy, F.H., and Chen. Y.-J., (1995) "A Thirty Year Perspective of Broms' Lateral Loading Models, as Applied to Drilled Shafts," *Bengt B. Broms Symposium on Geotechnical Engineering*, Singapore, pp. 225-240.

Wang, Shih-Tower, and Reese, L.C., (1993) "COM624P-Laterally Loaded Pile Analysis Program for the Microcomputer, Version 2.0," Final Report, Report No. FHWA-SA-91-048.

Bhushan, K., Lee, L.J., and Grime, D.B. (1981) "Lateral Load Tests on Drilled Piers in Sand." *Drilled Piers and Caissons: Proceedings of a Session at the ASCE National Convention*, St Louis, MO, USA. Conference Code: 00225. P. 114-131.

Bhushan, K., and Askari, S. (1984) "Lateral-Load Tests on Drilled Pier Foundations for Solar Plant Heliostats." Laterally Loaded Deep Foundations: Analysis and Performance, ASTM STP 835, J.A. Langer, E.T. Mosley, and C. D. Thompson, Eds., ASTM, pp. 140-156.

References Related to Torsional Response of Drilled Shaft:

Carter, J.P., and Kulhawy, F.H., (1988) "Analysis and Design of Drilled Shaft Foundations Socketed into Rock," Cornell University, Ithaca, New York.

Chow, Y. K., (1985) "Torsional Response of Piles in Non-Homogeneous Soil," *Journal of Geotechnical Engineering*, ASCE, Vol. 111, pp. 942-947.

Dutt, R. N., (1976) "Torsional response of piles in sand," Ph.D. thesis, Univ. of Houston,Texas.

Guo, W.D., and Randolph, M.F., (1996) "Torsional Piles in Non-Homogeneous Media," *Computers and Geotechnics*, No. 19, pp. 265-287.

Hache, R.A.G., and Valsangker, A. J., (1988) "Torsional Resistance of Single Pile in Layered Soil," *Journal of Geotechnical Engineering*, ASCE, V. 114, pp. 216-220.

Lin, S.S., and AlKhaleefi, A.L. (1996) "Torsional Behavior of Cracked Reinforced Concrete Piles in Sand," *Journal of The Chinese Institute of Engineers*, Vol.19: (6), pp. 689-696.

O'Neill, Michael Wayne, (1964) "Determination of the Pile-Head, Torque-Twist Relationship for a Circular Pile Embedded in a Clay Soil," Master Thesis, The University of Texas at Austin.

O'Neill, M.W., and Dutt, R.N., (1976) discussion of "Torsional Response of Piles," by Harry G. Poulos, *Journal of Geotechnical Engineering Division*, ASCE, Vol. 102, No. GT6, Proc. Paper 12163, pp. 658-660.

Poulos, Harry G. (1975) "Torsional Response of Piles," *Journal of the Geotechnical Engineering Division*, V. 101, GT10, pp. 1019-1035.

Randolph, M. F. (1981) "Piles Subjected to Torsion," *Journal of the Geotechnical Engineering Division*, American Society of Civil Engineers, Vol.107, issue 8, pp. 1095-1111.

Stoll, U. W. (1972) "Torque Shear Test of Cylindrical Friction Piles," *Civil Engineering*, ASCE, Vol. 42, pp.63-65.

Tawfiq, K. (2000) " Drilled shaft under torsional loading conditions", *Final report Federal Highway Administration*, Florida Department of Transportation.

References Related to Strain Rate Effect:

Abrantes, Antonio E., and Yamamuro, Jerry A. (2002) "Experimental and data analysis techniques used for high strain rate tests on cohesionless soil", *Geotechnical Testing Journal*. v. 25 issue 2, p. 128-141.

Shibuya, Satoru, et al. (1996) "Strain rate effects on stress-strain behaviour of clay as observed in monotonic and cyclic triaxial tests", *Geotechnical Special Publication*, issue 61, p. 214-227.

Shibuya, Saturo, et al., (1995) "Strain rate effects on shear modulus and damping of normally consolidated clay", *Geotechnical Testing Journal*, v. 18 issue 3, p. 365-375.

Wedage, A. M.P., et al. (1998) "Strain rate dependent constitutive model for clays at residual strength", *Canadian Geotechnical Journal*, v. 35 issue 2, p. 364-374.

Nakase, Akio, and Kamei, Takeshi, (1986) "INFLUENCE OF STRAIN RATE ON UNDRAINED SHEAR CHARACTERISTICS OF K_0-CONSOLIDATED COHESIVE SOILS", *Soils and Foundations*, v. 26 issue 1, p. 85-95.

Seed, H.B., and Lundgren, R., (1954) "Investigation of the Effect of Transient Loadings on the Strength and Deformation Characteristics of Saturated Sands." *Proceedings of the American Society of Civil Engineers*, Vol. 54, pp. 1288-1306.

Whitman, R.V., and Healy, K.A., "Shear Strength of Sands During Rapid Loading," *Journal of the Soil mechanics and Foundations Division*, ASCE, Vol. 88, No. SM2, PP. 99-132.

Lee, K. L., Seed, H. B., and Dunlop, P., (1969) "Effect of Transient Loading on the Strength of Sand," *Proceedings of the 7th International Conference on Soil Mechanics and Foundation Engineering*, Vol. 1, Mexico City, Mexico, pp. 239-247.

Mesri, G., Febres-Cordero, E., Shields, D.R. and Castro,A., (1981) "Shear stress-strain-time behavior of clays," *Geotechnique*, London, England, 31(4), pp. 537-552.

Kulhawy, F. H., and Mayne, P. W., (1990) "Manual on Estimating Soil Properties for Foundation Design," Rep. No. EL-6800, *Electric Power Res. Inst.*, Palo Alto, Calif.

Casagrande, A., and Wilson, S. D., (1951) "Effect of rate of loading on the strength of clays and shales at constant water content," *Geotechnique*, London, U.K., 2(3), pp 251-263.

Graham, J., Crooks, J.H.A., and Bell, A.L.,(1983) "Time effects on the stress-strain behavior of natural soft clays," *Geotechnique*, London, U.K., 33(3), pp 327-340.

Richardson, A. M., and Whitman, R. V., (1963) "Effect of strain-rate upon undrained shear resistance of a saturated remoulded fat clay," *Geotechnique*, London, U.K., 13(4), pp 310-324.

Lefebvre, Guy, and LeBoeuf, Denis, (1987) "Rate effects and cyclic loading of sensitive clays," *Journal of Geotechnical Engineering*, ASCE, Vol. 113, No. 5, pp 476-489.

Sheahan, T.C., Ladd, C.C., and Germaine, J.T., (1996) "Rate-dependent undrained shear behavior of saturated clay," *Journal of Geotechnical Engineering*, ASCE, Vol. 122, No. 2, pp 99-108.

References Related to Cyclic Degradation

Long, James H., and Reese, Lymon C. (1984) "Testing and analysis of two offshore drilled shafts subjected to lateral loads", *ASTM Special Technical Publication*. p. 214-228.

Long, J. H., and Vanneste, G. (1994) "Effects of cyclic lateral loads on piles in sand" *ASCE Journal of Geotechnical Engineering*, Vol: 120(1), pp: 225-224.

Matasovic, N., and Vucetic, M. (1995) "Generalized cyclic-degradation-pore-pressure generation model for clays" *ASCE Journal of Geotechnical Engineering*, Vol: 121(1), pp: 33-42.

Poulos, H.G. (1982) "Single pile response to cyclic lateral load" *ASCE Journal of Geotechnical Engineering Div*, Vol: 108(GT3), pp: 355-375.

Vucetic, Mladen, and Dobry, Ricardo (1988) "Degradation of marine clays under cyclic loading"*, American Society Of Civil Engineers Journal Of Geotechnical Engineering.* v. 114 issue 2, p. 133-149.

Vucetic, M. (1994) "Cyclic threshold shear strains in soils" *ASCE Journal of Geotechnical Engineering,* Vol: 120(12), pp:208-28.

Yasuhara, K. (1994) "Post cyclic undrained strength for cohesive soils" *ASCE Journal of Geotechnical Engineering*, Vol: 120(11), pp:1969-79.